Aus der

Medizinischen Universitätsklinik und Poliklinik Tübingen

Abteilung Innere Medizin IV

(Schwerpunkt: Diabetologie, Endokrinologie und Nephrologie)

Bildung und Freisetzung von Lysophosphatidylcholinen in primären humanen Myotuben und deren Assoziation mit *In-vivo*- und weiteren *In-vitro*-Parametern der Spender

Inaugural-Dissertation
zur Erlangung des Doktorgrades
der Medizin

der Medizinischen Fakultät
der Eberhard Karls Universität
zu Tübingen

vorgelegt von

Wolf, Magnus Hermann

2021

Dekan:	Professor Dr. B. Pichler
1. Berichterstatter:	Professorin Dr. C. Weigert
2. Berichterstatter:	Professorin Dr. B. Munz
Tag der Disputation:	15.04.2021

Directory

List of Figures

List of Tables

List of Abbreviations

1^{st}pIS	First phase insulin secretion
AC	Acylcarnitine or adenylate cyclase (in the case of Figure 4)
ACC	Acetyl-CoA carboxylase
ACP	Acyl carrier protein
ACTB	β-Actin (gene)
AICAR	5-Aminoimidazole-4-carboxamide 1-β-D-ribofuranoside
AP-1	Activator protein 1
ARA	Arachidonic acid (C20:4)
AT	Anaerobic threshold
ATP	Adenosine 5'-triphosphate
BCA	Bicinchoninic acid
BMI	Body mass index (= weight [kg]/height² [m²])
bp	Base pair (of DNA) [unit of DNA length]
Bq	Becquerel [unit of radioactivity] (1 becquerel = 1 nuclear disintegration per second)
BEL	Bromoenol lactone
BSA	Bovine serum albumin
c	Concentration
c	*cis*-configuration of double bonds
C8-AC	*O*-Octanoyl-L-carnitine
C10-AC	*O*-Decanoyl-L-carnitine
$[D_3]$C10-AC	Trideuterated *O*-decanoyl-L-carnitine
C12-AC	*O*-Dodecanoyl-L-carnitine = *O*-Lauroyl-L-carnitine
cDNA	Complementary DNA
CDP	Cytidine 5'-diphosphate
CDP-DAG	3-CDP-1,2-diacyl-*sn*-glycerol
CE	Cholesteryl ester
CHOx	Carbohydrate oxidation
$CHOx_{clamp}$	Carbohydrate oxidation determined during steady-state phase of a euglycemic-hyperinsulinemic clamp
$CHOx_{fasting}$	Carbohydrate oxidation determined in fasting condition

CL	Cell lysate
CMP	Cytidine 5’-monophosphate
CoA	Coenzyme A
cpm	Counts per minute [unit of radioactivity]
CPT1B	Carnitine palmitoyltransferase 1β (gene)
CPT-1β	Carnitine palmitoyltransferase 1β (protein)
C_p	LightCycler® synonym for C_q
C_q	Quantification cycle number in quantitative PCR experiments
CRP	C-reactive protein
CTP	Cytidine 5’-triphosphate
DAG	1,2-Diacyl-*sn*-glycerol (diglyceride)
DHAP	Dihydroxyacetone phosphate
DMSO	Dimethyl sulfoxide
DNA	Deoxyribonucleic acid
dNTP	Deoxyribonucleoside triphosphate
DPBS	Dulbecco’s phosphate-buffered saline
EB	Elution buffer
EC	Enzyme classification (number)
EDTA	Ethylenediaminetetraacetate
EMCL	Extramyocellular lipid content
EMEM	Eagle’s minimal essential medium
EnExp	Energy expenditure
$EnExp_{clamp}$	Energy expenditure determined during steady-state phase of a euglycemic-hyperinsulinemic clamp
$EnExp_{fasting}$	Energy expenditure determined in fasting condition
ER	Endoplasmic reticulum
ESI-Q-TOF-MS	Electrospray ionization quadrupole time-of-flight mass spectrometry
FAD	Flavin adenine dinucleotide (oxidized form)
$FADH_2$	Flavin adenine dinucleotide (reduced form)
FAO	Fatty acid oxidation
FBS	Fetal bovine serum
FL	Fluorescein

G3P	*sn*-Glycerol 3-phosphate
GA3P	Glyceraldehyde 3-phosphate
GAPDH	Glyceraldehyde 3-phosphate dehydrogenase
GIR	Glucose infusion rate
GPC	*sn*-Glycero-3-phosphocholine
GPCPD	Glycerophosphocholine phosphodiesterase (glycerophosphocholine glycerophosphohydrolase)
GPCR	G protein-coupled receptor
h	Hour [unit of time]
HDL	High density lipoprotein
hMT	Human myotubes
HOMA-IR	Homeostatic model assessment of insulin resistance
HPLC	High-performance liquid chromatography
IGTT	Intraperitoneal glucose tolerance test
IL-8	Interleukin-8
IMCL	Intramyocellular lipid content
IP_3	Inositol trisphosphate
$iPLA_2$	Calcium-independent phospholipase A_2
IRS-1	Insulin receptor substrate 1
ISI	Insulin sensitivity index
ISI_{clamp}	Insulin sensitivity index calculated by use of results from a euglycemic-hyperinsulinemic clamp
ISI_{OGTT}	Insulin sensitivity index calculated by use of glucose and insulin concentrations during OGTT according to Matsuda and DeFronzo
JNK	c-Jun *N*-terminal kinase
LBM	Lean body mass
LC	L-Carnitine or LightCycler® (*e.g.* in the case of LC640 or LC705)
LCAD	Long-chain acyl-coenzyme A dehydrogenase
LCAT	Lecithin:cholesterol acyltransferase (phosphatidylcholine:sterol *O*-acyltransferase)
LDL	Low density lipoprotein

LipOx	Lipid oxidation
$LipOx_{clamp}$	Lipid oxidation determined during steady-state phase of a euglycemic-hyperinsulinemic clamp
$LipOx_{fasting}$	Lipid oxidation determined in fasting condition
LLAT	Lysolecithin acyltransferase
LPA	Lysophosphatidic acid (1-acyl-*sn*-glycerol 3-phosphate)
LPC	Lysophosphatidylcholine (1-acyl-*sn*-glycero-3-phosphocholine)
LPC C14:0	Tetradecanoyl lysophosphatidylcholine (myristoyl LPC)
LPC C14:1	Tetradecenoyl lysophosphatidylcholine (myristoleoyl LPC)
LPC C15:0	Pentadecanoyl lysophosphatidylcholine (pentadecyloyl LPC)
LPC C16:0	Hexadecanoyl lysophosphatidylcholine (palmitoyl LPC)
LPC C16:1	Hexadecenoyl lysophosphatidylcholine (palmitoleoyl LPC)
LPC C17:0	Heptadecanoyl lysophosphatidylcholine (margaroyl LPC)
LPC C17:1	Heptadecenoyl lysophosphatidylcholine
LPC C18:0	Octadecanoyl lysophosphatidylcholine (stearoyl LPC)
LPC C18:1	Octadecenoyl lysophosphatidylcholine (oleoyl LPC)
LPC C18:2	Octadecadienoyl lysophosphatidylcholine (linoleoyl LPC)
LPC C18:3	Octadecatrienoyl lysophosphatidylcholine (linolenoyl LPC)
LPC C19:0	Nonadecanoyl lysophosphatidylcholine (nonadecyloyl LPC)
LPC C20:0	Eicosanoyl lysophosphatidylcholine (arachidoyl LPC)
LPC C20:1	Eicosenoyl lysophosphatidylcholine (gondoyl LPC)
LPC C20:2	Eicosadienoyl lysophosphatidylcholine
LPC C20:3	Eicosatrienoyl lysophosphatidylcholine
LPC C20:4	Eicosatetraenoyl lysophosphatidylcholine (arachidonoyl LPC)
LPC C20:5	Eicosapentaenoyl lysophosphatidylcholine
LPC C22:0	Docosanoyl lysophosphatidylcholine (behenoyl LPC)
LPC C22:1	Docosenoyl lysophosphatidylcholine (erucoyl LPC)
LPC C22:3	Docosatrienoyl lysophosphatidylcholine
LPC C22:4	Docosatetraenoyl lysophosphatidylcholine (adrenoyl LPC)
LPC C22:5	Docosapentaenoyl lysophosphatidylcholine
LPC C22:6	Docosahexaenoyl lysophosphatidylcholine (cervonoyl LPC)
LPC C24:0	Tetracosanoyl lysophosphatidylcholine (lignoceroyl LPC)
LPC C26:0	Hexacosanoyl lysophosphatidylcholine (cerotoyl LPC)

LPL	Lipoprotein lipase (gene)
$LPLA_1$	Lysophospholipase A_1
LPLD	Lysophospholipase D
M	Mega- (= 10^6) or molar (= mol/l) [unit of concentration]
m	Milli- (= 10^{-3}), mass [physical quantity] or meter [unit of length]
MAPK	Mitogen-activated protein kinase
mcAC	Medium-chain acylcarnitine
MCAD	Medium-chain acyl-coenzyme A dehydrogenase
MCP1	Monocyte chemotactic protein 1 (CCL2)
MCR	Metabolic clearance rate
MEM	Modified Eagle's medium (in case of αMEM)
$MgCl_2$	Magnesium chloride
min	Minute [unit of time]
mRNA	Messenger RNA
MRS	Magnetic resonance spectroscopy
MS	Mass spectrometry
MSR	Macrophage scavenger receptor
mtDNA	Mitochondrial DNA
MT-ND1	(Mitochondrially encoded) NADH dehydrogenase 1 (gene)
µ	Micro- (= 10^{-6})
n	Nano- (= 10^{-9}) or amount of substance or nuclear or number
NAD^+	Nicotinamide adenine dinucleotide (dehydrogenated, oxidized)
$NADH/H^+$	Nicotinamide adenine dinucleotide (hydrogenated, reduced)
NEFA	Nonesterified fatty acid
OGTT	Oral glucose tolerance test
p	Pico- (= 10^{-12}) or p-value (probability value)
p*	Statistically significant difference ($p \leq 0.05$)
p**	Statistically highly significant difference ($p \leq 0.01$)
p***	Statistically very highly significant difference ($p \leq 0.001$)
p****	Statistically very highly significant difference ($p \leq 0.0001$)
PA	Phosphatidic acid (1,2-diacyl-*sn*-glycerol 3-phosphate)
$PACOCF_3$	Palmitoyl trifluoromethyl ketone

PBF	Percentage of body fat
PC	Phosphatidylcholine (lecithin; 1,2-diacyl-*sn*-glycero-3-phosphocholine)
PCR	Polymerase chain reaction
PDH	Pyruvate dehydrogenase multienzyme complex
PDK4	Pyruvate dehydrogenase kinase, isozyme 4 (gene)
PE	Phosphatidylethanolamine (ethanolamine cephalin)
PG	Phosphatidylglycerol
PGC-1α	Peroxisome proliferator-activated receptor γ coactivator 1α (prot.)
PH	Phosphate as 3’ end-linked molecule of hybridization probes
P_i	Inorganic phosphate
PI	Phosphatidylinositol
PIP_2	Phosphatidylinositol bisphosphate
PKC	Protein kinase C
PKCδ	Protein kinase C δ
PLA_1	Phospholipase A_1
PLA_2	Phospholipase A_2
PLC	Phospholipase C
PLD	Phospholipase D
PPARGC1A	Peroxisome proliferator-activated receptor γ coactivator 1α (gene)
PPARD	Peroxisome proliferator-activated receptor δ (gene)
PPARδ	Peroxisome proliferator-activated receptor δ (protein)
PS	Phosphatidylserine (serine cephalin)
PUFA	Polyunsaturated fatty acid
qPCR	Quantitative PCR
r	Pearson correlation coefficient
RNA	Ribonucleic acid
ROS	Reactive oxygen species
rpm	Revolutions per minute
RQ	Respiratory quotient
RQ_{clamp}	Respiratory quotient determined during steady-state phase of a euglycemic-hyperinsulinemic clamp
$RQ_{fasting}$	Respiratory quotient determined in fasting condition

RT	Reverse transcriptase
RT-qPCR	Reverse transcriptase quantitative PCR
s	Second [unit of time]
SAH	*S*-Adenosyl-L-homocysteine
SAM	*S*-Adenosyl-L-methionine
SCD-1	Stearoyl-CoA desaturase-1
siRNA	Small interfering RNA
sn	Stereochemical numbering
SN	Supernatant
$sPLA_2$	Secretory phospholipase A_2
STEAM	Stimulated echo acquisition mode
t	Time [physical quantity]
t	*trans*-configuration of double bonds
Taq	*Thermus aquaticus*
TE	Echo time
TG	Triacylglycerol (triglyceride)
TM	Trial Medium
TNF-α	Tumor necrosis factor-α
TR	Repetition time
TRIS	Tris(hydroxymethyl)aminomethane
TUEF	Tübingen Family study
UCP3	Uncoupling protein 3 (gene)
V	Volume [physical quantity]
$V(O_2)_{max}$	Maximal aerobic capacity
$V(O_2)_{perc}$	Percentage aerobic capacity of individually predicted peak $V(O_2)$
W	Watt [unit of power]
WHR	Waist-to-hip ratio
WHO	World Health Organization

1 Introduction

1.1 Lipids and phospholipids

Lipids represent a very heterogeneous group of substances consisting of different components linked with each other [1, 2]. These components include for example fatty acids, glycerol or sphingosine, phosphoric acid and sugars, amino acids, ethanolamine or choline as well as cholesterol [1]. Many lipids show an amphipathic character because their chemical structures feature both polar and nonpolar regions [1-3]. Thus, they exhibit both hydrophobic and hydrophilic behavior as well as the ability for aggregation into membranous structures [1].

Phospholipids represent the major constituent of biological membranes (40 % to 90 % of total membrane lipids) and thereby influence functioning of every living cell [1, 2, 4-6]. Phospholipids can be grouped into sphingophospholipids (containing sphingosine as central unit) and glycerophospholipids (containing glycerol as central unit) including phosphatidylcholines (PC), phosphatidylserines (PS), phosphatidylethanolamines (PE) [1] and phosphatidylinositols (PI).

Remarkably, the configurations of the two hydroxymethyl groups of glycerol (C-1 and C-3) are not equivalent, although glycerol is not chiral, because the C-1 group exhibits pro-*S* configuration and the C-3 group pro-*R* configuration [1]. That is to say, an increase of the priority in the *RS* system of the C-1 group, for example by formation of an ester bond, leads to *S* configuration of the product molecule, whereas the same reaction at C-3 results in a product molecule with *R* configuration [1]. The numbering of the carbon in the pro-*S* configuration as *sn*-1 and of the carbon in the pro-*R* configuration as *sn*-3 is defined by the stereochemical numbering (*sn*) system [1]. The chemical structure of glycerol is stereochemically illustrated in **Figure 1** (on the left).

PCs, also known as lecithin, are the most abundant phospholipid of animal cells [4, 7] and are predominantly found on the outside of plasma membranes [8], whereas PSs and PEs mostly occur in the inner cytosolic membrane layer [4, 8, 9]. PCs (1,2-diacyl-*sn*-glycero-3-phosphocholine) consist of a glycerol molecule linked *via* ester linkages with two fatty acids at *sn*-1 and *sn*-2 and *via* a phosphodiester group with choline at *sn*-3 [1]. The positively charged choline is able to loop back towards the negatively charged phosphate portion in order to build an ionic bond, although the methyl groups at choline's nitrogen atom attenuate this interaction sterically [1, 4]. The zwitterionically

charged phosphocholine group functions as hydrophilic "head", the nonpolar acyl groups as hydrophobic "tail" occupying approximately an equal cross-sectional area [1, 4]. This fact enables both molecule parts to interact closely with adjacent molecules in membranes [4]. Hydrophobic bonding and van der Waals forces act amongst fatty acyl groups, ionic and hydrogen bridge bonds amongst hydrophilic head groups [4]. Because of the steric hindrance at choline's nitrogen atom by the methyl groups, the phosphate groups of PCs are hydrogen-bridged *via* water molecules and the melting temperature of PCs is 10 °C – 30 °C lower than that of PEs [4].

Unlike the typically saturated acyl groups at *sn*-1, acyl groups at *sn*-2 are usually unsaturated [5, 10-15] containing between one and four double bonds (often represented by arachidonoyl C20:4 group) [1, 9] with the unsaturated groups decreasing the melting point [4, 9]. Whereas triacylglycerols (triglycerides; TG) are typically liquid at body temperature, pure phospholipids are solid [1]. Membrane fluidity adjustment is achieved by cholesterol according to the fluid mosaic model of Singer and Nicolson [4, 16].

1.1.1 Biosynthesis of phospholipids

Biosynthesis of phospholipids begins with nicotinamide adenine dinucleotide (NADH)-dependent reduction of dihydroxyacetone phosphate (DHAP), deriving for example from glycolysis, to *sn*-glycerol 3-phosphate which is converted by the consecutive action of two different acyltransferases plus acyl group-carrying coenzyme A (CoA) or acyl carrier protein (ACP) into 1,2-diacyl-*sn*-glycerol 3-phosphate (phosphatidic acid; PA) [5, 9, 10]. These consecutively acting acyltransferases are *sn*-glycerol 3-phosphate 1-*O*-acyltransferase (enzyme classification (EC) number 2.3.1.15) [5, 10, 11, 17-19], accepting both acyl-CoA and acyl-ACP as acyl donors [17, 18], and 1-acyl-*sn*-glycerol 3-phosphate 2-*O*-acyltransferase (EC 2.3.1.51) [5, 10, 11, 18] plus in some circumstances 2-acyl-*sn*-glycerol 3-phosphate 1-*O*-acyltransferase (EC 2.3.1.52) [10]. The last-named enzyme transfers acyl groups from acyl-CoA to *sn*-1 of 2-acyl-*sn*-glycerol 3-phosphate to build PA with saturated acyl-CoA thioesters representing the most effective acyl donors and stearoyl-CoA exceeding the effectiveness of palmitoyl-CoA [10]. In contrast, 1-acyl-*sn*-glycerol 3-phosphate 2-*O*-acyltransferase shows a significant specificity for transfer of unsaturated acyl groups [5] from acyl-CoA thioesters to *sn*-2 of 1-acyl-*sn*-glycerol 3-phosphate to build PA (effectiveness of acyl-donors: oleoyl-CoA > linoleoyl-CoA ≈ palmitoleoyl-CoA > palmitoyl-CoA ≈

myristoyl-CoA; almost ineffective: stearoyl-CoA, lauroyl-CoA and arachidonoyl-CoA) [10]. In accordance with these substrate preferences acyl groups at *sn*-1 of glycerol usually are saturated and those at *sn*-2 unsaturated [5, 9, 11-14]. Yamashita *et al.* therefore postulated in 1973 that the asymmetric acyl group distribution in glycerophospholipids might be primarily caused by the substrate specificity of acyltransferases during formation of PA and subordinately by a deacylation-reacylation cycle after *de novo* biosynthesis of phospholipids [10, 15]. There are both supportive [5, 12, 13] and partially inconsistent [20-22] findings with regard to this hypothesis. However, the nonrandom distribution of acyl groups in PAs was found to be considerably congruent with that in 1,2-diacyl-*sn*-glycerols (DAG), TGs and PCs [13]. More precisely, the nonrandom distribution of monounsaturated and doubly unsaturated acyl groups in glycerolipids seems to be predefined at the step of PA formation, whereas the incorporation of polyunsaturated fatty acids (PUFA) like arachidonic acid (C20:4; ARA) seems to be achieved by the deacylation-reacylation Lands cycle after *de novo* biosynthesis of glycerophospholipids [11, 15, 23].

For biosynthesis of triacylglycerols or glycoglycerolipids a specific phosphatidate phosphatase (EC 3.1.3.4) eliminates phosphate at *sn*-3 of PA with formation of DAG [9-11, 18, 24, 25]. DAGs also emerge from membrane phospholipid metabolism such as G_q protein-driven hydrolysis of PI derivatives and can be reconverted into PA by appropriate1,2-diacyl-*sn*-glycerol kinases (EC 2.7.1.107) [9, 26-31]. Biosynthesis of phospholipids continues with the reaction of PA and cytidine 5'-triphosphate (CTP) catalyzed by phosphatidate cytidylyltransferase (cytidine 5'-diphosphate (CDP)-diacylglycerol synthetase; EC 2.7.7.41) and resulting in the key compound 3-CDP-1,2-diacyl-*sn*-glycerol (CDP-DAG) and pyrophosphate [9, 25, 32-34]. Catalyzed by an integral membrane enzyme mostly of the endoplasmic reticulum (ER) but sometimes also of ribosomes or mitochondria, CDP-diacylglycerol:L-serine *O*-phosphatidyltransferase (phosphatidylserine synthetase; EC 2.7.8.8), serine replaces cytidine 5'-monophosphate (CMP) to form PS [33, 35-37] possibly being decarboxylated to PE [9, 33, 38, 39] by the pyridoxal-phosphate-dependent enzyme phosphatidylserine decarboxylase (EC 4.1.1.65) [35]. Like this latter, the majority of the enzymes of phospholipid biosynthesis act in close vicinity to or are integral components of the cytoplasmic membrane [9].

PCs can be obtained from PEs by threefold *S*-adenosyl-L-methionine (SAM)-assisted methylation [33, 39-47] representing a very important reaction in human metabolism [9]. It is catalyzed by the enzymes phosphatidylethanolamine *N*-methyltransferase (EC 2.1.1.17) [43, 48], yielding phosphatidyl-*N*-monomethylethanolamine, and by phosphatidyl-*N*-methylethanolamine *N*-methyltransferase (EC 2.1.1.71) [43, 48] yielding phosphatidyl-*N*,*N*-dimethylethanolamine in a first reaction step and PC in a second reaction step [43, 47, 48].

An alternative formation of PCs is represented by the Kennedy pathways [6, 7, 23, 39, 49] combining DAG from phospholipid metabolism and CDP-choline with diacylglycerol cholinephosphotransferase (EC 2.7.8.2) catalyzing this reaction [7, 50-55]. CDP-choline emerges after adenosine 5'-triphosphate (ATP)-dependent and choline kinase (EC 2.7.1.32)-catalyzed phosphorylation of free choline [7, 55, 56] followed by reaction with CTP [9, 41] catalyzed by choline phosphate cytidylyltransferase (EC 2.7.7.15) [7, 23, 49, 53-55, 57]. Analogously, the Kennedy pathway starting from free ethanolamine yields PE [39, 49] which might be methylated to PC as aforementioned [9, 43, 48]. These reactions take place both in the nucleus and at the cytosolic membrane bilayer leaflet [9, 57]. Patients with genetic defects of choline phosphate cytidylyltransferase, representing the rate-determining enzyme of the Kennedy pathways [7, 55], show pronounced symptoms such as severe nonalcoholic fatty liver disease, very low levels of high density lipoprotein (HDL) cholesterol, lipodystrophy, severe insulin resistance and diabetes [7].

Additionally, PS can be reconstituted from PE with serine directly replacing ethanolamine *via* catalysis by L-serine:phosphatidylethanolamine phosphatidyl-transferase (phosphatidylserine synthase 2; EC 2.7.8.29) [9, 58, 59]. As PS can be decarboxylated to PE again, this mechanism offers the possibility of catalyzing the degradation of serine to ethanolamine [9]. On the analogy of phosphatidyl-serine synthase 2 the enzyme L-serine:phosphatidylcholine phosphatidyltransferase (phosphatidylserine synthase 1) is also existing catalyzing the replacement of choline in PC by serine with formation of PS [58, 59].

Both pathways of PC biosynthesis, the CDP-DAG pathway with methylation of PE on the one hand and the Kennedy pathway *via* CDP-choline and DAG on the other hand, are illustrated in **Figure 2** with the relevance of these two pathways varying dependent

on the organism [57]: Whereas PCs are exclusively yielded by methylation of PEs in bacteria [47, 57], the yeast *Saccharomyces cerevisiae* is able to switch between both pathways [6, 57, 60]. Disturbance of the CDP-DAG pathway from PA by disruption of the enzymes PS synthase and PS decarboxylase in *Candida albicans* showed no obvious effects on the levels of PCs and PEs, but on the levels of other lipids such as phosphatidylglycerols (PG), PAs, PIs and PSs, as the alternative Kennedy pathways for PC and PE formation may compensate these disruptions [39]. In higher plants and animals, PCs are predominantly synthesized *via* CDP-choline and the Kennedy pathways [55, 61], but significant amounts of PCs are also obtained in the liver by methylation of PEs [55, 57] with this PE methyl transferase pathway apparently being restricted to liver cells [23, 55, 62]. In fact, methylation of ethanolamine phosphate and PE has also been detected in other tissues than liver but to a much lower extent and thus appearing quantitatively insignificant [63-65].

Investigations by DeLong and colleagues suggest that 70 % of hepatic PC biosynthesis results from the Kennedy pathway and the remaining 30 % from the CDP-DAG pathway and sequential methylation of PE [55]. While the exact contributions of the CDP-DAG pathway and the Kennedy pathway to PC and PE biosynthesis are not conclusively clarified [6], the absence of ethanolamine or choline in growth medium was shown to favor the CDP-DAG pathway [6] and high cellular levels of CTP were shown to favor the CDP-choline Kennedy pathway by a factor of two [6] pointing to a dynamic interplay of both pathways.

Choline can be produced in human body but as the bioavailabilities of the nutritionally ingested methionine and folate, needed for biosynthesis, usually are too low to meet the respective requirements, choline represents a (conditionally) essential dietary constituent [62, 64] forming part of PCs, lysophosphatidylcholines (LPCs), plasmalogens, sphingomyelins and the neurotransmitter acetylcholine [9].

1.1.2 Formation of lysophosphatidylcholines

As illustrated in **Figure 1** (in the middle), PCs are biochemically modified by site-specific phospholipases [10, 66, 67]: Hydrolytic removal of the acyl group at *sn*-1 occurs by phospholipase A_1 (PLA_1; phosphatidylcholine 1-acylhydrolase; EC 3.1.1.32) and yields a 2-monoacyl-*sn*-glycero-3-phosphocholine [66, 68-71], whereas phospholipase C (PLC; phosphatidylcholine cholinephosphohydrolase; EC 3.1.4.3)

hydrolytically eliminates choline phosphate at *sn*-3 with formation of 1,2-diacyl-*sn*-glycerol (DAG) [66, 72-76] and phospholipase D (PLD; phosphatidylcholine phosphatidohydrolase; EC 3.1.4.4) produces a PA (1,2-diacyl-*sn*-glycerol 3-phosphate) by enzymatic dissociation of choline [5, 10, 64, 66, 77].

Lysophosphatidylcholines (LPC; 1-acyl-*sn*-glycero-3-phosphocholine) are produced from PCs by phospholipase A_2 (PLA_2; phosphatidylcholine 2-acylhydrolase; EC 3.1.1.4) which removes the fatty acid at *sn*-2 resulting in the structural formula shown in **Figure 1** (on the right side) [10, 14, 23, 66, 67, 70, 78-83]. Pharmacological inhibition of PLA_2 by bromoenol lactone (BEL) or palmitoyl trifluoromethyl ketone ($PACOCF_3$) prevents PLA_2-dependent hydrolysis of PC and thus formation of LPC [67, 79]. Alternative pathways for LPC production from PC have been reported for lecithin:cholesterol acyltransferase (LCAT; phosphatidylcholine:sterol *O*-acyltransferase; EC 2.3.1.43) [84, 85] catalyzing the apolipoprotein A-I-dependent esterification of HDL cholesterol with acyl groups from *sn*-2 of PCs [85, 86] or for reactive oxygen species (ROS) [87-89]. The retransfer of the acyl group is catalyzed by lysolecithin acyltransferase (LLAT; lysophosphatidylcholine acyltransferase or 1-acyl-*sn*-glycero-3-phosphocholine *O*-acyltransferase; EC 2.3.1.23) (see **Figure 3**) [11, 15, 23] preferring unsaturated acyl-CoA derivatives and possibly enabling the incorporation of long-chain and polyunsaturated acyl groups into PCs by this Lands cycle [2, 11, 15].

As the phosphodiester group, choline and glycerol are defined decidedly, LPC species exclusively differ in regard to the length and the degree of unsaturation of the acyl group predominantly bound at *sn*-1. Therefore, LPC species are particularized by an affix indicating the length and the degree of unsaturation of the acyl group [1]. Notably, Croset *et al.* reported in 2000 a biochemical equilibrium for the actual positioning of the acyl group at *sn*-1 or *sn*-2 in LPCs with a rapid isomerization of 20 % of 1-lyso-2-[^{14}C]C18:2(*n*-6)-*sn*-glycero-3-phosphocholine (GPC) to 1-[^{14}C]C18:2(*n*-6)-2-lyso-GPC taking place in plasma within 2 minutes [3]. Additionally, approximately 50 % of polyunsaturated fatty acyl groups were found to be located at the *sn*-2 position in LPCs [3]. These findings are in accordance with the observations that unsaturated fatty acyl groups are predominantly bound at the *sn*-2 position in PCs [5, 10-15, 90] and that polyunsaturated fatty acids like ARA (C20:4) seem to be incorporated at the *sn*-2 position *via* the Lands deacylation-reacylation cycle catalyzed by PLA_2 and LLAT [2,

11, 15] as mentioned above. Recently, acyl migration from *sn*-2 to *sn*-1 was shown to depend on the length and the degree of unsaturation of the acyl group exemplified by increasing acyl migration rates for LPC C22:6, LPC C20:4, LPC C18:1 and LPC C16:0 with the isomerization rate being 2- to 5-fold higher for LPC C16:0 than for LPC C22:6 [90]. Storage for 4 weeks at – 20 °C in an organic solvent resulted in 10 % acyl migration for *sn*-2 LPC C22:6 but 55 % acyl migration for *sn*-2 LPC C16:0 [90].

The degradation of LPCs occurs both *via* hydrolysis of the *sn*-1 fatty acyl group by PLA_1 (EC 3.1.1.32) or rather by lysophospholipase A_1 ($LPLA_1$; lysophosphatidylcholine acylhydrolase or phospholipase B; EC 3.1.1.5) [91-95] to form *sn*-glycero-3-phosphocholine (GPC) and *via* hydrolysis of choline by lysophospholipase D (LPLD; *e.g.* autotaxin) [83, 96] to form 1-acyl-*sn*-glycerol 3-phosphate (lysophosphatidic acid; LPA). The subsequent conversion of LPA by $LPLA_1$ [91] or of GPC by glycerophosphocholine phosphodiesterase (GPCPD; glycerophosphocholine glycerophosphohydrolase; EC 3.1.4.2) [76, 97, 98] both yield *sn*-glycerol 3-phosphate (G3P) which might be oxidized to glyceraldehyde 3-phosphate (GA3P) representing a central metabolite of glycolysis and thus of energy metabolism. The enzymatic activity of PLA_1 for hydrolysis of LPCs with formation of GPC was reported to reach only 2 % to 5 % of the enzymatic activity for hydrolysis of PCs [68]. LPCs in the outer membrane leaflet are completely degraded by lysophospholipase *in vitro* [99-102] but those in the inner leaflet are not [100-102].

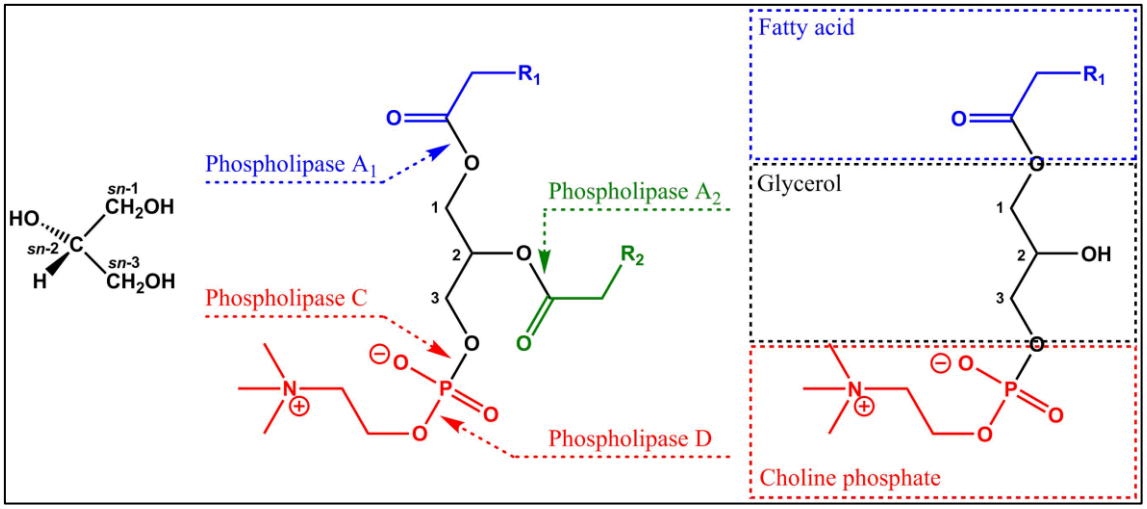

Figure 1: Stereochemical presentation and numbering (*sn*) of glycerol (on the left), site-specific points of action of phospholipases at glycerophospholipids (in the middle) and detailed illustration of the components of lysophosphatidylcholines (on the right). Sources: [10, 66].

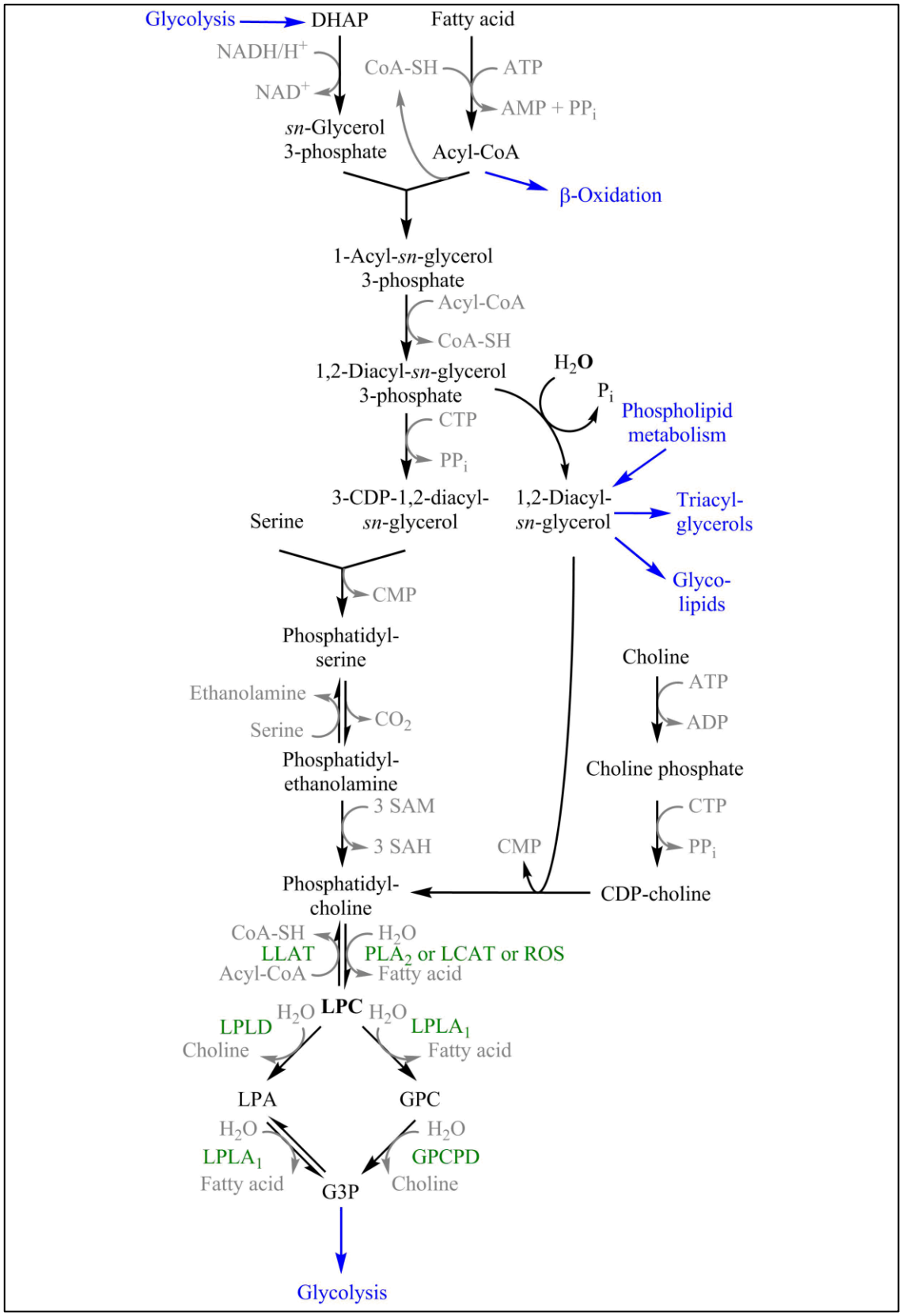

Figure 2: *De novo* biosynthesis of lysophosphatidylcholines (LPC).
Please refer to text and the List of Abbreviations for clarification of designations.

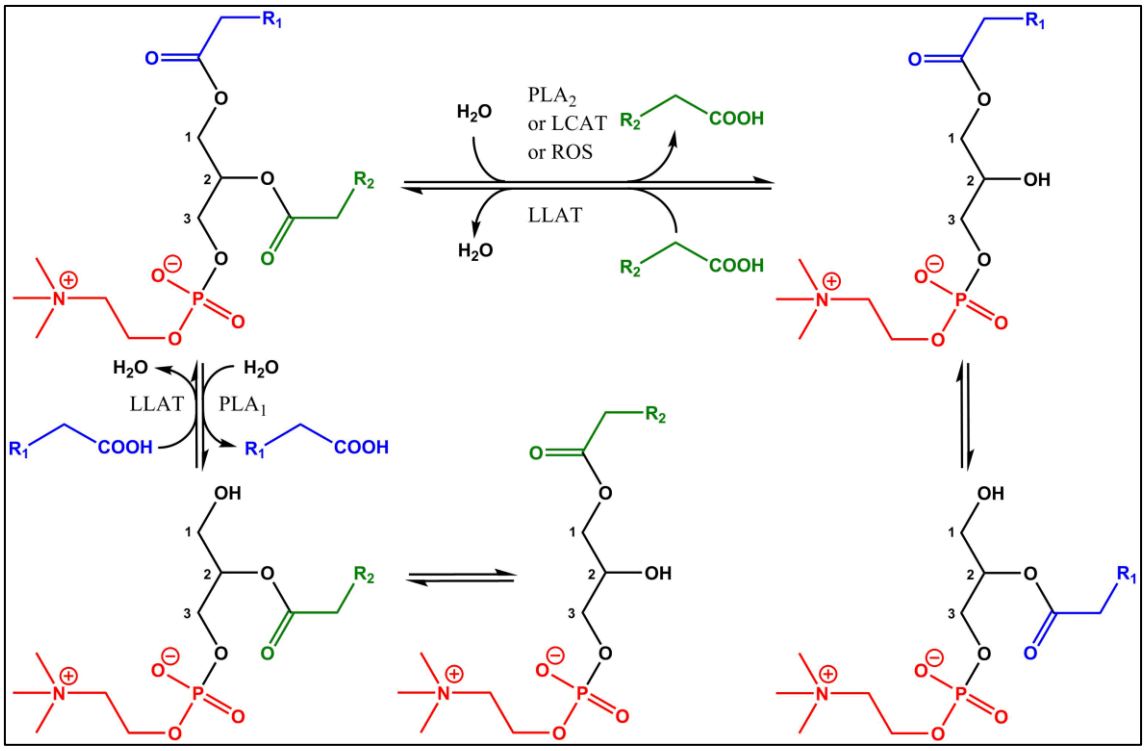

Figure 3: Formation of lysophosphatidylcholines (LPC) from phosphatidylcholines by phospholipase A_2 (PLA_2), lecithin:cholesterol acyltransferase (LCAT), reactive oxygen species (ROS) or phospholipase A_1 (PLA_1) and biochemical reversal of this process by lysolecithin acyltransferase (LLAT). An equilibrium has been reported in solution for the actual positioning of the acyl group at *sn*-1 or *sn*-2 in LPCs.
Sources: [3, 10, 11, 14, 15, 23, 67, 70, 78-85, 87-89].

1.1.3 Transport of lysophosphatidylcholines in the circulation

Multifarious forms of the transport of LPCs in blood are described: Associations between low density lipoprotein (LDL) and various LPC species (LPC C14:0, LPC C15:0, LPC C16:0, LPC C17:0, LPC C17:1, LPC C18:0, LPC C20:0, LPC C20:1, LPC C22:0, LPC C22:1, LPC C22:5 and LPC C24:0) were reported by Heilbronn *et al.* [84] and Sakai *et al.* found the LPC content of oxidized LDL particles (644 nmol/mg ± 53 nmol/mg) to be approximately 29 times greater than that of nonoxidized LDL particles (22 nmol/mg ± 10 nmol/mg protein) [78]. However, neither Wallace *et al.* [103] nor Barber *et al.* [104] found any associations of lipoproteins with any plasma LPC species in their human cohorts. Alternatively, as long ago as 1982, Buckley *et al.* already interpreted the stimulating effect of albumin on LCAT activity *in vitro* as consequence of the complexing of the LPC product by albumin [85] and reports by Schmitz [105], Croset [3], Kim [106] and Ojala [107] also support the hypothesis that LPCs predominantly circulate bound to albumin [108], although incorporation into

LDL particles [84, 108] and HDL particles [108, 109] as well as binding to alpha-1 acid glycoprotein [107] also seem to occur.

LPCs bound to lipoproteins or albumin have been suggested as transport mode for PUFAs with the ARA (C20:4) concentration from LPCs in plasma exceeding that from nonesterified fatty acids (NEFA) bound to albumin by a factor of two in humans [3].

1.1.4 Signal transduction of lysophosphatidylcholines

Han *et al.* observed in cultured L6 myotubes that pertussis toxin inhibiting the $G\alpha_i$ protein [110, 111] reversed the LPC-mediated pathobiochemical effects like insulin resistance emerging after palmitate supplementation [67]. Thus it seems that LPC signal transduction occurs at least in part *via* $G\alpha_i$ protein-coupled receptors ($G_{(}\alpha_{i)}$PCR). Further $G\alpha_i$-driven LPC signaling involves phosphorylation of c-Jun *N*-terminal kinase (JNK) [67, 80] phosphorylating insulin receptor substrate 1 (IRS-1) at Ser307 [67] as illustrated in **Figure 4**. Notably, JNK phosphorylation is also observed in obesity-induced insulin resistance [112, 113] with JNK representing a member of the mitogen-activated protein kinase (MAPK) family and activating activator protein 1 (AP-1) [80]. Congruously, exogenous LPC promoted AP-1 binding to deoxyribonucleic acid (DNA) and transcriptional activity independently from AP-1 activators like protein kinase C (PKC) or other MAPK family members like ERK1 or ERK2 [80].

LPCs have also been reported as ligands of the G protein-coupled receptor (GPCR) GPR4 [111] and of the immunoregulatory lymphocyte-expressed GPCR G2A whose genetic ablation is associated with autoimmunity [110] but both publications were withdrawn because they couldn't be reproduced.

In contrast to the aforementioned pathobiochemical effects of LPCs *via* $G\alpha_i$PCR signaling in L6 myotubes [67] involving JNK phosphorylation, which is also observed in obesity-induced insulin resistance [112, 113], both uptake of glucose in cultured adipocytes by means of an insulin-independent mechanism [114] and glucose-mediated insulin secretion from pancreatic beta-cells are promoted by LPCs [115]. According to these latter findings blood glucose concentration in diabetic mice is reduced by LPCs [114] attributing biochemical relevance to LPCs in insulin-dependent and -independent glucose homeostasis [103, 104, 114]. Furthermore, LPCs function as important signaling molecules influencing crucial cellular processes such as proliferation, tumor cell invasion and inflammation [78, 80, 103, 104, 116-119].

LPCs also represent a major phospholipid component of oxidized LDL particles [78] and may be in part responsible for some of the biochemical effects of the oxidized LDL particles. These oxidized LDL particles increase the proliferation of murine resident peritoneal macrophages by a factor of two [78, 120, 121], enhance the proliferation of human monocyte-derived macrophages [122], induce chemoattraction of monocytes [123, 124], deteriorate the endothelium-dependent arterial relaxation [125] and cytotoxically damage endothelial cells [126].

Oxidized LDL particles were shown to induce inositol trisphosphate (IP_3) accumulation in both human smooth muscle cells [127] and murine macrophages [128] with elevated intracellular Ca^{2+} levels being fittingly found in the latter [128]. Thus, various oxidized LDL-induced signal transductions seem to involve G_q protein-coupled receptors and PKC. In line with this, the dose-dependent stimulation of glucose uptake into cultured adipocytes by LPCs is associated with activation of protein kinase C δ (PKCδ) [114].

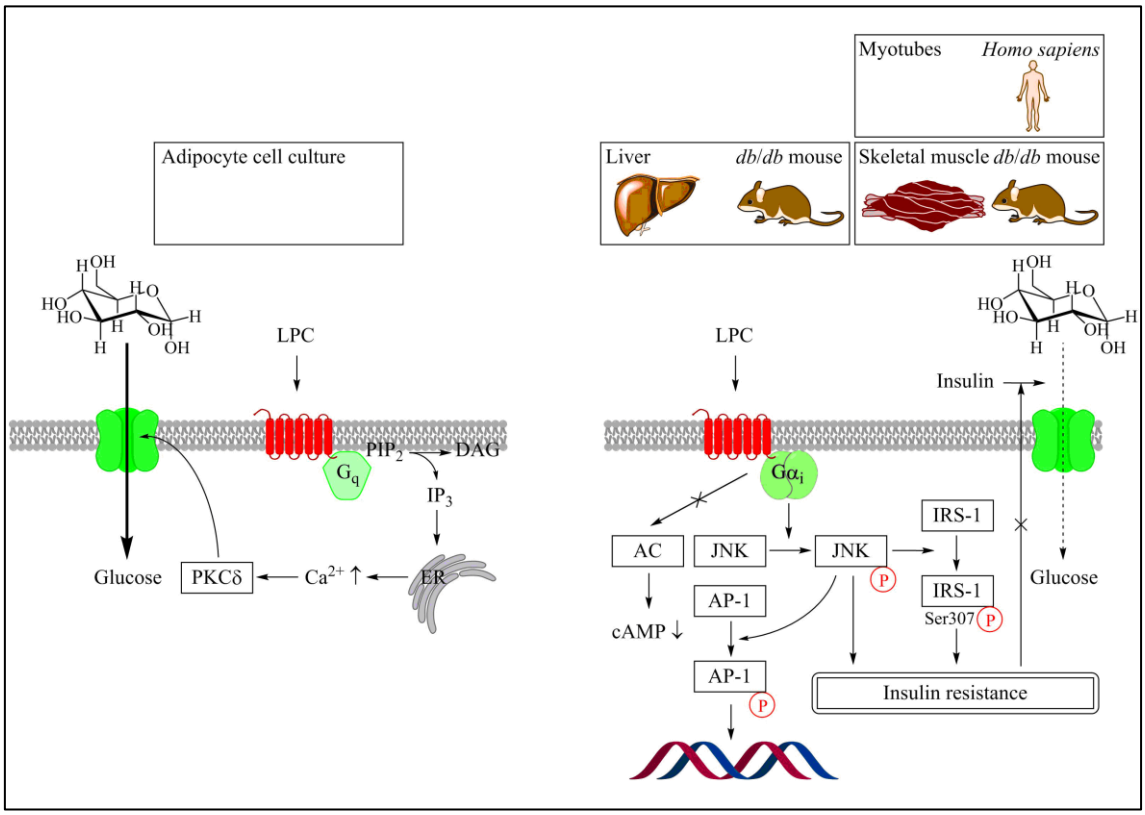

Figure 4: LPC signaling in cultured adipocytes and myotubes as well as liver and skeletal muscle of mice. Abbreviations: AC, adenylate cyclase; AP-1, activator protein 1; DAG, 1,2-diacyl-*sn*-glycerol; ER, endoplasmic reticulum; IP_3, inositol trisphosphate; IRS-1, insulin receptor substrate 1; JNK, c-Jun *N*-terminal kinase; LPC, lysophosphatidylcholine; PIP_2, phosphatidylinositol bisphosphate; PKCδ, protein kinase C δ.

1.1.5 Transmembrane import and export of lysophosphatidylcholines

Another important consideration concerns the biochemical mechanisms enabling LPC molecules to cross the cytoplasmic membrane either to be incorporated into cells or to be released from them. Noncatalyzed transbilayer transport of PCs [129] or LPCs [130] in PC vesicles takes an enormously long time with half-times of days and migration of [*N*-$^{13}CH_3$]dioleoyl PC from the outer to the inner monolayer of dimyristoyl PC vesicles showed a half-time of about 12 hours [129]. Less than 2 % of the applied [*N*-$^{13}CH_3$]LPC C16:0 was monitored after 40 hours in the inner monolayer of dioleoyl PC vesicles [130] suggesting an enormously slow transport [100, 130] whose half-time was assessed as approximately 100 hours at 37 °C [100]. However, equilibration between the two membrane leaflets of sarcoplasmic reticulum membranes after administration of [*N*-$^{13}CH_3$]-labeled LPC C16:0 occurred *in vitro* within 30 minutes at 20 °C with 42 % of [*N*-$^{13}CH_3$]LPCs incorporated into the inner leaflet [101] but the majority incorporated into the outer leaflet [130].

Exogenous [*N*-$^{13}CH_3$]LPC C16:0 was integrated into the outer monolayer of glycophorin-containing dioleoyl PC vesicles partially migrating afterwards to the inner monolayer with a half-time of approximately 1.5 hours at 4 °C and the half-time of the complete LPC transbilayer transport was assessed as approximately 1 hour at 37 °C [99] indicating a promoted transport of phospholipids by glycophorin [131]. In murine macrophages, about 10 % of [^{14}C]LPCs from [^{14}C]LPC-labeled oxidized LDL particles were intracellularly incorporated after 10 hours from whom approximately 50 % were shown to be internalized as major phospholipid component of oxidized LDLs by their endocytosis *via* macrophage scavenger receptors (MSR) with oxidized LDL-induced macrophage proliferation decreasing in MSR knockout mice [78]. As oxidized LDL particles bind to a variety of other receptors such as Fc receptor, CD 36 and SR-BI [78, 132-141] and LPCs represent a major component of oxidized LDL, their endocytosis may also offer a pathway for LPC internalization in other cells and tissues. Furthermore, nonspecific LPC transfer accounted for uptake of the other half of [^{14}C]LPCs with membrane entrainment *via* aqueous diffusion or lipid exchange reaction [78] potentially followed by flip-flop transfer to the inner leaflet of the plasma cell membrane [99, 101, 129]. Incorporation of PCs into the outer membrane layer is catalyzed by PC exchange proteins [129, 142]. By flip-flop mechanism, phospholipids

such as PCs or LPCs can switch between the outer and inner membrane layer [8, 99, 101, 129] or pass the bilayer by this means [4, 8, 99, 129]. This process lasts many seconds and thus occurs very slowly in comparison to the lateral diffusion of phospholipids (exchange frequency about 10^7 per second), but increase of intracellular Ca^{2+} concentration activates the enzyme scramblase which substantially accelerates this procedure [4] and lipid peroxidation was also described to facilitate this flip-flop mechanism of phospholipids [8, 142].

1.1.6 Relevance of lysophosphatidylcholines in physiologic processes

The term "lysophosphatidylcholines" refers to their remarkably detergent property potentially inducing lysis of cells [1, 4, 93]. The cytolytic toxicity of some snake venoms is due to LPC-producing phospholipases exemplified by phospholipase A from cobra venom [1, 4].

As PCs are the most abundant phospholipids in humans [4, 7] with ARA (C20:4) usually being bound at *sn*-2 of glycerol, phospholipase A_2-dependent hydrolysis of PCs to LPCs represents an important source of arachidonate which functions as precursor molecule in the biosynthesis of eicosanoids like prostaglandins [66]. Phospholipase A_2 activity may be influenced by G_q proteins specifically inducing the conversion of PI into DAG and inositol phosphate derivatives such as IP_3 [66].

Additionally, as stated above, LPCs bound to lipoproteins or albumin might function as transport mechanism for PUFAs supplying tissues and organs which require a lot of them such as the brain [3].

Furthermore, small amounts of LPCs (as well as of DAGs) in the presence of Ca^{2+} promote the formation of an inverted hexagonal H_{II} phase of phospholipids instead of bilayer organization [4] although Barsukov *et al.* reported that LPC (up to a proportion of 15 %) did neither affect the bilayer structure of vesicles nor promote flip-flop migration of phospholipids [8].

A plethora of additional physiologic functions arises from biochemical LPC metabolization like hydrolytic removal of choline by LPLD [83, 96] with formation of LPA which is released by activated platelets as signaling molecule into the blood [1, 9].

1.1.7 Relevance of lysophosphatidylcholines in pathophysiologic processes

The plasma lipidome is influenced by a variety of genetic, physiologic, pathophysiologic and nutritional parameters [84, 103, 104, 143]. Whereas various PC species (and PE species) significantly differed between genders in a study by Wallace *et al.* [103], LPCs did not. However, studying a markedly larger cohort (1076 subjects *vs.* 39 subjects), 20 out of 21 LPC species were found to be increased in males relative to females [144]: LPC C14:0, LPC C15:0, LPC C16:0, LPC C16:1, LPC C17:0, LPC C17:1, LPC C18:0, LPC C18:1, LPC C18:2, LPC C18:3, LPC C20:0, LPC C20:1, LPC C20:2, LPC C20:3, LPC C20:4, LPC C20:5, LPC C22:0, LPC C22:1, LPC C22:6 and LPC C24:0. Similarly, significant relationships between LPCs and age were observed (positive associations with LPC C15:0, LPC C17:0, LPC C18:0, LPC C20:0, LPC C20:1, LPC C20:2, LPC C22:0, LPC C22:1, LPC C24:0 and LPC C26:0 plus a negative association with LPC C18:2) when many subjects were involved [144] but lacked in small cohorts [84, 103]. Neither did blood glucose concentration [104], NEFAs [84, 104], TGs [84, 104], HDL cholesterol levels [84, 104] nor total cholesterol levels [84, 104] influence circulating LPC concentrations.

Whereas Heilbronn *et al.* found significant positive correlations of LDL cholesterol levels with LPC C14:0, LPC C15:0, LPC C16:0, LPC C17:0, LPC C17:1, LPC C18:0, LPC C20:0, LPC C20:1, LPC C22:0, LPC C22:1, LPC C22:5 and LPC C24:0 [84], both Wallace *et al.* and Barber *et al.* did not observe any association of LPCs with plasma lipoproteins (in contrast to specific PC or PE species) [103, 104]. That is one reason why it is assumed that LPC transport in the human body predominantly occurs by binding to albumin [3, 103, 105].

Moreover, smokers showed increased levels of LPC C16:1 and decreased levels of LPC C15:0 in comparison with nonsmokers [144].

1.1.7.1 Obesity and insulin resistance

The plasma lipidome is associated with obesity [104] and insulin resistance [104, 145-149] and plasma profiles of both total LPCs [104, 144] and individual LPC species [84, 103, 104, 144] are altered by body mass index (BMI = weight [kg]/height² [m²]). Significant negative associations of BMI were reported with total LPCs [104, 144] as well as with LPC C15:0 [104, 144], LPC C16:0 [103, 144], LPC C18:0 [103, 104, 144], LPC C18:1 [103, 104, 144], LPC C18:2 [103, 104, 144], LPC C18:3 [144], LPC C20:0

[104, 144], LPC C20:1 [104, 144], LPC C20:2 [104, 144], LPC C20:4 [103, 104, 144], LPC C22:0 [144], LPC C22:1 [144], LPC C22:6 [144], LPC C24:0 [144] and LPC C26:0 [144] but not with LPC C14:0 [104, 144], LPC C16:1 [104, 144], LPC C20:3 [104, 144] and LPC C20:5 [104, 144]. Moreover, Barber *et al.* measured in obese relative to lean subjects significant lower concentrations of total LPCs as well as of LPC C15:0, LPC C18:0, LPC C18:1, LPC C18:2 and LPC C20:4 plus similar trends for LPC C20:0 and LPC C20:1 [104]. Furthermore, alterations of BMI (ΔBMI) in 28-day overfed human subjects negatively associated with alterations of LPC C17:0, LPC C22:1 and LPC C22:6 [84].

However, the comparison of monozygotic twins with differing weights showed increased LPC concentrations in the obese siblings with only ether phospholipids decreasing with obesity [150].

Reduced LPC levels in the circulation are found in pathophysiologic circumstances like overfeeding [84, 104], obesity [103, 104, 144, 149, 151], nonalcoholic steatohepatitis [152], impaired glucose tolerance [153], insulin resistance in combination with nonalcoholic fatty liver [154] and type 2 diabetes mellitus [104, 155]. The relevance of decreased LPC levels in pathobiochemical processes is also underlined by negative associations of LPC species with insulin resistance quantified by homeostatic model assessment of insulin resistance (HOMA-IR) [103] in both human individuals (LPC C18:1, LPC C18:2 [103] and LPC C22:6 [84]) and mice (LPC C15:0, LPC C16:1, LPC 20:0 and LPC C20:1) [104]. In a human cohort, LPC C18:1 not only showed a strong negative association with HOMA-IR score but also represented the most significant predictor of HOMA-IR score in this study [103] pointing to a potential relevance in development of insulin resistance [103]. Furthermore, a negative correlation between HOMA-IR score and LPC C22:6 plus a positive correlation between glucose infusion rate (GIR) and LPC C22:6 were reported in humans with LPC C22:6 being the only one out of 333 detected lipid species negatively correlating with HOMA-IR score [84]. In the human cohort, Barber *et al.* found negative correlations between LPC C18:1, LPC C18:2, LPC C20:0, LPC C20:1, LPC C20:2 and LPC C22:6 and plasma insulin levels but not any association between LPC species and HOMA-IR score, whereas plasma lipidome profiling of mice fed for 12 weeks with a

high-fat diet revealed significant negative associations of LPC C16:1, LPC C20:0 and LPC C20:1 with HOMA-IR score [104].

Diabetic subjects show significantly reduced concentrations of both total LPCs and specific LPC species such as LPC C18:0, LPC C18:2, LPC C20:0, LPC C20:1, LPC C20:2 and LPC C20:4 in comparison to lean nondiabetic subjects [104]. Nevertheless, LPC concentrations were not reduced in relation to obese nondiabetic individuals [104] pointing to the possibility that obesity as confounder is the real reason for decreased LPC concentrations rather than diabetes. The identification of lipid species specifically associated with type 2 diabetes mellitus, but not with obesity, would be very valuable for early detection of an emerging diabetic state in obese individuals as well as for elucidation of the pathobiochemical mechanisms promoting the progression from obesity to insulin resistance and diabetes [104].

Because of the concomitance of decreased LPC levels, increased fat mass, impaired glucose tolerance and hyperinsulinemia in high-fat-fed mice, Barber *et al.* could not clarify whether diet, obesity or insulin resistance mainly caused the reduction of LPC levels [104]. But as regression analyses revealed major contribution predominantly from high-fat diet but also from adiposity (as percentage of body fat, PBF), these parameters appear more influential than insulin resistance *per se* [104].

In contrast to LPCs, concentrations of plasma NEFAs, DAGs and TGs are increased in obesity and type 2 diabetes mellitus [84, 104, 146-149] with particularly distinct alterations of saturated DAG and TG species (3.5 - 5.5-fold increase) [104, 149]. Notably, intravenously injected NEFAs induce insulin resistance in humans [156]. Saturated TGs are reduced in plasma by fasting-driven weight loss negatively correlating with insulin sensitivity [157]. Accordingly, the 12-week high-fat diet in C57Bl/6J mice led to increasing DAG and TG levels in plasma but to decreasing levels of most LPC species with the most distinct reduction of plasma LPCs within the first week coinciding with increasing fat mass, emerging insulin resistance and impairing glucose tolerance determined by intraperitoneal glucose tolerance test (IGTT) [104]. From the LPC profile alterations observed after 12 weeks of high-fat diet, more than 80 % were already existing after the first week [104]. In comparison to these changes in plasma, those in tissues like liver, adipose tissue or skeletal muscle were found to be weak [104]. Whereas LPC C20:0 and LPC C20:1 significantly decreased in liver and

LPC C16:1 and LPC C20:1 significantly decreased in skeletal muscle, an increase of LPC C17:0, LPC C18:0 and LPC C20:3 was observed in adipose tissue [104].
In accordance with these findings from high-fat-fed mice [104] human subjects overfed for 28 days showed significant reductions of 7 out of 22 LPC species [84]. Similarly, these alterations by overfeeding were accompanied by increases of body weight, fat mass (hepatic, abdominal and total), fasting serum insulin, fasting blood glucose and insulin resistance (indicated by elevated HOMA-IR score) but by decreased DAG levels plus unaltered TG and NEFA levels [84].
Nonetheless, weight loss following fasting did not alter LPC levels [157].

Otherwise, contradictory results have been reported by some studies [67, 79, 158-161] such as the detection of an increased intracellular total LPC concentration in the liver and skeletal muscle of diabetic *db/db* mice [67] or increased circulating total LPC levels in diabetic patients [158] or high-fat-fed rats [161]. This elevated LPC concentration in rats fed a 10-week high-fat diet was accompanied by significant augmentations of liver weight, hepatic exponent, serum alanine aminotransferase, serum TGs, serum cholesterol, serum lipoprotein A, serum LDL, serum insulin, insulin resistance index, serum NEFAs, serum secretory phospholipase A_2 ($sPLA_2$), serum leptin, liver TG content, liver cholesterol content, hepatic steatosis and $sPLA_2$ ribonucleic acid (RNA) expression [161]. Additionally, cell culture experiments with L6 myotubes stimulated with palmitate (C16:0), very similar to the present study, even suggested LPCs as mediator of NEFA-induced insulin resistance because pharmacological inhibition of calcium-independent phospholipase A_2 ($iPLA_2$) and thus of LPC production from PC (by $PACOCF_3$ or BEL) antagonized the pathobiochemical effects of palmitate (C16:0) leading to reinvigorated insulin-induced phosphorylation of Akt at Ser473 plus IRS-1 at Tyr612 as well as to attenuated palmitate-induced phosphorylation of JNK and of IRS-1 at Ser307 [67].
Consistently, exogenous LPC impaired insulin-induced Akt phosphorylation at Ser473 *via* PKC-α in rat aortic vascular smooth muscle cells in a dose-dependent manner as well as the insulin-induced tyrosine phosphorylation of IRS-1 suggesting *in vitro* insulin resistance [159]. These findings were verified in L6 myotubes with exogenous LPC also impairing insulin-induced Akt Ser473 and IRS-1 Tyr612 phosphorylation in a dose-dependent manner and enhancing JNK and IRS-1 Ser307 phosphorylation [67].

Moreover, LPC concentrations in both liver and skeletal muscle have been reported to be increased in obese diabetic *db/db* mice in comparison to C57BL/6 mice and reduction of these concentrations by BEL application resulted in an attenuated symptomatology with alleviated insulin resistance and diabetes found in these mice as well as a decreased LPC content plus diminished phosphorylation of JNK and of IRS-1 Ser307 in liver and muscle of these mice [67]. After 1-week BEL administration mice showed reduced nonfasting blood glucose levels and after 4-week administration additional improvements of glucose tolerance (determined by IGTT), HOMA-IR score and serum insulin levels without affecting food intake or weight [67]. Furthermore, similar findings were obtained with L6 myotubes whose intracellular LPC content was elevated by 12-hour stimulation with 600 µM to 1000 µM palmitate but unaltered when iPLA$_2$ inhibitors (PACOCF$_3$ or BEL) or iPLA$_2$β small interfering RNA (siRNA) and/or iPLA$_2$γ siRNA were additionally added and impairment of insulin-dependent 2-deoxyglucose uptake by palmitate was also reversed by PACOCF$_3$ [67].
Accordantly, *iPLA$_2$β*-null mice showed a superior insulin sensitivity than control mice after a high-fat diet [162] and *iPLA$_2$γ* disruption protected against high-fat diet-induced insulin resistance [163, 164]. *Vice versa*, insulin-dependent glucose uptake was significantly reduced by exogenous LPC [67]. Moreover, stimulation of primary human myotubes with 250 µM [$^{13}C_{16}$]palmitate also led to an increased intracellular LPC concentration [160]. Because of these findings reduction of intracellular LPC concentration by PLA$_2$ inhibitors was proposed for therapeutic treatment of obesity-induced insulin resistance [67].

1.1.7.2 Inflammation

LPC species are negatively correlated with important inflammatory markers such as interleukin-8 (IL-8), leptin, C-reactive protein (CRP), tumor necrosis factor-α (TNF-α) and monocyte chemotactic protein 1 (MCP1) [103] with an especially strong association found for LPC C18:1 and LPC C18:2 with leptin and CRP [103]. In another human cohort, this negative correlation with CRP was confirmed for LPC C18:2 and amplified for LPC C22:5 which was not detected in the prementioned study [84]. Revealingly, these inflammatory markers are positively correlated with obesity and insulin resistance [165, 166] with this interrelationship complying well with the aforementioned negative

associations between HOMA-IR score as measure of insulin resistance and various LPC species in mice [104] and humans [84, 103].

However, not only decreasing LPCs have been proposed as link between obesity, inflammation and insulin resistance and thus as mediators of insulin resistance [103], but also increasing LPCs [67, 80].

1.1.7.3 Atherosclerosis

With regard to the macrophage proliferation stimulated by oxidized LDL particles, the presence of LPCs is essential but not sufficient (without modified lipoproteins such as oxidized LDL) [78, 120, 122]. Applied by analogy to the human metabolism, increased macrophage proliferation could promote emergence of macrophage-derived foam cells and thus progression of atherosclerosis [78, 167-169]. LPCs show additional atherogenic effects like the induction of the vascular cell adhesion molecule-1 and the intercellular adhesion molecule-1 in endothelial cells [170], the induction of platelet-derived growth factor and heparin-binding epidermal growth factor-like protein in endothelial cells [171] and the reduction of fibrinolytic activity by increased release of plasminogen activator inhibitor-1 and decreased release of tissue-type plasminogen activator from endothelial cells [172].

1.2 Fatty acids

Fatty acids, the precursors of the acyl group constituents in LPCs, are important acyl group precursors of a great number of other metabolite classes but also exert critical pathobiochemical effects in nonesterified form: Circulating NEFAs, especially saturated entities, have been proposed as potential effector of type 2 diabetes as they play a crucial role in both pathobiochemical preconditions which are insulin resistance [67, 79, 113] and pancreatic β-cell failure [173, 174]. Notably, intravenously injected NEFAs induce insulin resistance in humans [156].

Not all fatty acids can be produced in human metabolism but have to be nutritionally ingested [1]. The precise chemical structure of fatty acids is meaningful as many (patho) biochemical functions differ depending on the length of the fatty acyl chain or on the degree of unsaturation: Pretreatment with palmitic acid (C16:0), the most abundant saturated NEFA *in vivo* [67], impairs insulin signaling and insulin-dependent glucose uptake in L6 myotubes [67] whereas pretreatment with oleic acid (C18:1), the most

abundant unsaturated NEFA *in vivo* [67], does not [67]. Other saturated NEFAs such as myristic acid (C14:0) or stearic acid (C18:0) were also reported to enhance JNK phosphorylation aggravating insulin resistance [113]. Total intracellular concentrations of LPCs and DAGs were increased in cultured L6 myotubes after stimulation with 600 µM palmitic acid (C16:0) but that of TGs was not whereas stimulation with 500 µM oleic acid (C18:1) led to increased intracellular TG content [67].

Already before, Listenberger *et al.* had reported this discrepancy between lipotoxicity-inducing palmitic acid (C16:0) poorly incorporated into TGs and lipotoxicity-preventing oleic acid (C18:1) promoting intracellular TG accumulation [175]. Deductive reasoning, plus the observation that oleic acid (C18:1) also induced lipotoxicity when TG biosynthesis was impaired, led to the hypothesis of unsaturated fatty acids preventing lipotoxicity by promotion of TG biosynthesis which also includes incorporation of saturated fatty acids that would otherwise enter different, potentially proapoptotic, pathways [175].

1.3 The Tübingen Family (TUEF) study

For all experiments skeletal muscle cells of twelve subjects of the Tübingen Family (TUEF) study were used. These twelve individuals were chosen to be young, lean and metabolically healthy.

1.3.1 Inclusion criteria and characteristics of the TUEF study

The Tübingen Family Study includes subjects of Caucasian origin at increased risk for development of type 2 diabetes [176]. The participants of the study came from Southern Germany and were not under antidiabetic medication [177]. Physical examination of the subjects did not reveal any pathologic findings [177], laboratory investigations were within normal range [177]. An oral glucose tolerance test (OGTT) was performed for all participants [177]. The absence of manifest diabetes in OGTT represented a necessary inclusion criterion for this study [177]. The majority of the subjects provided a positive family history of type 2 diabetes [177]. Euglycemic-hyperinsulinemic clamps were applied to a subset of subjects [177].

1.3.2 Determination of anthropometrics, physiologic parameters and metabolic traits of the subjects within the framework of the TUEF study

Testing procedure of the subjects was started at 7:00 a.m. after a 12 hours lasting fasting period overnight [177, 178]. Concentrations of blood glucose, plasma insulin, plasma C-peptide and NEFAs were determined from venous blood samples after 0 minutes (basal), 30 minutes, 60 minutes, 90 minutes and 120 minutes [176] during a 75 g OGTT [177] performed as suggested by the World Health Organization (WHO) [179]. Measurement of blood glucose concentrations was performed by use of a bedside glucose analyzer [176, 177] based on glucose-oxidase methodology [177], measurement of plasma insulin concentrations by microparticle enzyme immunoassay [176, 177] and measurement of plasma C-peptide concentrations by radioimmunoassay [176, 177]. Serum specimens were frozen immediately and stored at –20 °C until further analysis such as measurement of adiponectin concentrations by radioimmunoassay [177] or measurement of NEFA concentrations by enzymatic methodology [177].

Determination of glucose tolerance was performed in accordance to the Expert Committee on the Diagnosis and Classification of Diabetes Mellitus from 1997 [180]. The first phase insulin secretion (1^{st}pIS) was determined from insulin and glucose concentrations during OGTT (**Supplemental Equation 1**) [177, 181, 182]. Insulin sensitivity index (ISI) was also calculated by use of glucose and insulin concentrations from OGTT according to Matsuda and DeFronzo (**Supplemental Equation 2**) [177, 183] and specified as ISI_{OGTT}. Furthermore, insulin sensitivity (specified as ISI_{clamp}) was additionally measured during a euglycemic-hyperinsulinemic clamp [177, 178] which was performed at 7:00 a.m. after a 12 hours lasting overnight fasting period [177, 178]. Application of insulin and glucose was executed *via* a cannulated antecubital vein [177, 178] and collection of arterialized blood specimens was realized *via* a punctured dorsal hand vein of the contralateral arm under heating [177, 178]. Insulin was infused constantly for 2 hours at a flow rate of $1.0\ mU \cdot kg^{-1} \cdot min^{-1}$ under control of blood glucose concentrations every 5 minutes [177, 178]. The maintenance of the respective fasting glucose concentration was achieved by the application of an accordingly adapted glucose solution [177, 178]. ISI_{clamp} for systemic glucose uptake is calculated by the division of the mean GIR during the second hour of the euglycemic-hyperinsulinemic

clamp by the plasma insulin concentration during steady-state phase (**Supplemental Equation 3**) [177, 178].

Energy expenditure (EnExp) and respiratory quotient (RQ) were determined using a DELTATRAC^{TM} Metabolic Monitor [176] both under fasting conditions ($EnExp_{fasting}$ and $RQ_{fasting}$) and during steady-state phase of the euglycemic-hyperinsulinemic clamp ($EnExp_{clamp}$ and RQ_{clamp}) [177]. Bioelectrical impedance measurements were performed for determination of lean body mass (LBM) [176] and PBF [176, 177]. BMI was calculated by division of weight by the square of height [177]. Waist and hip circumferences for calculation of the waist-to-hip ratio (WHR) as a method of estimation for body fat distribution were determined in dorsal position [177]. Maximal aerobic capacity ($V(O_2)_{max}$) was quantified by a continuous, incremental exercise test to voluntary exhaustion on an electromagnetically braked cycle ergometer with a pedaling rate of 60 revolutions per minute (rpm) [178]. Warm-up was conducted for 2 minutes at 0 W before the test was started at an initial power output of 20 W which was increased every minute by stepwise increments of 40 W until exhaustion [178]. A spiroergometer was applied for measurement of oxygen consumption [178]. $V(O_2)_{max}$, an indicator of physical fitness, was also calculated as percentage ($V(O_2)_{perc}$) of the individually predicted peak $V(O_2)$ resulting from the anthropometrics sex, age and BMI of the respective subject [178, 184].

Proton magnetic resonance spectroscopy (^{1}H-MRS) was applied for determination and differentiation of intramyocellular lipid content (IMCL; inside myofibers) and extramyocellular lipid content (EMCL; between the muscle fibers) using a 1.5 Tesla whole-body imager [177, 178, 185]. A single-voxel stimulated echo acquisition mode (STEAM) technique was used for volume selection applying a repetition time (TR) of 2 seconds, an echo time (TE) of 10 milliseconds, 40 acquisitions and a volume of interest of (11 mm · 11 mm · 20 mm =) 2420 mm³ [177, 178]. IMCL and EMCL were quantified on the separation of two resonances in the lipid-CH_2-region [177]. The predominantly nonoxidative, fast-twitching, white *M. tibialis anterior* [178] was chosen as a representative muscle for mixed type I and type II fiber composition [177, 178]. As a muscle predominantly containing type I fibers with high oxidative capacity the slow-twitching, red *M. soleus* was selected [177, 178]. The preciseness of ^{1}H-MRS technique has been described as equal to biochemical or histological methods [186].

All participants gave informed written consent to the study design approved by the ethical committee of the Medical Faculty of the University of Tübingen [177].

1.4 Preceding own experimental work

The work in hand was initiated to investigate the lipid metabolism in cultured primary human myotubes obtained from 12 human subjects who were comprehensively phenotyped anthropometrically, physiologically and clinical-chemically within the framework of the TUEF study. Lipid parameters were studied in relationship to *in vivo* parameters of the donors reflecting insulin sensitivity and muscle lipid metabolism. Since insulin resistance is accompanied by increased NEFA blood levels, we decided to simulate an increased NEFA strain *in vitro* by stimulation with 125 µM [$^{13}C_{16}$]palmitate for 30 minutes, 4 hours or 24 hours choosing primary human myotubes as cell culture model in order to appreciate the central function of skeletal muscles in lipid metabolism and emergence of insulin resistance. The utilization of [$^{13}C_{16}$]palmitate enabled the definite detection and quantification of lipids produced *de novo* after the commencement of the palmitate stimulation incorporating activated derivatives or metabolites of the [^{13}C]-labeled stimulant. Cell lysates and supernatants of the primary human myotubes had already been analyzed by mass spectrometry for the investigation of the production and the release of acylcarnitines (AC) and the results have been published [187]. Additional *in vitro* parameters like expression levels of important genes of lipid metabolism and mitochondrial DNA content were assessed within the framework of these aforegoing experiments. The human donors were divided into two groups depending on their *in vivo* $RQ_{fasting}$ revealing a significantly superior production and release of medium-chain acylcarnitines (mcAC) in the donor group with high $RQ_{fasting}$ [187]. Released [$^{13}C_8$]-labeled *O*-octanoyl-L-carnitine ([$^{13}C_8$]C8-AC) and [$^{13}C_{10}$]-labeled *O*-decanoyl-L-carnitine ([$^{13}C_{10}$]C10-AC), isolated from supernatants, positively correlated with $RQ_{fasting}$ with a lower expression of medium-chain acyl-coenzyme A dehydrogenase (MCAD) in these myotubes blending in well with this association [187]. The results of this precedent work validated *in vitro* metabolomics analyses as appropriate method for decipherment of *in vivo* metabolism in skeletal muscle tissue.

1.5 Aims of the study

In this present study, lipid metabolism in cultured primary human myotubes was studied laying the focus on the lipid class of LPCs as they represent auspicious molecular compounds with a wide range of biochemical and pathobiochemical effects. Many of the functions and observations reported for LPCs are related to overfeeding, obesity, inflammation, insulin resistance and type 2 diabetes mellitus. However, concerning insulin resistance and type 2 diabetes mellitus obvious discrepancies are found in literature reporting both prodiabetogenic and antidiabetogenic effects of LPCs. Pancreas, liver, adipose tissue and skeletal muscles are all considered as relevant in pathogenesis of insulin resistance and type 2 diabetes mellitus with skeletal muscles playing a crucial role in development of insulin resistance. LPC species were analyzed by mass spectrometry in cell lysates and supernatants of the primary human myotubes stimulated with 125 µM [$^{13}C_{16}$]palmitate for 30 minutes, 4 hours or 24 hours

First aim of the study was to investigate the kinetics of LPC production and release which was rendered possible by the three different stimulation periods isolating intracellular LPCs from cell lysates and extracellular LPCs from supernatants for mass spectrometric measurements. Utilization of [$^{13}C_{16}$]palmitate allows differentiation of biosynthetic routes of LPC production and turnover.

Second aim of the study was to use the widespread individual characteristics of the skeletal muscle cells donors, both *in vivo* and *in vitro*, for extensive association analyses with *in vitro* intracellular and extracellular LPCs involving concentrations of both total LPCs and individual LPC species embracing unlabeled and [^{13}C]-labeled entities. Anthropometric as well as physiologic and clinical-chemical parameters reflecting insulin sensitivity and lipid metabolism *in vivo* were used. Moreover, *in vitro* experiments were performed with the primary human myotubes including determination of the individual [^{3}H]palmitate oxidation activities in order to amplify the phenotyping of the subjects biochemically.

With this experimental set-up we aimed to shed light on the specific biochemical function of LPCs in lipid metabolism and in physiologic processes possibly defining *in vivo* differences on a molecular level.

2 Materials and Methods

2.1 Materials

2.1.1 Cell culture media

αMEM Medium	BioWhittaker™ Lonza (1 g/l glucose, without L-glutamine)
Cloning Medium	400 ml αMEM Medium 400 ml Ham's F-12 Medium 200 ml fetal bovine serum (FBS; ≈ 20 %) Chicken extract (supernatant from a resuspension in 10 ml of a 1 : 1 mixture of αMEM Medium and Ham's F-12 Medium after centrifugation for 8 minutes at 3300 rpm and 20 C) 10 ml 10 kU/ml penicillin and 10 kU/ml streptomycin 10 ml 200 mM L-glutamine (2 mmol) 2 ml 250 µg/ml amphotericin B (500 µg)
EMEM Medium	BioWhittaker™ Lonza (1 g/l glucose, without L-glutamine)
Fetal bovine serum (FBS)	Thermo Scientific™ HyClone™ (100 nm sterile filtered)
Fusion Medium	500 ml αMEM Medium 10 ml FBS (≈ 2 %) 5 ml 10 kU/ml penicillin and 10 kU/ml streptomycin 5 ml 200 mM L-glutamine (1 mmol) 1 ml 250 µg/ml amphotericin B (250 µg)
Ham's F-12 Medium	BioWhittaker™ Lonza (1.8 g/l glucose, 146.2 mg/l L-glutamine)
Trial Medium	500 ml Eagle's minimal essential medium (EMEM) 10 ml FBS (≈ 2 %) 5 ml 10 kU/ml penicillin and 10 kU/ml streptomycin 5 ml 200 mM L-glutamine (1 mmol)

2.1.2 Chemicals and biochemicals

Acetonitrile	Merck
AICAR (≥ 98 %)	Sigma-Aldrich®
Amphotericin B	Sigma-Aldrich®
BSA	Sigma-Aldrich®
Buffer AW1	QIAGEN® (AllPrep DNA/RNA Mini Kit)

Buffer AW2	QIAGEN® (AllPrep DNA/RNA Mini Kit)
Buffer EB	QIAGEN® (10 mM TRIS-Cl (pH 8.5), AllPrep DNA/RNA Mini Kit and QIAquick® PCR Purification Kit)
Buffer PB	QIAGEN® (QIAquick® PCR Purification Kit)
Buffer PE	QIAGEN® (QIAquick® PCR Purification Kit)
Buffer RDD	QIAGEN® (RNase-Free DNase Set)
Buffer RLT	QIAGEN® (RNeasy® Mini Kit)
Buffer RLT Plus	QIAGEN® (AllPrep DNA/RNA Mini Kit)
Buffer RPE	QIAGEN® (AllPrep DNA/RNA Mini Kit and RNeasy® Mini Kit)
Buffer RW1	QIAGEN® (AllPrep DNA/RNA Mini Kit and RNeasy® Mini Kit)
L-Carnitine HCl (≥ 98 %)	Sigma-Aldrich®
Chicken extract	Sera Laboratories International
O-Decanoyl-L-carnitine HCl	Metabolic Laboratory, Vrije Universiteit Amsterdam Medical Center (Dr. Herman J. ten Brink)
[D_3]*O*-Decanoyl-L-carnitine HCl	Metabolic Laboratory, Vrije Universiteit Amsterdam Medical Center (Dr. Herman J. ten Brink)
DNase I (RNase-free)	QIAGEN® (RNase-Free DNase Set)
dNTP mix (PCR-grade)	Roche (Transcriptor First Strand cDNA Synthesis Kit)
O-Dodecanoyl-L-carnitine HCl	Metabolic Laboratory, Vrije Universiteit Amsterdam Medical Center (Dr. Herman J. ten Brink)
DPBS	BioWhittaker™ Lonza
Ethanol	Merck EMSURE®
Etomoxir (≥ 98 %)	Sigma-Aldrich® (50 mM in H_2O)
L-Glutamine (200 mM)	BioWhittaker™ Lonza
GW501516	Santa Cruz Biotechnology®
H_2O (PCR-grade)	Roche (Transcriptor First Strand cDNA Synthesis Kit)

H_2O (PCR quality)	QIAGEN® (RNeasy® Mini Kit)
[D_3]Leucine	Sigma-Aldrich® ISOTEC®
LPC C19:0	Avanti® Polar Lipids
Magnesium chloride	Roche
β-Mercaptoethanol (≥ 99 %)	Sigma-Aldrich®
Methanol	Merck EMSURE®
O-Octanoyl-L-carnitine-HCl	Metabolic Laboratory, Vrije Universiteit Amsterdam Medical Center (Dr. Herman J. ten Brink)
[^{3}H]Palmitate	PerkinElmer®
[$^{13}C_{16}$]Palmitate	Sigma-Aldrich® ISOTEC® (> 99 % ^{13}C atoms)
Penicillin-Streptomycin	BioWhittaker™ Lonza (10.000 U/ml penicillin, 10.000 U/ml streptomycin)
Protector RNase Inhibitor	Roche (Transcriptor First Strand cDNA Synthesis Kit)
Random hexamer primers	Roche (Transcriptor First Strand cDNA Synthesis Kit)
Scintillation liquid	PerkinElmer® Ultima Gold™
Transcriptor Reverse Transcriptase	Roche (Transcriptor First Strand cDNA Synthesis Kit)
Transcriptor RT Reaction Buffer	Roche (Transcriptor First Strand cDNA Synthesis Kit)
Trypsin-EDTA	BioWhittaker™ Lonza (120.000 U/l trypsin, 200 mg/l EDTA)

2.1.3 Laboratory equipment

Biological safety cabinet	Heraeus®	HERAsafe® HS 12
Centrifugal vacuum concentrator	CHRiST®	ALPHA RVC cmc-1
Centrifuges	Eppendorf®	Centrifuge 5415 R (4 °C)
	Heraeus®	Biofuge® fresco (refrigerated)
	Heraeus®	Biofuge® pico (nonrefrigerated)
	Heraeus®	Megafuge 2.0R

Condensation trap	CHRiST®	ALPHA 2–4 LDC-1
Electronic hand-held dispenser	Eppendorf®	Research® pro 0.5 µl – 10 µl
	Eppendorf®	Research® pro 5 µl – 100 µl
Electronic pipette controllers	Eppendorf®	Easypet®
	Andwin Scientific	Hirschmann® pipetus®
Electrophoresis system	Pharmacia Biotech	MultiPhor™ II
Hand-held dispenser tips	Eppendorf®	Combitips® plus capacity 1.0 ml
	Eppendorf®	Combitips® plus capacity 5.0 ml
	Eppendorf®	Combitips® capacity 12.5 ml
Heating shaker	Eppendorf®	ThermoMixer® comfort
Incubator	Heraeus®	Function Line BB 16 CU
Liquid scintillation counter	Packard®	Tri-Carb® 2900TR
Manual hand-held dispenser	Eppendorf®	Multipette® plus
Microplate reader	Bio-Rad®	Model 680
Microscope	Carl Zeiss	Axiovert 25
Photometer	Eppendorf®	BioPhotometer® 6131
Pipette filtertips	Eppendorf®	ep Dualfilter T.I.P.S.® 0.1 µl – 10 µl
	Eppendorf®	ep Dualfilter T.I.P.S.® 2 µl – 100 µl
	Eppendorf®	ep Dualfilter T.I.P.S.® 2 µl – 200 µl
Real-time PCR instruments	Roche	LightCycler® 2.0 (carousel-based)
	Roche	LightCycler® 480
Shaker	Scientific Industries	Vortex-Genie® G560-E

Single channel pipettes	Eppendorf®	Research® 0.1 µl – 2.5 µl
	Eppendorf®	Research® 0.5 µl – 10 µl
	Eppendorf®	Research® 10 µl – 100 µl
	Eppendorf®	Research® 100 µl – 1000 µl
Special accuracy weighing machine	Sartorius	MC1 Research RC 210 D
Thermal cycler	Eppendorf®	Mastercycler® gradient
Ultrasonic bath	Elma®	TRANSSONIC T 460 / H
Vacuum exhauster	Edwards™	RV3
Voltage source (gel electrophoresis)	LKB BIOCHROM	2103 Power Supply
Water bath	Julabo®	MB

2.1.4 Laboratory materials

AllPrep DNA spin columns	QIAGEN®	AllPrep DNA/RNA Mini Kit
Aspirating pipettes	Corning® costar®	STRIPETTE® (5 ml)
	Corning® costar®	STRIPETTE® (10 ml)
	Corning® costar®	STRIPETTE® (25 ml)
Collection tubes	QIAGEN®	RNeasy® Mini Kit
Conical tubes	Becton Dickinson™	Falcon® BLUE MAX™ Jr. 15 ml Polypropylene Conical Tube
	Becton Dickinson™	Falcon® BLUE MAX™ 50 ml Polypropylene Conical Tube
Extraction cartridges	Waters™ OASIS®	HLB 1 cc (30 mg sorbent)
Glass cuvette	Eppendorf®	UVette® (220 – 1600 nm)
Gloves	Ansell™	MICRO-TOUCH® HyGrip™ Latex Powder-Free Examination Gloves
	Kimberly-Clark™	KC500 Purple Nitrile™ Powder-Free Exam Gloves

QIAquick® spin columns	QIAGEN®	PCR Purification Kit
Microtiter plate	Greiner bio-one	96-Well Polystyrene Microplate
qPCR capillaries	Roche LightCycler®	Capillaries (20 µl)
Reaction vessels	Eppendorf®	PCR Tubes (0.2 ml)
	Eppendorf®	Safe-Lock Tubes (1.5 ml)
	Eppendorf®	Safe-Lock Tubes (2.0 ml)
RNeasy® spin columns	QIAGEN®	RNeasy® Mini Kit
Tissue culture plates	TPP®	Tissue Culture Plate 92006 (growth surface 8.960 cm²)
Tissue culture dishes	TPP®	Tissue Culture Dish 93100 (growth surface 60.1 cm²)
	TPP®	Tissue Culture Dish 93150 (growth surface 147.8 cm²)

2.1.5 Computer software

ChemBioDraw® Ultra	PerkinElmer®	Version 13.0.2.3021
EndNote®	Thomson Reuters	Version X4.0.2 (Bld 5149)
Excel® 2010	Microsoft®	Version 14.0.7149.5000
JMP®	SAS®	Version 11.2.0 (64-Bit)
LightCycler® software	Roche LightCycler®	Version 3.5
LightCycler® 480 software	Roche LightCycler®	Release 1.5.0
Office Professional Plus 2010	Microsoft®	
Windows® 2000 Professional	Microsoft®	
Windows® 7 Home Premium	Microsoft®	Service Pack 1 (64-Bit)
Word 2010	Microsoft®	Version 14.0.7149.5000

2.1.6 Computer hardware

Hewlett-Packard™	Compaq dc7600 Convertible Minitower
Lenovo®	IdeaPad Z560 M37BMGE W7HP

2.1.7 Kits

BCA protein quantification	Thermo Scientific™	Pierce™ BCA Protein Assay Kit
Bradford protein quant.	Bio-Rad®	Protein Assay
Cell lysate homogenization	QIAGEN®	QIAshredder™
DNA and RNA purification	QIAGEN®	AllPrep DNA/RNA Mini Kit
Duplex PCR	Roche LightCycler®	FastStart DNA Master HybProbe
PCR product purification	QIAGEN®	QIAquick® PCR Purification Kit
Quantitative PCR	Roche LightCycler®	FastStart DNA Master SYBR® Green I Kit
Reverse transcription	Roche	Transcriptor First Strand cDNA Synthesis Kit
RNA purification	QIAGEN®	RNeasy® Mini Kit

2.1.8 Primer pairs for RT-qPCR experiments

The primer sequences as well as the number of base pairs (bp) of the corresponding amplicons are listed in **Table 1** for all primers used in reverse transcriptase (RT) quantitative polymerase chain reaction (RT-qPCR) experiments.

Table 1: Primer sequences and lengths in base pairs (bp) of the respective amplicons plus manufacturers of the primer pairs used in reverse transcriptase quantitative polymerase chain reactions (RT-qPCR).

Gene	Strand	Sequence (5‘ → 3‘)	Amplicon bp number	Manu-facturer
ACTB	Template	GAGCAAGAGAGGCATCCTCA	238 bp	TIB MOLBIOL®
	Complementary	AGCCTGGATAGCAACGTACA		
CPT1B	Template	CTCCTTTCCTTGCTGAGGTC	177 bp	TIB MOLBIOL®
	Complementary	TCTCGCCTGCAATCATGTAG		
PDK4	Template	CATGAAGCAGCTACTGGACT	416 bp	Invitrogen™
	Complementary	GGTTCATCAGCATCCGAGTA		
PPARD	Template	AAGAGGAAGTGGCAGAGGCA	415 bp	Invitrogen™
	Complementary	TGCCACCAGCTTCCTCTTCT		
PPARGC1A	Template	TGTGGAACTCTCTGGAACTG	232 bp	Invitrogen™
	Complementary	TGAGGACTTGCTGAGTTGTG		
UCP3	Template	ATGGACGCCTACAGAACCAT	312 bp	gibco™ BRL®
	Complementary	CTGGGCCACCATCTTTATCA		

The investigated genes were those of β-actin (*ACTB*), carnitine palmitoyltransferase 1β (*CPT1B*), pyruvate dehydrogenase kinase isozyme 4 (*PDK4*), peroxisome proliferator-activated receptor δ (*PPARD*), peroxisome proliferator-activated receptor γ coactivator 1α (*PPARGC1A*) and uncoupling protein 3 (*UCP3*).

2.1.9 Primer pairs and hybridization probes for duplex PCR experiments

The mitochondrially encoded gene of NADH dehydrogenase 1 (*MT-ND1*) as well as the gene of the (genomically encoded) lipoprotein lipase (*LPL*) were analyzed in duplex PCR experiments for quantification of mitochondrial DNA (mtDNA) content (in relation to genomic DNA) using primer pairs, whose sequences, resulting amplicon lengths (in bp numbers) and manufacturer are listed in **Table 2**, as well as hybridization probes, whose sequences are summarized in **Table 3**. The hybridization probes are working in pairs with one probe being linked to fluorescein (FL) at its 3' end and the other probe being linked to a chromophore (LC640 or LC705) at its 5' end and to phosphate (PH) at its 3' hydroxyl group.

Table 2: Primer sequences, base pair (bp) numbers of the respective amplicons and manufacturer of the primer pairs used in duplex PCR experiments for quantification of mitochondrial DNA content in relation to genomic DNA.

Gene	Strand	Sequence (5' → 3')	Amplicon bp number	Manu-facturer
MT-ND1	Template	TCTAGGCTATATACAACTACGCAA	182 bp	TIB MOLBIOL®
	Complementary	GGGTTCATAGTAGAAGAGCGAT		
LPL	Template	GCTGGACCTAACTTTGAGTATG	197 bp	
	Complementary	CGGATAGCTTCTCCAATGTTA		

Table 3: Sequences of hybridization probes applied in duplex PCR experiments for quantification of mitochondrial DNA content in relation to genomic DNA. The hybridization probes were designed as pairs being coupled either with fluorescein (FL) at the 3' end or a chromophoric molecule (LC640 respectively LC705) at the 5' end plus phosphate (PH) at the 3' hydroxyl group.

Amplicon	Strand	Sequence (5' → 3')	Manu-facturer
MT-ND1	Template	CGCCACATCTACCATCACCCTCTACA--FL	TIB MOLBIOL®
		LC640-CACCGCCCCGACCTTAGCTCT--phosphate	
LPL	Complementary	TTCGGGTAAATGTCAACATGCCCA--FL	
		LC705-CTGGTTTCTGGATTCCAATGCTTCG--PH	

2.2 Methods

The positive vote of the ethics commission of the medical faculty of the University of Tübingen concerning this present dissertation is documented under the reference number 179/97.

2.2.1 Cultivation of human muscle cells

For all experiments, human muscle cells from twelve different donors were cultivated. These muscle cells are satellite cells which were obtained from percutaneous needle muscle biopsies of the *M. vastus lateralis* of the *M. quadriceps*. Until their utilization these satellite cells were stored in aliquots in liquid nitrogen. The proliferation of these satellite cells is induced by the additives in the Cloning Medium (chicken extract and fetal bovine serum (FBS)) which is applied for their cultivation. These proliferating muscle cells are termed myoblasts and after having fused they are named myotubes. For the experiments, one aliquot per each donor was distributed among all corresponding tissue culture vessels and cultivated with Cloning Medium until fusion.

The base area of the particular tissue culture plate or dish thereby determined the applied volume of the cell culture medium: For each well of the 6-well plates 2 ml medium were used, for 10 cm dishes 7 ml and for 15 cm dishes 18 ml.

During proliferation phase, Cloning Medium was changed every 2 to 4 days until the myoblasts reached 80 % to 95 % confluency (depending on cell culture vessel and experiment as described in detail below). Subsequently, the differentiation into human myotubes was induced by the cultivation of the myoblasts in Fusion Medium with a lower content of FBS (≈ 2 % FBS in lieu of ≈ 20 % FBS in Cloning Medium).

The cultivation of the muscle cells of the twelve different donors was performed in three batches of four donors each whose muscle cells were cultivated simultaneously in six 15 cm dishes, six 10 cm dishes and four 6-well plates respectively.

The muscle biopsies were resuspended in 11 ml Cloning Medium for cell culture initiation. Concerning the first batch of donors, 500 µl of the particular muscle cell suspension were added to each 15 cm dish (with 18 ml Cloning Medium submitted), 250 µl to each 10 cm dish (with 7 ml Cloning Medium submitted) and 100 µl to each well of the 6-well plates (with 2 ml Cloning Medium submitted). Due to the observation that the confluency pursued for initiation of differentiation into myotubes was reached at obvious later time in 15 cm dishes and 10 cm dishes, the volumes of the muscle cell

suspensions for addition to these dishes were raised to 750 µl for each 15 cm dish and accordingly to 300 µl for each 10 cm dish for the second and the third batch. The added volume of the suspension to each well of the 6-well plates (100 µl) was not changed.

As illustrated in **Figure 5**, the primary human myotubes in the 15 cm dishes were used for the mass spectrometric investigation of the production and release of LPCs after cultivation with [$^{13}C_{16}$]palmitate. The mtDNA content as well as the expressions of important genes of fatty acid metabolism after incubation with L-carnitine (LC), an equimolar mcAC mixture of *O*-octanoyl-L-carnitine (C8-AC), *O*-decanoyl-L-carnitine (C10-AC) and *O*-dodecanoyl-L-carnitine (*O*-lauroyl-L-carnitine; C12-AC) or L-carnitine plus GW501516, a receptor agonist of peroxisome proliferator-activated receptor δ (PPARδ), were determined in the primary human myotubes of the 10 cm dishes. For correlation analyses with LPC concentrations, obtained from the experiments with the 15 cm dishes, the results of the mcAC incubation are not taken into account in this present work, as they do not significantly differ from the results of the LC incubation [187, 188].

The myotubes of the 6-well plates were used for analysis of *PDK4* expression after stimulation with fatty acids (oleic acid (C18:1) and palmitic acid (C16:0); O/P) and/or mcACs in either glucose-free RPMI medium or glucose-containing Eagle's minimal essential medium (EMEM), but as the correlation analyses between the results of these investigations and the determined LPC concentrations are excluded from this present work, this experimental set-up is not shown in **Figure 5**.

The palmitate oxidation activity was determined in primary human myotubes which had been cultured in four 6-well plates per each donor as charted in **Figure 6**. The muscle cells of the twelve donors were divided in the same three batches of four donors each as described above. For cell culture initiation, one muscle biopsy aliquot of the respective donor was resuspended in 7.5 ml Cloning Medium whereof 200 µl were added to each well of the four corresponding 6-well plates with 2 ml Cloning Medium having been submitted before per each well. Out of the five different stimulation modes, solely the results of the stimulation with 100 µM L-carnitine (contr.) as well as the results of the stimulation with 100 µM L-carnitine plus 1 µM GW501516 (GW) are included in this present work in the correlation studies with the mass spectrometrically determined LPC concentrations.

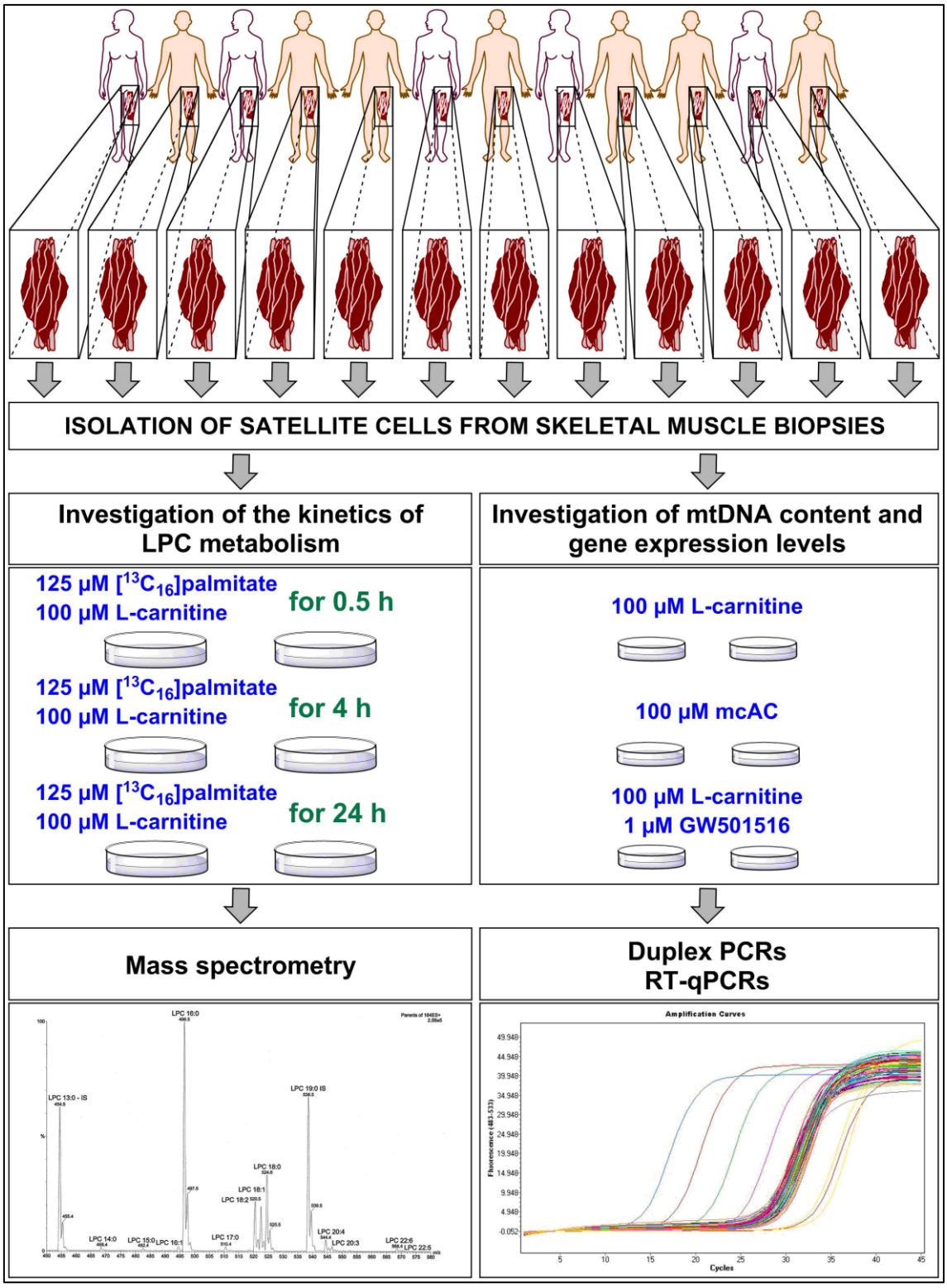

Figure 5: Visualization of the experiments performed with primary human myotubes of 12 different donors distributing the cell suspensions among different cell culture vessels: The myotubes cultivated in 15 cm dishes were used for mass spectrometric quantification of lysophosphatidylcholines (LPC) and the mitochondrial DNA (mtDNA) content as well as various gene expression levels were investigated in myotubes cultivated in 10 cm dishes with the results from the incubation with medium-chain acylcarnitines (mcAC) being unconsidered in this present work. LPC mass spectrogram from [189].

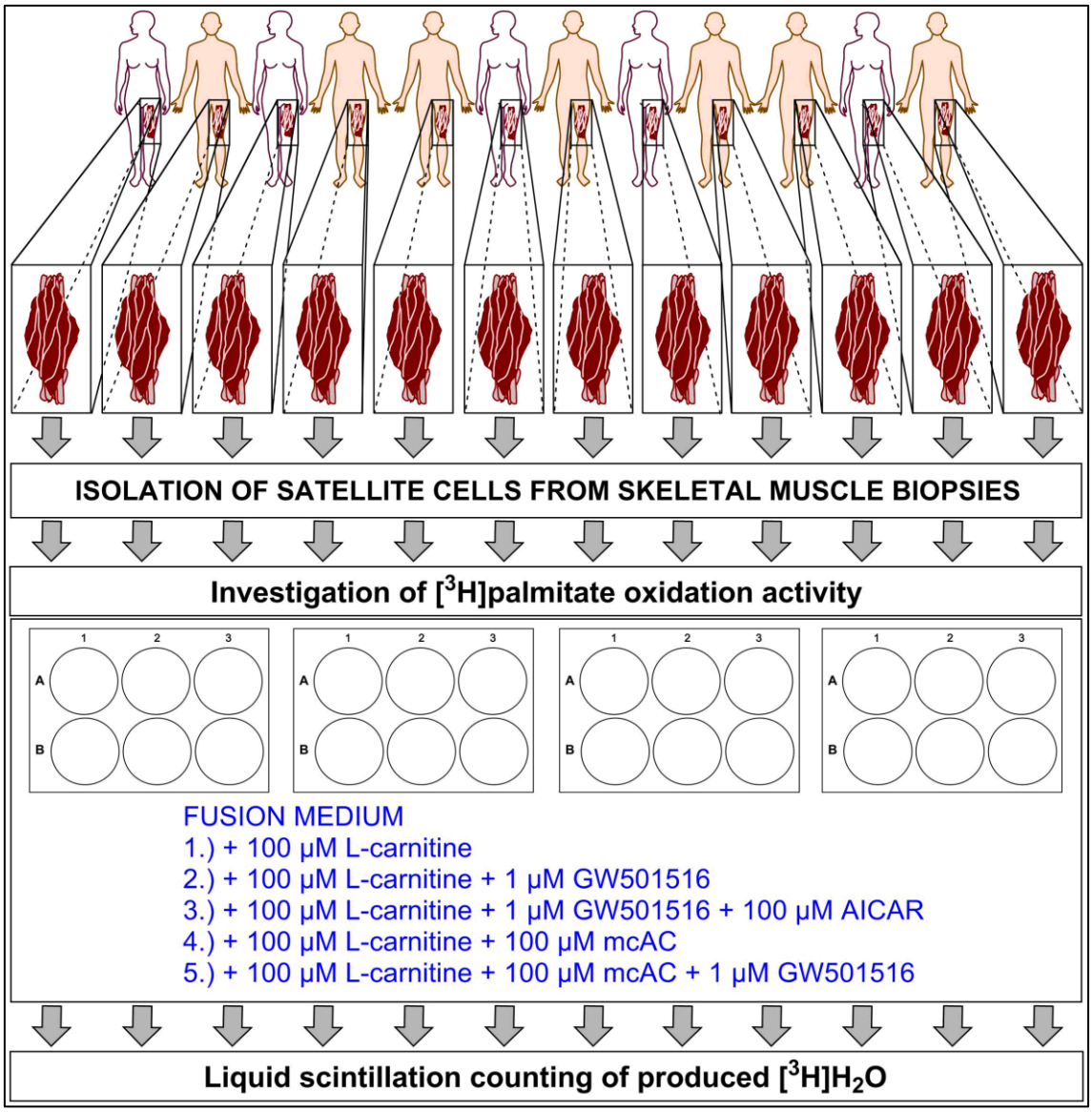

Figure 6: Schematic representation of the experimental set-up for determination of [^{3}H]palmitate oxidation activity in primary human myotubes from 12 different human donors applying four 6-well plates per each donor as cell culture vessels. During fusion phase the muscle cells were incubated for seven days with Fusion Medium containing 100 µM L-carnitine and supplemented with 1 µM GW501516, 1 µM GW501516 + 100 µM 5-aminoimidazole-4-carboxamide 1-β-D-ribofuranoside (AICAR), 100 µM equimolar medium-chain acylcarnitine (mcAC) combination (C8-, C10- and C12-AC) or 100 µM equimolar mcAC combination plus 1 µM GW501516. In this present work, results of the correlation analyses with the mass spectrometrically determined LPC concentrations are exclusively shown for the incubation mode with L-carnitine and the incubation mode with L-carnitine plus GW501516, as congruent results are obtained with other incubation modes and for the sake of clarity.

2.2.2 Investigation of intracellular and extracellular kinetics of lysophosphatidylcholines after cultivation with [$^{13}C_{16}$]palmitate

The primary human skeletal muscle cell cultures of the twelve donors in the 15 cm dishes were supplied for 9 to 19 days with Cloning Medium until 90 % to 95 % confluency. Afterwards differentiation into myotubes was induced by replacing the Cloning Medium with Fusion Medium which was renewed after 3 days. The 24-hour stimulation was begun 6 days after differentiation initiation in two of the six 15 cm dishes per each donor respectively by replacing the Fusion Medium with 15 ml Trial Medium plus L-carnitine in a final concentration of 100 µM as well as [$^{13}C_{16}$]palmitate in a final concentration of 125 µM. The subsequent day, Trial Medium plus L-carnitine and [$^{13}C_{16}$]palmitate was added for 4 hours or for 30 minutes to respectively two of the remaining four 15 cm dishes per each donor with the result that all 15 cm dishes of each donor could be finished simultaneously. LPCs were isolated from both supernatant and cell lysate.

2.2.2.1 Isolation of lysophosphatidylcholines from supernatant

At the end of the stimulation periods, 13 ml of each supernatant were decanted in a 15 ml tube respectively. The residuals of the supernatants were discarded. Further isolation steps were resumed approximately 3 hours later after the isolation of lysophosphatidylcholines from the cell lysates. Until then, the supernatants were stored at 4 °C in the refrigerator. Subsequently, the supernatants were centrifuged for 5 minutes at 3,300 rpm and 4 °C and afterwards transferred into other 15 ml tubes. The addition of 1 µl 1.5 µg/ml [D_3]*O*-decanoyl-L-carnitine ([D_3]C10-AC), 0.535 µl 2 mg/ml [D_3]leucine and 1 µl 1.47 mg/ml LPC C19:0 per each supernatant as internal standards for the mass spectrometric measurements proceeded to storage of the supernatants at – 80 °C. Internal standards were not added to the supernatants of the first two donors since the protocol was changed afterwards.

Protein precipitation and lyophilization of supernatants were performed after having stored them for 3 to 29 days at – 80 °C. Due to capacity issues, the protein precipitation was accomplished for each of the donors individually. For this purpose the supernatants of the respective donor were thawed for approximately 3 hours at 4 °C. Twelve 2 ml Eppendorf® reaction vessels with always 1000 µl acetonitrile submitted were prepared for each of the thawed supernatants. Acetonitrile was submitted with a manual hand-

held dispenser. Each time 1000 µl of the corresponding supernatant were added to the twelve prepared reaction vessels respectively with a 1000 µl pipette. These assays were mixed for 3 minutes with a shaker device, incubated for 2 minutes at room temperature and centrifuged for 20 minutes at 13,200 rpm and 4 °C. Two 15 ml tubes were prepared for each batch of twelve centrifuged reaction vessels from whose supernatants 1900 µl (95 %) were transferred into the 15 ml tubes respectively. The volume in these tubes was reduced to less than 7 ml respectively by use of a centrifugal vacuum concentrator within 2 hours in order to pool the contents of the always two related 15 ml tubes and to continue centrifugal vacuum concentration in these pooled tubes overnight. The next morning (after approximately 18 hours), the concentration procedure had proceeded to a volume less than 2 ml with the result that the samples could be transferred into 2 ml Eppendorf® reaction vessels. Lyophilization of samples was continued until entire drying through centrifugal vacuum concentration until the next day.

2.2.2.2 Isolation of lysophosphatidylcholines from cell lysate

After aspiration of the supernatants (see above), the cells in the 15 cm dishes were washed three times with 5 ml Dulbecco's phosphate-buffered saline (DPBS) containing 0.5 % bovine serum albumin (BSA), twice with 5 ml (pure) DPBS and once with 10 ml (pure) DPBS. Afterwards, the cells were trypsinized with 4 ml trypsin plus ethylenediaminetetraacetate (EDTA) per each 15 cm dish at 37 °C. The activity of trypsin was stopped by the addition of 8 ml Cloning Medium. The cell suspensions were pipetted up and down 20 times with a 10 ml pipette and transferred into 15 ml tubes which were centrifuged for 4 minutes at 900 rpm and 4 °C. After centrifugation the supernatants were aspirated and discarded. The pellets were resuspended with 1000 µl DPBS pipetting up and down 30 times, transferred into 1.5 ml Eppendorf® reaction vessels and centrifuged for 2 minutes at 5,600 rpm and 4 °C. The supernatants were aspirated using a water-jet aspirator pump, after which the cells were resuspended in 400 µl H_2O (high-performance liquid chromatography (HPLC)-grade) and disrupted by sonicating them twice for in each case 5 minutes while cooling with iced water. The cell lysates were mixed with a shaker device before 20 µl of each sample were transferred into another 1.5 ml Eppendorf® reaction vessel respectively and stored at – 80 °C until the execution of the Bradford protein quantification (see **2.2.5**). Aliquots

for protein quantification were not taken from the cell lysates of the donors M11 and M42, since the protocol was changed not until after their workup.

In the remaining cell lysates, protein precipitation was initiated by adding always 600 µl acetonitrile plus 1 µl 1.5 µg/ml [D_3]C10-AC, 1 µl 1.47 mg/ml LPC C19:0 and 0.535 µl 2 mg/ml [D_3]leucine as internal standards for the mass spectrometric measurements. Once again internal standards were not added to the cell lysates of the donors M11 and M42 during protein precipitation. Furthermore, each of the lyophilization procedures (except the one of the cell lysates of the donors M11 and M42) was accompanied by the lyophilization of one or two standard solutions consisting of 400 µl pure (HPLC-grade) H_2O plus 600 µl acetonitrile and internal standards for checking purposes. Their further workup was identical to the one of the cell lysates: After addition of acetonitrile the reaction vessels were mixed for 3 minutes with a shaker device, incubated for 2 minutes at room temperature and centrifuged for 20 minutes at 13,200 rpm and 4 °C.

Afterwards, always 900 µl (90 %) of the resulting supernatants were transferred into a 1.5 ml Eppendorf® reaction vessel respectively for lyophilization until entire drying by centrifugal vacuum concentration until the next day. The pellets and the residues of the supernatants were discarded.

2.2.2.3 Quantification of lysophosphatidylcholines by HPLC-MS

The quantification of lysophosphatidylcholines was accomplished through cooperation with the Key Laboratory of Separation Science for Analytical Chemistry of the Dalian Institute of Chemical Physics of the Chinese Academy of Sciences by Xinjie Zhao and Shili Chen in Dalian, China. An Aquity BEH T3 column (2.1 mm x 100 mm; 1.8 µm particle size; company: Waters™) coupled to a 6460 triple quadrupole mass spectrometer (Agilent Technologies©, Waldbronn, Germany) was used for separation. As mobile phase for gradient elution 0.1 % formic acid and acetonitrile were used. The peak areas were measured by use of MassHunter Quantitative Analysis Software. The concentrations of the individual lysophosphatidylcholine species were calculated as ratios to the internal standard LPC C19:0. For mass spectrometric measurement the deproteinized lyophilisates of the cell lysates were resuspended in 100 µl 20 % acetonitrile/H_2O whereof 1 µl was injected, whereas those of the

supernatants were resuspended in 200 µl 20 % acetonitrile/H_2O whereof 2 µl were injected.

2.2.3 Investigation of [^{3}H]palmitate oxidation activity

Palmitate oxidation activity of the human myotubes of the twelve donors (see **Table 10** and **Table 11**) was determined after different stimulation modes. For this purpose one aliquot from skeletal muscle biopsy of each of the donors was used for cell culture initiation in four 6-well plates, respectively. Once again the muscle cells of the twelve donors were divided into the three batches of in each case four donors cultured simultaneously.

The human myoblasts were cultivated in Cloning Medium until 70 % to 80 % confluency following which the four 6-well plates of each of the donors were divided into two batches of in each case two plates. These two batches were treated identically after a one-day distance of time respectively: During the following fusion phase the muscle cells were incubated for seven days with Fusion Medium containing 100 µM L-carnitine and supplemented with 1 µM GW501516, 1 µM GW501516 plus 100 µM 5-aminoimidazole-4-carboxamide 1-β-D-ribofuranoside (AICAR), 100 µM C8-/C10-/C12-AC combination (mcAC) or 100 µM mcAC plus 1 µM GW501516, respectively. These incubation modes were always performed in two wells for duplication check. The remaining four wells of each batch were supplied with Fusion Medium containing 100 µM L-carnitine without supplements. The medium with or without supplements was replaced twice during fusion phase: after two days and after five days. Incubation and thus fusion phase was terminated after seven days by aspiration of the medium and its replacement with 1 ml EMEM including 100 µM L-carnitine without any further supplements per each well. Afterwards, the subsequent determination of [^{3}H]palmitate oxidation activity was accomplished in the isotope laboratory of the University Tübingen: Etomoxir in a final concentration of 100 µM was added to two of the four wells without supplement addition during fusion phase. As Etomoxir represents an inhibitor of β-oxidation, these two wells of each batch were considered as references respectively. After an incubation of the 6-well plates for 30 minutes at 37 °C, 15 µl coupled [^{3}H]palmitate solution corresponding to a radioactivity of 0.185 MBq (see below) were added to all wells of all plates respectively followed by another incubation

at 37 °C for four hours. Thereafter, always 200 µl of the cell culture supernatants were transferred from each well into an extraction cartridge equilibrated before with 1 ml pure methanol and 1 ml distilled H_2O. Elution was initiated approximately 45 minutes later by addition of 800 µl distilled H_2O per each extraction cartridge and lasted 90 to 120 minutes. The eluate of each extraction cartridge was collected in a scintillation vial containing 5 ml scintillation liquid. Subsequently, the scintillation vials were capped, shaken, incubated overnight in the dark and measured the next day with a scintillation counter. Cells had not been added to two wells of an extra 6-well plate containing 1 ml EMEM including 100 µM L-carnitine per each well, but apart from that these wells were treated identically to the other wells with cells and considered as negative controls in liquid scintillation counting. The batches of two out of the twelve donors were treated on the same day without a distance of time.

Coupled [^{3}H]palmitate solution was prepared a few days prior to the termination of the fusion phase of the first batch in the isotope laboratory: After submission of 900 µl EMEM (without supplements) in four 2 ml Eppendorf® reaction vessels respectively, 500 µl 6 mM (unlabeled) palmitate and 100 µl [^{3}H]palmitate corresponding to a radioactivity of 18.5 MBq were augmented. The following incubation for three hours at 37 °C and 350 rpm was performed with a heating shaker. All samples were pooled in a 15 ml tube and mixed with a shaker device before being realiquoted into four 2 ml reaction vessels for storage at – 20 °C in order to avoid multiple freezing and thawing.

2.2.4 Bicinchoninic acid protein quantification

Since protein concentration could not be determined *via* the Bradford method (see **2.2.5**) after the investigation of [^{3}H]palmitate oxidation due to incompatibilities with supplements of the lysis buffer, protein concentration was determined with Pierce™ bicinchoninic acid (BCA) Protein Assay Kit.

There were differences in the lysis procedure between different donors: The myotubes of four donors were first trypsinized and then lyzed. For their first batch 150 µl Volker's lysis buffer were used, whereas this volume was increased to 500 µl for their second batch respectively. The myotubes of the eight other donors were lyzed directly by adding 500 µl Volker's lysis buffer to each well of the respective 6-well plates. Protein quantification was omitted for the first batch of one donor.

According to the manufacturer's specifications, 25 µl of serial dilutions of BSA in final concentrations of 1.0 µg/ml, 1.5 µg/ml, 2.0 µg/ml, 25 µg/ml, 125 µg/ml, 250 µg/ml, 500 µg/ml and 750 µg/ml or 25 µl of the 1 : 2 diluted cell lysates were submitted in the wells of a microtiter plate. After addition of 200 µl BCA Working Reagent to each well and incubation for 30 minutes at 37 °C, the plate was cooled to room temperature and the colorimetric measurement was performed at 562 nm with a microplate reader.

2.2.5 Bradford protein quantification

Serial dilutions of BSA in final concentrations of 50 µg/ml, 100 µg/ml, 200 µg/ml, 300 µg/ml, 400 µg/ml and 500 µg/ml (representing the linear range of this microtiter plate assay) were submitted in a volume of 10 µl in always four wells of a 96-well plate for calculation of a standard curve. Samples were measured in triplicate pipetting 10 µl of a 1 : 10 dilution in three wells respectively. Color reaction based on the Bradford dye-binding method [190] was initiated by adding always 200 µl dye reagent. After incubation at room temperature for 5 minutes, photometric measurement was performed with a microplate reader at 595 nm.

2.2.6 Analysis of gene expression and of mitochondrial DNA content

RNA and DNA were isolated simultaneously from human myotubes of the 10 cm dishes for investigation of both gene expression of important genes of fatty acid metabolism and mitochondrial DNA content. Proliferation phase of the human myoblasts had been performed for 8 to 16 days in Cloning Medium until 70 % to 90 % confluency, the subsequent fusion phase for 6 days in Fusion Medium. During this fusion phase, two 10 cm dishes per each donor had been supplemented with 100 µM L-carnitine, 100 µM C8-/C10-/C12-AC combination (mcAC) or 100 µM L-carnitine plus 1 µM GW501516, respectively. Fusion Medium plus corresponding supplements had been renewed twice during fusion phase: after 2 days and after 4 days.

Isolated RNA was purified and subsequently converted into complementary DNA (cDNA) by reverse transcription. Quantitative polymerase chain reaction (qPCR), using primers from different industrial suppliers (see **Table 1** and **Table 2**), was applied for quantification of these transcripts as well as for quantification of purified DNA samples.

2.2.6.1 Nucleic acid isolation and purification

Parallel isolation of both DNA and RNA as well as purification of DNA were based on the QIAGEN® AllPrep protocol "Simultaneous Purification of Genomic DNA and Total RNA from Animal Cells" of the QIAGEN® AllPrep DNA/RNA Mini Handbook from November 2005 (pages 19 - 25) which was adapted to the conditions of this experiment. All centrifugation steps were performed at 13,000 rpm with the nonrefrigerated Heraeus® Biofuge® pico. Due to the maximum capacity of the rotor accepting at most 24 collection tubes, four donors were combined for RNA purification from cell lysates of the 10 cm dishes (six dishes per each donor).

2.2.6.2 Simultaneous isolation of RNA and DNA

Both RNA and DNA were isolated from cell lysates of the 10 cm dishes. To that end, cell culture medium was aspirated finishing the fusion phase and, after a wash step with 5 ml DPBS per each dish, cells were lyzed by adding always 600 µl Buffer RLT Plus with 1 % (V/V) β-mercaptoethanol. Cell lysates were mechanically detached with a cell scraper, transferred into 1.5 ml reaction vessels, mixed with a shaker device and loaded on QIAshredder™ spin columns placed in 2 ml collection tubes. After a 2-minute centrifugation, columns were discarded and nucleic acid eluates were stored at – 80 °C until nucleic acid purification (RNA and DNA).

2.2.6.3 DNA purification

The nucleic acid eluates from the 10 cm dishes were thawed by incubating for 2 minutes in a water bath (37 °C), mixed by pipetting, transferred to AllPrep DNA spin columns placed in 2 ml collection tubes and centrifuged for 30 seconds. DNA purification from these AllPrep DNA spin columns was performed directly after RNA purification from the flow-throughs (see **2.2.6.4**). Until then, AllPrep DNA spin columns, transferred into new collection tubes, were incubated at 4 °C. Subsequently, spin columns were washed with always 500 µl Buffer AW1 centrifuging for 30 seconds and with 500 µl Buffer AW2 centrifuging for 2 minutes. DNA was eluted with 50 µl elution buffer (Buffer EB) in 1.5 ml reaction vessels incubating for 1 minute at room temperature and centrifuging for 1 minute at maximum speed. DNA eluates were stored at – 80 °C until photometric DNA quantification (see **2.2.6.5**).

2.2.6.4 RNA purification

RNA was purified from samples of the 10 cm dishes using the flow-throughs of AllPrep DNA spin columns (see **2.2.6.3**). RNA was precipitated by adding always 600 µl 70 % ethanol to the AllPrep DNA spin column flow-throughs. Samples were mixed thoroughly by pipetting and transferred into QIAGEN® RNeasy® mini spin columns binding RNA during purification procedure. After centrifugation for 30 seconds the flow-through was discarded and RNA was washed with always 350 µl Buffer RW1 centrifuging once more for 30 seconds and discarding the flow-through completely.
Subsequently, DNase digestion was performed with 70 µl Buffer RDD plus 10 µl DNase I per each column incubating for 15 minutes at room temperature.
Three wash steps followed: The first was performed with always 350 µl Buffer RW1 centrifuging for 30 seconds, the second with 500 µl Buffer RPE centrifuging again for 30 seconds and the third with 500 µl Buffer RPE centrifuging for 2 minutes. For entire drying, the columns were transferred into new collection tubes and centrifuged for 1 minute. Subsequently, RNA was eluted with 30 µl RNase-free H_2O in lettered 1.5 ml Eppendorf® reaction vessels centrifuging for 1 minute. The eluates were retransferred into the corresponding column in order to increase RNA concentration for reverse transcription. After having incubated them for 1 minute at room temperature, they were again centrifuged for 1 minute. RNA eluates were stored at – 80 °C until thawing once for photometric RNA quantification (see **2.2.6.5**) and another time for reverse transcription (see **2.2.6.6**).

2.2.6.5 Photometric nucleic acid quantification

Nucleic acid quantification was performed photometrically. Always 6 µl of the respective RNA eluate were added to 80 µl H_2O (HPLC-grade) for RNA quantification and always 10 µl of the respective DNA eluate were added to 70 µl H_2O (HPLC-grade) for DNA quantification. Absorptions of these dilutions were measured at 260 nm (for nucleic acid quantification) and at 280 nm (for assessment of nucleic acid purity).

2.2.6.6 Reverse transcription

A dilution with a total volume of 11 µl and a total RNA content of 1 µg was prepared from each of the RNA samples individually. For this, the volume of H_2O (PCR quality) missing by way of calculation for a total volume of 11 µl was submitted in 0.2 ml

Eppendorf® reaction vessels and the corresponding volume of the individual RNA samples containing 1 µg RNA was added. These dilutions were mixed with a shaker device, briefly centrifuged and transferred to the thermo block of a thermal cycler heating for 10 minutes at 65 °C to denature RNA secondary structures before cooling down to 4 °C within 1 minute. Thereafter, samples were incubated for 5 minutes on ice.
Components for reverse transcription with Roche Transcriptor First Strand cDNA Synthesis Kit were prepared for all samples as master mix. For each of the RNA samples 2 µl 600 µM random hexamer primers, 4 µl Transcriptor RT reaction buffer, 2 µl deoxyribonucleoside triphosphate (dNTP) mix, 0.5 µl Thermostable Protector RNase inhibitor and 0.5 µl Transcriptor reverse transcriptase were included in the calculation (see **Table 4**). Inhibitor and reverse transcriptase were added to the master mix just before usage and stored up to that time and afterwards at – 20 °C. To each of the RNA dilutions (V = 11 µl; m(RNA) = 1 µg) 9 µl of the master mix were added resulting in a total volume of 20 µl and a final RNA concentration of 50 mg/l.

Table 4: Components of reverse transcription reaction. RNA dilutions (V = 11 µl, m(RNA) = 1 µg) were submitted individually. Random hexamer primers, buffer, deoxyribonucleoside triphosphate (dNTP) mix, RNase inhibitor and the enzyme reverse transcriptase were prepared as master mix.

Component	Volume	Final concentration
Total RNA (91 mg/l)	11 µl	50 mg/l
Random hexamer primers (600 µM)	2 µl	60 µM
RT reaction buffer (5x)	4 µl	1x (8 mM $MgCl_2$)
dNTP mix (10 mM each)	2 µl	1 mM each
RNase inhibitor (40 U/µl)	0.5 µl	1.0 U/µl (20 U)
Reverse transcriptase (20 U/µl)	0.5 µl	0.5 U/µl (10 U)

Reverse transcription was performed for 10 minutes at 25 °C, for 30 minutes at 55 °C and for 5 minutes at 85 °C in a thermal cycler. Subsequently, the samples were incubated at 4 °C. Five 2 µl aliquots of each cDNA sample were transferred into 0.5 ml reaction vessels and stored at – 20 °C along with the nonaliquoted residue.
After exhaustion of all five 2 µl aliquots of the cDNA samples from the 10 cm dishes, four more 2 µl aliquots were produced from the prior nonaliquoted residues.

2.2.6.7 Quantitative polymerase chain reaction (qPCR)

Dilutions of an amplicon standard solution with defined concentration were applied for quantification of corresponding PCR products by calculation of a fluorescence intensity

calibration curve. A specific amplicon standard solution with a concentration of 5 ng/µl was prepared for each of the analyzed genes from its PCR product (see **2.2.6.10**).

Nine serial 1 : 10 dilutions of these standard solutions were produced submitting always 18 µl H_2O (PCR-grade) and adding 2 µl of the higher concentrated dilution, respectively. From the six low concentrated of altogether nine 1 : 10 dilutions, 2 µl were transferred into 0.5 ml Eppendorf® reaction vessels as templates for the calibration curve of RT-qPCR experiments. For the calibration curve of duplex PCR experiments 2 µl of the first until fifth 1 : 10 dilution of the *MT-ND1* standard solution (corresponding to 1 : 10^1 until 1 : 10^5 dilutions) were combined with 2 µl of the third until seventh 1 : 10 dilution of the *LPL* standard solution (corresponding to 1 : 10^3 until 1 : 10^7 dilutions), respectively.

The cDNA samples had been aliquoted at 2 µl directly after reverse transcription (see **2.2.6.6**). The remaining RT-qPCR components were added as master mix resulting in the compositions shown in **Table 5** as a function of $MgCl_2$ final concentration.

Table 5: Components of RT-qPCR experiments on LightCycler® instruments depending on $MgCl_2$ final concentration. Previously aliquoted cDNA samples (2 µl) were applied as templates. The other constituents were added as master mix. According to the optimal $MgCl_2$ final concentration (3 mM, 4 mM or 5 mM) of the respective gene-specific primers, volumes of 25 mM $MgCl_2$ varied from 1.6 µl to 3.2 µl. Volumes of upstream and downstream primers (0.5 µl each) and of LightCycler® FastStart DNA Master SYBR® Green I Reaction Mix (2.0 µl) did not vary. Reaction mix contained FastStart *Thermus aquaticus* (*Taq*) DNA Polymerase, reaction buffer, dNTP mix, SYBR® Green I dye and 10 mM $MgCl_2$. H_2O was added for a total volume of 20 µl. When using *PPARD*-specific primers, 1 µl H_2O was replaced by 1 µl dimethyl sulfoxide (DMSO).

Component	**Volume**			**Final concentration**		
H_2O (PCR-grade)	13.4 µl	12.6 µl	11.8 µl			
$MgCl_2$ (25 mM)	1.6 µl	2.4 µl	3.2 µl	3 mM	4 mM	5 mM
Upstream primer (20 µM)	0.5 µl			500 nM		
Downstream primer (20 µM)	0.5 µl			500 nM		
LightCycler® FastStart SYBR® Green I Reaction Mix including LightCycler® FastStart *Taq* DNA Polymerase (10x)	2.0 µl			1x		
cDNA	2.0 µl					

RT-qPCR program parameters depending on the analyzed gene are summarized in **Table 6**. Optimal $MgCl_2$ concentrations as well as optimal annealing temperatures of the individual primers had been determined by other members of the research group applying $MgCl_2$ titrations and gradient PCRs, respectively.

Table 6: Amplification program parameters for RT-qPCRs with gene-specific primers of *ACTB* (β-actin), *UCP3*, *CPT1B* (CPT-1β), *PPARD* (PPARδ), *PDK4* or *PPARGC1A* (PGC-1α). Annealing temperature optima of the primers were experimentally determined by gradient PCRs, optimal $MgCl_2$ final concentrations (3 mM, 4 mM or 5 mM) by $MgCl_2$ titrations. Annealing temperatures for melting curve analysis were chosen to be 2 °C above those for the amplification phase. Duration of elongation period (in seconds) was calculated by dividing the respective amplicon's number of base pairs by 25 (duration of elongation [s] = bp number of the amplicon/25).

Analyzed Gene		***ACTB***	***UCP3***	***CPT1B***	***PPARD***	***PDK4***	***PPARGC1A***
$MgCl_2$ concentration		5 mM	4 mM	3 mM	3 mM	3 mM	4 mM
Activation of FastStart *Taq* DNA Polymerase		95 °C					
		10 min					
Amplification: 45 cycles	Denaturation	95 °C					
		15 s					
	Annealing	67 °C	62 °C	68 °C	67 °C	62 °C	65 °C
		10 s					
	Elongation	72 °C					
		11 s	13 s	13 s	16 s	17 s	10 s
Melting curve analysis	Denaturation	95 °C					
		5 s					
	Annealing	69 °C	65 °C	70 °C	69 °C	64 °C	67 °C
		10 s					
	Melting	until 98 °C					
		increase of 0.1 °C/s					
Cooling		40 °C					
		30 s					

Components of duplex PCR experiments including different hybridization probes are outlined in **Table 7**. Primers and hybridization probes of the mitochondrially encoded *MT-ND1* gene were applied in combination with those of the chromosomally encoded *LPL* gene in the same samples. Final concentration of $MgCl_2$ (4 mM) was optimized by means of $MgCl_2$ titration. The primer pairs of the two genes were chosen because they showed similar annealing temperatures and very good specificities in a gradient PCR. **Table 8** lists the program parameters of the duplex PCR.

Table 7: Duplex PCR components. Hybridization probes and primer pairs for both genes (*MT-ND1* and *LPL*) were applied contemporaneously in the same samples. The primers *MT-ND1*_S and *LPL*_F were selected as upstream primers, *MT-ND1*_A and *LPL*_A as downstream primers. *MT-ND1* hybridization probes were complementary to the template strand; *LPL* hybridization probes were complementary to the complementary strand. LightCycler® FastStart HybProbe Reaction Mix contained LightCycler® FastStart *Taq* DNA Polymerase, reaction buffer, dNTP mix (with dUTP instead of dTTP) and 10 mM $MgCl_2$.

Component	Volume	Final concentration
H_2O (PCR-grade)	2.6 µl	
$MgCl_2$ (25 mM)	2.4 µl	4 mM
***MT-ND1* fluorescein-coupled probe (2 µM)**	2.0 µl	200 nM
***MT-ND1* LC640-coupled probe (2 µM)**	2.0 µl	200 nM
***LPL* fluorescein-coupled probe (2 µM)**	2.0 µl	200 nM
***LPL* LC705-coupled probe (2 µM)**	2.0 µl	200 nM
***MT-ND1* upstream primer (4 µM)**	0.5 µl	100 nM
***MT-ND1* downstream primer (4 µM)**	0.5 µl	100 nM
***LPL* upstream primer (20 µM)**	1.0 µl	1000 nM
***LPL* downstream primer (20 µM)**	1.0 µl	1000 nM
LightCycler® FastStart HybProbe Reaction Mix including FastStart *Taq* DNA Polymerase (10x)	2.0 µl	1x
DNA (15 ng/µl)	2.0 µl	1.5 ng/µl

Table 8: Duplex PCR program parameters using *MT-ND1* and *LPL* primer pairs and hybridization probes for mitochondrial DNA quantification. Optimal annealing temperature for both primer pairs was revealed at 64 °C by a gradient PCR. Base pair numbers of the two amplicons were chosen to be similar and in this way compatible for implementation of the (mutual) elongation duration (10 seconds). Amplification of both duplex PCR products was monitored by measuring the fluorescence intensities at the two corresponding wavelengths once after each amplification cycle at 64 °C, whereas melting curves resulted from continuous measurement of fluorescence intensities during heating.

Process		Temperature	Duration
Activation of FastStart *Taq* DNA Polymerase		95 °C	10 min
Amplification: 55 cycles	Denaturation	95 °C	15 s
	Annealing	64 °C	10 s
	Elongation	72 °C	10 s
Melting curve analysis	Denaturation	95 °C	5 s
	Annealing	60 °C	30 s
	Melting	until 98 °C	Increase of 0.1 °C/s
Cooling		40 °C	30 s

Pretrials and duplex PCRs were performed on a carousel-based LightCycler® 2.0 whereas all other qPCR experiments were performed on a LightCycler® 480 instrument.

2.2.6.8 Duplex PCRs on LightCycler® 2.0 instrument

Eluates from DNA purification (see **2.2.6.3**) were applied as templates in duplex PCR experiments at a concentration of 15 ng/µl and a volume of 2 µl (resulting in 30 ng). All other components of the duplex PCR (depicted in **Table 7**) were added as master mix. As the reaction vessels for the calibration curve contained 2 µl of both *MT-ND1* and *LPL* serially diluted standard solution, the master mix containing the remaining components was initially prepared for addition of always 16 µl master mix per standard dilution. After preparation of these standard dilutions, the master mix was diluted with H_2O for addition of always 18 µl master mix per sample.

After centrifuging until 7,000 rpm the reaction solutions were transferred into qPCR capillaries which were capped and centrifuged at 4 °C until 2,000 rpm. Subsequently, the capillaries were placed in the carousel of the LightCycler® 2.0 instrument performing the duplex PCR with the parameters demonstrated in **Table 8**. Quantification cycle numbers (C_q or C_p values), identifying the first cycle number with significantly higher fluorescence intensity than the background, were determined using the LightCycler® 2.0 software (version 3.5) on Windows© 2000 Professional. Concentrations of the samples were calculated based on their C_q values relating to those of the standard dilutions. Both C_q values and concentrations of the samples were used for evaluation referring the results of the *MT-ND1* PCR reaction to those of the *LPL* PCR reaction.

2.2.6.9 RT-qPCRs on LightCycler® 480 instrument

Aliquots of cDNA samples at 2 µl (see **2.2.6.6** for cDNA preparation) were thawed on ice for being used as templates in RT-qPCR experiments. The six lowest concentrated of altogether nine 1 : 10 serial dilutions of a 5 ng/µl amplicon-specific standard solution served as templates for the calibration curve. The remaining components depicted in **Table 5** were included in 18 µl of the prepared master mix.

The solutions were centrifuged until 7,000 rpm and pipetted into wells of a white microtiter plate which was covered and centrifuged for 1 minute at 3,300 rpm and 4 °C. Subsequently, RT-qPCRs were conducted using the LightCycler® 480 instrument and the appropriate gene-specific amplification program (see **Table 6**).

LightCycler® 480 software (release 1.5.0) was used for PCR product quantification referring the C_q values of the samples to those of the standard dilutions. Concentrations of *ACTB* were applied for normalization of the related concentrations of other genes.

2.2.6.10 Preparation of amplicon-specific standard solutions for qPCR experiments

Amplicon-specific PCR products from previously performed LightCycler® runs were purified using the QIAGEN® QIAquick® PCR Purification Kit, quantified by photometrical measurement and adjusted to a concentration of 5 ng/µl for preparation of standard solutions. Serial 1 : 10 dilutions of these standard solutions were applied in qPCR experiments for calibration curve computation.

For PCR product purification, three or four samples of a preceding PCR with the same primers (*e.g.* in the context of pretrials) were applied adding always 100 µl Buffer PB preparatory to their transfer into one common QIAquick® spin column placed in a 2.0 ml collection tube. After 1-minute centrifugation at 13,000 rpm and room temperature the flow-through was discarded and the column was washed with 750 µl Buffer PE. After another centrifugation reapplying the same parameters the flow-through was again discarded and the column once again centrifuged in order to secure complete drying. Purified DNA was eluted with 50 µl Buffer EB into a 1.5 ml Eppendorf® reaction vessel.

2.2.6.11 Establishment of primer pairs

As different primer pairs exhibit different optima in consideration of annealing temperature as well as of $MgCl_2$ final concentration, these parameters were specifically optimized for every applied primer pair by gradient PCRs and $MgCl_2$ titrations. With the exception of the *MT-ND1* and *LPL* primer pairs, establishment had been already performed by other members of the research group, so that the procedure was leftover only for these two primer pairs. Gradient PCR with *MT-ND1* and *LPL* primer pairs was performed simultaneously but separately on Eppendorf® Mastercycler® gradient thermal cycler. LightCycler® 2.0 instrument was used for $MgCl_2$ titration.

Detailed descriptions of the performance of the gradient PCR, the polyacrylamide gel electrophoresis and the silver staining of the polyacrylamide gel as well as the

$MgCl_2$ titration for primer establishment already formed part of my diploma thesis [188] and are not included in this work again.

2.2.7 Statistics

All data as well as multiple transformations of them were analyzed in regard to their normal distribution applying Shapiro-Wilk W tests in JMP® (version 11.2.0) software (SAS Institute, Cary, NC, USA). Based on the results of these Shapiro-Wilk W tests on the one hand and on comparisons with transformations reported in studies and publications with much more subjects [176-178, 183, 191-209] on the other hand, the respective transformation was chosen for each parameter individually. In order to ameliorate the commensurability of the results the same transformation was chosen for all variants of a given parameter *en bloc* even if the Shapiro-Wilk W tests showed discordant results. That is why always the same transformation was invariably selected for all lysophosphatidylcholine species or for all stimulation modes of an analyzed gene.
Correlation analyses were performed for detection of associations between the formation or release of LPCs and anthropometric, physiologic, genetic or metabolic traits in JMP® (version 11.2.0) software (SAS Institute, Cary, NC, USA). The results of these correlation analyses are expressed in the respective Pearson correlation coefficients (r) as well as probability values (p-values) specifying the number of measurements (n) for each correlation if they are different from n = 10.
Data normally distributed without any transformation are presented as means ± standard deviation. Variables with log-normal distribution are shown as geometric means ± geometric standard deviation.
Differences between groups or correlation results with p-values ≤ 0.05 are considered statistically significant (p*), those with p-values ≤ 0.01 highly significant (p**) and those with p-values ≤ 0.001 very highly significant (p***). Results with p-values ≤ 0.0001 are marked with four asterisks (p****).
Differences of the amounts of the individual LPC species between pure Trial Medium and cell culture supernatants using the sums of unlabeled plus corresponding [^{13}C]-labeled LPC amounts were examined by unpaired Student's *t*-tests in JMP® version 11.2.0 software (SAS Institute, Cary, NC, USA).
Differences between LPC concentrations at different stimulation periods were analyzed applying pairwise *t*-tests in JMP®.

2.2.7.1 Decision-making procedure on transformations of parameters

Transformations of anthropometric, physiologic and metabolic parameters for the correlation analyses were individually chosen for each parameter on the basis of both the results of the Shapiro-Wilk W tests and the transformation selections which were reported in studies with a large number of subjects. This contrasting juxtaposition is exemplarily depicted in **Table 9** for some parameters.

Table 9: Parameter-specific distribution assessment based on the reports from publications with a large number of subjects and the results of Shapiro-Wilk W tests in JMP® (W) exemplified for the parameters age, body mass index (BMI), basal insulin prior to the beginning of the OGTT (Ins (0)), plasma triglycerides (TGs), total plasma cholesterol (cholest.) and insulin sensitivity index determined during OGTT (ISI_{OGTT}). Abbreviations: normal distribution (ND), number of subjects (n).

		n	Age	BMI	Ins (0)	TGs	Cholest.	ISI_{OGTT}
Reports from studies with a large number of subjects	**UKPDS [201]**	**3867**	ND	ND	log-ND	log-ND	ND	
	UKPDS [200]	**1704**	ND	ND	log-ND	log-ND	ND	
	UKPDS [199]	**2078**	ND	ND	no ND	no ND	ND	log-ND
	ACCORD [192]	**10251**	ND	ND		no ND	ND	
	ADVANCE [196]	**360**	ND	ND		ND	ND	
	DIGAMI [198]	**620**	ND	ND				
	DIGAMI [197]	**1253**	ND	ND		ND	ND	
	TUEF [202]	**725**	ND	ND				ND
	TUEF [177]	**502**	ND	ND	ND			ND
	Matsuda & DeFronzo [183]	**153**	ND	ND	ND			
Shapiro-Wilk W	**Untransformed [x]**	**10**	0.41	0.97	0.98	0.82	0.53	0.09
	Logarithmic function [ln(x)]	**10**	0.21	0.90	0.24	0.79	0.69	0.47
	Reciprocity [1/x]	**10**	0.09	0.76	0.00	0.25	0.39	0.61
	Exponentiation [x^2]	**10**	0.61	0.99	0.85	0.27	0.14	0.00
	Root function [$\sqrt{x}$]	**10**	0.30	0.94	0.75	0.88	0.67	0.25
Assumed distribution			**ND**	**ND**	**log-ND**	**log-ND**	**ND**	**log-ND**

2.2.7.2 Anthropometric, physiologic and metabolic phenotyping of the donors

Measurements of anthropometric, physiologic and metabolic parameters of the donors were performed *in vivo* within the context of the Tübingen Family (TUEF) study. The expressions of various genes of fatty acid metabolism as well as the activity of fatty acid oxidation (FAO) were determined by *in vitro* experiments using human myotubes (see above). The results are listed in **Table 10** and **Table 11** for both the cohort of 12 donors and the cohort of 10 donors (without M11 and M42) as all 12 donors were incorporated into the comparisons of LPC amounts between pure Trial Medium and cell culture supernatants but only 10 donors were taken into consideration for all other investigations for whom LPC amounts were referred to the protein concentration of the corresponding cell lysate. For the first two donors this protein concentration of the cell lysate is missing which is why these donors were consequentially excluded.

Table 10: Anthropometric, physiologic and metabolic phenotyping of both the cohort involving 12 donors (n = 12) and the cohort involving 10 donors (n = 10). Depending on the respective transformation (TN), data are presented as arithmetic mean ± standard deviation (SD) for the normally distributed parameters and as geometric mean for the log-normally distributed parameters (ln) raising the base *e* to the power of the mean of the ln-transformed values ($mean_{LN}$). The measure of dispersion for these log-normally distributed parameters was calculated by raising the base *e* to the power of both the difference ($mean_{LN} - SD_{LN}$) and the sum ($mean_{LN} + SD_{LN}$) of the mean and the standard deviation of the logarithmized values (SD_{LN}).

Parameter	Unit	TN	**Arithmetic mean** ± SD **Geometric mean** ($e^{(mean_{LN} - SD_{LN})}$, $e^{(mean_{LN} + SD_{LN})}$)	
			n = 12 (7 ♂, 5 ♀)	**n = 10** (6 ♂, 4 ♀)
Age	years	none	**24.1** ± 3.0	**24.1** ± 3.2
Height	cm	none	**173** ± 8	**174** ± 8
Weight	kg	none	**65.7** ± 7.3	**65.9** ± 7.9
Body mass index (BMI)	kg/m²	none	**21.8** ± 1.8	**21.8** ± 1.9
Waist-to-hip ratio (WHR)	AU (ratio)	none	**0.77** ± 0.06	**0.77** ± 0.06
Lean body mass (LBM)	kg	none	**52.3** ± 6.2	**52.5** ± 6.5
Percentage of body fat (PBF)	%	ln	**19.1** (13.5, 27.1)	**18.9** (13.0, 27.6)
Max. aerobic capacity $V(O_2)_{max}$	ml/kg/min	none	**41.6** ± 10.5	**41.5** ± 11.3
Perc. aerobic capacity $V(O_2)_{perc}$	%	none	**112** ± 18	**112** ± 21
Respiratory quotient ($RQ_{fasting}$)	AU (ratio)	ln	**0.84** (0.78, 0.91)	**0.86** (0.80, 0.92)
Respiratory quotient (RQ_{clamp})	AU (ratio)	ln	**0.90** (0.83, 0.97)	**0.92** (0.87, 0.97)
Carbohydrate oxid. ($CHOx_{fasting}$)	mg/kg/min	none	**172.2** ± 99.0	**186.2** ± 94.0
Carbohydrate oxid. ($CHOx_{clamp}$)	mg/kg/min	none	**246.3** ± 74.6	**257.4** ± 69.7
Lipid oxidation ($LipOx_{fasting}$)	mg/kg/min	none	**59.9** ± 35.7	**54.8** ± 33.7
Lipid oxidation ($LipOx_{clamp}$)	mg/kg/min	none	**43.1** ± 25.1	**40.2** ± 24.8
Energy expenditure ($EnExp_{fasting}$)	kcal/24 h	ln	**1565** (1303, 1879)	**1570** (1294, 1906)
Energy expenditure ($EnExp_{clamp}$)	kcal/24 h	ln	**1709** (1503, 1943)	**1723** (1508, 1968)
Anaerobic threshold (AT)	ml/kg/min	none	**21.2** ± 7.3	**20.9** ± 8.2
C-peptide; 0 min OGTT	pmol/l	ln	**481** (330, 700)	**508** (344, 751)
C-peptide; 30 min OGTT	pmol/l	ln	**2312** (1714, 3118)	**2472** (1864, 3277)
C-peptide; 60 min OGTT	pmol/l	ln	**2878** (1975, 4193)	**3006** (2035, 4439)
C-peptide; 90 min OGTT	pmol/l	ln	**2278** (1581, 3282)	**2417** (1667, 3504)
C-peptide; 120 min OGTT	pmol/l	ln	**2102** (1635, 2704)	**2093** (1599, 2741)
Insulin; 0 min OGTT	pmol/l	ln	**32.9** (22.7, 47.7)	**34.0** (23.2, 49.9)
Insulin; 30 min OGTT	pmol/l	ln	**313.0** (220.8, 443.7)	**324.5** (223.2, 471.8)
Insulin; 60 min OGTT	pmol/l	ln	**326.7** (185.9, 574.0)	**341.4** (185.0, 630.0)
Insulin; 90 min OGTT	pmol/l	ln	**178.1** (103.2, 307.4)	**180.7** (101.2, 322.7)
Insulin; 120 min OGTT	pmol/l	ln	**176.9** (129.3, 242.0)	**169.8** (122.4, 235.6)
Proinsulin; 0 min OGTT	pmol/l	ln	**1.64** (0.67, 4.05)	**1.86** (0.70, 4.95)
Proinsulin; 30 min OGTT	pmol/l	ln	**3.88** (2.03, 7.44)	**3.88** (1.91, 7.89)
Proinsulin; 60 min OGTT	pmol/l	ln	**8.42** (4.55, 15.55)	**8.40** (4.32, 16.33)
Proinsulin; 90 min OGTT	pmol/l	ln	**7.93** (4.17, 15.09)	**7.93** (3.90, 16.11)
Proinsulin; 120 min OGTT	pmol/l	ln	**8.12** (4.27, 15.43)	**7.67** (3.85, 15.26)
Glucose; 0 min OGTT	mmol/l	ln	**4.72** (4.30, 5.17)	**4.67** (4.24, 5.14)
Glucose; 30 min OGTT	mmol/l	ln	**7.85** (6.77, 9.11)	**7.85** (6.67, 9.24)
Glucose; 60 min OGTT	mmol/l	ln	**6.61** (5.41, 8.08)	**6.59** (5.28, 8.23)
Glucose; 90 min OGTT	mmol/l	ln	**4.90** (4.12, 5.82)	**4.71** (4.00, 5.55)
Glucose; 120 min OGTT	mmol/l	ln	**5.16** (4.09, 6.50)	**4.83** (3.99, 5.86)
Glycerol; 0 min OGTT	µmol/l	ln	**65.3** (42.8, 99.8)	**67.2** (42.5, 106.1)
Glycerol; 30 min OGTT	µmol/l	ln	**38.7** (22.5, 66.4)	**42.5** (26.8, 67.4)
Glycerol; 60 min OGTT	µmol/l	ln	**39.8** (22.8, 69.6)	**45.7** (31.4, 66.5)
Glycerol; 90 min OGTT	µmol/l	ln	**33.4** (18.4, 60.8)	**37.5** (24.9, 56.3)
Glycerol; 120 min OGTT	µmol/l	ln	**31.1** (17.5, 55.2)	**33.8** (21.7, 52.7)

Table 11: Physiologic, genetic and metabolic traits of both the cohort involving 12 donors (n = 12) and the cohort involving 10 donors (n = 10). Depending on the respective transformation (TN), data are presented as arithmetic mean ± standard deviation (SD) for the normally distributed parameters and as geometric mean for the log-normally distributed parameters (ln) raising the base *e* to the power of the mean of the ln-transformed values ($mean_{LN}$). The measure of dispersion for these log-normally distributed parameters was calculated by raising the base *e* to the power of both the difference ($mean_{LN} - SD_{LN}$) and the sum ($mean_{LN} + SD_{LN}$) of the mean and the standard deviation of the logarithmized values (SD_{LN}).

Parameter	Unit	TN	**Arithmetic mean** ± SD **Geometric mean** ($e^{(mean_{LN} - SD_{LN})}$, $e^{(mean_{LN} + SD_{LN})}$)	
			n = 12 (7 ♂, 5 ♀)	**n = 10** (6 ♂, 4 ♀)
NEFAs; 0 min OGTT	µmol/l	ln	**374.8** (214.2, 655.8)	**339.2** (193.9, 593.2)
NEFAs; 30 min OGTT	µmol/l	ln	**147.7** (67.0, 325.7)	**133.3** (58.0, 306.8)
NEFAs; 60 min OGTT	µmol/l	ln	**63.4** (33.2, 121.0)	**61.6** (30.4, 124.6)
NEFAs; 90 min OGTT	µmol/l	ln	**34.8** (13.6, 89.3)	**35.8** (14.6, 88.2)
NEFAs; 120 min OGTT	µmol/l	ln	**25.8** (10.9, 60.8)	**24.9** (11.3, 54.8)
1st phase insulin secretion (1stpIS)	pmol/l	ln	**894** (686, 1166)	**921** (697, 1216)
Insulin sensitivity index (ISI_{OGTT})	AU	ln	**22.7** (16.5, 31.2)	**22.4** (15.8, 31.8)
Insulin sensitivity index (ISI_{clamp})	µmol/kg/min/pM	ln	**0.112** (0.106, 0.119)	**0.113** (0.107, 0.120)
Glucose infusion rate (GIR)	µmol/kg/min	ln	**35.3** (29.2, 42.8)	**36.0** (29.2, 44.2)
Metabolic clearance rate (MCR)	ml/kg/min	ln	**7.42** (5.71, 9.64)	**7.71** (5.88, 10.11)
IMCL, *M. tibialis*	AU (ratio)	ln	**2.48** (1.79, 3.43)	**2.58** (1.85, 3.59)
IMCL, *M. soleus*	AU (ratio)	ln	**8.15** (5.05, 13.15)	**8.54** (5.19, 14.04)
EMCL, *M. tibialis anterior*	AU (ratio)	ln	**1.38** (0.68, 2.81)	**1.59** (0.82, 3.08)
EMCL, *M. tibialis posterior*	AU (ratio)	ln	**1.55** (1.10, 2.18)	**1.64** (1.17, 2.29)
EMCL, *M. soleus*	AU (ratio)	ln	**2.30** (1.66, 3.18)	**2.50** (1.92, 3.25)
EMCL, *M. GC lateralis*	AU (ratio)	ln	**1.86** (1.30, 2.66)	**1.92** (1.32, 2.81)
EMCL, *M. GC medialis*	AU (ratio)	ln	**1.63** (1.07, 2.47)	**1.76** (1.19, 2.62)
EMCL, *Mm. peronei*	AU (ratio)	ln	**2.74** (1.66, 4.50)	**2.72** (1.58, 4.70)
Triglycerides (TGs), plasma	mg/dl	ln	**71.2** (49.3, 102.9)	**75.6** (55.3, 103.4)
Total cholesterol, plasma	mg/dl	none	**180.7** ± 38.8	**178.9** ± 42.7
HDL cholesterol, plasma	mg/dl	none	**60.0** ± 14.0	**58.1** ± 14.2
LDL cholesterol, plasma	mg/dl	none	**109.6** ± 32.5	**109.6** ± 35.4
Leptin, serum	ng/dl	ln	**5.05** (1.71, 14.87)	**4.89** (1.51, 15.87)
$Adiponectin_{OGTT}$, plasma	µg/ml	ln	**13.73** (9.05, 20.82)	**14.56** (9.20, 23.02)
$Adiponectin_{clamp}$, plasma	µg/ml	ln	**12.03** (8.25, 17.55)	**12.03** (8.25, 17.55)
Creatinine, plasma	mg/dl	ln	**0.94** (0.76, 1.17)	**0.96** (0.81, 1.13)
Albumin/creatinine, urine	mg/g	ln	**7.38** (2.70, 20.17)	**8.16** (2.96, 22.45)
***MT-ND1/LPL*,** LC	AU (ratio)	ln	**0.8456** (0.8324, 0.8590)	**0.8479** (0.8348, 0.8612)
***MT-ND1/LPL*,** GW501516	AU (ratio)	ln	**0.8467** (0.8300, 0.8637)	**0.8482** (0.8302, 0.8665)
***CPT1B/ACTB*,** LC	AU (ratio)	ln	**0.0597** (0.0404, 0.0880)	**0.0604** (0.0415, 0.0877)
***CPT1B/ACTB*,** GW501516	AU (ratio)	ln	**0.4820** (0.2980, 0.7794)	**0.4933** (0.3139, 0.7751)
***PDK4/ACTB*,** LC	AU (ratio)	ln	**0.0062** (0.0037, 0.0104)	**0.0057** (0.0034, 0.0096)
***PDK4/ACTB*,** GW501516	AU (ratio)	ln	**0.0565** (0.0355, 0.0898)	**0.0578** (0.0379, 0.0884)
***PPARD/ACTB*,** LC	AU (ratio)	ln	**0.0774** (0.0583, 0.1029)	**0.0824** (0.0629, 0.1080)
***UCP3/ACTB*,** LC	AU (ratio)	ln	**$9.72 \cdot 10^{-5}$** ($7.27 \cdot 10^{-5}$, $12.98 \cdot 10^{-5}$)	**$10.20 \cdot 10^{-5}$** ($7.59 \cdot 10^{-5}$, $13.69 \cdot 10^{-5}$)
***PPARGC1A/ACTB*,** LC	AU (ratio)	ln	**0.0898** (0.0323, 0.2494)	**0.1096** (0.0435, 0.2761)
PDK4/ACTB (EMEM), contr.	AU (ratio)	ln	**0.1515** (0.0884, 0.2596)	**0.1442** (0.0838, 0.2480)
PDK4/ACTB (EMEM), O/P	AU (ratio)	ln	**1.6065** (0.9323, 2.7684)	**1.5224** (0.8819, 2.6283)
PDK4/ACTB (RPMI), contr.	AU (ratio)	ln	**0.1801** (0.1316, 0.2465)	**0.1915** (0.1466, 0.2501)
PDK4/ACTB (RPMI), O/P	AU (ratio)	ln	**1.5679** (1.0865, 2.2624)	**1.5818** (1.1126, 2.2490)
Fatty acid oxidation (FAO), contr	cpm/protein	ln	**478** (425, 538)	**472** (435, 511)
Fatty acid oxidation (FAO), GW	cpm/protein	ln	**602** (544, 667)	**595** (534, 663)
Fatty acid oxidation (FAO), AC	cpm/protein	ln	**604** (535, 681)	**594** (526, 671)
relative FAO, GW501516	AU (ratio)	ln	**1.33** (1.22, 1.45)	**1.34** (1.24, 1.46)
relative FAO, AC	AU (ratio)	ln	**1.23** (1.15, 1.32)	**1.23** (1.15, 1.32)

3 Results

3.1 Lysophosphatidylcholines in Trial Medium

All 19 (unlabeled) [^{12}C]LPC species detected in the cell culture supernatants of primary human myotubes are also found in pure Trial Medium. **Figure 7**, **Figure 8** and **Figure 9** illustrate the amounts of all these LPC species in Trial Medium in comparison to those in the cell culture supernatants after stimulation periods of 30 minutes, 4 hours or 24 hours with 100 µM L-carnitine and 125 µM [$^{13}C_{16}$]palmitate. **Figure 7** shows the results of LPC species containing acyl groups which are composed of 14, 16 or 18 carbon atoms with LPC C14:0 (**Figure 7** A) significantly (p*) increasing after 4-hour stimulation and with LPC C14:0, LPC C16:1 (**Figure 7** C), LPC C18:2 (**Figure 7** F) and LPC C18:3 (**Figure 7** G) showing similar trends after the 30-minute stimulation.

In contrast, a significant decrease of LPC C18:1 (**Figure 7** E; p*) and very highly significant decreases ($p < 0.0001$*) of LPC C18:0 (**Figure 7** D), LPC C18:2 and LPC C18:3 are observed after 24 hours of stimulation. Levels of LPC C16:0 (**Figure 7** B) do not significantly vary.

The time course profiles of the C_{20} acyl group-containing LPC species (**Figure 8**) are similar in appearance: Whereas LPC C20:2 (**Figure 8** C) and LPC C20:5 (**Figure 8** F) tend to increase after 30 minutes of stimulation, highly or very highly significant decreases of LPC C20:0 (**Figure 8** A; p**), LPC C20:2 (p**), LPC C20:3 (**Figure 8** D; p****), LPC C20:4 (**Figure 8** E; p****) and LPC C20:5 (p****) are found after 24 hours with only LPC C20:1 (**Figure 8** B) lacking any significant alterations.

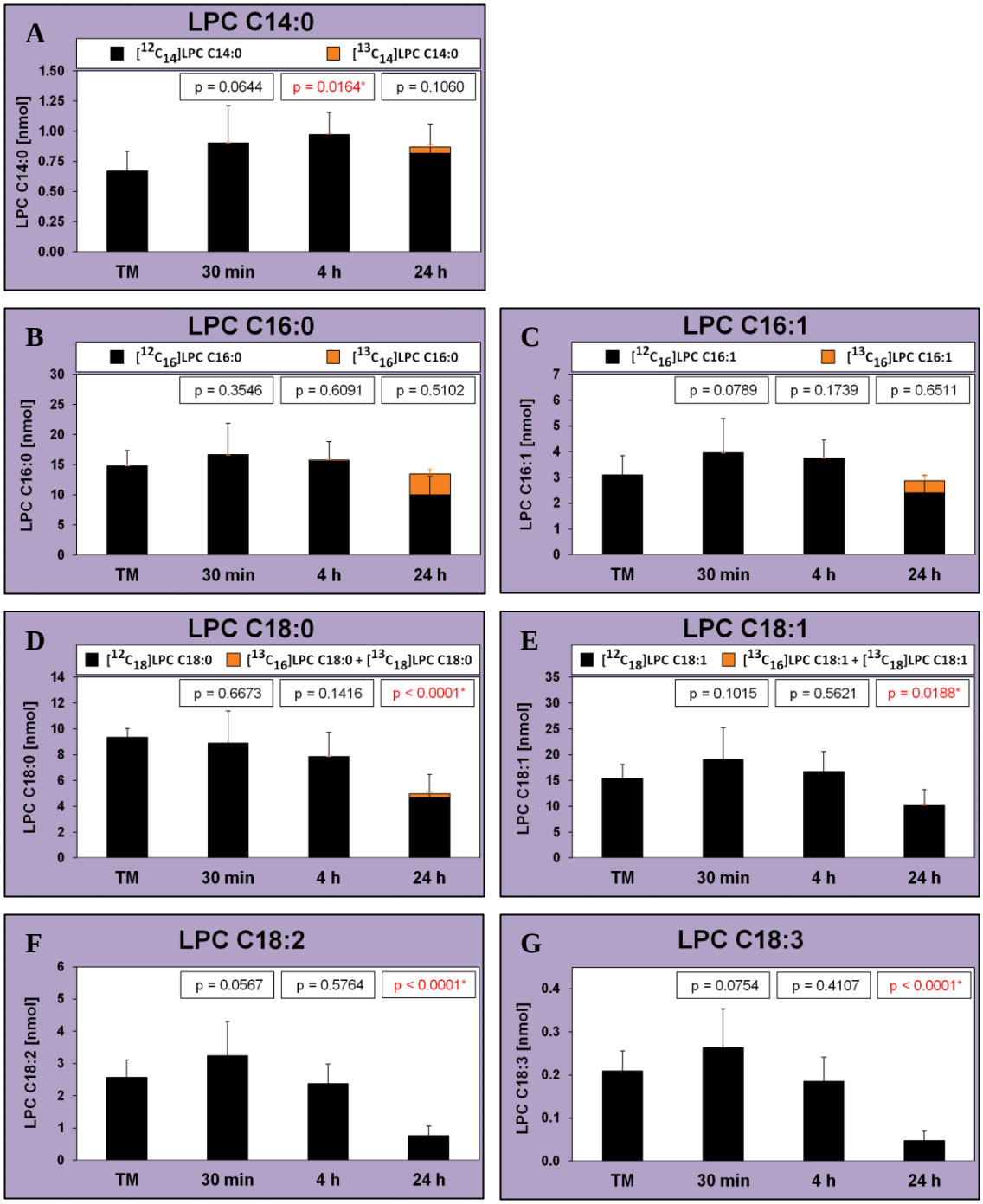

Figure 7: Amount of lysophosphatidylcholine (LPC) species (in nmol) containing a fatty acyl chain composed of 14 to 18 carbon atoms in pure Trial Medium (TM) or in cell culture supernatant (SN) of primary human myotubes stimulated with 100 µM L-carnitine plus 125 µM [$^{13}C_{16}$]palmitate in 15 ml TM for 30 minutes (30 min), 4 hours (4 h) or 24 hours (24 h). Quintuplicate analysis of TM was performed (n_{TM} = 5), supernatants were obtained from cultivated myotubes from 12 different donors in duplicate (n_{SN} = 24 for the 4-hour and 24-hour stimulation periods but n_{SN} = 22 for the 30-min stimulation period because of fungal contaminations in two cell culture dishes). Amounts of [^{13}C]-labeled LPCs are shown in orange. Data are presented as mean ± standard deviation and p-values are the results of unpaired Student's *t*-tests for every pair in JMP® estimating the significance of the change of the sums of unlabeled plus corresponding [^{13}C]-labeled LPC amounts in SN in comparison to pure TM. (A) LPC C14:0, (B) LPC C16:0, (C) LPC C16:1, (D) LPC C18:0, (E) LPC C18:1, (F) LPC C18:2 (G) LPC C18:3.

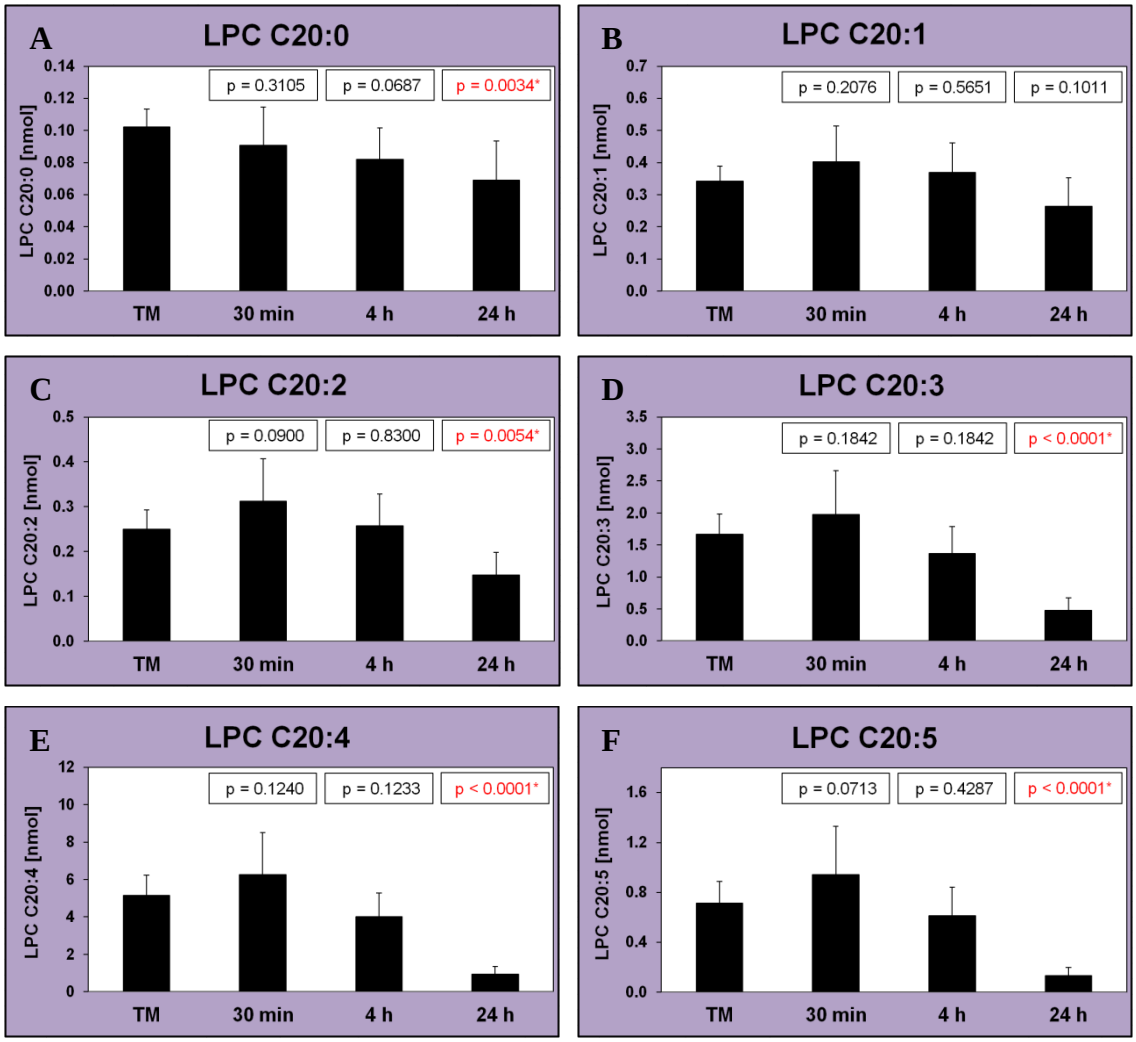

Figure 8: Lysophosphatidylcholine (LPC) species (in nmol) with C_{20} fatty acyl groups distinguished by their degree of unsaturation in pure Trial Medium (TM) or in cell culture supernatant (SN) from cultivated primary human myotubes previously stimulated for 30 minutes (30 min), 4 hours (4 h) or 24 hours (24 h) with 100 µM L-carnitine and 125 µM [$^{13}C_{16}$]palmitate in 15 ml Trial Medium. Detected LPC species with a C_{20} acyl group are LPC C20:0 (A), LPC C20:1 (B), LPC C20:2 (C), LPC C20:3 (D), LPC C20:4 (E) and LPC C20:5 (F). Trial Medium was measured in quintuplicate ($n_{TM} = 5$), primary human myotubes from 12 different individuals were examined for the 4-hour and the 24-hour stimulation periods in duplicate ($n_{SN} = 24$) but the myotubes of two dishes of the 30-minute stimulation showed fungal contaminations ($n_{SN} = 22$). Differences of LPC amounts between pure Trial Medium and supernatants were analyzed using unpaired Student's *t*-tests for every pair in JMP®. Results are expressed as mean ± standard deviation.

The kinetics of LPC species with acyl chains constituted of 22 carbon atoms, depicted in **Figure 9**, differ depending on their degree of unsaturation: While the species LPC C22:0 (**Figure 9** A), LPC C22:1 (**Figure 9** B) and LPC C22:3 (**Figure 9** C) with a low number of double bonds do not significantly change over time, the species with more double bonds LPC C22:4 (**Figure 9** D), LPC C22:5 (**Figure 9** E) and LPC C22:6 (**Figure 9** F) diminish significantly (p*) after 4 hours of stimulation and very highly significantly ($p < 0.0001$*) after 24 hours.

In pure Trial Medium, negligible amounts of [^{13}C]-labeled LPCs are detected (as discussed in **9.2**). Labeled [^{13}C]LPCs are also found in significant amounts in the supernatants of the cultivated cells indicating incorporation of the labeled palmitate and release of the labeled LPCs. The seven [^{13}C]-labeled LPC species found in supernatants ([$^{13}C_{14}$]LPC C14:0, [$^{13}C_{16}$]LPC C16:0, [$^{13}C_{16}$]LPC C16:1, [$^{13}C_{16}$]LPC C18:0, [$^{13}C_{18}$]LPC C18:0, [$^{13}C_{16}$]LPC C18:1 and [$^{13}C_{18}$]LPC C18:1) are illustrated by orange columns in the respective diagrams of **Figure 7**. The kinetics of [^{13}C]-labeled LPCs will be discussed in detail in the following chapter (see **Figure 18** and **Figure 19**).

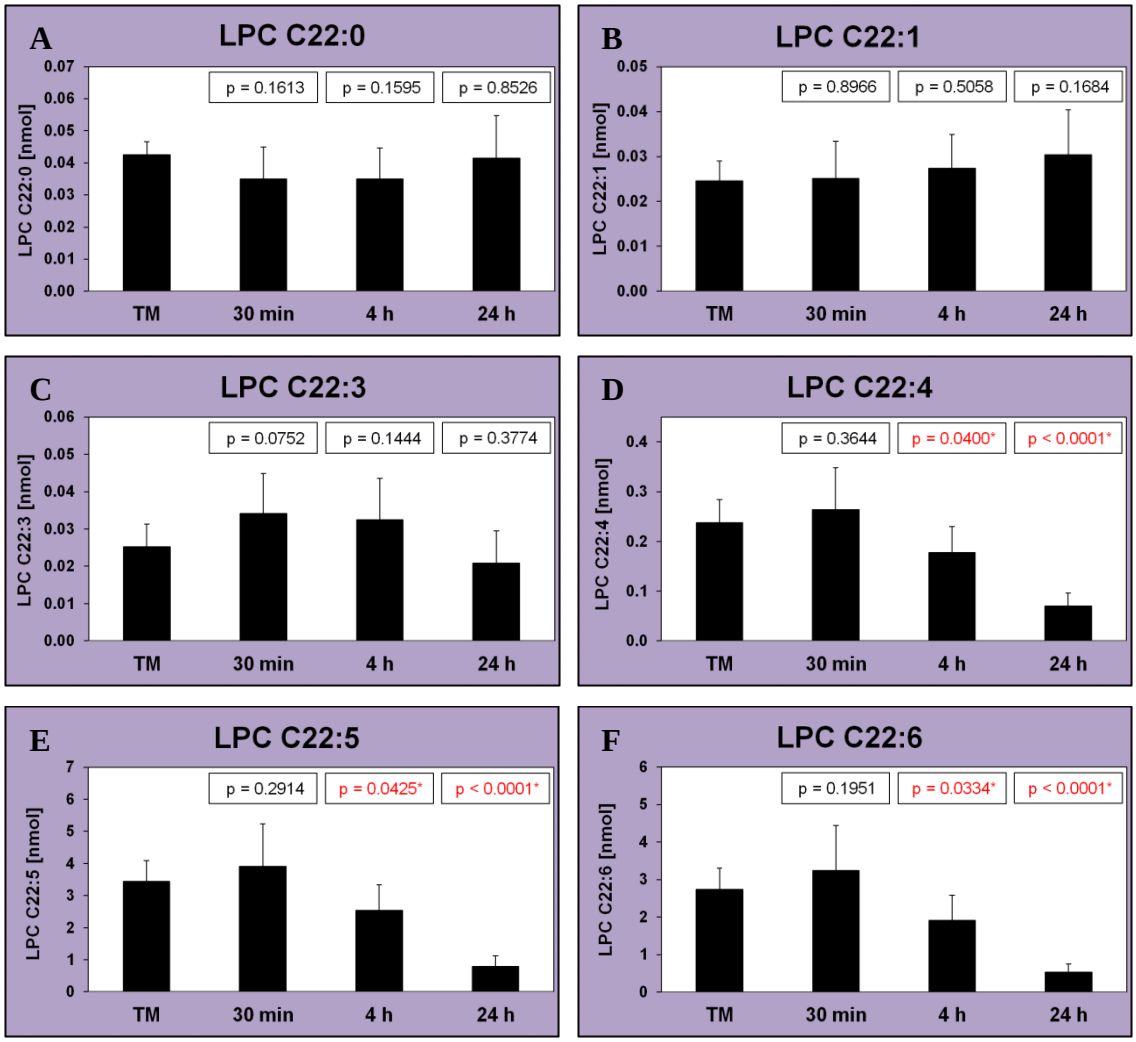

Figure 9: Comparison of the amounts of lysophosphatidylcholine (LPC) species (in nmol) with an acyl chain constituted of 22 carbon atoms in pure Trial Medium (TM) *versus* cell culture supernatants (SN). Quintuplicate analysis of the Trial Medium was performed ($n_{TM} = 5$), supernatants were obtained from cultivated primary human myotubes from 12 different subjects in duplicate ($n_{SN} = 24$ for the 4-hour and the 24-hour stimulation periods but $n_{SN} = 22$ for the 30-minute stimulation period because of fungal contaminations in two cell culture dishes). Human myotubes were stimulated with 100 µM L-carnitine plus 125 µM [$^{13}C_{16}$]palmitate in 15 ml Trial Medium for 30 minutes (30 min), 4 hours (4 h) or 24 hours (24 h) prior to aspiration of the supernatants. LPC species with C_{22} acyl groups differing in the number of double bonds were specified as LPC C22:0 (A), LPC C22:1 (B), LPC C22:3 (C), LPC C22:4 (D), LPC C22:5 (E) and LPC C22:6 (F). Differences of the amounts of the individual LPC species between pure Trial Medium and supernatants were examined by unpaired Student's *t*-tests for every pair in JMP® and results are given as p-values. Data represent the mean ± standard deviation.

3.2 Lysophosphatidylcholines in cell lysate and supernatant

LPC amounts from both cell lysates and supernatants of cultivated primary human myotubes were referred to the protein mass determined in the corresponding cell lysate for analysis of LPC time course changes after stimulation of the myotubes with 100 µM L-carnitine and 125 µM [$^{13}C_{16}$]palmitate for 30 minutes, 4 hours or 24 hours.

Time course kinetics of total LPC concentrations (in pmol/mg protein) in cell lysate (**Figure 10** A and **Figure 10** C), cell culture supernatant (**Figure 10** B and **Figure 10** D) or cell lysate plus supernatant (**Figure 10** E) are separately depicted for [^{12}C]LPCs (black columns) and [^{13}C]LPCs (colorful columns) with **Figure 10** A and **Figure 10** B showing the results of significance tests between the sums of [^{12}C]LPCs plus [^{13}C]LPCs of the different stimulation periods and **Figure 10** C, **Figure 10** D and **Figure 10** E separately showing the results of significance tests between either [^{12}C]LPCs (black lines) or [^{13}C]LPCs (colorful lines) of the different stimulation periods.

Unlabeled [^{12}C]LPCs and (labeled) [^{13}C]LPCs show fundamentally different profiles: Whilst total [^{12}C]LPCs highly significantly decrease after 24 hours of stimulation in both cell lysates (*vs*. 4-hour stimulation: p**) and supernatants (*vs*. 30-minute stimulation: p****, *vs*. 4-hour stimulation: p***), [^{13}C]-labeled LPC species show a continuous highly significant increase in cell lysates (*vs*. 30-minute and *vs*. 4-hour stimulations: p**) and supernatants (always $p < 0.0001$* for all comparisons). As the sums of total [^{12}C]LPCs plus total [^{13}C]LPCs in cell lysates (**Figure 10** A) significantly increase after 4 hours (*vs*. 30-minute stimulation) remaining unaltered after 24 hours (*vs*. 4-hour stimulation: $p = 0.9740$), the highly significant decrease of [^{12}C]LPCs in cell lysates after 24 hours (*vs*. 4-hour stimulation; **Figure 10** C) seems to be compensated by the highly significant increase of [^{13}C]LPCs in cell lysates after 24 hours (**Figure 10** C). As opposed to this, the very highly significant decrease of [^{12}C]LPCs in supernatants after 24 hours (**Figure 10** D) is not adequately compensated by the very highly significant increase of [^{13}C]LPCs (**Figure 10** D), as the sums of total [^{12}C]LPCs plus total [^{13}C]LPCs in supernatants (**Figure 10** B) also very highly significantly (p***) decrease after 24 hours. Altogether, the sums of total [^{12}C]LPCs plus total [^{13}C]LPCs intracellularly show a significant increase after 4 hours of stimulation (**Figure 10** A) and extracellularly a very highly significant decrease after 24 hours (**Figure 10** B).

Similarly, [^{12}C]LPCs tend to be increased after 4 hours in cell lysates (**Figure 10** C) but not in supernatants (p = 0.8425; **Figure 10** D).

As the LPC concentrations in supernatant are more than 20-fold greater than those in cell lysate, the changes of the total sum of both intra- and extracellular LPC concentrations (**Figure 10** E) largely reflect the results from supernatant (**Figure 10** D).

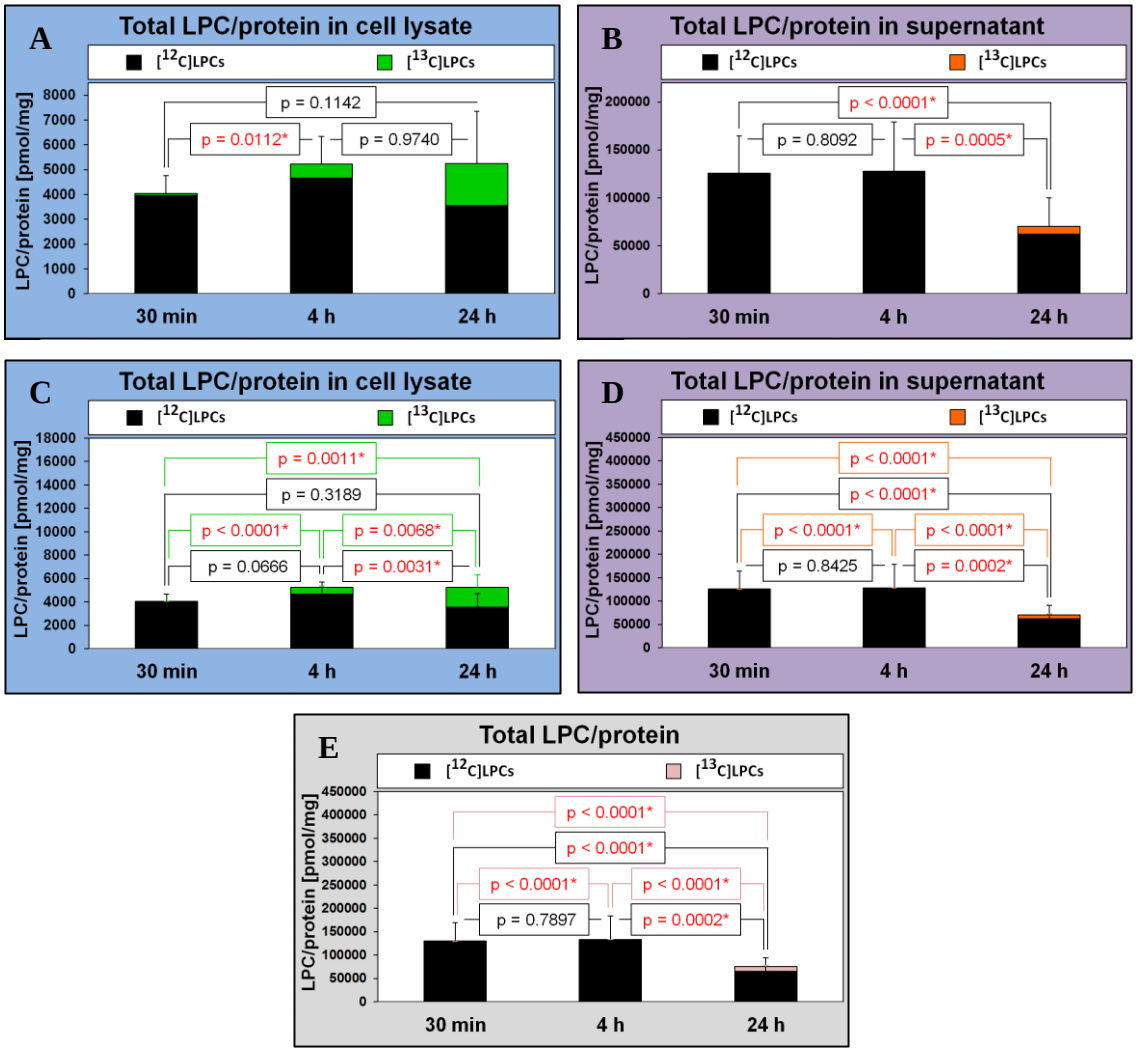

Figure 10: Total concentrations of all lysophosphatidylcholine (LPC) species detected in cell lysates (A and C), supernatants (B and D) or cell lysates plus supernatants (E) from cultivated primary human myotubes of 10 different individuals (n = 10). Stimulation of the human myotubes with 100 µM L-carnitine and 125 µM [$^{13}C_{16}$]palmitate for 30 minutes (30 min), 4 hours (4 h) or 24 hours (24 h) proceeded to isolation of LPCs from cell lysates and supernatants. LPC concentrations are depicted in pmol LPC/mg protein and represent the mean ± standard deviation. [^{12}C]LPCs are illustrated in black, [^{13}C]LPCs in color. Pairwise Student's *t*-tests were applied in JMP® for analysis of the changes between the different stimulation periods investigating the sums of total [^{12}C]LPCs plus total [^{13}C]LPCs (A and B) or investigating the total concentrations of either [^{12}C]LPCs or [^{13}C]LPCs (C, D and E).

Comparative species-specific profiling of all individual LPC species reveals LPC C16:0, LPC C18:0 and LPC C18:1 as the most abundant species in both cell lysates (**Figure 11** A) and supernatants (**Figure 11** B). Mid-level concentrations are observed for LPC C16:1 and LPC C20:4. The concentrations of LPC C14:0, LPC C18:2, LPC C20:3, LPC C20:5, LPC C22:5 and LPC C22:6 are slightly lower and very low concentrations are measured for LPC C14:1, LPC C18:3, LPC C20:0, LPC C20:1, LPC C20:2, LPC C22:0, LPC C22:1, LPC C22:3 and LPC C22:4.

Out of the 20 different [^{12}C]-species detected in total 18 (90 %) are detected both intra- and extracellularly. LPC C14:1 is exclusively monitored in cell lysates and LPC C22:0 only in supernatants with both compounds being of vanishingly low abundance.

All 7 [^{13}C]-species, which are [$^{13}C_{14}$]LPC C14:0, [$^{13}C_{16}$]LPC C16:0, [$^{13}C_{16}$]LPC C16:1, [$^{13}C_{16}$]LPC C18:0, [$^{13}C_{18}$]LPC C18:0, [$^{13}C_{16}$]LPC C18:1 and [$^{13}C_{18}$]LPC C18:1, emerge in cell lysates and supernatants but their appearance is to some extent delayed in supernatants.

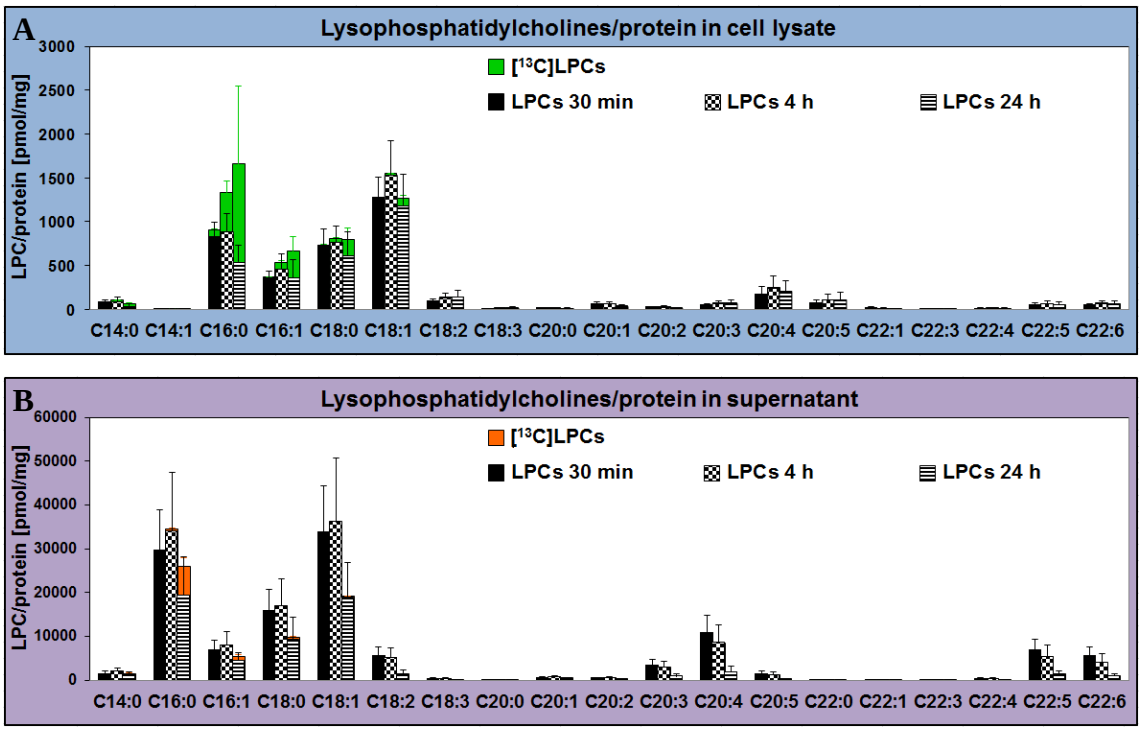

Figure 11: Comparison of the concentrations (in pmol LPC/mg protein) of all individual lysophosphatidylcholine (LPC) species isolated from cell lysates (A) and supernatants (B) of primary human myotubes previously stimulated with 100 µM L-carnitine and 125 µM [$^{13}C_{16}$]palmitate for 30 minutes (30 min), 4 hours (4 h) or 24 hours (24 h). Human myotubes from 10 different donors were included in the analysis (n = 10). Concentrations of the 30-min *stimuli* are demonstrated as filled columns, those of the 4-h *stimuli* in checker and those of the 24-h *stimuli* in stripes. [^{12}C]LPCs are shown in black, [^{13}C]LPCs in color. Data are presented as mean ± standard deviation.

Figure 12 individually illustrates the kinetics of both intra- and extracellular LPC species whose fatty acyl chains are composed of 14 or 16 carbon atoms. Considering unlabeled [^{12}C]LPCs, the comparison of the concentrations after 24-hour *versus* 4-hour stimulation reveals reduced concentrations after 24 hours for all species of this category with intracellular LPC C16:1 (**Figure 12** F) marginally missing the significance, whereas intracellular LPC C14:0 (**Figure 12** A; p***), extracellular LPC C14:0 (**Figure 12** B; p**), intracellular LPC C14:1 (**Figure 12** C; p**), intracellular LPC C16:0 (**Figure 12** D; p****), extracellular LPC C16:0 (**Figure 12** E; p**) and extracellular LPC C16:1 (**Figure 12** G; p***) show a highly significant decline. The comparison of the concentrations after 24-hour *versus* 30-minute stimulation also uncovers significant declines after 24 hours of stimulation for intracellular LPC C14:0 (p***), intracellular LPC C14:1 (p*), intracellular LPC C16:0 (p**), extracellular LPC C16:0 (p***) and extracellular LPC C16:1 (p**). Extracellular LPC C14:0 significantly increases after 4 hours of stimulation in comparison to the 30-minute time point.

In contrast, [^{13}C]-labeled LPC species show opposed time course changes continuously increasing over time with [$^{13}C_{14}$]LPC C14:0 accounting for approximately 30 % of total [^{12}C+^{13}C]LPC C14:0, [$^{13}C_{16}$]LPC C16:0 accounting for approximately 67 % of total [^{12}C+^{13}C]LPC C16:0 and [$^{13}C_{16}$]LPC C16:1 accounting for approximately 46 % of total [^{12}C+^{13}C]LPC C16:1 in cell lysates after 24 hours of stimulation.

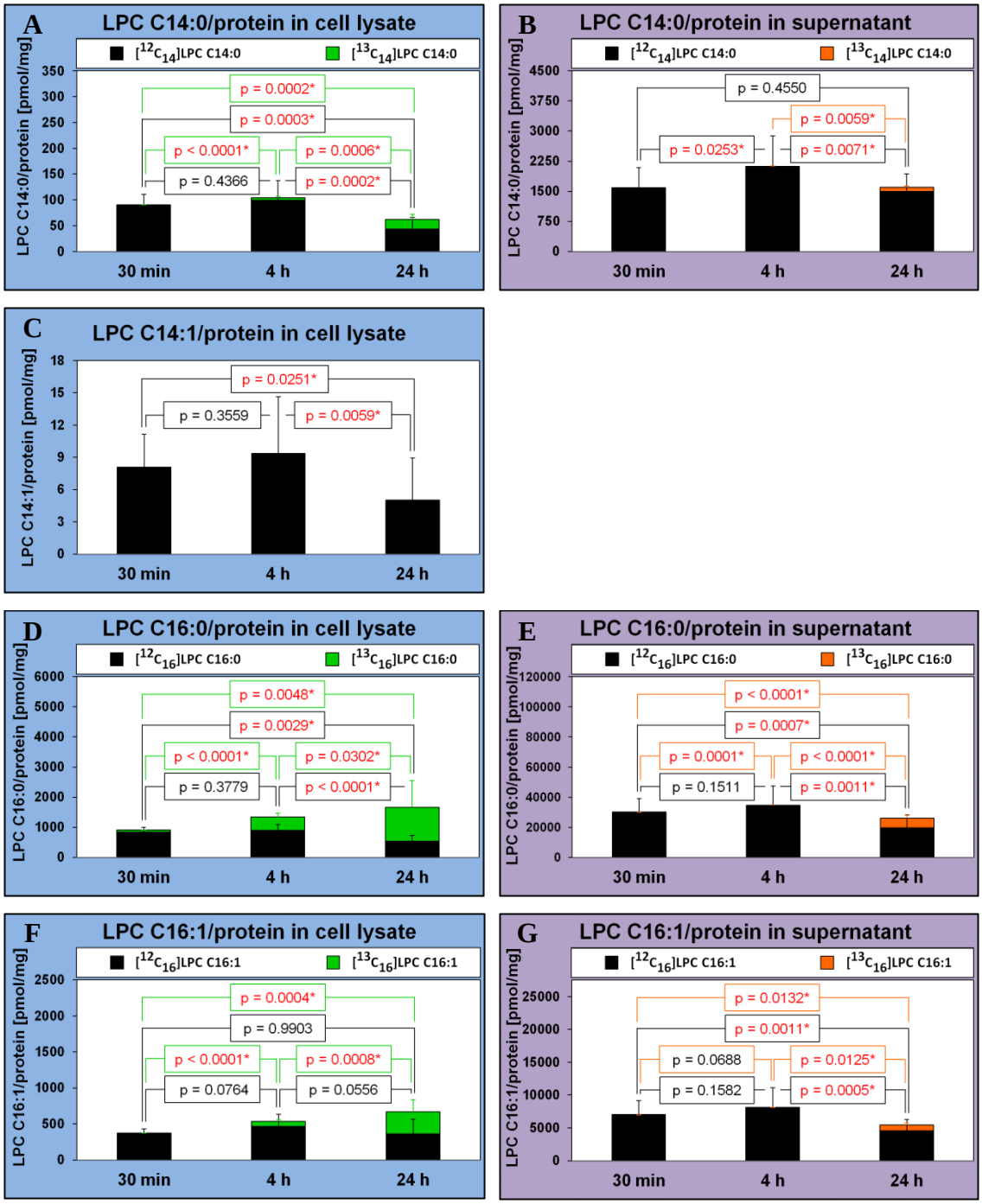

Figure 12: Time course demonstration of concentrations of lysophosphatidylcholine (LPC) species (in pmol LPC/mg protein) with fatty acyl groups containing 14 or 16 carbon atoms: LPC C14:0 (A + B), LPC C14:1 (C), LPC C16:0 (D + E) and LPC C16:1 (F + G). LPCs were isolated from both cell lysates (A, C, D and F) and supernatants (B, E and G) of primary human myotubes from 10 different subjects (n = 10). Stimulation of myotubes with 100 µM L-carnitine and 125 µM [$^{13}C_{16}$]palmitate was performed for 30 minutes (30 min), 4 hours (4 h) or 24 hours (24 h). [^{12}C]LPCs are illustrated in black, [^{13}C]LPCs in green (cell lysates) or orange (supernatants). Concentrations are shown as mean ± standard deviation. Differences of LPC concentrations between the stimulation periods were examined by pairwise Student's *t*-tests in JMP®, the results are indicated as p-values.

Time course studies of the concentrations of the C_{18} acyl group-containing LPC species stimulating for 30 minutes, 4 hours or 24 hours with 100 µM L-carnitine and 125 µM [$^{13}C_{16}$]palmitate are depicted in **Figure 13** in both cell lysates and supernatants. Kinetics of the [^{12}C]LPC species indicate basically different shifts between cell lysates and supernatants: Whereas intracellular LPC C18:2 (**Figure 13** E; p*) and intracellular LPC C18:3 (**Figure 13** G; p*) show significantly increased concentrations after 4 hours (*versus* 30 minutes) of stimulation and intracellular LPC C18:1 (**Figure 13** C) an analog trend, all extracellular [^{12}C]-species of this category show very highly significant decreases after 24 hours or more specifically LPC C18:0 (**Figure 13** B; *vs*. 30 min: p****, *vs*. 4 h: p***), LPC C18:1 (**Figure 13** D; *vs*. 30 min: p****, *vs*. 4 h: p ***), LPC C18:2 (**Figure 13** F; *vs*. 30 min: p****, *vs*. 4 h: p****) and LPC C18:3 (**Figure 13** H; *vs*. 30 min: p****, *vs*. 4 h: p***). Intracellular LPC C18:0 (**Figure 13** A) and LPC C18:1 decrease after 24 hours against 4-hour stimulations (LPC C18:0: p*; LPC C18:1: p**) but not against 30-minute stimulations.

Both [^{13}C]LPC C18:0 (**Figure 13** A and B) and [^{13}C]LPC C18:1 (**Figure 13** C and D) increase with time intra- and extracellularly but to a lesser extent than [^{13}C]LPC C16:0 and [^{13}C]LPC C16:1 (**Figure 12**): After 24 hours of stimulation [^{13}C]LPC C18:0 accounts for approximately 21.8 % of total [^{12}C+^{13}C]LPC C18:0 in cell lysates and for 5.7 % of total [^{12}C+^{13}C]LPC C18:0 in supernatants as does [^{13}C]LPC C18:1 for approximately 6.8 % of total [^{12}C+^{13}C]LPC C18:1 in cell lysates and for 1.5 % of total [^{12}C+^{13}C]LPC C18:1 in supernatants. Notably, both [$^{13}C_{16}$]- and [$^{13}C_{18}$]-labeled C_{18} acyl group-containing LPC species are detected. Differences of [^{13}C]-species between different stimulation periods shown in **Figure 13** refer to the sums of the [$^{13}C_{16}$]- plus the analog [$^{13}C_{18}$]-derivatives. Unraveled analyses of [$^{13}C_{16}$]C_{18} *versus* [$^{13}C_{18}$]C_{18} acyl chain-containing LPC species are depicted in **Figure 19** separately showing all [^{13}C]-species in detail as they are in some cases barely distinguishable in the illustrations of total LPC concentrations.

Extracellular appearance of [^{13}C]-labeled C_{18} acyl group-containing species is delayed with [$^{13}C_{16}$]LPC C18:0 (**Figure 13** B) emerging after 4 hours and [$^{13}C_{18}$]LPC C18:0 (**Figure 13** B), [$^{13}C_{16}$]LPC C18:1 (**Figure 13** D) and [$^{13}C_{18}$]LPC C18:1 (**Figure 13** D) emerging after 24 hours of stimulation in supernatants.

Labeled [^{13}C]LPC C18:2 or [^{13}C]LPC C18:3 are not detected.

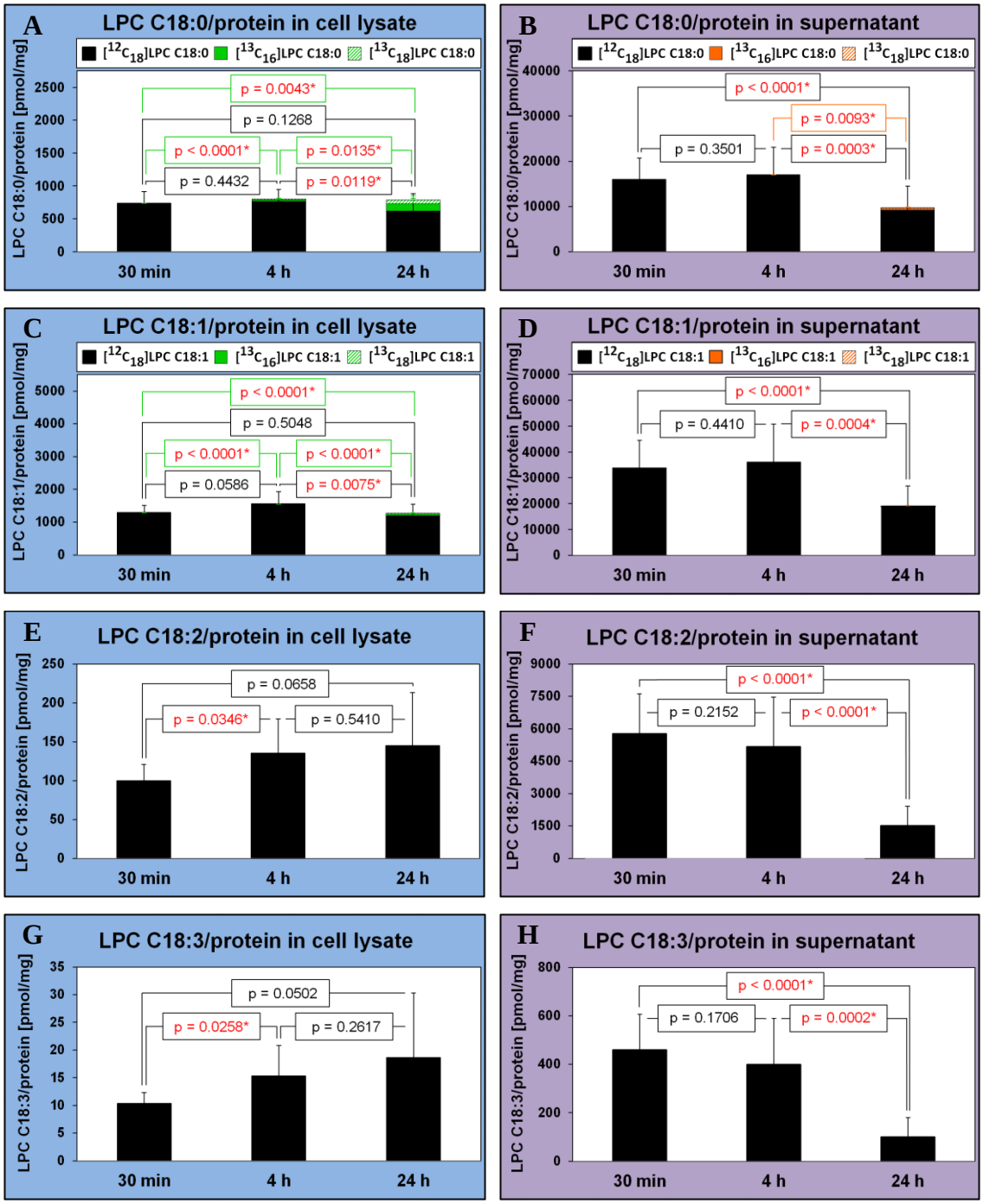

Figure 13: Comparison of the time course changes of the concentrations of the C_{18} fatty acyl group-containing LPC species LPC C18:0 (A + B), LPC C18:1 (C + D), LPC C18:2 (E + F) and LPC C18:3 (G + H) in cell lysates (A, C, E and G) *versus* supernatants (B, D, F and H) of primary human myotubes from 10 different donors (n = 10). Prior to LPC isolation, myotubes were stimulated with 100 µM L-carnitine and 125 µM [$^{13}C_{16}$]palmitate for 30 minutes (30 min), 4 hours (4 h) or 24 hours (24 h). Concentrations are expressed as pmol LPC/mg protein and represent the mean ± standard deviation. Pairwise Student's *t*-tests were used for analysis of the differences between different stimulation periods. Black columns demonstrate [^{12}C]LPC concentrations, green (cell lysates) and orange (supernatants) columns concentrations of [^{13}C]LPC species.

The comparison of the time course changes of the species LPC C20:0 (**Figure 14** A and B), LPC C20:1 (**Figure 14** C and D) and LPC C20:2 (**Figure 14** E and F) implicating C_{20} acyl groups with few double bonds on the one hand with the polyunsaturated species LPC C20:3 (**Figure 15** A and B), LPC C20:4 (**Figure 15** C and D) and LPC C20:5 (**Figure 15** E and F) on the other hand unveils differences concerning the intracellular kinetics: While significant decreases after 24 hours are found for intracellular LPC C20:1 (**Figure 14** C; *vs*. 30 min: p***, *vs*. 4 h: p***) and intracellular LPC C20:2 (**Figure 14** E; *vs*. 30 min: p**, *vs*. 4 h: p**) as well as a respective trend for intracellular LPC C20:0 (**Figure 14** A), significant increments after 4 hours and partly after 24 hours of stimulation are featured by the polyunsaturated intracellular species LPC C20:3 (**Figure 15** A; 30 min *vs*. 4 h: p**; 30 min *vs*. 24 h: p*), LPC C20:4 (**Figure 15** C; 30 min *vs*. 4 h: p*) and LPC C20:5 (**Figure 15** E; 30 min *vs*. 4 h: p**). LPC C20:2 does show both a trend to be increased after 4 hours and a highly significant decline after 24 hours (p**).

Extracellular kinetics also exhibit distinct declines in the course of time with polyunsaturated extracellular species showing an earlier and more pronounced decrease: LPC C20:3 (**Figure 15** B; 30 min *vs*. 4 h: p*), LPC C20:4 (**Figure 15** D; 30 min *vs*. 4 h: p*) and LPC C20:5 (**Figure 15** F; 30 min *vs*. 4 h: p*) are already significantly decreased after 4 hours, but LPC C20:0 (**Figure 14** B), LPC C20:1 (**Figure 14** D) and LPC C20:2 (**Figure 14** F) are not. All extracellular C_{20} acyl group-containing species are consistently decreased after 24 hours or more specifically LPC C20:0 (*vs*. 30 min: p*, *vs*. 4 h: p*), LPC C20:1 (*vs*. 30 min: p***, *vs*. 4 h: p***), LPC C20:2 (*vs*. 30 min: p****, *vs*. 4 h: p***), LPC C20:3 (*vs*. 30 min: p****, *vs*. 4 h: p***), LPC C20:4 (*vs*. 30 min: p****, *vs*. 4 h: p****) and LPC C20:5 (*vs*. 30 min: p****, *vs*. 4 h: p***).

Labeled [^{13}C]C_{20} acyl group-containing species are not detected.

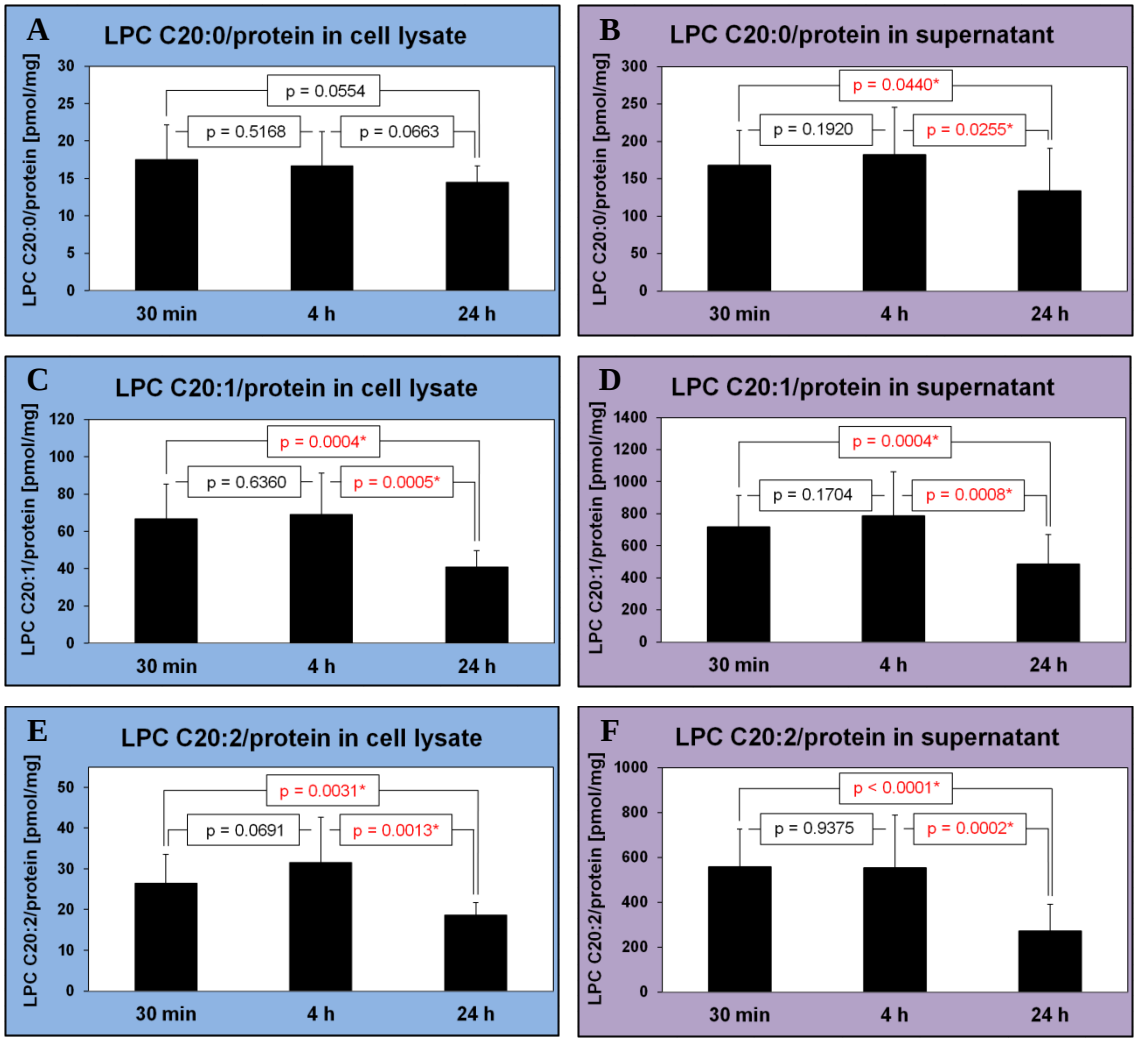

Figure 14: Graphical representation of the concentrations of LPC C20:0 (A + B), LPC C20:1 (C + D) and LPC C20:2 (E + F) in pmol referred to mg of protein after stimulation of primary human myotubes from 10 different individuals (n = 10) for 30 minutes (30 min), 4 hours (4 h) or 24 hours (24 h) with 100 µM L-carnitine plus 125 µM [$^{13}C_{16}$]palmitate. Lysophosphatidylcholines (LPC) were isolated from both cell lysates (A, C and E) and supernatants (B, D and F). Data are demonstrated as mean ± standard deviation and p-values are the results of pairwise Student's *t*-tests in JMP®.

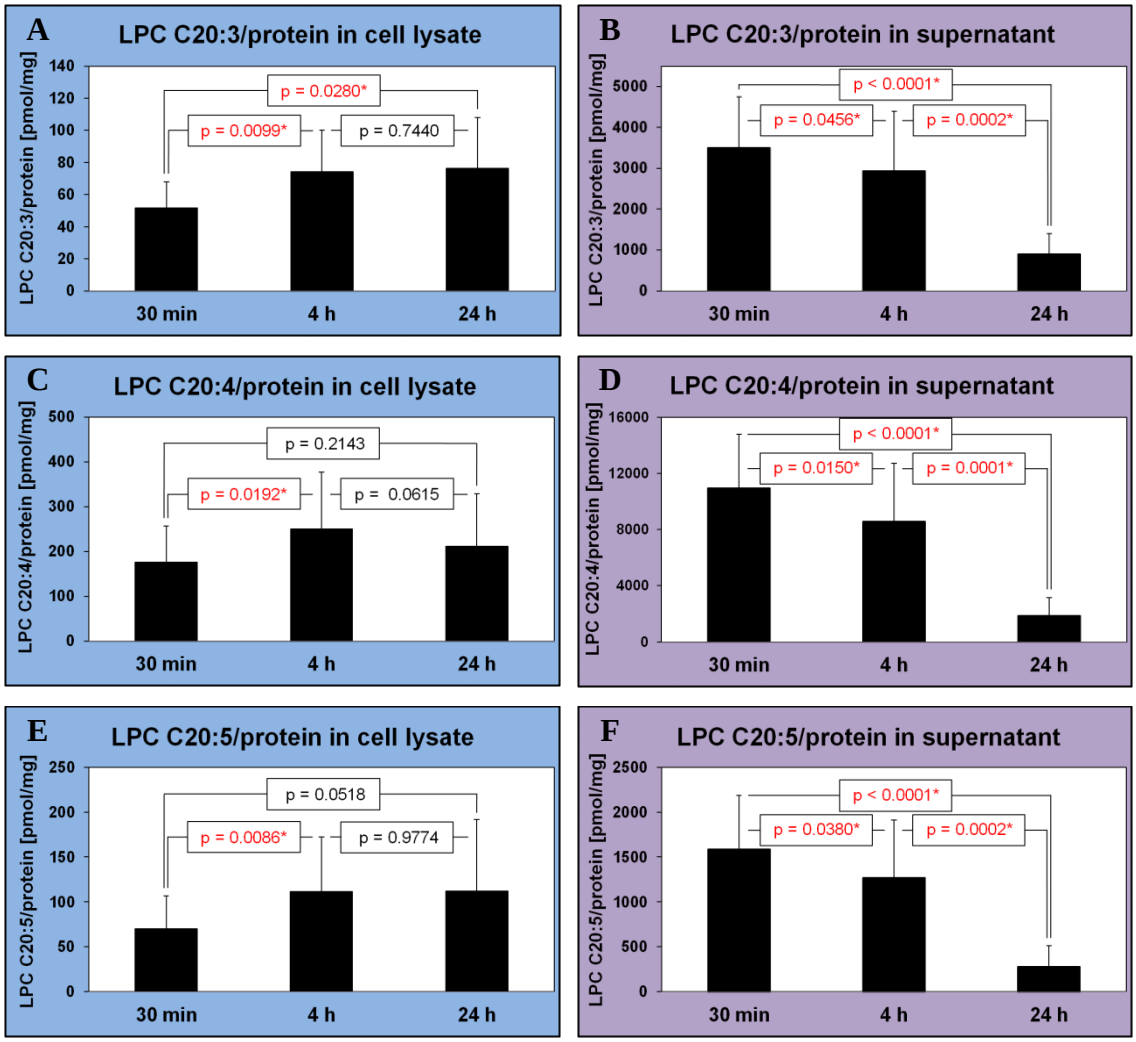

Figure 15: Concentrations of the lysophosphatidylcholine (LPC) species LPC C20:3 (A + B), LPC C20:4 (C + D) and LPC C20:5 (E + F) (in pmol/mg protein in cell lysate) as a result of the stimulation of primary human myotubes with 100 µM L-carnitine and 125 µM [$^{13}C_{16}$]palmitate for 30 minutes (30 min), 4 hours (4 h) or 24 hours (24 h). LPC species were isolated from both cell lysates (A + C + E) and supernatants (B + D + F) of myotubes from 10 different subjects (n = 10). Columns plus error bars represent the means and standard deviations of the concentrations. Significance of changes was tested using pairwise Student's *t*-tests in JMP®.

As mentioned above for the C_{20} acyl group-containing LPC species (**Figure 14** and **Figure 15**), LPC species containing C_{22} acyl groups (**Figure 16** and **Figure 17**) also show different intra- and extracellular time course changes depending on their degree of unsaturation. Intracellularly, the higher the degree of unsaturation the weaker the decrease of the concentrations in the course of time and the higher the increases after 4 hours: Intracellular LPC C22:1 (**Figure 16** B) significantly diminishes after 4 hours (*vs*. 30 min: p*) and after 24 hours (*vs*. 30 min: p**, *vs*. 4 h: p**) but intracellular LPC C22:3 (**Figure 16** D) only diminishes after 24 hours (*vs*. 30 min: p**, *vs*. 4 h: p***) and LPC C22:4 (**Figure 17** A) and LPC C22:5 (**Figure 17** C) exclusively diminish after 24 hours when compared with the 4-hour *stimuli* (LPC C22:4: p**; LPC C22:5: p*). Intracellular LPC C22:6 (**Figure 17** E) shows no decreases. *Vice versa*, intracellular LPC C22:1 and LPC C22:3 lack increases whereas significant augmentations are found after 4 hours for the polyunsaturated intracellular species LPC C22:4 (*vs*. 30 min: p*), LPC C22:5 (*vs*. 30 min: p*) and LPC C22:6 (*vs*. 30 min: p*). As mentioned above, intracellular LPC C22:0 is not detectable.

Extracellularly, mirror-inverted, the lower the degree of unsaturation the weaker the decrease of the concentrations in the course of time and the higher the increases after 4 hours: Significant declines between all stimulation periods are exhibited by the polyunsaturated extracellular species LPC C22:4 (**Figure 17** B; 30 min *vs*. 4 h: p*, 4 h *vs*. 24 h: p****, 30 min *vs*. 24 h: p****), LPC C22:5 (**Figure 17** D; 30 min *vs*. 4 h: p*, 4 h *vs*. 24 h: p***, 30 min *vs*. 24 h: p****) and LPC C22:6 (**Figure 17** F; 30 min *vs*. 4 h: p**, 4 h *vs*. 24 h: p***, 30 min *vs*. 24 h: p****) whereas LPC C22:0 (**Figure 16** A) and LPC C22:1 (**Figure 16** C) lack any decline and LPC C22:3 (**Figure 16** E) declines not before 24 hours of stimulation (*vs*. 30 min: p****, *vs*. 4 h: p***). *Vice versa*, polyunsaturated extracellular species do not increase whilst LPC C22:0 (p*) and LPC C22:1 (p**) are significantly elevated after 4 hours (*vs*. 30 minutes) of stimulation.

Labeled [^{13}C]C_{22} acyl group-containing species are not detected.

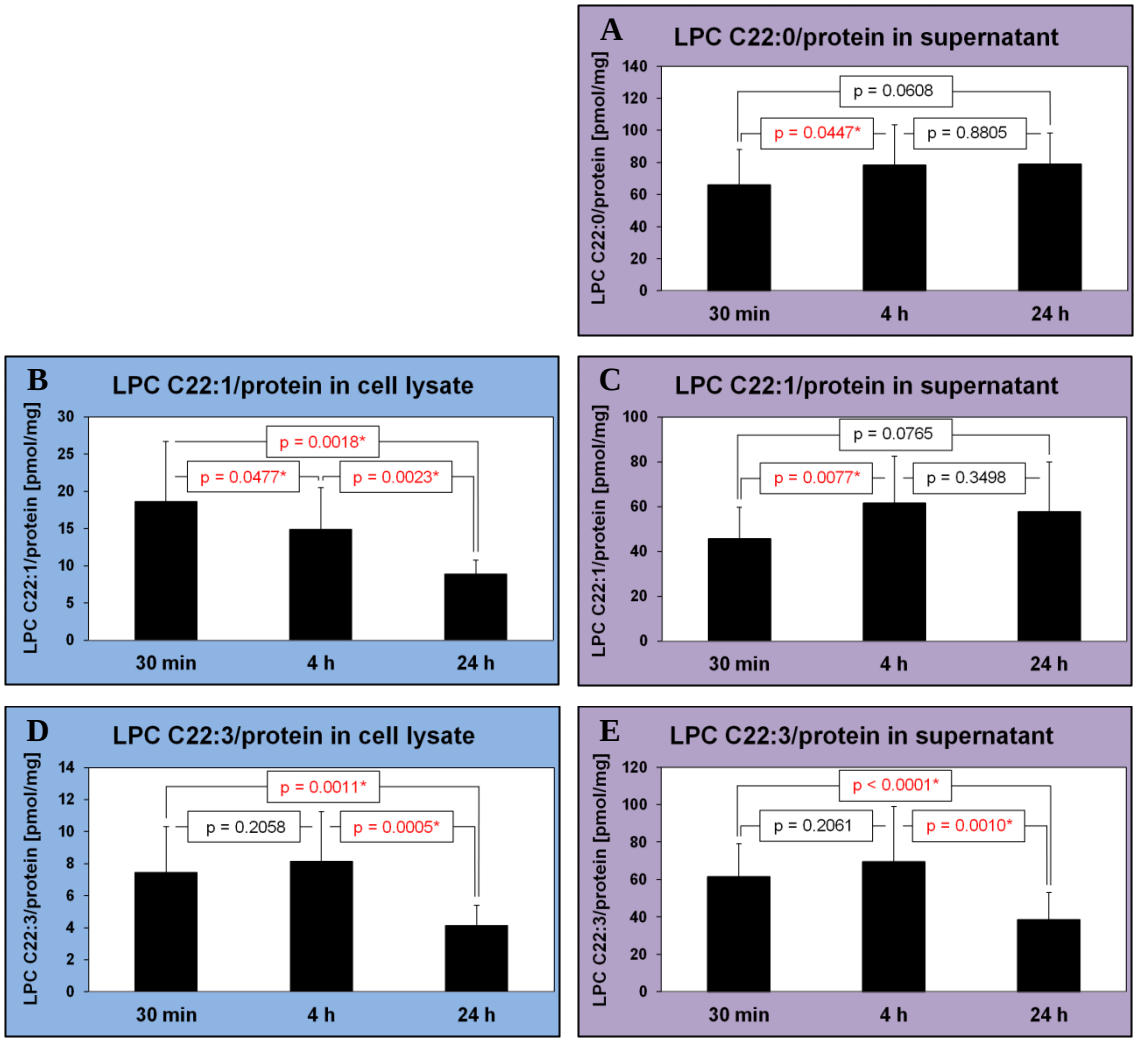

Figure 16: Time course study of the concentrations of the lysophosphatidylcholine (LPC) species LPC C22:0 (A), LPC C22:1 (B + C) and LPC C22:3 (D + E) (in pmol LPC/mg protein) in cell lysates (B + D) or supernatants (A + C + E) of primary human myotubes stimulated for 30 minutes (30 min), 4 hours (4 h) or 24 hours (24 h) with 100 µM L-carnitine and 125 µM [$^{13}C_{16}$]palmitate. Myotubes from 10 individuals were included in the analysis (n = 10). Data are expressed as mean ± standard deviation and differences between stimulation periods were analyzed by pairwise Student's *t*-tests in JMP®.

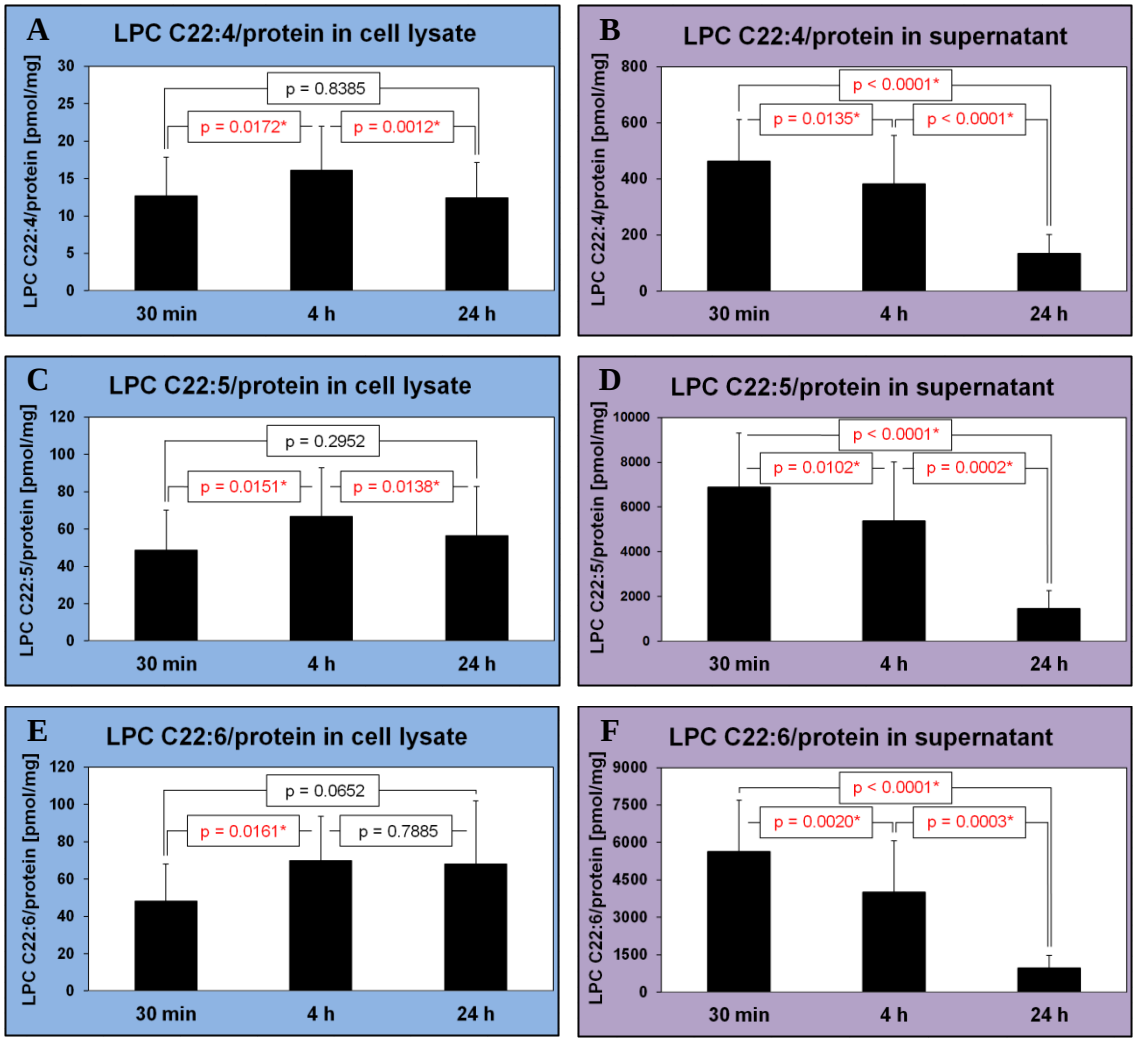

Figure 17: Comparison of the concentrations of the lysophosphatidylcholine (LPC) species LPC C22:4 (A + B), LPC C22:5 (C + D) and LPC C22:6 (E + F) (in pmol) in relation to the protein mass (in mg) in the cell lysates of cultivated primary human myotubes from 10 donors (n = 10). LPCs were isolated from cell lysates (A + C + E) and supernatants (B + D + F) of the myotubes after having them stimulated for 30 minutes (30 min), 4 hours (4 h) and 24 hours (24 h) with 100 µM L-carnitine and 125 µM [$^{13}C_{16}$]palmitate. Data are presented as mean ± standard deviation and p-values are the results of pairwise Student's *t*-tests in JMP® assessing the significance of the changes.

Since the concentrations of the [^{13}C]LPC species mostly are considerably lower than those of their unlabeled analogs, **Figure 18** and **Figure 19** separately illustrate the [^{13}C]LPC profiles. The by far most abundant [^{13}C]-compound in both cell lysate and supernatant is [$^{13}C_{16}$]LPC C16:0, followed by [$^{13}C_{16}$]LPC C16:1, [^{13}C]LPC C18:0, [^{13}C]LPC C18:1 and [$^{13}C_{14}$]LPC C14:0 in that order with [^{13}C]LPC C18:0 and [^{13}C]LPC C18:1 summing up the [$^{13}C_{16}$]- and [$^{13}C_{18}$]-derivatives, respectively. As depicted in these figures all [^{13}C]-labeled species continuously increase in the course of time both intracellularly and extracellularly.

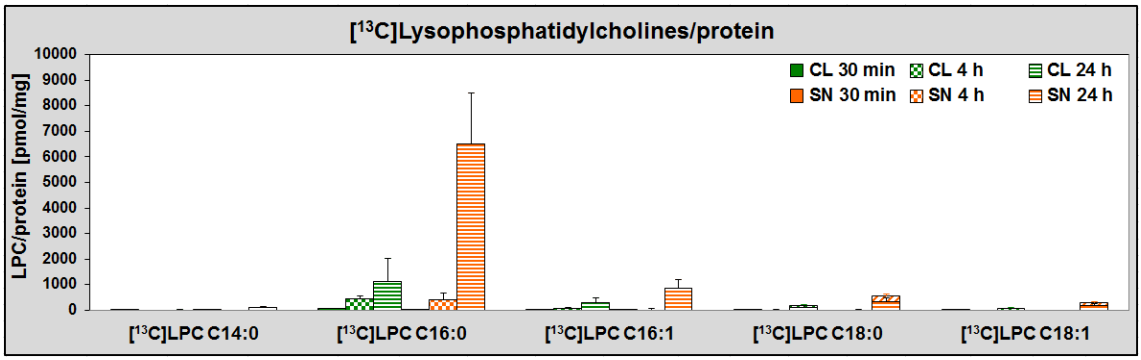

Figure 18: Visualization of the time course profile of all [^{13}C]-labeled lysophosphatidylcholine (LPC) species detected in cell lysates (CL; green columns) or supernatants (SN; orange columns) of primary human myotubes from 10 different subjects (n = 10) after stimulation with 100 µM L-carnitine plus 125 µM [$^{13}C_{16}$]palmitate for 30 minutes (30 min; filled columns), 4 hours (4 h; checkered columns) or 24 hours (24 h; striped columns). Concentrations are depicted in the unit pmol LPC/mg protein and represent the mean ± standard deviation.

Both total concentrations of all [^{13}C]-species and individual concentrations of the specific [^{13}C]-species permanently keep rising over time, intra- and extracellularly, as substantiated by **Figure 19**. Analyzing the total sums of all [^{13}C]-compounds (**Figure 19** A) in cell lysates (CL) *versus* supernatants (SN) reveals higher intracellular than extracellular levels after 30-minute (CL: 85 pmol/mg ± 14 pmol/mg; SN: 17 pmol/mg ± 8 pmol/mg) and 4-hour stimulation (CL: 570 pmol/mg ± 137 pmol/mg; SN: 461 pmol/mg ± 287 pmol/mg) but extracellular concentrations multiply exceed those in cell lysates after 24 hours. This observation is reflected by [$^{13}C_{16}$]LPC C16:0 (**Figure 19** C; CL(30 min): 69 pmol/mg ± 12 pmol/mg; SN(30 min): 14 pmol/mg ± 7 pmol/mg; CL(4 h): 441 pmol/mg ± 122 pmol/mg; SN(4 h): 404 pmol/mg ± 259 pmol/mg) but [$^{13}C_{16}$]LPC C16:1 (**Figure 19** D) does show higher intracellular concentrations after 4 hours (CL: 69 pmol/mg ± 24 pmol/mg; SN: 39 pmol/mg ± 24 pmol/mg) but lower intracellular concentrations not only after 24-hour stimulation period but also after 30 minutes (CL: 8 pmol/mg ± 3 pmol/mg; SN: 10 pmol/mg ± 3 pmol/mg) and the extracellular concentration of [$^{13}C_{14}$]LPC C14:0 (**Figure 19** B) already beggars the intracellular concentration after 4 hours (CL: 5 pmol/mg ± 2 pmol/mg; SN: 16 pmol/mg ± 11 pmol/mg). [$^{13}C_{14}$]LPC C14:0 and [^{13}C]LPC C18:0 (specified as [$^{13}C_{16}$]LPC C18:0 plus [$^{13}C_{18}$]LPC C18:0 in **Figure 19** E) are not detected in supernatants after 30 minutes and [^{13}C]LPC C18:1 (specified as [$^{13}C_{16}$]LPC C18:1 plus [$^{13}C_{18}$]LPC C18:1 in **Figure 19** F) extracellularly appears not before 24 hours of stimulation.

Intracellularly, all detected [^{13}C]LPC species are already present after 30 minutes of stimulation subsequently increasing whereas emergence of the [^{13}C]-metabolites in supernatants is delayed for all species: After 30 minutes [$^{13}C_{16}$]LPC C16:0 is found in the supernatants of only 8 (out of the 10) donors, [$^{13}C_{16}$]LPC C16:1 of 4 donors and [$^{13}C_{14}$]LPC C14:0, [$^{13}C_{16}$]LPC C18:0, [$^{13}C_{18}$]LPC C18:0, [$^{13}C_{16}$]LPC C18:1 and [$^{13}C_{18}$]LPC C18:1 are not monitored at all. After 4 hours supernatants of all donors contain [$^{13}C_{16}$]LPC C16:0 and [$^{13}C_{16}$]LPC C16:1, but only 5 donors feature [$^{13}C_{16}$]LPC C18:0, 3 donors feature [$^{13}C_{14}$]LPC C14:0 and one single donor features [$^{13}C_{18}$]LPC C18:0. After 24 hours all [^{13}C]-species are detected in the supernatants of all donors' human myotubes with [$^{13}C_{16}$]LPC C18:1 and [$^{13}C_{18}$]LPC C18:1 not arising before. Consequently, results of the pairwise Student's *t*-tests have to be interpreted taking account of these missing values.

All (tendentially) significant time course alterations of total LPCs as well as of all specific [^{12}C]- and/or [^{13}C]-species in both cell lysates and supernatants are listed in **Table 12** in order to provide a patterned overview. As aforementioned this synopsis underlines the two principal findings of permanently increasing [^{13}C]LPC species on the one hand and decreasing [^{12}C]LPC species in the course of time on the other hand. Comparing the LPC amounts in the supernatants with those in pure Trial Medium, of the one part, and comparing the extracellular LPC concentrations (referred to the protein mass of the corresponding cell lysate) between the different stimulation periods, of the other part, yield congruent results.

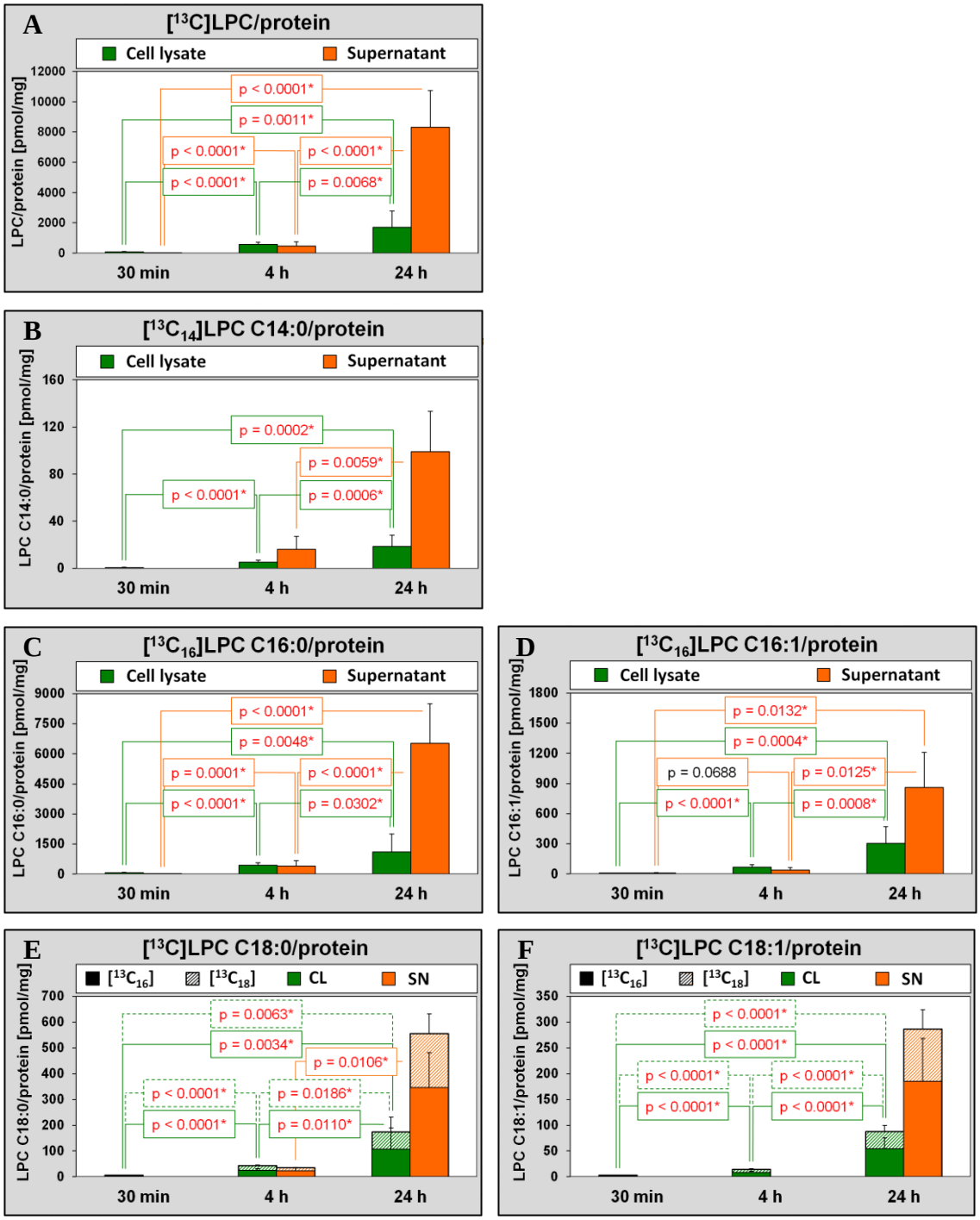

Figure 19: Time course changes of [^{13}C]lysophosphatidylcholines (LPC) isolated from both cell lysates (CL; green columns) and supernatants (SN; orange columns) of primary human myotubes (n = 10) stimulated for 30 minutes (30 min), 4 hours (4 h) or 24 hours (24 h) with 100 µM L-carnitine and 125 µM [$^{13}C_{16}$]palmitate. With regard to the LPC species with a C_{18} acyl group, results of species with a completely [^{13}C]-labeled acyl group ([$^{13}C_{18}$]LPC C18:0 and [$^{13}C_{18}$]LPC C18:1) are depicted by striped columns (and dashed lines), those of species with incompletely labeled acyl groups ([$^{13}C_{16}$]LPC C18:0 and [$^{13}C_{16}$]LPC C18:1) by filled columns. Diagrams show the concentrations (in pmol LPC/mg protein) of total [^{13}C]LPCs (A) as well as of the species [^{13}C]LPC C14:0 (B), [^{13}C]LPC C16:0 (C), [^{13}C]LPC C16:1 (D), [^{13}C]LPC C18:0 (E) and [^{13}C]LPC C18:1 (F) as means ± standard deviations. Differences between stimulation periods were analyzed applying pairwise Student's *t*-tests in JMP®.

Table 12: Schematic representation of the levels of significance (by arrows) and relative changes (by colors) in the LPC time course studies from cell lysates and supernatants of primary human myotubes stimulated with 100 µM L-carnitine and 125 µM [$^{13}C_{16}$]palmitate for 30 minutes (0.5 h), 4 hours (4 h) or 24 hours (24 h). Differences between the three different stimulation periods were examined by pairwise Student's *t*-tests in JMP® considering results from 10 donors. LPC amounts (in nmol) in the supernatants were also compared with those in pure Trial Medium (TM) with results from 12 donors being involved in analysis by means of unpaired Student's *t*-tests. Relative changes are elucidated by backgrounds colored with different intensities of green (relative increase > + 25 % | + 50 % | + 100 % | + 200 % | + 400 %) or red (relative decrease < - 20 % | - 33 % | - 50 % | - 67 % | - 80 %), respectively. The arrows reflect the level of significance with a parenthesized arrow showing relative decreases ((↓)) or relative increases ((↑)) with a tendency to statistical significance ($0.10 \geq p > 0.05$), one arrow showing significant ($0.05 \geq p > 0.01$), two arrows showing highly significant ($0.01 \geq p > 0.001$), three arrows showing very highly significant ($0.001 \geq p > 0.0001$) changes and four arrows showing decreases (↓↓↓↓) or increases (↑↑↑↑) with $p \leq 0.0001$. Crossed out boxes indicate unfeasible comparisons because of nonexistent values.

		CELL LYSATE			SUPERNATANT					
		4 h	24 h		0.5 h	4 h		24 h		
		vs. 0.5 h	*vs.* 0.5 h	*vs.* 4 h	*vs.* TM	*vs.* TM	*vs.* 0.5 h	*vs.* TM	*vs.* 0.5 h	*vs.* 4 h
Total [^{12}C]LPCs		(↑)		↓↓				↓↓↓	↓↓↓↓	↓↓↓
[^{12}C]LPCs + [^{13}C]LPCs		↑						↓↓	↓↓↓↓	↓↓↓
Total [^{13}C]LPCs		↑↑↑↑	↑↑	↑↑			↑↑↑↑		↑↑↑↑	↑↑↑↑
[^{12}C]LPC species	LPC C14:0		↓↓↓	↓↓↓	(↑)	↑	↑			↓↓
	LPC C14:1		↓	↓↓						
	LPC C16:0		↓↓	↓↓↓↓				↓	↓↓↓	↓↓
	LPC C16:1	(↑)		(↓)	(↑)				↓↓	↓↓↓
	LPC C18:0			↓				↓↓↓↓	↓↓↓↓	↓↓↓
	LPC C18:1	(↑)		↓↓				↓	↓↓↓↓	↓↓↓
	LPC C18:2	↑	(↑)		(↑)			↓↓↓↓	↓↓↓↓	↓↓↓↓
	LPC C18:3	↑	(↑)		(↑)			↓↓↓↓	↓↓↓↓	↓↓↓
	LPC C20:0		(↓)	(↓)		(↓)		↓↓	↓	↓
	LPC C20:1		↓↓↓	↓↓↓					↓↓↓	↓↓↓
	LPC C20:2	(↑)	↓↓	↓↓	(↑)			↓↓	↓↓↓↓	↓↓↓
	LPC C20:3	↑↑	↑				↓	↓↓↓↓	↓↓↓↓	↓↓↓
	LPC C20:4	↑		(↓)			↓	↓↓↓↓	↓↓↓↓	↓↓↓↓
	LPC C20:5	↑↑	(↑)		(↑)		↓	↓↓↓↓	↓↓↓↓	↓↓↓
	LPC C22:0						↑		(↑)	
	LPC C22:1	↓	↓↓	↓↓			↑↑		(↑)	
	LPC C22:3		↓↓	↓↓↓	(↑)				↓↓↓↓	↓↓↓
	LPC C22:4	↑		↓↓		↓	↓	↓↓↓↓	↓↓↓↓	↓↓↓↓
	LPC C22:5	↑		↓		↓	↓	↓↓↓↓	↓↓↓↓	↓↓↓
	LPC C22:6	↑	(↑)			↓	↓↓	↓↓↓↓	↓↓↓↓	↓↓↓
[^{12}C] + [^{13}C]	Total LPC C14:0		↓	↓↓	(↑)	↑	↑			↓
	Total LPC C16:0	↑↑	(↑)							↓
	Total LPC C16:1	↑	↑		(↑)				↓	↓↓
	Total LPC C18:0							↓↓↓↓	↓↓↓	↓↓↓
	Total LPC C18:1	(↑)		↓				↓	↓↓↓↓	↓↓↓
[^{13}C]LPC species	[$^{13}C_{14}$]LPC C14:0	↑↑↑↑	↑↑↑	↑↑↑						↑↑
	[$^{13}C_{16}$]LPC C16:0	↑↑↑↑	↑↑	↑			↑↑↑↑		↑↑↑↑	↑↑↑↑
	[$^{13}C_{16}$]LPC C16:1	↑↑↑↑	↑↑↑	↑↑↑			(↑)		↑	↑
	[$^{13}C_{16}$]LPC C18:0	↑↑↑↑	↑↑	↑						↑
	[$^{13}C_{18}$]LPC C18:0	↑↑↑↑	↑↑	↑						
	[$^{13}C_{16}$]LPC C18:1	↑↑↑↑	↑↑↑↑	↑↑↑↑						
	[$^{13}C_{18}$]LPC C18:1	↑↑↑↑	↑↑↑↑	↑↑↑↑						

3.3 Correlation analyses

Age, sex, lean body mass and body fat have been described as relevant covariates in several association studies [210-212]. Therefore, correlation analyses between logarithmically transformed sums of intra- or extracellular LPCs and anthropometrics of the donors were performed. In addition, potential associations of LPC concentrations were investigated with *in vivo* and *in vitro* parameters of lipid oxidation, insulin sensitivity and muscle lipid content with their determination being described in section **1.3.2** and their specifications being listed in **Table 10** plus **Table 11**.

3.3.1 Correlation analyses with anthropometric parameters

The investigation of a potential gender difference in LPC concentrations by unpaired Student's *t*-tests, whose results are depicted in **Supplemental Table 1**, reveals no single LPC species significantly differing between male and female donors.

Age, height, weight, WHR and LBM do not show any significant correlation with sums of unlabeled (^{12}C) or labeled (^{13}C) intra- or extracellular LPCs (**Table 13**).

Species-specific correlation analyses were also performed and are represented by color coding in the heat maps of **Table 20**, **Table 21** and **Table 22**. The significant results are shown in detail (r-values and p-values) in the Supplemental Data section.

In these species-specific analyses, no single significant association is found for height and LBM. Age exclusively correlates with extracellular [$^{13}C_{18}$]LPC C18:1 (24 h: r = - 0.65, p = 0.0406*) and intracellular LPC C22:3 but this latter association is confirmed for all three points in time (30 min: r = - 0.65, p = 0.0413*; 4 h: r = - 0.67, p = 0.0336*; 24 h: r = - 0.77, p = 0.0091*). WHR correlates at the time of 4 hours with extracellular LPC C22:0 (r = + 0.74, p = 0.0142*) and extracellular LPC C22:1 (r = + 0.66, p = 0.0397*) and weight solely correlates significantly with intracellular LPC C18:0 at the time of 30 minutes (r = + 0.77, p = 0.0092*) and at the time of 4 hours (r = + 0.69, p = 0.0258*).

Significant positive correlations of extracellular [^{13}C]LPCs after 30 minutes of [$^{13}C_{16}$]palmitate stimulation are found with BMI and PBF (**Table 13**) but no significant correlation is found with any specific extracellular [^{13}C]-species at this stimulation time point of 30 minutes (**Table 20**). PBF also correlates with total intracellular [^{12}C]LPCs at

the same time point (**Table 13**) with this positive correlation being retained in species-specific analysis for LPC C18:0 (r = + 0.82, p = 0.0038*; **Table 21**) and tendentially for LPC C16:0, LPC C18:1, LPC C18:2 and LPC C20:3. Intracellular LPC C18:0 (**Table 21**) also correlates with PBF at the time of 4 hours (r = + 0.78, p = 0.0073*) and 24 hours (r = + 0.84, p = 0.0023*) and with BMI at the time of 4 hours (r = + 0.91, p = 0.0003*) and 24 hours (r = + 0.76, p = 0.0113*) as well as a clear trend at the time of 30 minutes (r = + 0.63, p = 0.0519).
Moreover, PBF correlates positively with intracellular [$^{13}C_{18}$]LPC C18:0 after 30 minutes (r = + 0.69, p = 0.0279*), 4 hours (r = + 0.61, p = 0.0626) and 24 hours (r = + 0.67, p = 0.0339*) as illustrated in **Table 20**.

Notably, none of the extracellular [^{13}C]LPC species at the time of 30 minutes correlates with BMI ($p \geq 0.1872$; **Table 20**) although their sum does (r = + 0.68, p = 0.0441*; **Table 13**), whereas at the time of 24 hours extracellular [$^{13}C_{16}$]LPC C18:1 (r = - 0.71, p = 0.0220*) and extracellular [$^{13}C_{18}$]LPC C18:1 (r = - 0.65, p = 0.0428*) correlate with BMI (**Table 20**) although the sum of extracellular [^{13}C]LPC species at the time of 24 hours doesn't (r = - 0.19, p = 0.5960; **Table 13**).

The aerobic capacity $V(O_2)_{max}$ negatively correlates with total extracellular [^{13}C]LPCs after 30 minutes of [$^{13}C_{16}$]palmitate stimulation (**Table 13**). This negative association of $V(O_2)_{max}$ is confirmed in species-specific analysis (**Table 20**) for [$^{13}C_{16}$]LPC C16:0 (r = - 0.91, p = 0.0042*, n = 7) and tendentially for [$^{13}C_{16}$]LPC C16:1 (n = 3). By contrast, $V(O_2)_{max}$ positively correlates after 24 hours with extracellular [$^{13}C_{16}$]LPC C16:1 (r = + 0.70, p = 0.0509, n = 8) and extracellular [$^{13}C_{18}$]LPC C18:1 (r = + 0.75, p = 0.0324*, n = 8).

In conclusion, a consistent observation is the positive correlation of intracellular LPC C18:0 with parameters of body fat content.

Table 13: Correlation analyses between total concentrations of [^{12}C]- or [^{13}C]-labeled lysophosphatidylcholines (LPC) in cell lysates or supernatants of primary human myotubes after different stimulation periods and the anthropometric *in vivo* parameters age, height, weight, body mass index (BMI), waist-to-hip ratio (WHR), lean body mass (LBM), percentage of body fat (PBF) and maximal aerobic capacity ($V(O_2)_m$). Human myotubes from 10 different individuals (n = 10) were stimulated for 30 minutes (0.5), 4 hours (4) or 24 hours (24) with 100 µM L-carnitine and 125 µM [$^{13}C_{16}$]palmitate. LPC amounts were mass spectrometrically quantified and referred to the protein mass of the corresponding cell lysate. As Shapiro-Wilk W tests in JMP® revealed log-normal distributions for LPC concentrations and PBF, these variables were $\log_e$-transformed (ln) for utilization in correlation analyses.

		TP		Age	Height	Weight	BMI	WHR	LBM	PBF [ln]	$V(O_2)_m$
CELL LYSATE	[^{12}C]LPC	0.5	r	- 0.20	+ 0.22	+ 0.29	+ 0.17	- 0.13	- 0.17	+ 0.66	- 0.55
			p	0.5781	0.5406	0.4247	0.6487	0.7102	0.6433	0.0386	0.1581
			n	10	10	10	10	10	10	10	8
		4	r	+ 0.04	- 0.05	+ 0.30	+ 0.47	- 0.02	0.00	+ 0.48	- 0.24
			p	0.9216	0.8944	0.3956	0.1729	0.9626	0.9948	0.1556	0.5666
			n	10	10	10	10	10	10	10	8
		24	r	+ 0.11	- 0.10	+ 0.18	+ 0.32	- 0.40	- 0.10	+ 0.37	- 0.34
			p	0.7524	0.7860	0.6264	0.3697	0.2473	0.7733	0.2903	0.4057
			n	10	10	10	10	10	10	10	8
	[^{13}C]LPC	0.5	r	- 0.51	+ 0.22	+ 0.22	+ 0.09	+ 0.17	+ 0.12	+ 0.20	- 0.32
			p	0.1302	0.5432	0.5477	0.8114	0.6296	0.7511	0.5787	0.4444
			n	10	10	10	10	10	10	10	8
		4	r	+ 0.27	- 0.53	- 0.19	+ 0.27	- 0.04	- 0.08	- 0.15	- 0.09
			p	0.4556	0.1184	0.5934	0.4496	0.9041	0.8178	0.6745	0.8357
			n	10	10	10	10	10	10	10	8
		24	r	+ 0.37	- 0.45	- 0.04	+ 0.40	- 0.37	- 0.31	+ 0.28	- 0.43
			p	0.2984	0.1914	0.9041	0.2543	0.2979	0.3833	0.4266	0.2862
			n	10	10	10	10	10	10	10	8
SUPERNATANT	[^{12}C]LPC	0.5	r	- 0.17	+ 0.17	+ 0.31	+ 0.29	+ 0.15	- 0.04	+ 0.55	- 0.23
			p	0.6339	0.6465	0.3758	0.4170	0.6840	0.9167	0.1019	0.5903
			n	10	10	10	10	10	10	10	8
		4	r	- 0.49	+ 0.22	+ 0.21	+ 0.10	+ 0.39	+ 0.17	+ 0.15	+ 0.12
			p	0.1487	0.5388	0.5629	0.7762	0.2587	0.6316	0.6880	0.7792
			n	10	10	10	10	10	10	10	8
		24	r	- 0.28	+ 0.15	+ 0.22	+ 0.19	+ 0.21	0.00	+ 0.34	- 0.03
			p	0.4256	0.6894	0.5423	0.5909	0.5666	0.9937	0.3423	0.9366
			n	10	10	10	10	10	10	10	8
	[^{13}C]LPC	0.5	r	+ 0.22	- 0.11	+ 0.44	+ 0.68	- 0.08	- 0.12	+ 0.73	- 0.89
			p	0.5613	0.7699	0.2387	0.0441	0.8463	0.7562	0.0270	0.0065
			n	9	9	9	9	9	9	9	7
		4	r	- 0.42	- 0.08	- 0.36	- 0.42	+ 0.23	+ 0.10	- 0.52	+ 0.45
			p	0.2264	0.8305	0.3118	0.2316	0.5184	0.7824	0.1277	0.2625
			n	10	10	10	10	10	10	10	8
		24	r	- 0.26	- 0.33	- 0.40	- 0.19	+ 0.07	- 0.17	- 0.29	+ 0.25
			p	0.4628	0.3466	0.2554	0.5960	0.8494	0.6443	0.4152	0.5464
			n	10	10	10	10	10	10	10	8

3.3.2 Correlation analyses with physiologic parameters of substrate oxidation

Both $EnExp_{fasting}$ and $EnExp_{clamp}$ show not a single relationship with LPCs, neither with individual species (**Supplemental Table 2**, **Supplemental Table 3** and **Supplemental Table 4**) nor with the sums (**Supplemental Table 5**), neither with intracellular nor with extracellular concentrations, neither with [^{12}C]- nor with [^{13}C]-isotopes.

RQ measured in fasting condition ($RQ_{fasting}$) does not show any correlation with the sums of intra- or extracellular LPCs, neither with [^{12}C]- nor with [^{13}C]-labeled derivatives (**Table 14**).

The positive relationship of RQ measured during steady-state phase of a euglycemic-hyperinsulinemic clamp (RQ_{clamp}) with 24-hour intracellular [^{12}C]LPCs and 24-hour intracellular [^{13}C]LPCs (**Table 14**) is reflected by 7 out of 19 [^{12}C]LPC species and 4 out of 7 [^{13}C]LPC species as shown in **Table 15** as well as in the **Supplemental Data** section.

In contrast, the sum of extracellular [^{13}C]LPCs after 4 hours negatively correlates with RQ_{clamp} (**Table 14**) which is also observed for extracellular [$^{13}C_{16}$]LPC C16:0 after 4 hours (r = - 0.64, p = 0.0456*; **Table 20**).

Intracellularly, exclusively LPC C20:2 after 30 minutes as well as LPC C22:3 after 30 minutes and after 4 hours correlate negatively with RQ_{clamp} (**Table 15**). *Vice versa*, the only extracellular species correlating positively with RQ_{clamp} is LPC C20:5 after 24 hours (r = + 0.65, p = 0.0406*; **Table 22**).

Well in accordance with RQ, only carbohydrate oxidation (CHOx) and lipid oxidation (LipOx) determined *in vivo* during steady-state phase of a euglycemic-hyperinsulinemic clamp ($CHOx_{clamp}$ and $LipOx_{clamp}$) show profound correlations with several intracellular LPC species (**Table 21**) with $CHOx_{clamp}$ reflecting the positive association of RQ_{clamp} and with $LipOx_{clamp}$ reflecting an opposite association.

In agreement with the results for RQ reported above, concerning [^{12}C]-species, the discrepancy between fasting condition and steady-state phase of the clamp is elucidated as not a single [^{12}C]-species associates with $CHOx_{fasting}$ (n = 9) but 6 out of 19 intracellular species (32 %) positively associate with $CHOx_{clamp}$ (n = 9) – predominantly

those with polyunsaturated long-chain acyl groups (**Table 21**): LPC C20:3, LPC C20:4, LPC C20:5, LPC C22:4, LPC C22:5 and LPC C22:6.
In addition, also 8 out of 19 extracellular [^{12}C]-species (42 %) positively associate with $CHOx_{clamp}$ (n = 9) – again predominantly those with polyunsaturated long-chain acyl groups (**Table 22**): LPC C18:0, LPC C18:2, LPC C20:3, LPC C20:4, LPC C20:5, LPC C22:4, LPC C22:5 and LPC C22:6. Extracellular [^{13}C]-metabolites lack significant associations (**Table 20**).

Well in line, inverse relationships with $LipOx_{clamp}$ are observed for 4 out of 7 intracellular [^{13}C]-species (**Table 20**) as well as for 6 out of 19 intracellular [^{12}C]-species (**Table 21**).
Moreover, the sum of intracellular [^{12}C]LPCs after 24 hours correlates negatively with both $LipOx_{fasting}$ and $LipOx_{clamp}$ (**Table 14**), but, once more, species-specific evaluation reveals fewer associations for fasting condition than for the clamp as only 2 [^{12}C]-species (11 %) correlate with $LipOx_{fasting}$ whereas 6 species (32 %) correlate with $LipOx_{clamp}$ (**Table 21**) which are LPC C16:0, LPC C18:0, LPC C20:3, LPC C20:4, LPC C20:5 and LPC C22:5. Similarly, not a single [^{13}C]-labeled metabolite correlates with $LipOx_{fasting}$ while $LipOx_{clamp}$ correlates negatively with 4 out of 7 intracellular species (57 %) which are [$^{13}C_{16}$]LPC C16:0, [$^{13}C_{16}$]LPC C18:0, [$^{13}C_{18}$]LPC C18:0 and [$^{13}C_{18}$]LPC C18:1 (**Table 20**).

To conclude, a higher carbohydrate oxidation during euglycemic-hyperinsulinemic clamp correlates with higher intracellular and partly extracellular long-chain acyl LPC concentrations in human myotubes from these donors. Higher *in vivo* lipid oxidation during the clamp is negatively associated with *in vitro* LPC concentrations.

Table 14: Results of the correlation analyses between the total *in vitro* concentrations of intracellular (cell lysate) or extracellular (supernatant) [^{12}C]- or [^{13}C]-labeled lysophosphatidylcholines (LPC) with reference to the protein mass of the matching cell lysate and the physiologic *in vivo* parameters of the donors respiratory quotient (RQ), carbohydrate oxidation (CHOx) and lipid oxidation (LipOx) measured both in fasting condition (fasting) and during steady-state phase of a euglycemic-hyperinsulinemic clamp (clamp). LPC isolation was performed from primary human myotubes of 10 different subjects (n = 10) after having stimulated for 30 minutes (0.5), 4 hours (4) or 24 hours (24) with 100 µM L-carnitine and 125 µM [$^{13}C_{16}$]palmitate. Gaussian distribution was objected for the concentrations of some LPC species as well as for $RQ_{fasting}$ and RQ_{clamp} by Shapiro-Wilk W tests in JMP®, but log-normal distributions were attested. Consequently, values of these parameters were log_e-transformed (ln) for correlation analyses.

		TP		RQ fasting [ln]	RQ clamp [ln]	CHOx fasting	CHOx clamp	LipOx fasting	LipOx clamp
CELL LYSATE	[^{12}C]LPC	0.5	r	+ 0.15	+ 0.27	+ 0.17	+ 0.51	- 0.29	- 0.58
			p	0.6738	0.4574	0.6696	0.1592	0.4467	0.0995
			n	10	10	9	9	9	9
		4	r	+ 0.02	+ 0.55	+ 0.07	+ 0.31	- 0.28	- 0.46
			p	0.9552	0.1002	0.8577	0.4211	0.4729	0.2077
			n	10	10	9	9	9	9
		24	r	+ 0.36	+ 0.79	+ 0.33	+ 0.44	- 0.73	- 0.79
			p	0.3024	0.0067	0.3933	0.2358	0.0266	0.0112
			n	10	10	9	9	9	9
	[^{13}C]LPC	0.5	r	+ 0.28	+ 0.27	+ 0.28	+ 0.42	- 0.31	- 0.36
			p	0.4369	0.4578	0.4600	0.2653	0.4128	0.3457
			n	10	10	9	9	9	9
		4	r	+ 0.01	+ 0.22	- 0.13	- 0.32	- 0.01	+ 0.12
			p	0.9676	0.5406	0.7384	0.4082	0.9799	0.7579
			n	10	10	9	9	9	9
		24	r	+ 0.40	+ 0.82	+ 0.21	+ 0.27	- 0.56	- 0.64
			p	0.2528	0.0034	0.5846	0.4867	0.1133	0.0645
			n	10	10	9	9	9	9
SUPERNATANT	[^{12}C]LPC	0.5	r	- 0.01	+ 0.35	+ 0.16	+ 0.57	- 0.09	- 0.42
			p	0.9860	0.3250	0.6818	0.1054	0.8265	0.2621
			n	10	10	9	9	9	9
		4	r	+ 0.05	+ 0.09	+ 0.32	+ 0.51	+ 0.08	- 0.04
			p	0.9008	0.8070	0.4035	0.1573	0.8310	0.9131
			n	10	10	9	9	9	9
		24	r	+ 0.26	+ 0.45	+ 0.39	+ 0.66	- 0.30	- 0.48
			p	0.4743	0.1883	0.2982	0.0547	0.4259	0.1872
			n	10	10	9	9	9	9
	[^{13}C]LPC	0.5	r	- 0.16	+ 0.34	- 0.15	+ 0.13	+ 0.22	- 0.22
			p	0.6775	0.3777	0.7263	0.7534	0.5987	0.6000
			n	9	9	8	8	8	8
		4	r	- 0.16	- 0.65	- 0.08	- 0.27	+ 0.39	+ 0.66
			p	0.6581	0.0405	0.8361	0.4782	0.2998	0.0539
			n	10	10	9	9	9	9
		24	r	+ 0.34	+ 0.01	+ 0.25	+ 0.07	- 0.26	- 0.01
			p	0.3385	0.9824	0.5200	0.8504	0.4986	0.9897
			n	10	10	9	9	9	9

Table 15: Results of the species-specific correlation analyses between intracellular [^{12}C]- or [^{13}C]-labeled lysophosphatidylcholine (LPC) species and the respiratory quotient measured during steady-state phase of a euglycemic-hyperinsulinemic clamp (RQ_{clamp}). Stimulations of primary human myotubes from 10 subjects with 100 µM L-carnitine and 125 µM [$^{13}C_{16}$]palmitate were performed for 30 minutes (0.5), 4 hours (4) or 24 hours (24).

Species		**C14:0**		**C14:1**	**C16:0**		**C16:1**		
Isotope		**[^{12}C]**	**[$^{13}C_{14}$]**		**[^{12}C]**	**[$^{13}C_{16}$]**	**[^{12}C]**	**[$^{13}C_{16}$]**	
0.5	r	- 0.08	+ 0.43	- 0.17	+ 0.13	+ 0.15	- 0.09	+ 0.28	
	p	0.8296	0.2116	0.6488	0.7289	0.6742	0.8095	0.4387	
	n	10	10	10	10	10	10	10	
4	r	+ 0.05	+ 0.01	- 0.15	+ 0.52	+ 0.25	+ 0.14	- 0.20	
	p	0.8894	0.9676	0.6883	0.1225	0.4873	0.6955	0.5740	
	n	10	10	10	10	10	10	10	
24	r	+ 0.32	+ 0.53	+ 0.03	+ 0.78	+ 0.84	+ 0.29	+ 0.25	
	p	0.3678	0.1167	0.9284	0.0075	0.0026	0.4247	0.4795	
	n	10	10	10	10	10	10	10	
Species		**C18:0**			**C18:1**			**C18:2**	**C18:3**
Isotope		**[^{12}C]**	**[$^{13}C_{16}$]**	**[$^{13}C_{18}$]**	**[^{12}C]**	**[$^{13}C_{16}$]**	**[$^{13}C_{18}$]**		
0.5	r	+ 0.33	+ 0.31	+ 0.37	+ 0.09	+ 0.47	+ 0.56	+ 0.23	+ 0.01
	p	0.3445	0.3807	0.2912	0.8085	0.1740	0.0889	0.5150	0.9774
	n	10	10	10	10	10	10	10	10
4	r	+ 0.52	+ 0.22	+ 0.44	+ 0.42	- 0.38	+ 0.60	+ 0.42	+ 0.19
	p	0.1198	0.5361	0.2005	0.2216	0.2788	0.0656	0.2213	0.6085
	n	10	10	10	10	10	10	10	10
24	r	+ 0.83	+ 0.80	+ 0.83	+ 0.70	+ 0.27	+ 0.75	+ 0.60	+ 0.19
	p	0.0030	0.0056	0.0028	0.0244	0.4534	0.0124	0.0681	0.6041
	n	10	10	10	10	10	10	10	10
Species		**C20:0**	**C20:1**	**C20:2**	**C20:3**	**C20:4**	**C20:5**		
0.5	r	- 0.39	- 0.54	- 0.73	+ 0.27	+ 0.61	+ 0.67		
	p	0.2636	0.1087	0.0159	0.4589	0.0636	0.0353		
	n	10	10	10	10	10	10		
4	r	- 0.58	- 0.47	- 0.52	+ 0.48	+ 0.67	+ 0.66		
	p	0.0790	0.1716	0.1200	0.1624	0.0331	0.0383		
	n	10	10	10	10	10	10		
24	r	- 0.35	+ 0.13	+ 0.01	+ 0.74	+ 0.77	+ 0.66		
	p	0.3277	0.7248	0.9727	0.0142	0.0096	0.0378		
	n	10	10	10	10	10	10		
Species		**C22:1**	**C22:3**	**C22:4**	**C22:5**	**C22:6**			
0.5	r	- 0.50	- 0.79	+ 0.22	+ 0.49	+ 0.38			
	p	0.1404	0.0071	0.5509	0.1538	0.2833			
	n	10	10	10	10	10			
4	r	- 0.56	- 0.66	+ 0.39	+ 0.61	+ 0.48			
	p	0.0915	0.0393	0.2626	0.0603	0.1634			
	n	10	10	10	10	10			
24	r	+ 0.05	- 0.17	+ 0.63	+ 0.73	+ 0.62			
	p	0.8910	0.6309	0.0525	0.0156	0.0534			
	n	10	10	10	10	10			

3.3.3 Correlation analyses with *in vivo* markers of insulin sensitivity

The metabolic parameters ISI_{OGTT}, measured during OGTT, as well as ISI_{clamp}, measured during steady-state phase of a euglycemic-hyperinsulinemic clamp, lack significant relationships with the sums of intra- or extracellular [^{12}C]- or [^{13}C]-labeled LPCs as depicted in **Table 16**, but species-specific correlation analyses (**Table 20**, **Table 21** and **Table 22**) reveal negative associations of ISI_{OGTT} (n = 10) with intracellular LPC C20:4 (0.5 h: r = - 0.79, p = 0.0069*; 4 h: r = - 0.60, p = 0.0654; 24 h: r = - 0.60, p = 0.0657), LPC C20:5 (0.5 h: r = - 0.70, p = 0.0237*), LPC C22:5 (0.5 h: r = - 0.66, p = 0.0381*) and LPC C22:6 (0.5 h: r = - 0.69, p = 0.0264*) plus extracellular LPC C20:3 (24 h: r = - 0.65, p = 0.0436*), LPC C20:4 (24 h: r = - 0.63, p = 0.0494*), LPC C22:5 (24 h: r = - 0.73, p = 0.0168*) and LPC C22:6 (24 h: r = - 0.73, p = 0.0165*) and negative associations of ISI_{clamp} (n = 10) with intracellular [$^{13}C_{16}$]LPC C16:1 (0.5 h: r = - 0.67, p = 0.0332*) plus extracellular LPC C22:5 (24 h: r = - 0.64, p = 0.0454*) and LPC C22:6 (24 h: r = - 0.64, p = 0.0447*).

In conclusion – and in concert with the correlation analyses with the metabolic parameters RQ, CHOx and LipOx (see chapter **3.3.2**) – the most profound associations, once again, are found for the LPC species containing polyunsaturated long-chain acyl groups.

Table 16: Association studies between the total amounts of [^{12}C]- or [^{13}C]-labeled lysophosphatidylcholines (LPC) as related to the protein mass of the matching cell lysate and the metabolic *in vivo* parameter insulin sensitivity index (ISI) assessed both by an oral glucose tolerance test (OGTT) and by a euglycemic-hyperinsulinemic clamp (clamp). LPC profile time course changes were investigated in both the cell lysates and supernatants of primary human myotubes from 10 different donors (n = 10) stimulating with 100 µM L-carnitine and 125 µM [$^{13}C_{16}$]palmitate for 30 minutes (0.5), 4 hours (4) or 24 hours (24). As Shapiro-Wilk W tests favored log-normal distributions for all parameters of this table, all these variables were $\log_e$-transformed (ln) for correlation studies. Glucose and insulin concentrations from OGTT were used for assessment of ISI_{OGTT} according to Matsuda and DeFronzo (**Supplemental Equation 2**). Euglycemic-hyperinsulinemic clamp was performed after a 12-hour overnight fasting period calculating ISI_{clamp} by division of the mean GIR during the second hour of the clamp by the insulin concentration during steady-state phase (**Supplemental Equation 3**).

		TP		ISI OGTT [ln]	ISI clamp [ln]
CELL LYSATE	[^{12}C]LPC	0.5	r	- 0.39	- 0.11
			p	0.2710	0.7585
			n	10	10
		4	r	- 0.08	+ 0.16
			p	0.8286	0.6678
			n	10	10
		24	r	- 0.28	+ 0.03
			p	0.4323	0.9395
			n	10	10
	[^{13}C]LPC	0.5	r	- 0.49	- 0.27
			p	0.1485	0.4590
			n	10	10
		4	r	+ 0.41	+ 0.33
			p	0.2442	0.3523
			n	10	10
		24	r	- 0.23	- 0.15
			p	0.5312	0.6781
			n	10	10
SUPERNATANT	[^{12}C]LPC	0.5	r	- 0.42	- 0.27
			p	0.2286	0.4554
			n	10	10
		4	r	- 0.21	- 0.22
			p	0.5589	0.5403
			n	10	10
		24	r	- 0.49	- 0.46
			p	0.1488	0.1853
			n	10	10
	[^{13}C]LPC	0.5	r	- 0.14	+ 0.13
			p	0.7105	0.7404
			n	9	9
		4	r	+ 0.54	+ 0.41
			p	0.1046	0.2454
			n	10	10
		24	r	+ 0.21	+ 0.03
			p	0.5551	0.9262
			n	10	10

3.3.4 Correlation analyses with *in vivo* muscular lipid content

No significant correlations are observed between *in vivo* IMCL and *in vitro* total LPCs (**Table 17**). IMCL of *M. tibialis* neither associates with any individual species, whereas IMCL of *M. soleus* (n = 7) associates inversely with four [^{12}C]- (**Table 21**) plus one [^{13}C]- (**Table 20**) intracellular LPC species.

Significant relationships with LPC levels are observed for EMCL of different muscles with both intracellular [^{12}C]- (**Table 17** and **Table 21**) and intra- plus extracellular [^{13}C]LPC levels (**Table 17** and **Table 20**) positively correlating with EMCL such as EMCL of *M. tibialis anterior* (*M. tib. ant.*; n = 6) positively correlates with total intracellular [^{12}C]LPCs after 30-minute stimulation (**Table 17**) reflected by individual correlations with LPC C18:1, LPC C18:2, LPC C20:1, LPC C20:3 and LPC C22:4 (**Table 21**). EMCLs (n = 6) of other muscles lack significant relationships with [^{12}C]LPC sums but correlate with specific intracellular [^{12}C]-species (**Table 21**).
Moreover, after 30 minutes of stimulation, intracellular [$^{13}C_{18}$]LPC C18:0 associates with EMCL of *Mm. tibiales anterior et posterior* and extracellular [$^{13}C_{16}$]LPC C16:0 with EMCL of *M. gastrocnemius lateralis* (*M. GC lat.*; n = 5) reflecting the significant correlation with total extracellular [^{13}C]LPCs (0.5 h: r = + 0.89, p = 0.0458*; n = 5).

Table 17: Results of the correlation analyses between the total *in vitro* intracellular (cell lysate) or extracellular (supernatant) concentrations of [^{12}C]- or [^{13}C]-labeled lysophosphatidylcholines (LPC) from cultivated primary human myotubes and the *in vivo* intra- (IMCL) or extramyocellular (EMCL) lipid content of the donor muscles *M. tibialis* (*tibialis*), *M. soleus* (*soleus*), *M. gastrocnemius* (*GC*) or *M. peroneus* (*peron.*). Concerning EMCL *M. tibialis* was specified in *M. tibialis anterior* (*tib. ant.*) *et posterior* (*tib. post.*) and *M. gastrocnemius* was specified in *M. gastrocnemius lateralis* (*GC lat.*) *et medialis* (*GC med.*). Myotubes were stimulated for 30 minutes (0.5), 4 hours (4) or 24 hours (24) with 100 µM L-carnitine plus 125 µM [$^{13}C_{16}$]palmitate in the *in vitro* experiments followed by isolation and mass spectrometric quantification of LPCs whose concentrations were referred to the protein mass in the matching cell lysate. Log-normal distribution was suggested by Shapiro-Wilk W tests in JMP® for both the *in vitro* LPC concentrations and the *in vivo* intra- and extramyocellular lipid contents which is why all parameters of this table were $\log_e$-transformed (ln) for correlation analyses. Quantification and differentiation of IMCL and EMCL were enabled by proton magnetic resonance spectroscopy (^{1}H-MRS).

		TP		IMCL *tibialis* [ln]	IMCL *soleus* [ln]	EMCL *tib. ant.* [ln]	EMCL *tib. post.* [ln]	EMCL *soleus* [ln]	EMCL *GC lat.* [ln]	EMCL *GC med.* [ln]	EMCL *peron.* [ln]
CELL LYSATE	[^{12}C]LPC	**0.5**	r	+ 0.35	- 0.55	+ 0.85	+ 0.69	+ 0.41	+ 0.60	+ 0.61	+ 0.64
			p	0.4362	0.2031	0.0309	0.1328	0.4251	0.2095	0.2030	0.1718
			n	7	7	6	6	6	6	6	6
		4	r	- 0.26	- 0.39	+ 0.55	+ 0.72	+ 0.36	+ 0.08	+ 0.24	+ 0.41
			p	0.5747	0.3930	0.2613	0.1069	0.4872	0.8809	0.6443	0.4144
			n	7	7	6	6	6	6	6	6
		24	r	0.00	- 0.44	+ 0.46	+ 0.51	+ 0.01	- 0.09	+ 0.03	+ 0.25
			p	0.9962	0.3180	0.3609	0.3064	0.9823	0.8616	0.9626	0.6389
			n	7	7	6	6	6	6	6	6
	[^{13}C]LPC	**0.5**	r	+ 0.54	- 0.14	+ 0.22	+ 0.15	+ 0.02	+ 0.06	+ 0.07	+ 0.02
			p	0.2091	0.7677	0.6712	0.7740	0.9759	0.9102	0.8965	0.9768
			n	7	7	6	6	6	6	6	6
		4	r	- 0.46	+ 0.14	- 0.20	- 0.05	+ 0.07	- 0.17	- 0.11	- 0.18
			p	0.3031	0.7710	0.6976	0.9220	0.8884	0.7510	0.8349	0.7295
			n	7	7	6	6	6	6	6	6
		24	r	- 0.20	- 0.50	+ 0.20	+ 0.19	- 0.26	- 0.21	- 0.18	- 0.07
			p	0.6685	0.2508	0.7012	0.7189	0.6219	0.6913	0.7305	0.8923
			n	7	7	6	6	6	6	6	6
SUPERNATANT	[^{12}C]LPC	**0.5**	r	+ 0.05	- 0.43	+ 0.68	+ 0.75	+ 0.41	+ 0.33	+ 0.42	+ 0.52
			p	0.9145	0.3352	0.1357	0.0876	0.4192	0.5221	0.4115	0.2957
			n	7	7	6	6	6	6	6	6
		4	r	- 0.25	- 0.18	+ 0.18	+ 0.36	+ 0.27	+ 0.06	+ 0.13	+ 0.14
			p	0.5836	0.6986	0.7302	0.4813	0.5983	0.9120	0.8007	0.7979
			n	7	7	6	6	6	6	6	6
		24	r	- 0.23	- 0.46	+ 0.15	+ 0.31	- 0.06	- 0.14	- 0.11	- 0.02
			p	0.6274	0.2970	0.7793	0.5475	0.9105	0.7905	0.8420	0.9688
			n	7	7	6	6	6	6	6	6
	[^{13}C]LPC	**0.5**	r	+ 0.55	+ 0.03	+ 0.84	+ 0.64	+ 0.87	+ 0.89	+ 0.95	+ 0.86
			p	0.2551	0.9507	0.0766	0.2433	0.0572	0.0458	0.0145	0.0616
			n	6	6	5	5	5	5	5	5
		4	r	- 0.33	- 0.04	- 0.21	- 0.12	+ 0.01	- 0.06	- 0.09	- 0.24
			p	0.4736	0.9359	0.6862	0.8263	0.9787	0.9047	0.8712	0.6489
			n	7	7	6	6	6	6	6	6
		24	r	- 0.48	- 0.24	- 0.39	- 0.30	- 0.30	- 0.26	- 0.34	- 0.49
			p	0.2705	0.6003	0.4442	0.5573	0.5597	0.6136	0.5050	0.3249
			n	7	7	6	6	6	6	6	6

3.3.5 Correlation analyses with mitochondrial DNA content and gene expression data of cultured human myotubes

Intra- and extracellular LPC levels were also tested for their association with *in vitro* mtDNA content and with the *in vitro* expression of genes related to lipid oxidation whose determination is described in chapter **2.2.6**.

Data were obtained from 'control cells' incubated with L-carnitine or cells incubated with L-carnitine plus the PPARδ receptor agonist GW501516 in order to stimulate the oxidative capacity-increasing effect of PPARδ whose expression is increased *inter alia* after exercise.

The expression levels of both *CPT1B* and *PDK4* (referred to the expression of *ACTB*) are markedly increased when incubated with GW501516 ($p < 0.0001$*) [188] whereas those of the other investigated genes *PPARD*, *UCP3* and *PPARGC1A* remain unaltered [188]. Because of this and due to the observation that correlation analyses reveal similar patterns for the corresponding incubations, **Table 18** shows the results of the incubations with L-carnitine plus GW501516 exclusively for the genes *CPT1B* and *PDK4* but for all other genes these results are not shown.

The mtDNA content, quantified by the ratio of mitochondrial *MT-ND1* to chromosomal *LPL*, is not significantly changed by incubating with GW501516, but different results are obtained in the correlation analyses as presented in **Table 18**: Whereas the sums of intracellular [^{12}C]LPCs, extracellular [^{12}C]LPCs and intracellular [^{13}C]LPCs all show significant inverse relationships with mtDNA content after 30-minute incubation with L-carnitine, no significant associations are found at all with LPC sums for the incubation with GW501516.

These findings are witnessed by species-specific analyses with markedly less LPC species significantly correlating with mtDNA content after the incubation with GW501516 than after the incubation with L-carnitine as depicted in **Table 20**, **Table 21** and **Table 22**.

In contrast to these observations, the negative associations of *CPT1B* expression as well as of *PDK4* expression with *in vitro* LPC concentrations are markedly more comprehensive for the incubation with GW501516 than they are for the incubation with L-carnitine. This insight is supported by the correlation analyses with total LPC sums

(**Table 18**), as significant correlations with LPC sums are exclusively found for the incubation with GW501516 between *CPT1B* expression and the extracellular [^{12}C]LPC sum and between *PDK4* expression and the extracellular [^{13}C]LPC sum.

In species-specific investigations, the inverse relationship between the *CPT1B* expression and extracellular LPCs is mirrored by 2 out of 7 [^{13}C]-species (29 %; **Table 20**) as well as by 15 out of 19 [^{12}C]-species (79 %; **Table 22**) for the incubation with GW501516: [$^{13}C_{16}$]LPC C18:0, [$^{13}C_{16}$]LPC C18:1, LPC C14:0, LPC C16:0, LPC C16:1, LPC C18:1, LPC C18:2, LPC C18:3, LPC C20:1, LPC C20:2, LPC C20:3, LPC C20:4, LPC C22:1, LPC C22:3, LPC C22:4, LPC C22:5 and LPC C22:6. In contrast, no single extracellular [^{12}C]- nor [^{13}C]-labeled species associates with the *CPT1B* expression after the incubation with L-carnitine.

The inverse relationship between the *PDK4* expression and the extracellular [^{13}C]LPC sum is mirrored by the three species [$^{13}C_{16}$]LPC C16:0 (4 h: r = - 0.67, p = 0.0328*; n = 10), [$^{13}C_{16}$]LPC C18:1 (24 h: r = - 0.82, p = 0.0036*; n = 10) and [$^{13}C_{18}$]LPC C18:1 (24 h: r = - 0.69, p = 0.0285*; n = 10) for the incubation with GW501516 but not for the incubation with L-carnitine (**Table 20**). After incubation with GW501516, no single extracellular [^{12}C]-species (**Table 22**) significantly correlates with *PDK4* expression but 5 intracellular [^{12}C]-species do (**Table 21**): LPC C14:0, LPC C14:1, LPC C16:1, LPC C20:2 and LPC C22:1.

No significant correlation is found between total *in vitro* LPC concentrations and *in vitro* expression of *PPARD*, *UCP3* or *PPARGC1A* (**Table 18**) and significant associations with specific species occur only sporadically (**Table 20**, **Table 21** and **Table 22**).

Table 18: Association studies between the total concentrations of [^{12}C]- or [^{13}C]-labeled lysophosphatidylcholines (LPC) and the amount of (mitochondrially encoded) NADH dehydrogenase 1 (*MT-ND1*) as well as the gene expressions of carnitine palmitoyltransferase 1β (*CPT1B*), pyruvate dehydrogenase kinase isozyme 4 (*PDK4*), peroxisome proliferator-activated receptor δ (*PPARD*), uncoupling protein 3 (*UCP3*) or peroxisome proliferator-activated receptor γ coactivator 1α (*PPARGC1A*; below: *PGC1A*). LPC concentrations were referred to the protein mass in the corresponding cell lysate, the amount of *MT-ND1* was referred to that of (chromosomally encoded) lipoprotein lipase (*LPL*) and the expressions of the other genes to that of β-actin (*ACTB*). Nucleic acids were investigated in primary human myotubes from 10 different individuals (n = 10) after incubation for 6 days during fusion phase with 100 µM L-carnitine (LC) or 100 µM L-carnitine plus 1 µM GW501516 (GW). LPCs were isolated from both cell lysates and supernatants after stimulation with 100 µM L-carnitine and 125 µM [$^{13}C_{16}$]palmitate for 30 minutes (0.5), 4 hours (4) or 24 hours (24). All variables of this table were $\log_e$-transformed (ln) as Shapiro-Wilk W tests in JMP® revealed a bias towards log-normal distributions for all these parameters.

		TP		*MT-ND1* / *LPL* (LC) [ln]	*MT-ND1* / *LPL* (GW) [ln]	*CPT1B* / *ACTB* (LC) [ln]	*CPT1B* / *ACTB* (GW) [ln]	*PDK4* / *ACTB* (LC) [ln]	*PDK4* / *ACTB* (GW) [ln]	*PPARD* / *ACTB* (LC) [ln]	*UCP3* / *ACTB* (LC) [ln]	*PGC1A* / *ACTB* (LC) [ln]
CELL LYSATE	[^{12}C]LPC	0.5	r	- 0.67	- 0.62	+ 0.30	- 0.34	- 0.40	- 0.35	- 0.14	- 0.27	- 0.18
			p	0.0336	0.0572	0.3929	0.3304	0.2580	0.3229	0.6990	0.4489	0.6160
			n	10	10	10	10	10	10	10	10	10
		4	r	- 0.58	- 0.23	+ 0.33	- 0.27	+ 0.09	- 0.09	+ 0.38	+ 0.06	- 0.02
			p	0.0776	0.5250	0.3549	0.4463	0.8124	0.7988	0.2783	0.8722	0.9536
			n	10	10	10	10	10	10	10	10	10
		24	r	- 0.50	- 0.35	+ 0.45	+ 0.15	+ 0.37	+ 0.11	+ 0.48	+ 0.11	- 0.26
			p	0.1427	0.3172	0.1878	0.6805	0.2943	0.7647	0.1612	0.7674	0.4731
			n	10	10	10	10	10	10	10	10	10
	[^{13}C]LPC	0.5	r	- 0.66	- 0.30	+ 0.50	- 0.26	- 0.21	- 0.22	- 0.15	- 0.33	- 0.09
			p	0.0373	0.3926	0.1382	0.4690	0.5533	0.5352	0.6887	0.3461	0.7956
			n	10	10	10	10	10	10	10	10	10
		4	r	+ 0.30	+ 0.58	- 0.04	+ 0.01	+ 0.30	+ 0.18	+ 0.33	+ 0.21	+ 0.05
			p	0.4063	0.0784	0.9072	0.9810	0.4013	0.6123	0.3523	0.5563	0.8906
			n	10	10	10	10	10	10	10	10	10
		24	r	- 0.18	+ 0.05	+ 0.18	+ 0.15	+ 0.48	+ 0.44	+ 0.41	+ 0.07	- 0.11
			p	0.6127	0.8838	0.6279	0.6704	0.1582	0.2031	0.2409	0.8518	0.7629
			n	10	10	10	10	10	10	10	10	10
SUPERNATANT	[^{12}C]LPC	0.5	r	- 0.73	- 0.49	+ 0.26	- 0.55	- 0.22	- 0.22	- 0.06	- 0.27	+ 0.03
			p	0.0172	0.1539	0.4648	0.1000	0.5459	0.5428	0.8629	0.4499	0.9302
			n	10	10	10	10	10	10	10	10	10
		4	r	- 0.45	- 0.10	+ 0.03	- 0.69	- 0.38	- 0.29	- 0.31	- 0.48	+ 0.10
			p	0.1963	0.7842	0.9370	0.0281	0.2821	0.4142	0.3824	0.1591	0.7890
			n	10	10	10	10	10	10	10	10	10
		24	r	- 0.62	- 0.28	+ 0.05	- 0.46	- 0.14	+ 0.01	- 0.14	- 0.45	+ 0.01
			p	0.0537	0.4393	0.8860	0.1776	0.6915	0.9758	0.6988	0.1911	0.9793
			n	10	10	10	10	10	10	10	10	10
	[^{13}C]LPC	0.5	r	- 0.32	- 0.01	+ 0.62	- 0.04	- 0.02	+ 0.07	+ 0.20	+ 0.21	+ 0.38
			p	0.4046	0.9713	0.0731	0.9273	0.9507	0.8549	0.6022	0.5858	0.3067
			n	9	9	9	9	9	9	9	9	9
		4	r	+ 0.36	+ 0.30	- 0.32	- 0.62	- 0.53	- 0.69	- 0.44	- 0.27	- 0.20
			p	0.3026	0.4040	0.3648	0.0559	0.1183	0.0274	0.2031	0.4425	0.5849
			n	10	10	10	10	10	10	10	10	10
		24	r	+ 0.17	+ 0.37	- 0.46	- 0.53	- 0.29	- 0.20	- 0.32	- 0.48	- 0.28
			p	0.6361	0.2878	0.1830	0.1174	0.4236	0.5808	0.3745	0.1606	0.4253
			n	10	10	10	10	10	10	10	10	10

3.3.6 Correlation analyses with *in vitro* [^{3}H]palmitate oxidation activity

Potential associations of mass spectrometrically determined *in vitro* LPC concentrations were also investigated with *in vitro* [^{3}H]palmitate oxidation (FAO) activity after incubation with either 100 µM L-carnitine or 100 µM L-carnitine plus 1 µM GW501516 with the PPARδ receptor agonist GW501516 increasing the FAO activity by approximately 30 % ($p = 0.0006$*) [188].

Correlation analyses of palmitate oxidation activity with the total intra- and extracellular LPC sums (**Table 19**) reveal markedly stronger relationships with extracellular [^{12}C]LPCs than with intracellular [^{12}C]LPCs as significant associations with extracellular [^{12}C]LPC sums are found at all three stimulation time points for the incubation with GW501516 but not with intracellular [^{12}C]LPC sums ($p \geq 0.16$).

This observation is confirmed by species-specific analyses as markedly more widespread associations are found for extracellular [^{12}C]-species (**Table 22**) than are for intracellular [^{12}C]-species (**Table 21**): Intracellularly, only 3 out of 19 [^{12}C]-species (16 %; incubation without GW501516) and 5 species (26 %; incubation with GW501516) significantly associate with FAO activity, whereas 5 species (26 %; incubation without GW501516) and 17 species (89 %; incubation with GW501516) do extracellularly.

Additionally, this contrasting juxtaposition elucidates the enhancement of the associations by the incubation with GW501516. This effect of GW501516 is also confirmed by the results of the [^{13}C]LPC species (**Table 20**) as only one out of seven intracellular (14 %) and none out of seven extracellular (0 %) [^{13}C]LPC species significantly correlate with FAO activity after incubation without GW501516 but 3 intracellular (43 %) and 1 extracellular (14 %) [^{13}C]LPC species do after incubation with GW501516.

Moreover, once more, the most conspicuous relationships are found with LPC species containing polyunsaturated long-chain fatty acyl groups: Palmitate oxidation activity exclusively associates with intracellular LPC C20:3, LPC C20:4, LPC C22:4, LPC C22:5 plus LPC C22:6 (**Table 21**) and with all extracellular [^{12}C]-species apart from LPC C22:0 and LPC C22:1 (**Table 22**) after incubation with GW501516.

Table 19: Correlation analyses for the total sums of [^{12}C]- or [^{13}C]-labeled lysophosphatidylcholines (LPC) with the fatty acid oxidation (FAO) activities quantified by [^{3}H]$_2$O produced within 4 hours from [^{3}H]palmitate after the incubation of human myotubes (hMT) during fusion phase for 7 days with 100 µM L-carnitine (LC) or 100 µM LC plus 1 µM GW501516 (GW). Lipidomic analysis was performed by isolating LPCs from cell lysates and supernatants of hMT stimulated for 30 minutes (0.5), 4 hours (4) or 24 hours (24) with 100 µM L-carnitine and 125 µM [$^{13}C_{16}$]palmitate, quantifying them mass spectrometrically, referring their amounts to the protein mass in the matching cell lysate and $\log_e$-transforming (ln) them as Shapiro-Wilk W tests in JMP® suggested log-normal distributions for all data.

		TP		FAO LC [ln]	FAO GW [ln]
CELL LYSATE	[^{12}C]LPC	0.5	r	+ 0.40	+ 0.48
			p	0.2462	0.1601
			n	10	10
		4	r	- 0.10	+ 0.30
			p	0.7899	0.3972
			n	10	10
		24	r	- 0.09	+ 0.05
			p	0.7981	0.8824
			n	10	10
	[^{13}C]LPC	0.5	r	+ 0.55	+ 0.44
			p	0.1012	0.2049
			n	10	10
		4	r	- 0.47	- 0.36
			p	0.1723	0.3026
			n	10	10
		24	r	- 0.19	- 0.06
			p	0.6071	0.8767
			n	10	10
SUPERNATANT	[^{12}C]LPC	0.5	r	+ 0.34	+ 0.77
			p	0.3306	0.0088
			n	10	10
		4	r	+ 0.51	+ 0.75
			p	0.1358	0.0118
			n	10	10
		24	r	+ 0.52	+ 0.71
			p	0.1208	0.0211
			n	10	10
	[^{13}C]LPC	0.5	r	- 0.16	+ 0.18
			p	0.6729	0.6445
			n	9	9
		4	r	+ 0.07	+ 0.01
			p	0.8384	0.9706
			n	10	10
		24	r	+ 0.24	+ 0.04
			p	0.4987	0.9151
			n	10	10

Table 20: Heat map for the correlations of [^{12}C]- or [^{13}C]-sums and of the individual [^{13}C]-species with the *in vivo* and *in vitro* parameters of the donors. The Pearson correlation coefficient r is visualized by color coding for all correlations with $p \leq 0.05$ and $n \geq 6$ according to the following color keys:

r > 0.0 | r > + 0.1 | r > + 0.2 | r > + 0.3 | r > + 0.4 | r > + 0.5 | r > + 0.6 | r > + 0.7 | r > + 0.8 | r > + 0.9 |
r < 0.0 | r < - 0.1 | r < - 0.2 | r < - 0.3 | r < - 0.4 | r < - 0.5 | r < - 0.6 | r < - 0.7 | r < - 0.8 | r < - 0.9 |

Please refer to the List of Abbreviations for specification of abbreviations.

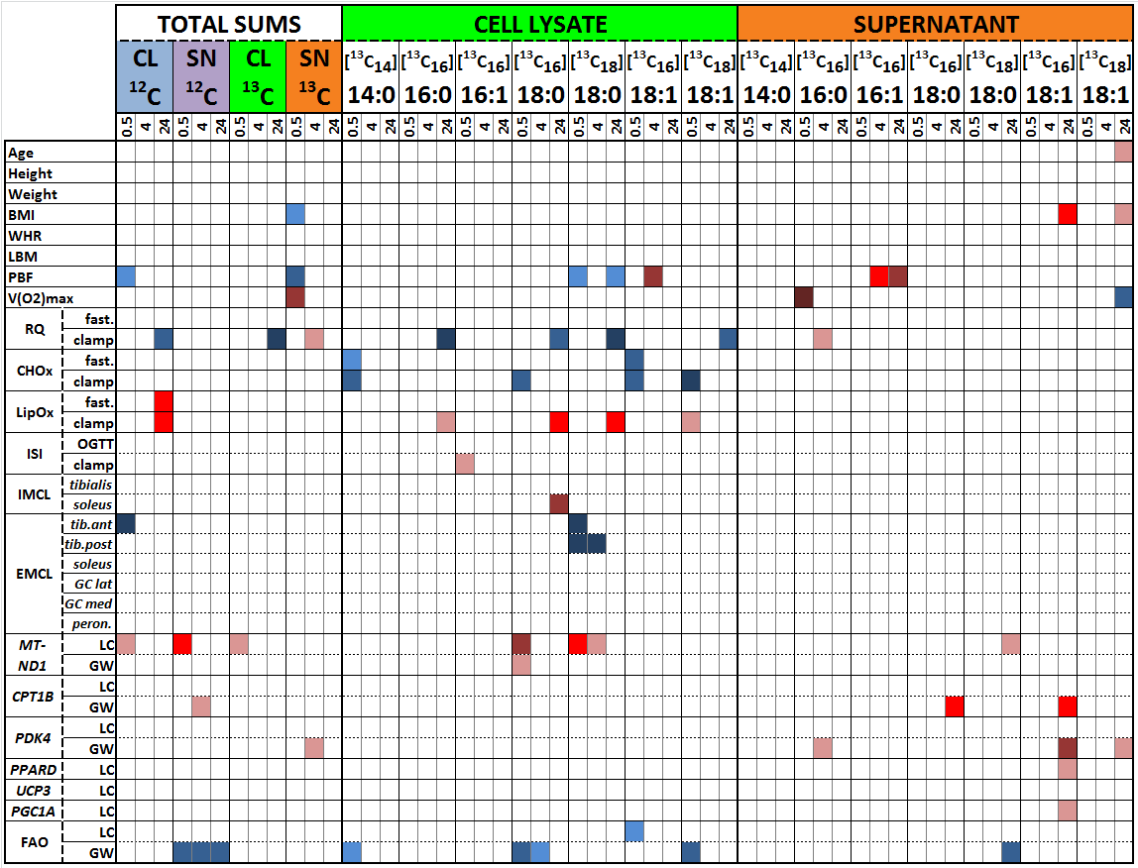

Table 21: Heat map of the species-specific associations of the intracellular [^{12}C]-species with the *in vivo* and *in vitro* parameters of the donors. The Pearson correlation coefficient r is visualized by color coding for all correlations with $p \leq 0.05$ and $n \geq 6$ according to the following color keys:

r > 0.0 | r > + 0.1 | r > + 0.2 | r > + 0.3 | r > + 0.4 | r > + 0.5 | r > + 0.6 | r > + 0.7 | r > + 0.8 | r > + 0.9 |
r < 0.0 | r < - 0.1 | r < - 0.2 | r < - 0.3 | r < - 0.4 | r < - 0.5 | r < - 0.6 | r < - 0.7 | r < - 0.8 | r < - 0.9 |

Please refer to the List of Abbreviations for specification of abbreviations.

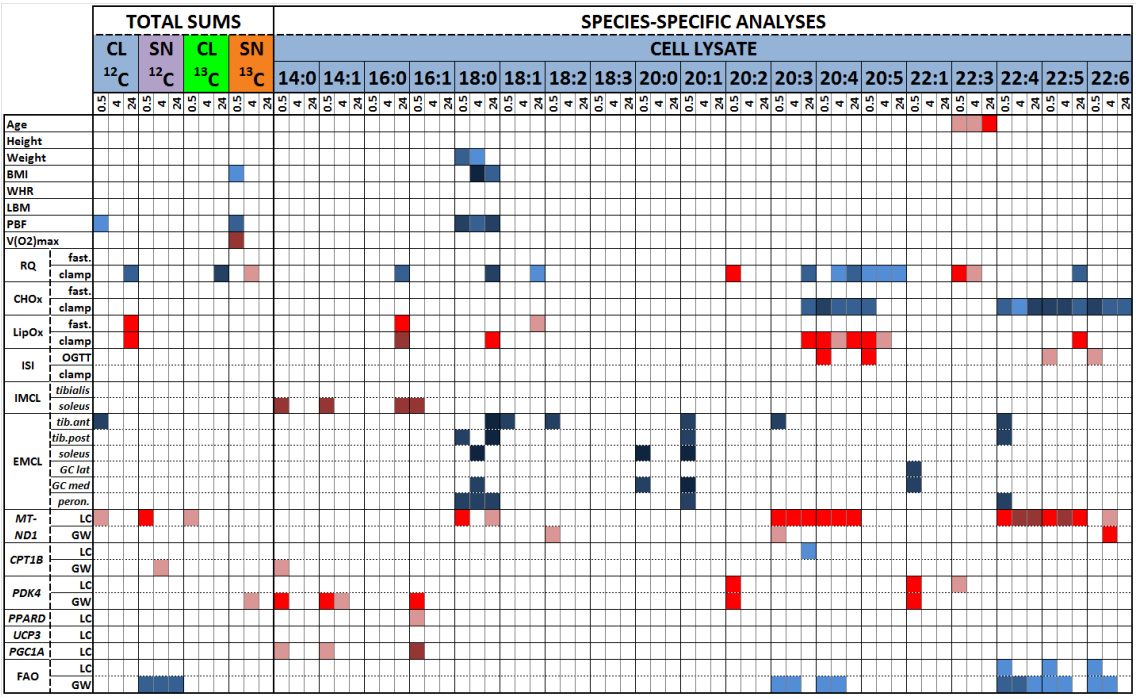

Table 22: Heat map of the species-specific associations of the extracellular [^{12}C]-species with the *in vivo* and *in vitro* parameters of the donors. The Pearson correlation coefficient r is visualized by color coding for all correlations with $p \leq 0.05$ and $n \geq 6$ according to the following color keys:

r > 0.0 | r > + 0.1 | r > + 0.2 | r > + 0.3 | r > + 0.4 | r > + 0.5 | r > + 0.6 | r > + 0.7 | r > + 0.8 | r > + 0.9 |
r < 0.0 | r < - 0.1 | r < - 0.2 | r < - 0.3 | r < - 0.4 | r < - 0.5 | r < - 0.6 | r < - 0.7 | r < - 0.8 | r < - 0.9 |

Please refer to the List of Abbreviations for specification of abbreviations.

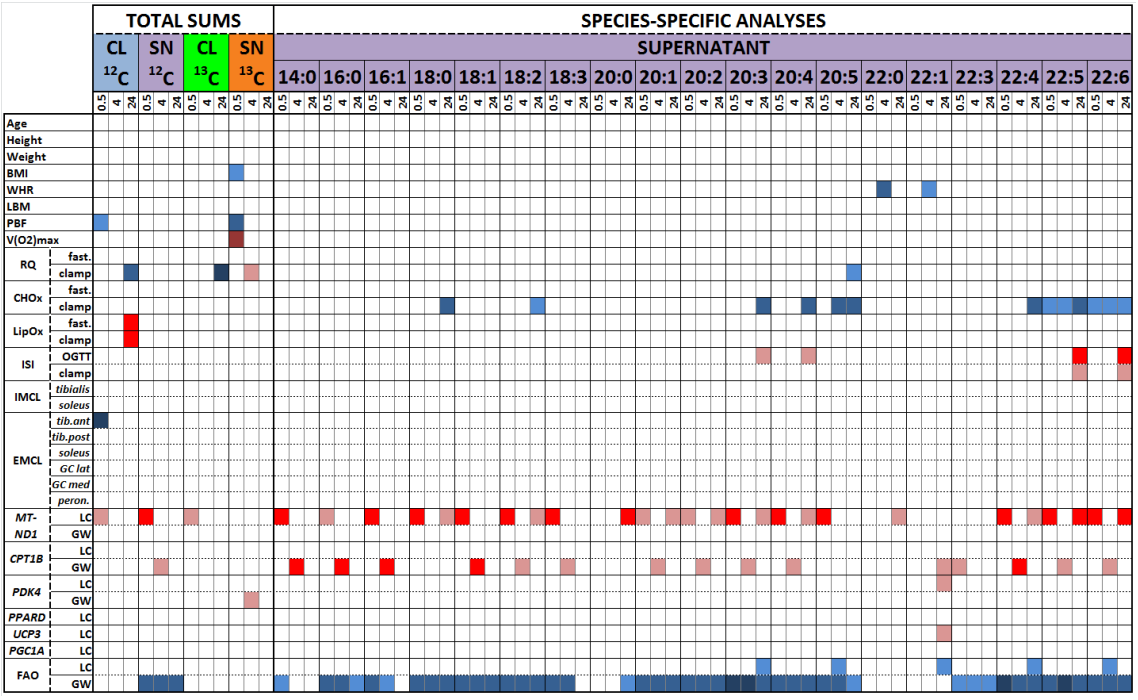

4 Discussion

4.1 Intra- and extracellular lysophosphatidylcholine profiles

The chemical structure of fatty acids hypothetically enables the construction of an enormous variety of different fatty acids. In fact, a relatively restricted assortment is found in nature characteristically differing between different biological organisms [1]. Naturally occurring fatty acids typically feature straight carbon chains with an even number of carbon atoms and eventually one or more nonconjugated *cis*-configured double bonds [1]. Fatty acids with odd-numbered carbon atoms, branched carbon chains, hydroxyl groups, triple bonds, conjugated or *trans*-configured double bonds do also exist, but are rare and often exclusively found in characteristic organisms [1]. The prevalent fatty acids in the human organism are palmitic acid (C16:0), stearic acid (C18:0) and oleic acid (C18:1(9*c*)). Fatty acids containing longer carbon chains (C_{20}, C_{22} and C_{24}) occur in distinctly lower quantities [1]. Phospholipids in human retinal photoreceptor membranes contain acyl groups with up to 36 carbon atoms (C_{36}) [1].

In accordance with these annotations, exclusively even-numbered, nonbranched acyl groups were found as LPC components in this present work with LPC C18:1 being the most abundant and LPC C16:0 being the second most abundant LPC species. The number of carbon atoms of the fatty acyl groups varied from 14 to 22, the number of double bonds from 0 in various species to 6 in LPC C22:6. In total 7 different [^{13}C]-labeled and 20 different unlabeled LPC species were detected. All [^{13}C]-labeled compounds were also found as unlabeled analogs and all of them emerged in both cell lysate and supernatant. Whereas LPC C22:0 was absent in cell lysates, LPC C14:1 was not detected in supernatants so that 19 different LPC species occurred in cell lysates and supernatants, respectively. However, it should be noted that LPC species containing shorter acyl groups might not be covered by our approach because of their more hydrophilic properties.

Notably, Wallace *et al.* found only 5 LPC species [103], Barber *et al.* 15 species [104], Weir *et al.* 21 species [144] and Heilbronn *et al.* 22 species [84]. As shown in the detailed listing of all these detected LPC species in **Table 23**, no hydroxylated or branched LPC species were monitored at all, but odd-numbered LPC species such as LPC C15:0 [84, 104, 144], LPC C17:0 [84, 104, 144] and LPC C17:1 [84, 144], which were not found in this present work, were reported.

Table 23: Comparison of LPC species detected in this present project in both cell lysates and supernatants with LPC species found in human blood samples by Wallace *et al.* [103], Barber *et al.* [104], Heilbronn *et al.* [84] and Weir *et al.* [144] Monitored species are represented by green color whereas absent species are represented by red color.

#	LPC species	Cell lysate	Supernatant	Wallace *et al.* *Mol. Biosyst.* 2014	Barber *et al.* *PLoS One* 2012	Heilbronn *et al.* *Obesity* 2013	Weir *et al.* *J. Lipid Res.* 2013
1	**LPC C14:0**						
2	**LPC C14:1**						
3	**LPC C15:0**						
4	**LPC C16:0**						
5	**LPC C16:1**						
6	**LPC C17:0**						
7	**LPC C17:1**						
8	**LPC C18:0**						
9	**LPC C18:1**						
10	**LPC C18:2**						
11	**LPC C18:3**						
12	**LPC C20:0**						
13	**LPC C20:1**						
14	**LPC C20:2**						
15	**LPC C20:3**						
16	**LPC C20:4**						
17	**LPC C20:5**						
18	**LPC C22:0**						
19	**LPC C22:1**						
20	**LPC C22:3**						
21	**LPC C22:4**						
22	**LPC C22:5**						
23	**LPC C22:6**						
24	**LPC C24:0**						
25	**LPC C26:0**						
Total number of species		**19**	**19**	**5**	**15**	**22**	**21**

4.2 Lysophosphatidylcholines in Trial Medium and cell culture supernatants

When compared with the amounts of LPC species in pure Trial Medium, solely 7 out of 19 [^{12}C]LPC species (37 %) detected in the cell culture supernatants of primary human myotubes tended to be higher after the 30-minute stimulation with 100 µM L-carnitine and 125 µM [$^{13}C_{16}$]palmitate (LPC C14:0, LPC C16:1, LPC C18:2, LPC C18:3, LPC C20:2, LPC C20:5 and LPC C22:3). Moreover, after 24 hours of stimulation, the amounts of the majority of the extracellular LPC species were significantly lower than

in pure Trial Medium suggesting appreciably high LPC amounts in pure Trial Medium. As specified in chapter **2.1.1**, 13 ml pure Trial Medium consisted of 12.5 ml EMEM Medium, 250 µl FBS (final concentration in Trial Medium: 2 %), 125 µl 10 kU/ml penicillin plus 10 kU/ml streptomycin (final concentration in Trial Medium: 100 U/ml, respectively) and 125 µl 200 mM L-glutamine (final concentration in Trial Medium: 2 mM). Thus, the origin of LPCs in pure Trial Medium has to stem from one of these constituents with FBS appearing most auspicious as FBS contains serum proteins such as albumin [106] or lipoproteins which are known to bind LPC species (*inter alia*) [3, 105, 106]. In this present study, the amounts of substance of LPC C16:0 and LPC C18:1 in 13 ml pure Trial Medium were determined as 14.76 nmol (± 2.62 nmol) and 15.43 nmol (± 2.69 nmol), respectively, corresponding to concentrations of 1.14 µM LPC C16:0 and 1.19 µM LPC C18:1 in pure Trial Medium or 59.0 µM LPC C16:0 and 61.7 µM LPC C18:1 in FBS.

In accordance with these expectations, Barber *et al.* reported concentrations for LPC C16:0 of 34.1 µM and for LPC C18:1 of 15.9 µM in plasma from lean human subjects [104]. In plasma from mice, concentrations for LPC C16:0 of 35.8 µM and for LPC C18:1 of 25.5 µM were detected [104]. Hence, the origin of LPCs in Trial Medium from FBS appears reasonable.

4.3 Kinetics of unlabeled lysophosphatidylcholines

Comparing extracellular LPC amounts in supernatants from cultured primary human myotubes with those in pure Trial Medium reveals that 13 out of 19 LPC species (68 %) significantly decreased after 24 hours of stimulation as a function of both chain length of the acyl group and their degree of unsaturation with longer chain length and major unsaturation promoting decreases over time. Accordingly, LPC C14:0 and LPC C16:1 as species with shorter acyl chains did not decrease after 24 hours of stimulation. The degree of unsaturation only seems to play an important role if the acyl group is consisted of 22 carbon atoms: LPC C22:0, LPC C22:1 and LPC C22:3 remained unaltered, whereas LPC C22:4, LPC C22:5 and LPC C22:6 showed significant declines after 4 hours plus very highly significant declines ($p < 0.0001$*) after 24 hours. Concerning LPC species containing an acyl group with less than 22 carbon atoms, not only the polyunsaturated species LPC C20:3, LPC C20:4 and LPC C20:5 distinctly

decreased after 24 hours ($p < 0.0001$*) but also LPC C18:0, LPC C18:1, LPC C18:2, LPC C18:3, LPC C20:0 and LPC C20:2 showed similar kinetics.

These reductions of extracellular LPC concentrations might be caused by continuous degradation of LPCs in supernatant or by artefacts such as (cumulative) adherence to the plastic walls of the cell culture vessels, but these assumptions are thwarted by trends to increase after 30 minutes by 7 out of 19 species (37 %) plus after 4 hours by LPC C14:0 as well as by the nondecreasing species LPC C14:0, LPC C16:1, LPC C20:1, LPC C22:0, LPC C22:1 and LPC C22:3.
Physicochemical affinity differences concerning the adherence to the plastic walls as well as biochemical affinity differences to degradative enzymes such as phospholipases in the supernatants appear implausible for explanation of divergent kinetics between different species as structurally highly similar LPC species showed incongruent kinetics: Whereas LPC C20:1 did not change, the more saturated LPC C20:0 as well as the more unsaturated LPC C20:2 showed highly significant declines after 24 hours with their acyl group chain being composed of the exact same number of carbon atoms.

Another reason for the extensive declines of most LPC species in supernatant may be found in cellular uptake, either into the intracellular compartment and/or into membranous structures accounting for the amphiphilic character of LPCs. Intracellular uptake of extracellular LPCs does hereby not necessarily cohere with increased intracellular LPC levels, as LPCs might be rapidly metabolized by LLAT (EC 2.3.1.23) with formation of the respective phosphatidylcholine (PC) species or by LPLD with formation of the respective LPA species or by $LPLA_1$ (EC 3.1.1.5) with formation of GPC as depicted in detail in **Figure 2**. As neither these direct derivatives nor any of the multifaceted subsequent metabolites were covered by our targeted stable isotope dilution-based metabolomics approach, no reliable statements can be derived from our results upon the metabolic turnover of LPCs after their (intra-) cellular uptake. To answer this question, a stable isotope-assisted lipidomics approach combined with nontargeted isotopomer filtering covering the respective lipid metabolite classes could be applied [160].

Alternative experiments for further elucidation of (dynamic) LPC production and metabolization could be performed using pharmacological inhibitors in order to investigate the precise role of individual enzymes in the complex metabolome, *exempli gratia* the role of PLA_2 for LPC formation from PCs pharmacologically inhibiting the PLA_2 enzyme by BEL or by $PACOCF_3$ (see chapter **1.1.2**). This pharmacological inhibition experiment would be of peculiar interest because LPCs can also be produced by LCAT, PLA_1 or ROS [87-89] as illustrated in detail in **Figure 3**.
Potential incorporation of LPCs into membranous structures is neither embraced by investigation of supernatants nor by investigation of cell lysates as these membranous structures are discarded as cell debris during the isolation procedure of LPCs from supernatants (see chapter **2.2.2.1**) and cell lysates (see chapter **2.2.2.2**).

There is evidence to suggest that the alterations of [^{12}C]LPCs after both 4 hours and 24 hours occur as a function of the degree of unsaturation of the respectively equivalent acyl group chain length: A higher degree of unsaturation seems to promote intracellular increases as well as extracellular decreases as visualized in **Figure 20** (always focusing on LPC species of the respectively equivalent acyl group chain length).

This dependence of LPC dynamics on the degree of unsaturation of respectively equivalent acyl group chain lengths may be the consequence of differing binding affinities with a major degree of unsaturation implicating a higher binding affinity with, for example, transmembrane transport proteins and/or metabolizing enzymes entailing a greater decline for more unsaturated species in supernatants.
Another explanation may be found in a facilitated (noncatalyzed) transmembrane migration for more unsaturated LPC species. Revealingly, as elaborated in detail in chapter **1.1.5**, equilibration between the two membrane leaflets of sarcoplasmic reticulum membranes after administration of [*N*-$^{13}CH_3$]-labeled LPC C16:0 was completed *in vitro* within 30 minutes at 20 °C [101]. Interestingly, the majority of [*N*-$^{13}CH_3$]LPCs was incorporated into the outer leaflet [130], with approximately 42 % of [*N*-$^{13}CH_3$]LPCs being incorporated into the inner leaflet [101], pointing again to the beforehand discussed possibility of an incorporation of LPCs into the membrane instead of a (complete) transmembrane migration.

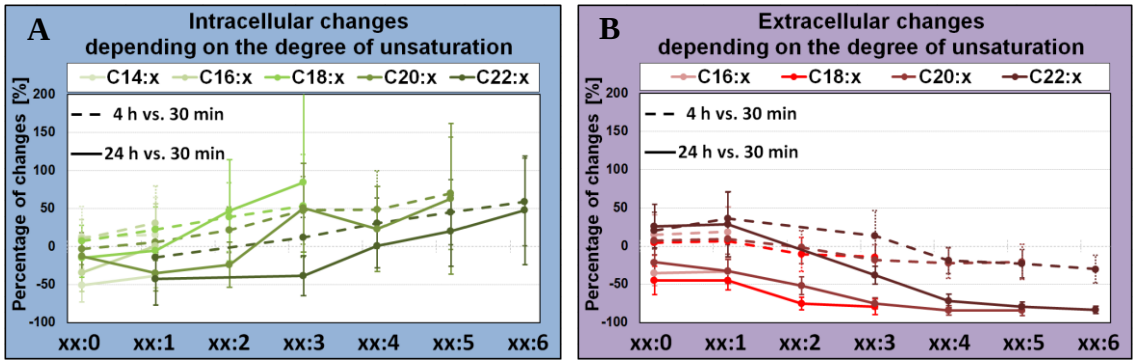

Figure 20: Visualization of the impact of the degree of unsaturation of the lysophosphatidylcholine (LPC) species on the extent of alteration of the intra- (A) and extracellular (B) species. Data are presented as mean ± standard deviation of individual percentage change in relation to the LPC concentrations after 30 minutes of stimulation with 125 µM [$^{13}C_{16}$]palmitate (30 min). The relative percentage changes after 4 hours of stimulation (4 h) are plotted as dashed lines, those after 24 hours (24 h) as solid lines.

However, as all myotubes were stimulated with 125 µM [$^{13}C_{16}$]palmitate we do not know exactly if the decreases are indeed the consequence of the stimulation or if similar kinetics would have been observed without fatty acid stimulation. Therefore, LPC profiling experiments without fatty acid load or with differing concentrations of [$^{13}C_{16}$]palmitate would be valuable for the elucidation of the actual role of the fatty acid *stimulus*.

In fact, previously performed lipidomics experiments of our research group partly offer such experimental designs [160]. So intracellular LPC content was unaltered in primary human myotubes (n = 4) without fatty acid stimulation after 12 hours and after 24 hours but increased approximately twofold after 12 hours of stimulation with 250 µM [$^{13}C_{16}$]palmitate and increased approximately threefold after 24 hours of stimulation in comparison to the control cells cultured without addition of palmitate [160]. Similarly, another publication reported an increased total intracellular LPC content in L6 myotubes after 12-hour stimulation with 600 µM to 1000 µM palmitic acid (C16:0) leading to an approximately twofold to fourfold increase of the LPC content [67]. These elevated intracellular LPC concentrations seem to be the result of an enhanced PLA_2 activity, as this palmitate-induced increase was prevented by pretreatment with the $iPLA_2$ inhibitors $PACOCF_3$ or BEL as well as by transfection with $iPLA_2\beta$ siRNA and/or $iPLA_2\gamma$ siRNA [67]. But as there are existing additional PLA_2 isozymes, further studies will have to elucidate the isozyme-specific relevancies [67].

These reports substantially differ from our findings of predominantly decreasing intracellular [^{12}C]LPC species in response to stimulation with 100 µM L-carnitine and 125 µM [$^{13}C_{16}$]palmitate with 7 species (≈ 37 %) significantly decreased but only 1 species (≈ 5 %) significantly increased after 24 hours (*vs*. 30 minutes). These inconsistencies may be caused by the markedly higher palmitate concentrations which were between 600 µM and 1000 µM in the study by Han *et al.* [67] and 250 µM in the study by Li *et al.* [160].

Most importantly, stimulation was performed with unlabeled [^{12}C]palmitate which is why LPC content was not distinguished into [^{12}C]- and [^{13}C]LPCs and species-specific profiling was omitted [67]. So these results should be compared with our sums of [^{12}C]- plus [^{13}C]LPCs consistently showing significant increases of total intracellular LPCs after 4 hours of stimulation as depicted in **Figure 10** A.

The observation that total intracellular LPCs kept on increasing over 24 hours when stimulated with 250 µM [$^{13}C_{16}$]palmitate [160] but remained constantly elevated without further increase after 4 hours of stimulation with 125 µM [$^{13}C_{16}$]palmitate (24 hours *vs*. 4 hours: $p = 0.9740$; **Figure 10** A) may be indicative of a steady-state coping mechanism.

As total extracellular LPCs are reduced not before 24 hours of stimulation (**Figure 10** B) (intra-) cellular LPC uptake might be compensated by LPC formation (for example directly from PCs by the action of phospholipases) until reaching this steady state.

The discrepancies between increasing intracellular and decreasing extracellular total LPC concentrations raise the question whether the intra- or extracellular LPCs determine the (patho-) biochemical function as intracellular LPCs were proposed to also participate in cell signaling by integration into the cytosolic cell membrane and laterally binding to the binding sites of cell receptors [67, 213].

4.4 Production and release of [^{13}C]-labeled lysophosphatidylcholines

In contrast to the [^{12}C]LPC species, all [^{13}C]LPC species distinctly and permanently increased in the course of time without exception both intra- and extracellularly.

Worth mentioning, different [^{13}C]-labeled LPC species are not directly convertible as visualized in **Figure 21**, but they specifically emerge from a plethora of complex

subsequent reactions including among others fatty acid desaturation by the enzyme stearoyl-CoA desaturase-1 (SCD-1, represented in dark blue color) and/or fatty acid elongation (represented in bright blue color) and/or reaction sequences of β-oxidation (represented in purple color).

Notably, the complex reactions illustrated in **Figure 21** represent a distinct simplification of the actual metabolic pathways as many of these reactions occur in different cell compartments: glycolysis takes place in the cytosol [214], whereas fatty acid oxidation happens primarily in mitochondria [214-216] but partially, albeit by diverging reaction sequences leading to production of H_2O_2, also in peroxisomes [215, 216] as well as in the endoplasmic reticulum [216]. The fatty acid elongation is primarily located at the outer mitochondrial membrane but may also be performed in peroxisomes [217]. The pyruvate dehydrogenase reaction takes place in mitochondria [218]. The occurrence of the metabolic reactions in different cell compartments necessarily implies (noncatalyzed) diffusion and/or (catalyzed) transport mechanisms. For example, the import of acyl-CoA intermediates into mitochondria is not possible but requires the transesterification of the acyl group on L-carnitine with the emerging acylcarnitine crossing the mitochondrial membrane by interaction with specific transport proteins, followed by enzymatically catalyzed retransesterification of the acyl group on coenzyme A restoring the acyl-CoA intermediate. All these complex transport mechanisms are disregarded in **Figure 21**.

Interindividual differences in concentrations of this huge variety of metabolites can be considered as correlates of divergent control mechanisms of metabolism which can be differentiated in, first, the regulation of (substrate or enzyme) locations, second, the regulation of (substrate or enzyme) amounts and, third, the regulation of the (enzymatic) catalytic activity [219]. Interindividual differences in metabolic activities are often attributed to different enzyme activities of specific pacemaker enzymes catalyzing rate-limiting steps in specific reaction sequences. However, enzymes which are not known as pacemaker enzymes in normal or healthy state might become rate-determining when metabolic circumstances or strains are changing [219] like, for example, in pathobiochemical circumstances such as adiposity, insulin resistance or diabetes.

Therefore, the simple investigation of the concentrations of isolated metabolites might be inappropriate to meet the high requirements for elucidation of interindividual differences in the complex metabolic network [219]. As opposed to this, a more sophisticated approach satisfying these requirements might be represented by the combination of repetitive targeted mass spectrometric analyses from the same samples for quantification of all the intermediate metabolites of the complex network and their evaluation by calculation of the specific mass action ratios ($[P_1]^c \cdot [P_2]^d / [E_1]^a [E_2]^b$ for the biochemical reaction $a\ E_1 + b\ E_2 \rightarrow c\ P_1 + d\ P_2$) with a rate-determining reaction in these metabolic circumstances being identified if the calculated ratio distinctly remains under the known equilibrium constant for this reaction [219] or significantly varies between individuals. By this effortful approach, the multiple enzymatic activities of the entire metabolic network might be assessed and interindividually compared.

Furthermore, an alternative method for elucidation of complex metabolic pathways was proposed: The investigation of substrate fluxes (F) enables the identification of rate-determining enzymes by calculation of a sensitivity coefficient Z for each individual enzyme (Z_i) corresponding to the quotient of the relative flux change (dF/F) divided by the relative change in the individual enzyme amount ($d[E_i]/[E_i]$) with the sensitivity coefficient ranging from almost “1” for rate-determining (pacemaker) enzymes to almost “0” for very active enzymes [219].

However, this approach still would fail to identify interindividual differences in reaction rates that are caused by discrepancies in diffusion or transport processes of compounds through specific membranes which can also function as rate-limiting pacemaker step [219].

The investigation of interindividual differences depending on definite cell organelles such as mitochondria or peroxisomes might be accomplished by performing metabolomics analyses after their specific isolation from cell lysates.

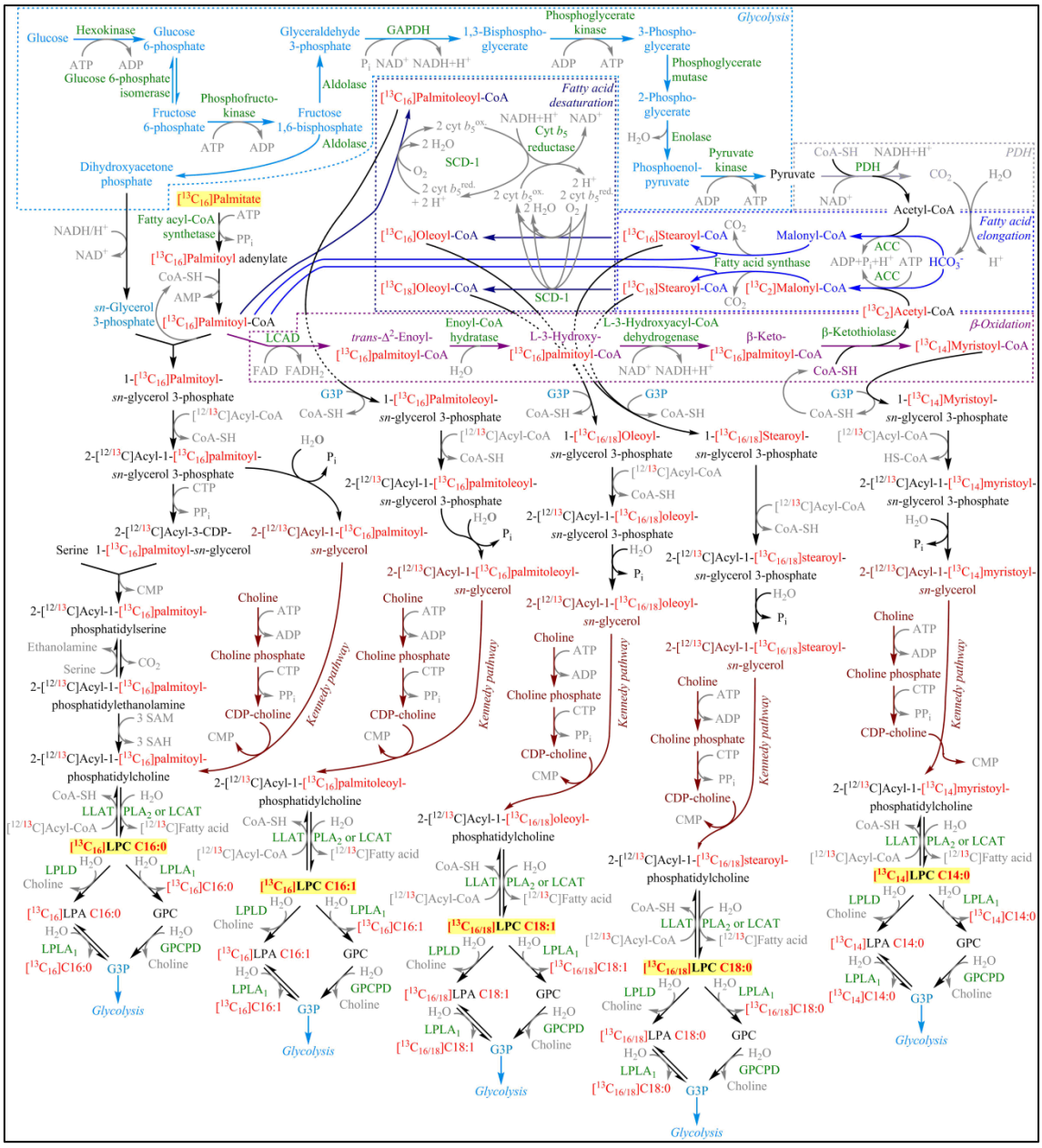

Figure 21: Biochemical formation and degradation of the seven detected [^{13}C]-labeled LPC species after stimulation of primary human myotubes with [$^{13}C_{16}$]palmitate.

Abbreviations: ACC = acetyl-CoA carboxylase, CDP = cytidine 5'-diphosphate, CDP-DAG = 3-CDP-1,2-diacyl-*sn*-glycerol, CMP = cytidine 5'-monophosphate, CoA-SH = coenzyme A, CTP = cytidine 5'-triphosphate, cyt $b_5^{ox.}$ = cytochrome b_5 (oxidized form), cyt $b_5^{red.}$ = cytochrome b_5 (reduced form), FAD = flavin adenine dinucleotide (oxidized form), $FADH_2$ = flavin adenine dinucleotide (reduced form), G3P = *sn*-glycerol 3-phosphate, GAPDH = glyceraldehyde 3-phosphate dehydrogenase, GPC = *sn*-glycero-3-phosphocholine, GPCPD = glycerophosphocholine phosphodiesterase, LCAD = long-chain acyl-CoA dehydrogenase, LCAT = lecithin:cholesterol acyltransferase, LLAT = lysolecithin acyl-transferase, LPA = lysophosphatidic acid, LPC = lysophosphatidylcholine, $LPLA_1$ = lysophospholipase A_1, LPLD = lysophospholipase D, NAD^+ = nicotinamide adenine dinucleotide (oxidized form), $NADH/H^+$ = nicotinamide adenine dinucleotide (reduced form), PDH = pyruvate dehydrogenase multi-enzyme complex, P_i = inorganic phosphate, PLA_2 = phospholipase A_2, SAH = *S*-adenosyl-L-homocysteine, SAM = *S*-adenosyl-L-methionine, SCD-1 = stearoyl-CoA desaturase-1.

4.5 Correlation analyses

4.5.1 Statistical considerations

It is very important to emphasize that the correlation analyses included an immense abundance of data (7 intracellular [^{13}C]-species, 7 extracellular [^{13}C]-species, 19 intracellular [^{12}C]-species and 19 extracellular [^{12}C]-species at always 3 stimulation periods *versus* 88 anthropometric, physiologic and biochemical variables) resulting in an enormous number of tests ($n \approx 13{,}500$). Thus, the probability increases that some of the statistically significant associations may be caused by a type 1 error. Bonferroni-Holm correction could reduce the risk for type 1 errors, but as the work in hand was intended as a explorative and hypotheses generating project with a low number of subjects ($n = 12$), correction methods were not executed. In lieu thereof, detected statistically significant associations should be verified in subsequent hypothesis-based studies with a major number of subjects for assessment of biochemical relevance. Reasonableness of adjustments for multiple comparisons is challenged anyway to some extent, because reducing the type 1 error for void associations by correcting procedures leads to an increase of type 2 errors for those associations which are not void [220]. Subsequently, important and relevant findings could get lost by correcting procedures [220]. Furthermore, the universal null hypothesis, which represents the basis for the endorsement of adjustments in performing multiple comparisons [220], assumes, that the variables are independent of each other [177]. Contradictory to this fundamental assumption, many of the variables in this study were highly correlated. Anyhow, it should be mentioned that the majority of the significant findings would miss the statistical significance if an adjustment for multiple comparisons was applied.

4.5.2 Relevance of the results of LPC sums

Aligning the correlations found either for the LPC sums or for the individual LPC species reveals that the results of the sums are largely mirrored by the most abundant species which are [$^{13}C_{16}$]LPC C16:0, LPC C16:0, LPC C18:0 and LPC C18:1 as they exert mathematically major impacts.

4.5.3 Relationships with anthropometrics

Other publications realized statistical analyses using multivariate linear regression models [176-178, 185]. To some extent, other results could have been expected by

performing association analyses with adjusted data. For example, Stefan *et al.* adjusted PBF, WHR and BMI for age and sex, all other parameters additionally for PBF, C-peptide plasma concentrations additionally for glucose plasma concentrations at the equal instant of time during OGTT and 1^{st}pIS for ISI_{OGTT} [177]. Weyrich *et al.* adjusted PBF, WHR and BMI for age and sex, all other parameters additionally for PBF, insulin secretion additionally for ISI and basal EnExp additionally for LBM [176].

As outlined in detail in the chapters **3.3.1** as well as **9.7.2**, anthropometrics of the donors (*in vivo*) correlated with not more than 4 species (*in vitro*), respectively. As the statistical significance level is mathematically defined as the probability that the considered association is achieved or exceeded assuming the null hypothesis and thus void associations, this signifies that defining an arbitrary significance level of 0.05 (like in these correlation analyses) leads theoretically to 5 % of significant results even if the null hypothesis is accepted and the associations are void. Following this, the inclusion of 52 species into the correlation analyses implies the occurrence of between 2 and 3 (2.6) significant findings without rejection of the null hypothesis. As 3 different stimulation periods were taken into account, this number raises to approximately 8 (7.8) when referring to individual stimulation time points. As age showed significant relationships with 4 individual time points, height with none, weight with 2, BMI with 4, WHR with 2, LBM with none, PBF with 8 and $V(O_2)_{max}$ with 2, these associations may be caused stochastically.

Nevertheless, it's noticeable that intracellular LPC C18:0 was positively correlated with the three relative parameters weight (after 0.5 hour and 4 hours), BMI (after 4 hours and 24 hours) and PBF (after 0.5 hour, 4 hours and 24 hours) and that this positive correlation was confirmed by intracellular [$^{13}C_{18}$]LPC C18:0 (after 0.5 hour and 24 hours) suggesting intracellular LPC C18:0 as potential marker for *in vivo* fat mass. **Figure 22** exemplarily shows the significant associations of LPC C18:0 as well as of [$^{13}C_{18}$]LPC C18:0 with *in vivo* parameters of fat distribution (BMI and PBF) and fat oxidation (RQ_{clamp} and $LipOx_{clamp}$) as well as with *in vitro* mitochondrial DNA content.

Furthermore, $V(O_2)_{max}$ (and $V(O_2)_{perc}$) negatively associated with extracellular [$^{13}C_{16}$]LPC C16:0 (after 0.5 hour) representing the straight LPC derivative of the stimulant [$^{13}C_{16}$]palmitate. Thus, myotubes of donors with major maximal aerobic capacity may release the straight LPC derivative at the beginning to a lesser extent.

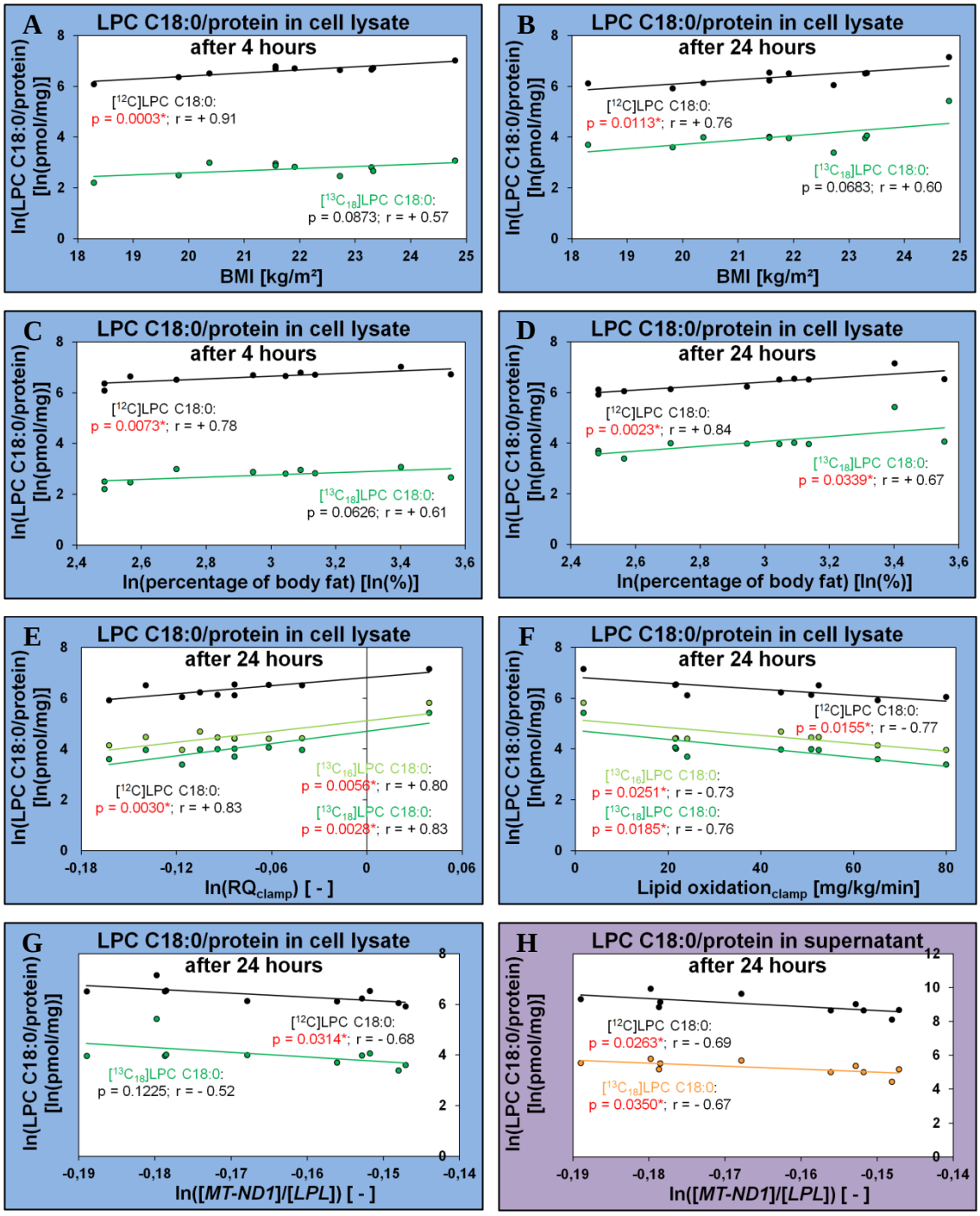

Figure 22: Correlations of the *in vitro* concentration of LPC C18:0 in cell lysates (A – G) or supernatants (H) of cultured primary human myotubes with the *in vivo* fat distribution- and fat oxidation-associated parameters body mass index (BMI; A and B), percentage of body fat (C and D), respiratory quotient (RQ; E) and lipid oxidation activity (F), both measured during steady-state phase of a euglycemic-hyperinsulinemic clamp, as well as the *in vitro* mitochondrial DNA content (G and H) assessed by the amount of the mitochondrially encoded NADH dehydrogenase 1 (*MT-ND1*) in relation to the amount of the (chromosomally encoded) lipoprotein lipase (*LPL*). Myotubes (n = 10 donors) stimulated for 30 minutes, 4 hours (A and C) or 24 hours (B, D, E, F, G and H) with 100 µM L-carnitine and 125 µM [$^{13}C_{16}$]palmitate were used for LPC isolation. The DNA content was investigated in myotubes incubated for 6 days during fusion phase with 100 µM L-carnitine. Correlations were performed in JMP®.

4.5.4 Relationships with physiologic parameters of energy metabolism

Physiologic parameters of energy metabolism of the donors such as RQ, *in vivo* CHOx and *in vivo* LipOx were determined both during fasting condition and during steady-state phase of a euglycemic-hyperinsulinemic clamp. Comparing the correlation analysis results of these physiologic conditions reveals fundamental discrepancies: $RQ_{fasting}$, $CHOx_{fasting}$ and $LipOx_{fasting}$ correlated with less than 5 % of the 52 monitored LPC species, respectively, whereas RQ_{clamp} correlated with 15 species (≈ 29 %), $CHOx_{clamp}$ with 18 species (≈ 35 %) and $LipOx_{clamp}$ with 10 species (≈ 19 %). These considerable differences suggest that the *in vitro* LPC levels measured after stimulation with a fatty acid load are associated with *in vivo* energy metabolism during euglycemic-hyperinsulinemic strain but not with basal energy metabolism during fasting condition.

Detailed analysis of the associated species highlights the relevance of their chemical structure, as solely the (intracellular) long-chain species LPC C20:2 and LPC C22:3, containing not more than three double bonds, exhibited a negative relationship with RQ_{clamp} (in favor of an enhanced lipid oxidation), whereas species containing shorter or long-chain polyunsaturated acyl groups showed correlations in favor of an enhanced carbohydrate oxidation: Positive correlations with RQ_{clamp} were found for intracellular [$^{13}C_{16}$]LPC C16:0, [$^{13}C_{16}$]LPC C18:0, [$^{13}C_{18}$]LPC C18:0, [$^{13}C_{18}$]LPC C18:1, LPC C16:0, LPC C18:0, LPC C18:1, LPC C20:3, LPC C20:4, LPC C20:5, LPC C22:5 and extracellular LPC C20:5 as well as positive correlations with $CHOx_{clamp}$ for intracellular [$^{13}C_{14}$]LPC C14:0, [$^{13}C_{16}$]LPC C18:0, [$^{13}C_{16}$]LPC C18:1, [$^{13}C_{18}$]LPC C18:1, LPC C20:3, LPC C20:4, LPC C20:5, LPC C22:4, LPC C22:5, LPC C22:6 and extracellular LPC C18:0, LPC C18:2, LPC C20:3, LPC C20:4, LPC C20:5, LPC C22:4, LPC C22:5 and LPC C22:6 plus negative correlations with $LipOx_{clamp}$ for intracellular [$^{13}C_{16}$]LPC C16:0, [$^{13}C_{16}$]LPC C18:0, [$^{13}C_{18}$]LPC C18:0, [$^{13}C_{18}$]LPC C18:1, LPC C16:0, LPC C18:0, LPC C20:3, LPC C20:4, LPC C20:5 and LPC C22:5.

Thus, the only species correlating with RQ_{clamp} ($r > 0$), $CHOx_{clamp}$ ($r > 0$) and $LipOx_{clamp}$ ($r < 0$) were intracellular [$^{13}C_{16}$]LPC C18:0, [$^{13}C_{18}$]LPC C18:1, LPC C20:3, LPC C20:4, LPC C20:5 and LPC C22:5. Additionally, the only species associating both intracellularly and extracellularly with $CHOx_{clamp}$ were LPC C20:3, LPC C20:4, LPC C20:5, LPC C22:4, LPC C22:5 and LPC C22:6 underlining the relevance of these

entities with polyunsaturated C_{20} or C_{22} acyl groups. Therefore, **Figure 23** exemplarily illustrates significant associations for these long-chain polyunsaturated species with *in vivo* $CHOx_{clamp}$ (**Figure 23** A, B, E and F) and $LipOx_{clamp}$ (**Figure 23** C and D) as well as with *in vitro* mitochondrial DNA content (**Figure 23** G and H).

Reasons for these varying interdependencies with parameters of energy metabolism depending on the length and the degree of unsaturation of the LPC acyl groups might be explained by differing binding affinities to (particularly rate-determining) enzymes of substrate oxidation pathways such as glycolysis, pyruvate dehydrogenase multienzyme complex, citric acid cycle, β-oxidation or oxidative phosphorylation. As oxidative phosphorylation takes place in mitochondria as β-oxidation does in mitochondria and/or peroxisomes, differing binding affinities to transport proteins might present another explanation. Interindividual differences in these enzyme activities and/or transport protein efficiencies could explain the found associations because both the alteration of specific LPC species levels and the preference of either carbohydrate or lipid oxidation might be resulting consequences. As the most profound associations were found with the long-chain polyunsaturated LPC species, whose complex acyl groups can partially be biosynthesized in peroxisomes, interindividual differences in peroxisomal (dys-) function might offer an additional rationale.

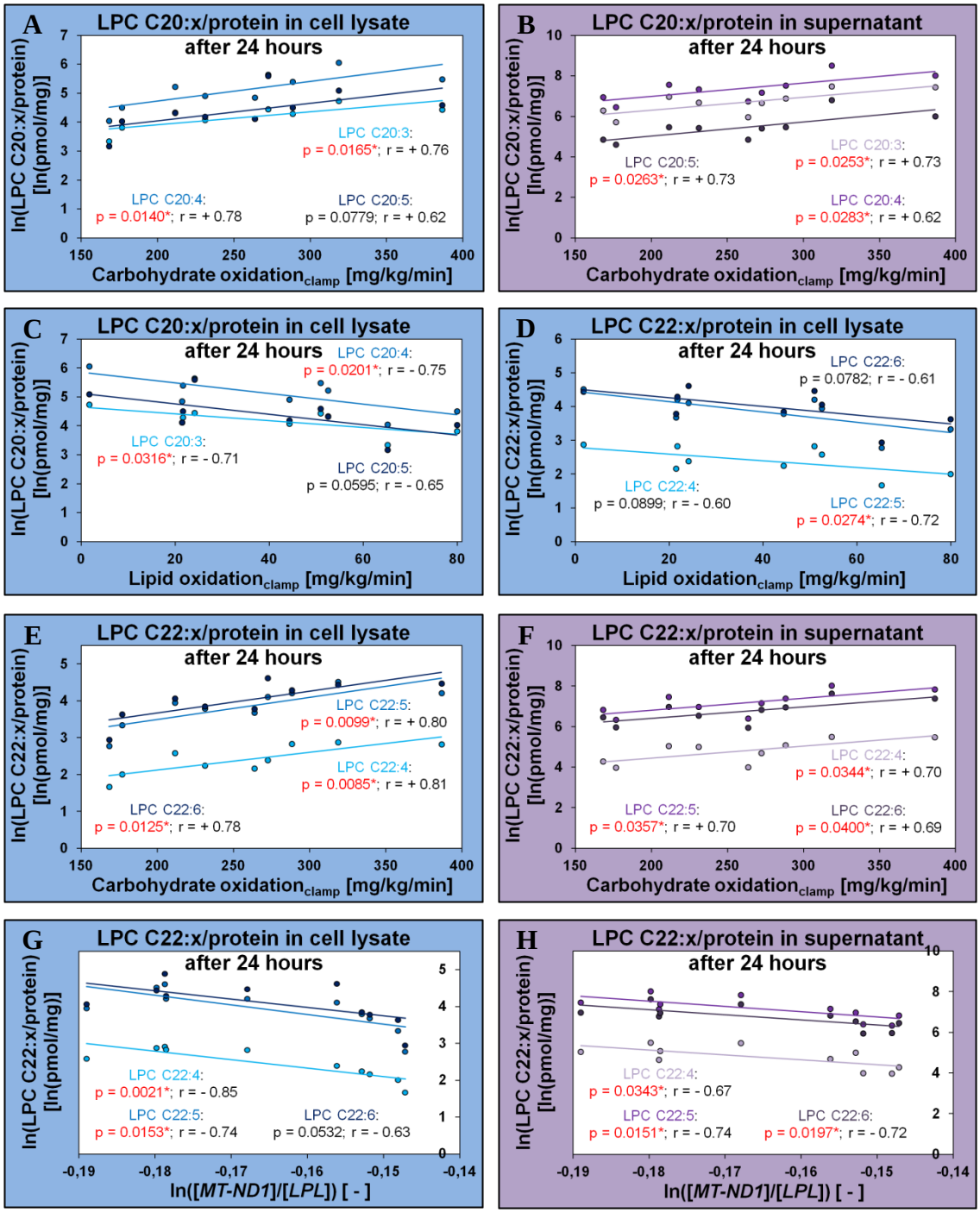

Figure 23: Correlations of long-chain polyunsaturated LPC species with *in vivo* parameters of substrate oxidation activity (A – F) as well as with *in vitro* mitochondrial DNA content (G and H). Isolation of LPCs was accomplished from both cell lysates (A, C, D, E and G) and supernatants (B, F and H) of cultured primary human myotubes from 10 donors (n = 10) stimulated for 30 minutes, 4 hours or 24 hours (A – H) with 100 µM L-carnitine and 125 µM [$^{13}C_{16}$]palmitate. The physiologic *in vivo* parameters carbohydrate oxidation activity (A, B, E and F) and lipid oxidation activity (C and D) were both measured during steady-state phase of a euglycemic-hyperinsulinemic clamp. Mitochondrial DNA content as approximate measure for substrate oxidation capacity was assessed by the amount of the mitochondrially encoded NADH dehydrogenase 1 (*MT-ND1*) in relation to the (chromosomally encoded) lipoprotein lipase (*LPL*) in myotubes incubated for 6 days during fusion phase with 100 µM L-carnitine.

4.5.5 Relationships with other *in vivo* metabolic markers

As concerns other *in vivo* metabolic parameters, a relevant number of 8 significant associations per parameter (as outlined in chapter **4.5.3**) was only reached by ISI determined during OGTT (ISI_{OGTT}) but not by ISI determined during the clamp (ISI_{clamp}). Since ISI_{OGTT} exclusively showed (inverse) correlations with polyunsaturated long-chain species, both intracellularly and extracellularly, but not with other species, the importance of species-specific lipidomics profiling is once more elucidated. Specifically, ISI_{OGTT} negatively correlated with intracellular LPC C20:4, LPC C20:5, LPC C22:5 and LPC C22:6 (always after 0.5 hour) as well as with extracellular LPC C20:3, LPC C20:4, LPC C22:5 and LPC C22:6 (always after 24 hours).

These observations are opposed by consistently reported *in vivo* data on strong negative correlations between circulating LPC levels and insulin resistance: A distinct inverse association of LPC C18:1 with HOMA-IR score reflecting insulin resistance (β = - 0.441, p = 0.006*) has been described by Wallace *et al.* [103] and additional negative associations of HOMA-IR score with LPC species were reported for both human individuals (LPC C18:1, LPC C18:2 [103] and LPC C22:6 [84]) and mice (LPC C15:0, LPC C16:1, LPC 20:0 and LPC C20:1) [104] with HOMA-IR score being considered as estimate of hepatic insulin resistance [84]. These reported negative associations with insulin resistance markedly confront the negative associations with insulin sensitivity which were found in the work in hand. One explanation for these oppositional observations may be differences in regard to the metabolic strain as both Wallace *et al.* and Heilbronn *et al.* performed *in vivo* lipidomics analyses after a 12-hour overnight fasting period in their human cohorts [84, 103] and mice were also fasted for 5 hours prior to plasma sampling [104] whereas *in vitro* LPC profiling of primary human myotubes in this project was directly conducted after the metabolic strain by a fatty acid load employing 125 µM [$^{13}C_{16}$]palmitate for 30 minutes, 4 hours or 24 hours.

However, based on the exclusively positive correlations of LPC species with *in vivo* $CHOx_{clamp}$ as well as the exclusively negative correlations with *in vivo* $LipOx_{clamp}$ in our study (see chapter **3.3.2**) positive relationships would have been expected with ISI as insulin favors glycolysis and inhibits lipolysis. Thus, the few negative correlations with ISI are difficult to explain and should not be overrated.

4.5.6 Relationships with *in vitro* [^{3}H]palmitate oxidation activity

As shown in detail in the chapters **3.3.6** and **9.7.5** as well as in the verbose species-specific correlation analyses in **Supplemental Table 2**, **Supplemental Table 3** plus **Supplemental Table 4**, the vast majority of the observed significant correlations of *in vitro* FAO activity of primary human myotubes with intracellular and extracellular LPC species had a positive direction (144 out of 146; ≈ 99 %) with only two correlations being inverse.

Therefore, high LPC concentrations seem to be indicative of a high *in vitro* FAO activity under metabolic strain by [^{3}H]palmitate. By contrast, *in vitro* LPC concentrations were exclusively negatively associated with *in vivo* $LipOx_{clamp}$ and accordingly positively associated with *in vivo* $CHOx_{clamp}$ plus *in vivo* RQ_{clamp} during a euglycemic-hyperinsulinemic clamp (see chapter **3.3.2**).

These observations suggest the assumption that high LPC levels may be indicative of a high β-oxidation activity under metabolic strain by a fatty acid load but also of a high glycolysis activity under metabolic strain by a combined insulin and glucose load. So there is evidence to suggest that, in the studied cohort of young (age: 24.1 years ± 3.2 years), lean (BMI: 21.8 kg/m² ± 1.9 kg/m²) and metabolically healthy donors, LPC levels may act as an indicator for metabolic flexibility.

Associations of [^{3}H]palmitate oxidation activity with LPC species were much more encompassing after incubation with the PPARδ receptor agonist GW501516 as elaborated in chapter **3.3.6**. Therefore, **Figure 24** displays the correlations of [^{3}H]palmitate oxidation activity after incubation with GW501516 during fusion phase with the long-chain polyunsaturated LPC species LPC C20:3 (**Figure 24** A and B), LPC C20:4 (**Figure 24** C and D), LPC C22:4 (**Figure 24** E and F) and LPC C22:5 (**Figure 24** G and H), as only long-chain polyunsaturated LPC species showed significant associations for both intracellular and extracellular concentrations with the FAO activity after incubation with the PPARδ receptor agonist.

Congruously, studies of our research group revealed the LPC-dependent activation of PPARδ showing an increased expression of its target genes such as *PDK4* [221]. Furthermore, LPC-dependent PPARδ activation ameliorated fatty acid-induced inflammation as well as ER stress in human myotubes [221].

As mentioned previously (see chapter **1.1.7.1**), a high-fat diet in mice led to reduction of LPC levels coinciding with developing obesity [104] which is not only associated with decreased LPC concentrations [103, 104] but also with increased concentrations of TGs and NEFAs [104, 146-148] and this present study revealed distinctly reduced concentrations of most LPC species after stimulation with [$^{13}C_{16}$]palmitate. So, taken together, decreasing LPC levels might be the consequence of increased levels of NEFAs, especially when obesity is simplistically considered as a quasi-experimental *in vivo* analog of an *in vitro* NEFA strain.
However, this hypothesis is disproved by the observations that there are no associations of NEFAs with any LPC species [84, 104]. But as the standardized concentration of [$^{13}C_{16}$]palmitate also caused inter-individually varying decreases of LPC species in this present project, LPC levels may not directly reflect the NEFA concentration but they may rather reflect the individual severity of the metabolic strain caused by the actual NEFA concentration with higher LPC levels revealing a superior coping capacity.

Furthermore, combined with the findings that LPCs stimulate glucose uptake in cultured adipocytes by a dose-dependent insulin-independent mechanism [114], reduced plasma LPC concentrations may cause an increase of blood glucose concentrations what initially might be compensated by hyperinsulinemia.
In fact, Barber *et al.* detected negative correlations of plasma insulin concentrations with LPC C18:1, LPC C18:2, LPC C20:0, LPC C20:1, LPC C20:2 and LPC C22:6 in their human cohort [104]. Consequently, LPCs might mediate metabolic changes in response to supernutrition and adiposity.

As fasting-driven weight loss leads to reduction of circulating NEFA [222] and TG [157, 222] levels and thus to a reduced metabolic strain by these lipids, concentrations of LPCs may recuperate what would be concordant with the hypothesis that LPCs mirror the individual intensity of the actual metabolic strain. However, weight loss following fasting did not alter LPC levels [157].

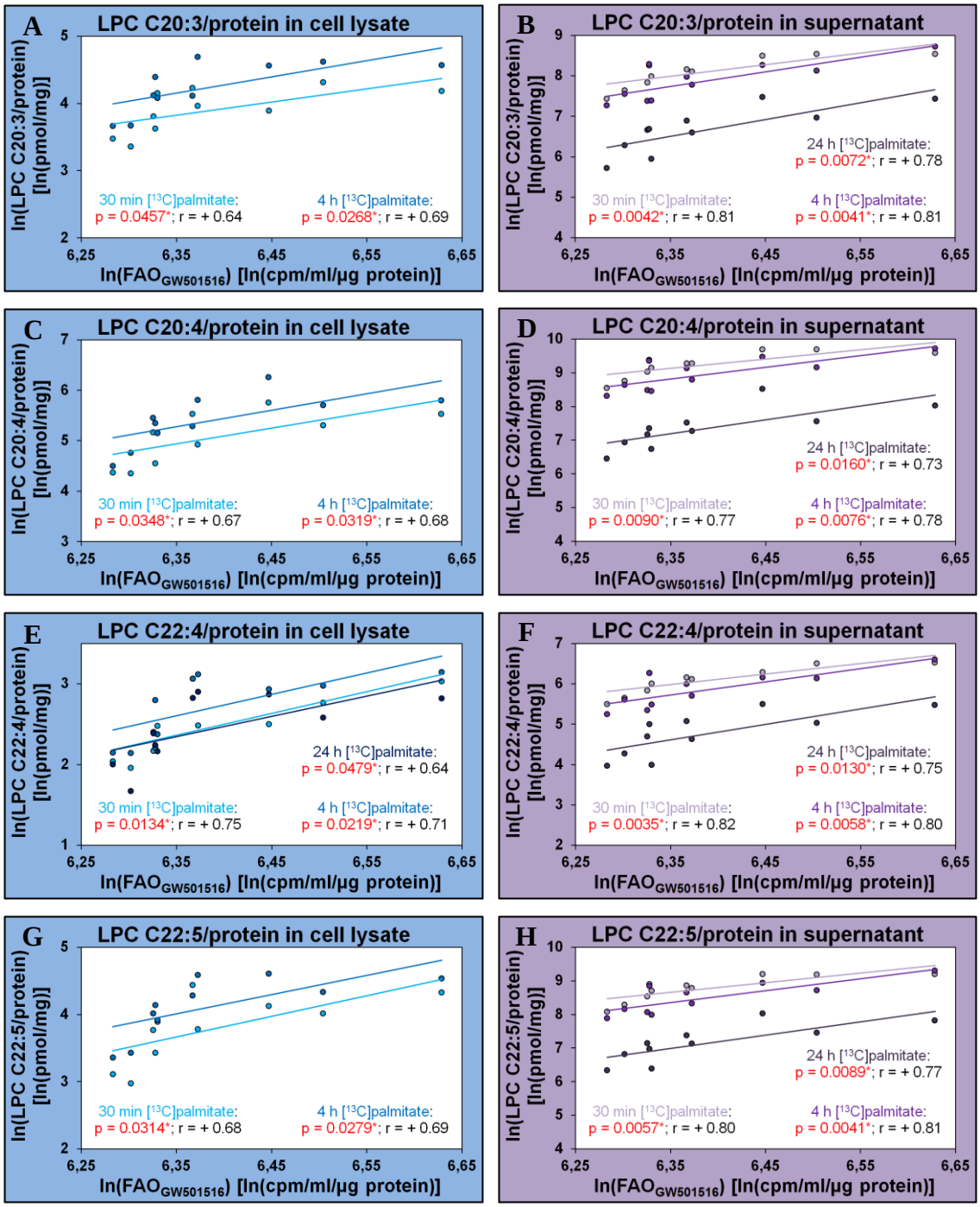

Figure 24: Correlations of long-chain polyunsaturated lysophosphatidylcholine (LPC) species in cell lysates (A, C, E and G) and supernatants (B, D, F and H) from primary human myotubes with the [^{3}H]palmitate fatty acid oxidation (FAO) activity determined after incubation with the PPARδ receptor agonist GW501516. For investigation of LPC kinetics, primary human myotubes from 10 donors (n = 10) were stimulated for 30 minutes (30 min), 4 hours (4 h) or 24 hours (24 h) with 100 µM L-carnitine and 125 µM [$^{13}C_{16}$]palmitate. The activity of FAO was quantified by [^{3}H]$_2$O produced within 4 hours from [^{3}H]palmitate after the incubation of primary human myotubes from the same 10 donors with 100 µM L-carnitine plus 1 µM GW501516 during fusion phase for 7 days. The most profound associations with [^{3}H]palmitate FAO activity in both cell lysates and supernatants were found for the long-chain polyunsaturated species LPC C20:3(A and B), LPC C20:4(C and D), LPC C22:4(E and F) and LPC C22:5(G and H). Correlation analyses were performed in JMP®.

4.5.7 Relationships with gene expression data

In contrast to the exclusively positive correlations of [^{3}H]palmitate oxidation activity in GW501516-incubated cells with LPC species, expression levels of *CPT1B* and *PDK4* showed exclusively negative associations. This is somewhat unexpected as GW501516-induced common pathways such as activation of PPARδ are considered to be responsible for the increase in fatty acid oxidation and gene expression in favor of an ameliorated oxidative capacity (for endurance exercise) [223]. This inconsistency at first sight might be explained by the complex reciprocal action between LPCs and PPAR, as on the one hand LPCs are known to activate PPAR [221, 224] but on the other hand LPC C16:0 levels are increased by pharmacological PPARα activation [224]. Simultaneous analysis of fatty acid oxidation activity, gene expression levels and LPC profiles in GW501516-treated cells (instead of different experiments with differing experimental set-ups as in this case) could represent an initial step for further elucidation of this complex reciprocity.

4.6 Alignment of *in vitro* results with reported *in vivo* findings

The hypothesis that the degree of unsaturation of the LPC acyl group may affect the dynamic character of the correspondent LPC species, as elaborated in the chapters **3.2**, **4.3** and **9.5** as well as visualized in **Figure 20**, is also supported by publications of *in vivo* data: Heilbronn *et al.* found 7 LPC species (LPC C15:0, LPC C16:0, LPC C16:1, LPC C17:0, LPC C20:4, LPC C22:5 and LPC C22:6) to be decreased but the 2 saturated long-chain LPC species LPC C22:0 and LPC C24:0 to be increased in overfeeding [84]. As juxtaposed in opposition in **Table 24**, these reports markedly agree with our findings of distinct decreases of extracellular LPC C16:0, LPC C16:1, LPC C20:4, LPC C22:5 and LPC C22:6 in the course of time whereas extracellular LPC C22:0 was significantly increased after 4 hours. In fact, LPC C22:0 was 1 of only 3 extracellular species (besides LPC C14:0 and LPC C22:1) which were increased after 4 hours. In this present study, LPC C15:0, LPC C17:0 and LPC C24:0 were not monitored.

Furthermore, as described in detail in the chapters **3.3.1** and **4.5.3**, intracellular LPC C18:0 was positively correlated with the three relative parameters weight, BMI and PBF with this positive correlation confirmed by intracellular [$^{13}C_{18}$]LPC C18:0 suggesting intracellular LPC C18:0 as potential marker for *in vivo* fat mass.

Interestingly, circulating LPC levels were repeatedly reported to be decreased in obesity [103, 104] and to be inversely associated with BMI [103, 104, 144], *inter alia* specifically for LPC C18:0 [103, 104, 144]. These reports could be squared with our findings by interpreting the decreased circulating (extracellular) levels as consequence of an increased (intra-) cellular uptake. However, Kim *et al.* reported decreased LPC C18:1 but increased LPC C14:0 as well as LPC C18:0 plasma levels in overweight subjects (BMI: 28.9 kg/m² ± 0.2 kg/m²) compared to normal weight subjects (BMI: 20.9 kg/m² ± 0.1 kg/m²) proposing them as potential plasma markers [225]. Furthermore, high-fat-fed pigs also were reported to exhibit increased LPC C18:0 levels in plasma [226] and Zucker (fa/fa) obese rats also showed increased levels of LPC C18:0 as well as of LPC C16:0 plus LPC C18:1 compared with wild-type animals [227]. Revealingly, exactly these three LPC species were shown to exert the most severe cytotoxic effect of all 11 studied LPC species [106].

As the donors of this study represented a cohort of young (age: 24.1 years ± 3.2 years), lean (BMI: 21.8 kg/m² ± 1.9 kg/m²) and metabolically healthy people with a small range of BMI (18.3 kg/m² - 24.8 kg/m²), results may deviate because of the limitation of the metabolic variations of the donors. More importantly, the reported *in vivo* associations may be the result of the interaction of various tissues and organs or, more precisely, these findings may be the consequence of the biochemical action of another tissue than skeletal muscle as for instance adipose tissue or hepatocytes of the liver.

As mentioned, associations reported *in vivo* between BMI and circulating LPC levels were not confirmed in this present project except for intracellular LPC C18:0, but as overfeeding and adiposity are associated with increased circulating NEFA levels [104, 146-148], *in vivo* overfeeding might be simplistically interpreted as a quasi-experimental analog for an *in vitro* metabolic strain by a fatty acid load (as in this present case). Therefore, **Table 24** compares the alterations of circulating LPC species *in vivo* in (emerging) obesity and after the *in vitro* fatty acid strain in human myotubes.

Revealingly, LPCs were repeatedly found to be decreased in obesity [103, 104, 144] and LPC C16:0, LPC C18:0, LPC C18:1, LPC C18:2 and LPC C20:4, representing all detected LPC species of that study [103], were negatively correlated with BMI [103]. Similarly, Barber *et al.* measured in obese relative to lean subjects significantly lower concentrations of total LPCs as well as of LPC C15:0, LPC C18:0, LPC C18:1,

LPC C18:2, LPC C20:2 and LPC C20:4 plus similar trends for LPC C20:0 and LPC C20:1 and confirmed negative associations with BMI for all these species and total LPCs [104]. In this present study, highly consistent with these reported associations, the ([^{12}C]- + [^{13}C]-) concentrations of LPC C18:0, LPC C18:1, LPC C18:2, LPC C20:0, LPC C20:1, LPC C20:2 and LPC C20:4 were significantly reduced in the supernatants after 24 hours (*vs.* 30 minutes) of stimulation with 125 µM [$^{13}C_{16}$]palmitate.
Additionally, Barber *et al.* found a marked reduction of plasma LPC concentrations in mice already after one week of high-fat diet persisting after three, six (and twelve) weeks of high-fat diet [104]: Specifically, LPC C14:0 (delayed response after 12 weeks), LPC C15:0, LPC C16:0 (after 3 weeks), LPC C16:1, LPC C18:1, LPC C18:2, LPC C20:0 (after 12 weeks), LPC C20:1 and LPC C20:5 significantly decreased, with LPC C16:1, LPC C20:1 and LPC C20:5 approximately diminishing by half, whereas the concentrations of LPC C18:0, LPC C20:0 (initially) and LPC C20:4 rose slightly but significantly [104]. Interestingly, total LPCs represented the only lipid class decreasing in plasma in consequence of this high-fat diet in mice [104]. The work in hand validated the decreases of extracellular LPC C14:0, LPC C16:0, LPC C16:1, LPC C18:1, LPC C18:2, LPC C20:0, LPC C20:1 and LPC C20:5 but distinct decreases instead of slight increases were observed for LPC C18:0 and LPC C20:4 and thus matching better with the alteration pattern of the obese human cohort (*vide supra*).
However, it needs to be emphasized that this comparison between observations *in vivo* in plasma/serum *versus* cell culture supernatants *in vitro* has to be interpreted with due care because of the restricted comparability and multiple additional influencing factors.

In skeletal muscle of the aforementioned mice, Barber *et al.* observed much more moderate changes with only LPC C16:1 and LPC C20:1 but not total LPCs significantly decreasing with high-fat diet [104]. These reports are consistent with our findings as intracellular total ([^{12}C]- + [^{13}C]-)LPCs did not significantly change after 24-hour (*vs*. 30-min) stimulation with only 6 species (≈ 32 %) significantly decreasing, whereas extracellular total LPCs markedly decreased after 24 hours (*vs*. 30-min stimulation: - 44 %, $p < 0.0001$*) with 15 species (≈ 79 %) significantly decreasing. Specific comparisons with the decreasing intramuscular species reported by Barber *et al.* consistently reveal significant decreases for intracellular LPC C20:1 but a significant increase of ([^{12}C]- + [^{13}C]-)LPC C16:1 after 24-hour (*vs*. 30-min) stimulation.

Table 24: Comparative juxtaposition of LPC alterations on the one hand after an *in vitro* fatty acid strain (in this present project; alterations refer to the sums of [^{12}C]- plus [^{13}C]-species, respectively) and on the other hand *in vivo* after overfeeding: Barber *et al.* investigated plasma lipid profile changes in 11 mice fed a high-fat diet (HFD) in comparison to baseline (B/L) after 1 week (wk), 3 wk or 6 wk as well as in 10 obese nondiabetic *vs.* 11 lean human subjects (human, obese *vs.* lean) [104]. Kus *et al.* reported plasma LPC differences in (in each case 4) mice fed a 6-week high-fat diet before being either refed for 3 hours after 10-hour fasting or left without refeeding for 14-hour fasting period [143]. Heilbronn *et al.* performed serum lipidomics analyses in 40 healthy human individuals overfed by 1,250 kcal/day for 28 days [84]. Weir *et al.* found profound negative associations between BMI and plasma LPC species in a cohort of more than 1000 human individuals [144]. In this present project, LPCs were isolated from cell lysates and supernatants of primary human myotubes (n = 10) stimulated with 100 µM L-carnitine and 125 µM [$^{13}C_{16}$]palmitate for 30 minutes (0.5 h), 4 hours (4 h) or 24 hours (24 h).
The arrows reflect the level of significance with a parenthesized arrow showing relative decreases ((↓)) or relative increases ((↑)) with a tendency to statistical significance ($0.10 \geq p > 0.05$), one arrow showing significant ($0.05 \geq p > 0.01$), two arrows showing highly significant ($0.01 \geq p > 0.001$), three arrows showing very highly significant ($0.001 \geq p > 0.0001$) changes and four arrows showing decreases (↓↓↓↓) or increases (↑↑↑↑) with $p \leq 0.0001$. Relative changes are elucidated by backgrounds colored with different intensities of green (relative increase > + 25 % | + 50 % | + 100 % | + 200 % | + 400 %) or red (relative decrease < - 20 % | - 33 % | - 50 % | - 67 % | - 80 %), respectively. The magnitude of β coefficients in the association study is also color-coded: β ≤ - 0.5 | - 1.0 | - 1.5 | - 2.0 | - 2.5.
Crossed out boxes indicate nondetected species in the respective study.

		CELL LYSATE			SUPERNATANT			Barber, *PLoS One*, 2012				Kus *PLoS One* 2011	Heil-bronn *Obes.* 2013	Weir *J.Lip. Res.* 2013
		4 h	24 h		4 h	24 h		1 wk HFD *vs.* B/L	3 wk HFD *vs.* B/L	6 wk HFD *vs.* B/L	human obese *vs.* lean			
		vs. 0.5 h	*vs.* 0.5 h	*vs.* 4 h	*vs.* 0.5 h	*vs.* 0.5 h	*vs.* 4 h							
Total [^{12}C]+[^{13}C]		↑				↓↓↓↓	↓↓↓				↓			- 1.4
([^{12}C]- + [^{13}C]-)LPC species	LPC C14:0		↓	↓↓	↑		↓							
	LPC C14:1		↓	↓↓										
	LPC C15:0							↓↓↓	↓↓↓	↓↓↓	↓		↓	- 1.4
	LPC C16:0	↑↑	(↑)				↓		↓↓	↓↓↓			↓	- 0.6
	LPC C16:1	↑	↑			↓	↓↓	↓↓↓	↓↓↓	↓↓↓			↓	
	LPC C17:0												↓	- 1.7
	LPC C17:1													- 1.6
	LPC C18:0					↓↓↓	↓↓↓	↑↑↑	↑↑↑	↑↑↑	↓↓	↑		- 1.0
	LPC C18:1	(↑)		↓		↓↓↓↓	↓↓↓	↓↓↓	↓↓↓	↓↓↓	↓	↑		- 1.8
	LPC C18:2	↑	(↑)			↓↓↓↓	↓↓↓↓	↓	↓	↓	↓↓	↑		- 2.7
	LPC C18:3	↑	(↑)			↓↓↓↓	↓↓↓							- 1.0
	LPC C20:0		(↓)	(↓)		↓	↓	↑↑↑	↑↑		(↓)			- 2.4
	LPC C20:1		↓↓↓	↓↓↓		↓↓↓	↓↓↓	↓↓↓	↓↓↓	↓↓↓	(↓)			- 2.4
	LPC C20:2	(↑)	↓↓	↓↓		↓↓↓↓	↓↓↓				↓			- 1.7
	LPC C20:3	↑↑	↑		↓	↓↓↓↓	↓↓↓					↑		
	LPC C20:4	↑		(↓)	↓	↓↓↓↓	↓↓↓↓	(↑)	(↑)	↑	↓	↑	↓	- 1.0
	LPC C20:5	↑↑	(↑)		↓	↓↓↓↓	↓↓↓	↓↓↓	↓↓↓	↓				
	LPC C22:0				↑	(↑)							↑	- 2.0
	LPC C22:1	↓	↓↓	↓↓	↑↑	(↑)								- 1.3
	LPC C22:3		↓↓	↓↓↓		↓↓↓↓	↓↓↓							
	LPC C22:4	↑		↓↓	↓	↓↓↓↓	↓↓↓↓							
	LPC C22:5	↑		↓	↓	↓↓↓↓	↓↓↓						↓	
	LPC C22:6	↑	(↑)		↓↓	↓↓↓↓	↓↓↓						↓	- 1.1
	LPC C24:0												↑	- 1.9
	LPC C26:0													- 1.8

By contrast, an increased serum total LPC concentration was reported in rats fed a 10-week high-fat diet without performing species-specific profiling [161]. These distinctions may stem from metabolic discrepancies between the organisms of human beings, mice and rats or, more likely, from the considerable differences of the experimental set-ups: Kinetics of *in vivo* plasma and serum LPCs of fat-overfed mice [104] and rats [161] were observed for weeks whereas kinetics of *in vitro* LPC concentrations from palmitate-stimulated human myotubes were observed for hours. And high-fat diet represents a much more heterogeneous stimulant containing a variety of lipids and fatty acids besides proteins and carbohydrates [104].

Remarkably, Kus *et al.*, also studying high-fat-fed mice, did not find any alterations of LPC concentrations when mice were fasted for 14 hours before sampling, but when mice were refed elevations of LPC C18:0, LPC C18:2 and LPC C20:4 were recognized in these high-fat-fed mice [143]. Thus, these results confirm the increases of LPC C18:0 and LPC C20:4 shown by Barber *et al.* but confront the decrease of LPC C18:2 [104].

4.7 Closing remarks on discrepancies between publications

First of all, it should be once again emphasized that divergent findings between *in vitro* results in this present work and published *in vivo* results are most likely the primary consequence of the restricted commensurability of these fundamentally distinct study designs. Most notably, the comparisons between LPC alterations on the one hand *in vitro* in cell culture supernatants after stimulation with a fatty acid load and on the other hand *in vivo* in serum or plasma of overfed or obese animals or human subjects have to be interpreted with all due caution, as circulating LPC concentrations are not only influenced by the secretory performances of each single cell type producing LPCs *in vivo* but also by the absorption capacity of each single cell type absorbing LPCs from circulation *in vivo* as well as by the enzymatic capacity for further metabolization of LPCs with their enzymatic degradation potentially taking place both intracellularly (catalyzed by cell enzymes) and extracellularly (catalyzed by circulating enzymes).

Additionally, discrepancies both between different studies and between this present work and published results may be explained by anthropometric, physiologic or metabolic differences of the investigated cohorts. Especially parameters like gender, age, BMI, insulin sensitivity, FAO activity, metabolic flexibility or physical fitness, comorbidities like obesity, insulin resistance or type 2 diabetes mellitus or therapeutic

procedures like exercising, diets, lifestyle interventions or medication with oral antihyperglycemic agents or antihypertensive drugs may act as substantial confounders and there may be differences in lipidome changes between Caucasian, Asian and Black individuals. So Wallace *et al.* and Heilbronn *et al.* investigated groups of metabolically healthy borderline normal weight subjects [84, 103] (**Supplemental Table 6**), whereas Barber *et al.* compared normal weight individuals with both obese nondiabetic subjects and obese patients with type 2 diabetes mellitus from whom some were being treated with diet (> 65 %), oral antidiabetics (> 30 %) and/or antihypertensives (> 30 %) [104]. Notably, high-fat-fed rats treated with metformin showed after 10 weeks reduced LPC levels compared to the high-fat-fed rats without metformin treatment [161] but as body weight, liver weight, serum TG levels, serum cholesterol levels, serum insulin levels, insulin resistance index, $sPLA_2$ levels, liver TG content, liver cholesterol content, hepatic steatosis and $sPLA_2$ mRNA expression were also ameliorated by metformin administration [161] the LPC reductions may not be directly caused by metformin. Furthermore, alimentary habits could influence the lipidome. Therefore, Heilbronn *et al.* provided for 3 days prior to the first sampling for each subject individually adjusted food according to their calculated baseline energy requirements and consisting of 30 % fat, 15 % protein and 55 % carbohydrates [84], whereas Barber *et al.* and Wallace *et al.* confined themselves to 10-hour to 12-hour overnight fasting periods [103, 104]. While [$^{13}C_{16}$]palmitate was used in this present study for stimulation, high-fat-fed mice received a diet whose energy derived 35 % from carbohydrates, 23 % from proteins and 42 % from fat including 24.7 % palmitic acid (C16:0), 15.7 % stearic acid (C18:0), 32.8 % oleic acid (C18:1) and 19.0 % linoleic acid (C18:2) [104].

Although cell culture experiments implicate many limitations such as the lack of interorganic communication mechanisms, they facilitate the clarification of specific issues by excluding influential variables. For example, influence of differing diets on the alterations of plasma LPC levels is difficult to consider in human cohorts [104] whereas a lipid load can be readily standardized in cell culture experiments.

In addition, fasting periods preceding to sampling may influence results [104, 143] and varied for example in studies with high-fat-fed mice between 5 hours [104] and 14 hours [143] with LPC alterations getting lost in consequence of the prolonged fasting period. Overfeeding studies not only differed in organism but also in intensity of

overnutrition and length of time resulting in markedly different metabolic strains reflected by a 7.5-fold increase of HOMA-IR score in mice overfed for 12 weeks [104] *versus* a 1.4-fold increase of HOMA-IR score in rats overfed for 10 weeks [161] and a 1.2-fold increase of HOMA-IR score in human subjects overfed for 4 weeks [84].

Moreover, discrepancies may be the result of differing determination methods and/or sample materials such as the analysis of the lipidome in plasma [103, 104, 144] *versus* serum [84]: Wallace *et al.* detected 325 lipid species in plasma [103], Weir *et al.* 312 lipid species in plasma [144] and Heilbronn *et al.* 333 lipid species in serum [84].

Furthermore, contradictory results concerning alterations of LPC levels may also be caused by the complex and highly dynamic kinetics of the specific LPC species possibly in combination with differing points in time for measurement. In plasma of high-fat-fed mice for example, LPC C15:0, LPC C16:1, LPC C18:1, LPC C18:2 and LPC C20:1 were already significantly decreased after 1 week of high-fat diet remaining at these levels during a 12-week high-fat diet and this kinetic applied analogously to the increasing LPC C18:0 species, but LPC C16:0 showed a delayed reduction after 3 weeks and LPC C20:4 a delayed elevation after 6 weeks [104]. Interestingly, LPC C20:0 was found to be initially increased after 1 week of overfeeding before declining slowly to be decreased after 12 weeks [104].

Therefore, it appears legitimate and reasonable to differentiate the LPC lipid class into specific LPC species as different LPC species may exert different biological functions. In consequence of both this insight and technological progress, differentiation of LPC lipids into specific LPC species tends to be routine standard in current studies [84, 103, 104, 144] whereas previous studies mostly omitted LPC specification [67, 78, 161].

The reproducibility of results of other studies is further complicated by the complexity of interaction mechanisms and by the abundance of multiple influencing factors. For example, the negative correlation between IMCL and insulin sensitivity [228, 229] is only found in untrained subjects but not in endurance-trained subjects [178]. Thus, this relationship seems to be modified by training. And HOMA-IR score (reflecting insulin resistance) is especially increased in humans showing both low plasma concentrations of LPC C18:1 plus LPC C18:2 and high concentrations of CRP or leptin [103].

Much more of these complex interactions exist among whom many may be still to discover.

5 Summary

Introduction: Lysophosphatidylcholines (LPCs) are considered as regulators of inflammation and atherosclerosis and increased intracellular and/or decreased circulating LPC concentrations have been multiply reported in obesity and insulin resistance. The aim of this study was to elucidate intracellular and extracellular LPC kinetics in primary human myotubes (hMT) after palmitate stimulation as correlate for an increased metabolic strain by free fatty acids and to reveal potential associations with *in vivo* characteristics of the donors and/or other *in vitro* results.

Methods: Myosatellite cells were obtained from muscle biopsies of the *M. vastus lateralis* from 12 lean, metabolically healthy participants of the Tübingen Family (TUEF) study involving anthropometric, physiologic and metabolic *in vivo* phenotyping of the donors in fasting condition, during an oral glucose tolerance test (OGTT) as well as during a euglycemic-hyperinsulinemic clamp (clamp). Myosatellite cells were isolated, proliferated and differentiated to primary hMTs which were stimulated for 30 minutes (0.5 h), 4 hours (4 h) or 24 hours (24 h) with 100 µM L-carnitine and 125 µM [$^{13}C_{16}$]palmitate. Intra- and extracellular [^{12}C]- and [^{13}C]LPCs were isolated and quantified by stable isotope dilution-based metabolomics analysis applying HPLC-ESI-Q-TOF-MS. Cultured hMTs were additionally used for investigation of mitochondrial DNA (mtDNA) content by duplex PCRs, of *in vitro* expression of important genes of fatty acid metabolism by RT-qPCRs and of [^{3}H]palmitate oxidation (FAO) activity by liquid scintillation counting.

Results: Mass spectrometric LPC profiling revealed 20 [^{12}C]-species, whereof in each case one was exclusively found intra- or extracellularly, and 7 [^{13}C]-labeled species. Permanently increasing concentrations were observed for the 7 [^{13}C]-species ([$^{13}C_{14}$]- to [$^{13}C_{18}$]-containing LPC species including LPC C16:1 and LPC C18:1) without exception both intra- and extracellularly. In contrast, most of the [^{12}C]-species were decreased after 24 hours in the supernatants and, to a lesser extent, also in the cell lysates. As a consequence, the total sum of all detected extracellular ([^{12}C]- + [^{13}C]-) species was decreased after 24 hours, whereas the total intracellular sum was unchanged. Species-specific analyses of the time course changes of the unlabeled [^{12}C]LPCs suggested an influence of both the length of the acyl group and its degree of unsaturation (in the form of the number of double bonds): The long-chain

polyunsaturated species LPC C20:3, LPC C20:4, LPC C20:5, LPC C22:4, LPC C22:5 and LPC C22:6 showed extracellularly the most profound decreases after 24 hours and intracellularly even increases after 4 hours.

Correlation analyses between the *in vivo* parameters of the donors and the *in vitro* LPC concentrations revealed a positive association of intracellular LPC C18:0 with measures of obesity and for the long-chain polyunsaturated LPC species positive associations with carbohydrate oxidation activity determined during steady-state phase of the clamp ($CHOx_{clamp}$) as well as negative associations with insulin sensitivity determined both during the OGTT and the clamp. Furthermore, the long-chain polyunsaturated LPC species correlated positively with *in vitro* FAO activity after stimulation with [^{3}H]palmitate and negatively with *in vitro* mtDNA content. Additionally, remarkable correlations were found for most extracellular LPC species with FAO activity in hMTs stimulated with the PPARδ receptor agonist GW501516.

Markedly less significant relationships were observed for the radiolabeled [^{13}C]LPC species.

In general, *in vitro* [^{12}C]- and [^{13}C]LPC levels determined in palmitate-strained condition were predominantly positively associated with both *in vitro* FAO activity after stimulation with [^{3}H]palmitate and *in vivo* $CHOx_{clamp}$ after stimulation with intravenous insulin plus glucose suggesting them as an indicator of high metabolic flexibility. Associations with parameters determined during fasting condition were substantially rarer and weaker.

Conclusion: The results of this project underline the importance of species-specific lipid profiling as the individual species considerably differed in both the kinetics and the correlation results. The most dynamic kinetics were observed for long-chain polyunsaturated LPC species also showing the most encompassing correlations with parameters of energy metabolism with lower concentrations potentially pointing to an impaired metabolic flexibility.

6 Zusammenfassung

Einleitung: Lysophosphatidylcholinen (LPCs) wird eine regulierende Funktion in der Entstehung von Entzündungen und Atherosklerose zugeschrieben und erhöhte intrazelluläre und/oder erniedrigte zirkulierende LPC-Konzentrationen im Blut wurden mehrfach im Rahmen von Fettleibigkeit und Insulinresistenz berichtet. Die Zielsetzung dieser Studie bestand in der Aufklärung der intrazellulären und extrazellulären LPC-Kinetik von primären humanen Myotuben (hMT) nach der Stimulation mit Palmitat als Korrelat für eine erhöhte metabolische Beanspruchung durch freie Fettsäuren sowie der Untersuchung auf mögliche Zusammenhänge mit *In-vivo*-Charakteristika der Donoren und/oder weiteren *In-vitro*-Ergebnissen.

Methoden: Muskelsatellitenzellen wurden von Muskelbiopsien des *M. vastus lateralis* bei 12 schlanken, metabolisch gesunden Teilnehmern der Tübinger Familienstudie (TUEF) gewonnen, die zusätzlich auch eine anthropometrische, physiologische und metabolische *In-vivo*-Phänotypisierung im Nüchternzustand, während eines oralen Glukosetoleranztestes (OGTT) sowie während einer euglykämischen-hyperinsulinämischen *Clamp* (Clamp) durchlaufen hatten. Die Satellitenzellen wurden isoliert, proliferiert und zu primären hMT differenziert, die 30 Minuten (0.5 h), 4 Stunden (4 h) oder 24 Stunden (24 h) mit 100 µM L-Carnitin und 125 µM [$^{13}C_{16}$]Palmitat stimuliert wurden. Intra- und extrazelluläre [^{12}C]- und [^{13}C]LPCs wurden isoliert und mittels Isotopenverdünnungsanalyse unter Einsatz von HPLC-ESI-Q-TOF-MS quantifiziert. Zellkulturen der hMTs wurden des Weiteren für die Bestimmung des mitochondrialen DNA (mtDNA)-Gehalts mittels Duplex-PCRs, der *In-vitro*-Expression wichtiger Gene des Fettsäurestoffwechsels mittels RT-qPCRs und der [^{3}H]Palmitat-Oxidationsaktivität (FAO) mittels Flüssigszintillationsdetektormethodik eingesetzt.

Ergebnisse: Die massenspektrometrische Profilanalyse der LPC-Spezies führte zur Detektion von 20 [^{12}C]-Spezies, von denen jeweils eine Spezies nur intra- bzw. extrazellulär auftrat, sowie von 7 [^{13}C]-markierten Spezies. Die Konzentrationen der 7 [^{13}C]-Spezies ([$^{13}C_{14}$]- bis [$^{13}C_{18}$]-enthaltende LPC-Spezies einschließlich LPC C16:1 und LPC C18:1) nahmen sowohl intra- als auch extrazellulär ausnahmslos ständig zu. Demgegenüber waren die meisten der [^{12}C]-Spezies nach 24 Stunden in den Überständen und, in geringerem Maße, auch in den Zelllysaten erniedrigt. In der Folge zeigte sich die Gesamtsumme aller detektierten extrazellulären ([^{12}C]- + [^{13}C]-)Spezies nach 24 Stunden erniedrigt, wogegen die intrazelluläre Gesamtsumme nach 24 Stunden nicht signifikant verändert war. Die speziesspezifische Auswertung der zeitabhängigen

Veränderungen der unmarkierten [^{12}C]LPCs wies darauf hin, dass deren Kinetik sowohl von der Kettenlänge der Acylgruppe als auch von deren Ungesättigtheitsgrad (in Form der Anzahl an Doppelbindungen) beeinflusst wird: Die langkettigen vielfach ungesättigten Spezies LPC C20:3, LPC C20:4, LPC C20:5, LPC C22:4, LPC C22:5 und LPC C22:6 wiesen extrazellulär die ausgeprägtesten Abnahmen nach 24 Stunden und intrazellulär sogar Zunahmen nach 4 Stunden auf.

Bei den Korrelationsanalysen zwischen den *In-vivo*-Parametern der Spender und den *In-vitro*-LPC-Konzentrationen ergaben sich eine positive Assoziation von intrazellulärem LPC C18:0 mit Messgrößen der Fettleibigkeit und für die langkettigen vielfach ungesättigten LPC-Spezies positive Assoziationen mit der Kohlenhydrat-oxidationsaktivität während der Fließgleichgewichtsphase der *Clamp* ($CHOx_{Clamp}$) sowie negative Assoziationen mit der, sowohl durch den OGTT als auch durch die *Clamp* ermittelten, Insulinsensitivität. Die langkettigen vielfach ungesättigten LPC-Spezies korrelierten zudem positiv mit der *In-vitro*-FAO-Aktivität nach Stimulation mit [^{3}H]Palmitat und negativ mit dem *In-vitro*-mtDNA-Gehalt. Außerdem zeigten sich für die meisten extrazellulären LPC-Spezies bemerkenswerte Korrelationen mit der FAO-Aktivität in hMTs, die mit dem PPARδ-Rezeptoragonisten GW501516 stimuliert worden waren.

Deutlich weniger signifikante Zusammenhänge wurden bei den radiomarkierten [^{13}C]LPC-Spezies beobachtet.

Im Allgemeinen waren die *In-vitro*-[^{12}C]- und -[^{13}C]LPC-Konzentrationen infolge der metabolischen Beanspruchung durch [$^{13}C_{16}$]Palmitat sowohl mit der *In-vitro*-FAO-Aktivität infolge der Stimulation mit [^{3}H]Palmitat als auch mit der *In-vivo*-$CHOx_{Clamp}$-Aktivität infolge der intravenösen Stimulation mit Insulin und Glukose überwiegend positiv assoziiert, weshalb LPCs eventuell als Gradmesser einer hohen metabolischen Flexibilität dienen könnten. Assoziationen mit während des Nüchternzustands ermittelten Parametern waren wesentlich seltener und schwächer.

Schlussfolgerung: Die Ergebnisse dieses Projekts verdeutlichen die Bedeutung der speziesspezifischen Profilanalyse bei Lipidquantifizierungen, da sich sowohl bei den Kinetiken als auch bei den Korrelationen beträchtliche Unterschiede zwischen den einzelnen Spezies ergaben. Langkettige vielfach ungesättigte LPC-Spezies wiesen die Kinetiken mit der größten Dynamik auf und zeigten auch die umfassendsten Korrelationen mit Parametern des Energiestoffwechsels, wobei niedrigere Konzentrationen auf eine beeinträchtigte metabolische Flexibilität hinweisen könnten.

7 List of Literature

1. Metzler, D. E. (2003), **Lipid structures**, in *Biochemistry – The Chemical Reactions of Living Cells*, Elsevier Science Academic Press. p. 380-389.
2. Bell, R. M. and Coleman, R. A. (1980), **Enzymes of glycerolipid synthesis in eukaryotes**. Annu Rev Biochem. **49**: p. 459-487.
3. Croset, M., Brossard, N., Polette, A. and Lagarde, M. (2000), **Characterization of plasma unsaturated lysophosphatidylcholines in human and rat**. Biochem J. **345 Pt 1**: p. 61-67.
4. Metzler, D. E. (2003), **The structure of membranes**, in *Biochemistry – The Chemical Reactions of Living Cells*, Elsevier Science Academic Press. p. 390-401.
5. Ray, T. K., Cronan, J. E., Jr., Mavis, R. D. and Vagelos, P. R. (1970), **The specific acylation of glycerol 3-phosphate to monoacylglycerol 3-phosphate in *Escherichia coli*. Evidence for a single enzyme conferring this specificity**. The Journal of biological chemistry. **245**(23): p. 6442-6448.
6. Carman, G. M. and Zeimetz, G. M. (1996), **Regulation of phospholipid biosynthesis in the yeast *Saccharomyces cerevisiae***. The Journal of biological chemistry. **271**(23): p. 13293-13296.
7. Payne, F., Lim, K., Girousse, A., Brown, R. J., Kory, N., Robbins, A., Xue, Y., Sleigh, A., Cochran, E., Adams, C., Dev Borman, A., Russel-Jones, D., Gorden, P., Semple, R. K., Saudek, V., O'Rahilly, S., Walther, T. C., Barroso, I. and Savage, D. B. (2014), **Mutations disrupting the Kennedy phosphatidylcholine pathway in humans with congenital lipodystrophy and fatty liver disease**. Proceedings of the National Academy of Sciences of the United States of America. **111**(24): p. 8901-8906.
8. Barsukov, L. I., Victorov, A. V., Vasilenko, I. A., Evstigneeva, R. P. and Bergelson, L. D. (1980), **Investigation of the inside-outside distribution, intermembrane exchange and transbilayer movement of phospholipids in sonicated vesicles by shift reagent NMR**. Biochim Biophys Acta. **598**(1): p. 153-168.
9. Metzler, D. E. (2003), **Phospholipids**, in *Biochemistry – The Chemical Reactions of Living Cells*. p. 1197-1201.
10. Yamashita, S., Hosaka, K. and Numa, S. (1973), **Acyl-donor specificities of partially purified 1-acylglycerophosphate acyltransferase, 2-acylglycerophosphate acyltransferase and 1-acylglycerophosphorylcholine acyltransferase from rat-liver microsomes**. Eur J Biochem. **38**(1): p. 25-31.
11. Hill, E. E., Husbands, D. R. and Lands, W. E. (1968), **The selective incorporation of ^{14}C-glycerol into different species of phosphatidic acid, phosphatidylethanolamine, and phosphatidylcholine**. The Journal of biological chemistry. **243**(17): p. 4440-4451.
12. Possmayer, F., Scherphof, G. L., Dubbelman, T., Van Golde, L. and Van Deenen, L. L. (1969), **Positional specificity of saturated and unsaturated fatty acids in phosphatidic acid from rat liver**. Biochim Biophys Acta. **176**(1): p. 95-110.
13. Elovson, J., Akesson, B. and Arvidson, G. (1969), **Positional specificity of liver 1,2-diglyceride biosynthesis *in vivo***. Biochim Biophys Acta. **176**(1): p. 214-217.
14. Hanahan, D. J., Brockerhoff, H. and Barron, E. J. (1960), **The site of attack of phospholipase (lecithinase) A on lecithin: a re-evaluation. Position of fatty acids on lecithins and triglycerides**. The Journal of biological chemistry. **235**: p. 1917-1923.

15. Miki, Y., Hosaka, K., Yamashita, S., Handa, H. and Numa, S. (1977), **Acyl-acceptor specificities of 1-acylglycerolphosphate acyltransferase and 1-acylglycerophosphorylcholine acyltransferase resolved from rat liver microsomes**. Eur J Biochem. **81**(3): p. 433-441.
16. Singer, S. J. and Nicolson, G. L. (1972), **The fluid mosaic model of the structure of cell membranes**. Science. **175**(4023): p. 720-731.
17. Bertrams, M. and Heinz, E. (1981), **Positional specificity and fatty acid selectivity of purified *sn*-glycerol 3-phosphate acyltransferases from chloroplasts**. Plant Physiol. **68**(3): p. 653-657.
18. Frentzen, M., Heinz, E., McKeon, T. A. and Stumpf, P. K. (1983), **Specificities and selectivities of glycerol 3-phosphate acyltransferase and monoacyl-glycerol 3-phosphate acyltransferase from pea and spinach chloroplasts**. Eur J Biochem. **129**(3): p. 629-636.
19. Green, P. R., Vanaman, T. C., Modrich, P. and Bell, R. M. (1983), **Partial NH_2- and COOH-terminal sequence and cyanogen bromide peptide analysis of *Escherichia coli* *sn*-glycerol 3-phosphate acyltransferase**. The Journal of biological chemistry. **258**(18): p. 10862-10866.
20. Lands, W. E. and Hart, P. (1964), **Metabolism of glycerolipids: V. Metabolism of phosphatidic acid**. Journal of lipid research. **5**: p. 81-87.
21. Hajra, A. K. (1968), **Biosynthesis of phosphatidic acid from dihydroxyacetone phosphate**. Biochem Biophys Res Commun. **33**(6): p. 929-935.
22. Abou-Issa, H. M. and Cleland, W. W. (1969), **Studies on the microsomal acylation of L-glycerol-3-phosphate. II. The specificity and properties of the rat liver enzyme**. Biochim Biophys Acta. **176**(4): p. 692-698.
23. Moessinger, C., Klizaite, K., Steinhagen, A., Philippou-Massier, J., Shevchenko, A., Hoch, M., Ejsing, C. S. and Thiele, C. (2014), **Two different pathways of phosphatidylcholine synthesis, the Kennedy Pathway and the Lands Cycle, differentially regulate cellular triacylglycerol storage**. BMC Cell Biol. **15**: p. 43.
24. Smith, S. W., Weiss, S. B. and Kennedy, E. P. (1957), **The enzymatic dephosphorylation of phosphatidic acids**. The Journal of biological chemistry. **228**(2): p. 915-922.
25. Carman, G. M. and Han, G. S. (2009), **Phosphatidic acid phosphatase, a key enzyme in the regulation of lipid synthesis**. The Journal of biological chemistry. **284**(5): p. 2593-2597.
26. Hokin, L. E. and Hokin, M. R. (1963), **Diglyceride kinase and other pathways for phosphatidic acid synthesis in the erythrocyte membrane**. Biochim Biophys Acta. **67**: p. 470-484.
27. Weissbach, H., Thomas, E. and Kaback, H. R. (1971), **Studies on the metabolism of ATP by isolated bacterial membranes: formation and metabolism of membrane-bound phosphatidic acid**. Arch Biochem Biophys. **147**(1): p. 249-254.
28. Daleo, G. R., Piras, M. M. and Piras, R. (1976), **Diglyceride kinase activity of microtubules. Characterization and comparison with the protein kinase and ATPase activities associated with vinblastine-isolated tubulin of chick embryonic muscles**. Eur J Biochem. **68**(2): p. 339-346.

29. Walsh, J. P. and Bell, R. M. (1986), ***sn*-1,2-Diacylglycerol kinase of *Escherichia coli*. Structural and kinetic analysis of the lipid cofactor dependence**. The Journal of biological chemistry. **261**(32): p. 15062-15069.
30. Russ, E., Kaiser, U. and Sandermann, H., Jr. (1988), **Lipid-dependent membrane enzymes. Purification to homogeneity and further characterization of diacylglycerol kinase from *Escherichia coli***. Eur J Biochem. **171**(1-2): p. 335-342.
31. Walsh, J. P. and Bell, R. M. (1992), **Diacylglycerol kinase from *Escherichia coli***. Methods Enzymol. **209**: p. 153-162.
32. Carter, J. R. and Kennedy, E. P. (1966), **Enzymatic synthesis of cytidine diphosphate diglyceride**. Journal of lipid research. **7**(5): p. 678-683.
33. McCaman, R. E. and Finnerty, W. R. (1968), **Biosynthesis of cytidine diphosphate-diglyceride by a particulate fraction from *Micrococcus cerificans***. The Journal of biological chemistry. **243**(19): p. 5074-5080.
34. Petzold, G. L. and Agranoff, B. W. (1967), **The biosynthesis of cytidine diphosphate diglyceride by embryonic chick brain**. The Journal of biological chemistry. **242**(6): p. 1187-1191.
35. Kanfer, J. and Kennedy, E. P. (1964), **Metabolism and function of bacterial lipids. II. Biosynthesis of phospholipids in *Escherichia coli***. The Journal of biological chemistry. **239**: p. 1720-1726.
36. Larson, T. J. and Dowhan, W. (1976), **Ribosomal-associated phosphatidylserine synthetase from *Escherichia coli*: purification by substrate-specific elution from phosphocellulose using cytidine 5'-diphospho-1,2-diacyl-*sn*-glycerol**. Biochemistry. **15**(24): p. 5212-5218.
37. Raetz, C. R. and Kennedy, E. P. (1974), **Partial purification and properties of phosphatidylserine synthetase from *Escherichia coli***. The Journal of biological chemistry. **249**(16): p. 5083-5045.
38. Satre, M. and Kennedy, E. P. (1978), **Identification of bound pyruvate essential for the activity of phosphatidylserine decarboxylase of *Escherichia coli***. The Journal of biological chemistry. **253**(2): p. 479-483.
39. Cassilly, C. D., Farmer, A. T., Montedonico, A. E., Smith, T. K., Campagna, S. R. and Reynolds, T. B. (2017), **Role of phosphatidylserine synthase in shaping the phospholipidome of *Candida albicans***. FEMS Yeast Res. **17**(2).
40. McMaster, C. R. and Bell, R. M. (1994), **Phosphatidylcholine biosynthesis *via* the CDP-choline pathway in *Saccharomyces cerevisiae*. Multiple mechanisms of regulation**. The Journal of biological chemistry. **269**(20): p. 14776-14783.
41. Kent, C. and Carman, G. M. (1999), **Interactions among pathways for phosphatidylcholine metabolism, CTP synthesis and secretion through the Golgi apparatus**. Trends Biochem Sci. **24**(4): p. 146-150.
42. Gibson, K. D., Wilson, J. D. and Udenfriend, S. (1961), **The enzymatic conversion of phospholipid ethanolamine to phospholipid choline in rat liver**. The Journal of biological chemistry. **236**: p. 673-679.
43. Scarborough, G. A. and Nyc, J. F. (1967), **Methylation of ethanolamine phosphatides by microsomes from normal and mutant strains of *Neurospora crassa***. The Journal of biological chemistry. **242**(2): p. 238-242.
44. Rehbinder, D. and Greenberg, D. M. (1965), **Studies on the methylation of ethanolamine phosphatides by liver preparations**. Arch Biochem Biophys. **109**: p. 110-115.

45. Morgan, T. E. (1969), **Isolation and characterization of lipid *N*-methyltransferase from dog lung**. Biochim Biophys Acta. **178**(1): p. 21-34.
46. Schneider, W. J. and Vance, D. E. (1979), **Conversion of phosphatidylethanolamine to phosphatidylcholine in rat liver. Partial purification and characterization of the enzymatic activities**. The Journal of biological chemistry. **254**(10): p. 3886-3891.
47. Arondel, V., Benning, C. and Somerville, C. R. (1993), **Isolation and functional expression in *Escherichia coli* of a gene encoding phosphatidylethanolamine methyltransferase (EC 2.1.1.17) from *Rhodobacter sphaeroides***. The Journal of biological chemistry. **268**(21): p. 16002-16008.
48. Hirata, F., Viveros, O. H., Diliberto, E. J., Jr. and Axelrod, J. (1978), **Identification and properties of two methyltransferases in conversion of phosphatidylethanolamine to phosphatidylcholine**. Proceedings of the National Academy of Sciences of the United States of America. **75**(4): p. 1718-1721.
49. Kennedy, E. P. and Weiss, S. B. (1956), **The function of cytidine coenzymes in the biosynthesis of phospholipids**. The Journal of biological chemistry. **222**(1): p. 193-214.
50. Coleman, R. and Bell, R. M. (1977), **Phospholipid synthesis in isolated fat cells. Studies of microsomal diacylglycerol cholinephosphotransferase and diacylglycerol ethanolaminephosphotransferase activities**. The Journal of biological chemistry. **252**(9): p. 3050-3056.
51. Lee, T. C., Blank, M. L., Fitzgerald, V. and Snyder, F. (1982), **Formation of alkylacyl- and diacylglycerophosphocholines *via* diacylglycerol cholinephosphotransferase in rat liver**. Biochim Biophys Acta. **713**(2): p. 479-483.
52. Parthasarathy, S., Cady, R. K., Kraushaar, D. S., Sladek, N. E. and Baumann, W. J. (1978), **Inhibition of diacylglycerol:CDPcholine cholinephosphotransferase activity by dimethylaminoethyl *p*-chlorophenoxyacetate**. Lipids. **13**(2): p. 161-164.
53. Borkenhagen, L. F. and Kennedy, E. P. (1957), **The enzymatic synthesis of cytidine diphosphate choline**. The Journal of biological chemistry. **227**(2): p. 951-962.
54. Banks, J. and Williams-Ashman, H. G. (1956), **Participation of cytidine coenzymes in the metabolism of choline by seminal vesicle**. The Journal of biological chemistry. **223**(1): p. 509-521.
55. Delong, C. J., Shen, Y. J., Thomas, M. J. and Cui, Z. (1999), **Molecular distinction of phosphatidylcholine synthesis between the CDP-choline pathway and phosphatidylethanolamine methylation pathway**. The Journal of biological chemistry. **274**(42): p. 29683-29688.
56. Wittenberg, J. and Kornberg, A. (1953), **Choline phosphokinase**. The Journal of biological chemistry. **202**(1): p. 431-444.
57. Kent, C. (1997), **CTP:phosphocholine cytidylyltransferase**. Biochim Biophys Acta. **1348**(1-2): p. 79-90.
58. Stone, S. J. and Vance, J. E. (1999), **Cloning and expression of murine liver phosphatidylserine synthase (*PSS*)-2: differential regulation of phospholipid metabolism by PSS1 and PSS2**. Biochem J. **342 (Pt 1)**: p. 57-64.
59. Tomohiro, S., Kawaguti, A., Kawabe, Y., Kitada, S. and Kuge, O. (2009), **Purification and characterization of human phosphatidylserine synthases 1 and 2**. Biochem J. **418**(2): p. 421-429.

60. Carman, G. M. and Henry, S. A. (1989), **Phospholipid biosynthesis in yeast**. Annu Rev Biochem. **58**: p. 635-669.
61. Sundler, R. and Akesson, B. (1975), **Biosynthesis of phosphatidylethanolamines and phosphatidylcholines from ethanolamine and choline in rat liver**. Biochem J. **146**(2): p. 309-315.
62. Jacobs, R. L., Zhao, Y., Koonen, D. P., Sletten, T., Su, B., Lingrell, S., Cao, G., Peake, D. A., Kuo, M. S., Proctor, S. D., Kennedy, B. P., Dyck, J. R. and Vance, D. E. (2010), **Impaired *de novo* choline synthesis explains why phosphatidylethanolamine *N*-methyltransferase-deficient mice are protected from diet-induced obesity**. The Journal of biological chemistry. **285**(29): p. 22403-22413.
63. Cui, Z. and Vance, D. E. (1996), **Expression of phosphatidylethanolamine *N*-methyltransferase-2 is markedly enhanced in long-term choline-deficient rats**. The Journal of biological chemistry. **271**(5): p. 2839-2843.
64. Andriamampandry, C., Freysz, L., Kanfer, J. N., Dreyfus, H. and Massarelli, R. (1989), **Conversion of ethanolamine, monomethylethanolamine and dimethylethanolamine to choline-containing compounds by neurons in culture and by the rat brain**. Biochem J. **264**(2): p. 555-562.
65. Andriamampandry, C., Massarelli, R. and Kanfer, J. N. (1992), **Properties of a partially purified phosphodimethylethanolamine methyltransferase from rat brain cytosol**. Biochem J. **288 (Pt 1)**: p. 267-272.
66. Metzler, D. E. (2003), **Phosphatidylinositol and the release of calcium ions**, in *Biochemistry - The Chemical Reactions of Living Cells*, Elsevier Science Academic Press. p. 563-566.
67. Han, M. S., Lim, Y. M., Quan, W., Kim, J. R., Chung, K. W., Kang, M., Kim, S., Park, S. Y., Han, J. S., Cheon, H. G., Dal Rhee, S., Park, T. S. and Lee, M. S. (2011), **Lysophosphatidylcholine as an effector of fatty acid-induced insulin resistance**. Journal of lipid research. **52**(6): p. 1234-1246.
68. Gatt, S. (1968), **Purification and properties of phospholipase A-1 from rat and calf brain**. Biochim Biophys Acta. **159**(2): p. 304-316.
69. Scandella, C. J. and Kornberg, A. (1971), **A membrane-bound phospholipase A1 purified from *Escherichia coli***. Biochemistry. **10**(24): p. 4447-4456.
70. Van Den Bosch, H. (1980), **Intracellular phospholipases A**. Biochim Biophys Acta. **604**(2): p. 191-246.
71. Van Den Bosch, H., Aarsman, A. J. and Van Deenen, L. L. (1974), **Isolation and properties of a phospholipase A1 activity from beef pancreas**. Biochim Biophys Acta. **348**(2): p. 197-209.
72. Druzhinina, K. V. and Kritsman, M. G. (1952), **Lecithinase C in animal tissue**. Biokhimiia. **17**(1): p. 77-81.
73. Little, C. and Otnass, A. B. (1975), **The metal ion dependence of phospholipase C from *Bacillus cereus***. Biochim Biophys Acta. **391**(2): p. 326-333.
74. Sheikhnejad, R. G. and Srivastava, P. N. (1986), **Isolation and properties of a phosphatidylcholine-specific phospholipase C from bull seminal plasma**. The Journal of biological chemistry. **261**(16): p. 7544-7549.
75. Takahashi, T., Sugahara, T. and Ohsaka, A. (1974), **Purification of *Clostridium perfringens* phospholipase C (alpha-toxin) by affinity chromatography on agarose-linked egg-yolk lipoprotein**. Biochim Biophys Acta. **351**(1): p. 155-171.
76. Dawson, R. M. (1956), **Liver glycerylphosphorylcholine diesterase**. Biochem J. **62**(4): p. 689-693.

77. Einset, E. and Clark, W. L. (1958), **The enzymatically catalyzed release of choline from lecithin**. The Journal of biological chemistry. **231**(2): p. 703-715.
78. Sakai, M., Miyazaki, A., Hakamata, H., Kodama, T., Suzuki, H., Kobori, S., Shichiri, M. and Horiuchi, S. (1996), **The scavenger receptor serves as a route for internalization of lysophosphatidylcholine in oxidized low density lipoprotein-induced macrophage proliferation**. The Journal of biological chemistry. **271**(44): p. 27346-27352.
79. Han, M. S., Park, S. Y., Shinzawa, K., Kim, S., Chung, K. W., Lee, J. H., Kwon, C. H., Lee, K. W., Park, C. K., Chung, W. J., Hwang, J. S., Yan, J. J., Song, D. K., Tsujimoto, Y. and Lee, M. S. (2008), **Lysophosphatidylcholine as a death effector in the lipoapoptosis of hepatocytes**. Journal of lipid research. **49**(1): p. 84-97.
80. Fang, X., Gibson, S., Flowers, M., Furui, T., Bast, R. C., Jr. and Mills, G. B. (1997), **Lysophosphatidylcholine stimulates activator protein 1 and the c-Jun *N*-terminal kinase activity**. The Journal of biological chemistry. **272**(21): p. 13683-13689.
81. Doery, H. M. and Pearson, J. E. (1961), **Haemolysins in venoms of Australian snakes. Observations on the haemolysins of the venoms of some Australian snakes and the separation of phospholipase A from the venom of *Pseudechis porphyriacus***. Biochem J. **78**: p. 820-827.
82. Moore, J. H. and Williams, D. L. (1964), **Some observations on the specificity of phospholipase A**. Biochim Biophys Acta. **84**: p. 41-54.
83. Sevastou, I., Kaffe, E., Mouratis, M. A. and Aidinis, V. (2013), **Lysoglycero-phospholipids in chronic inflammatory disorders: the PLA(2)/LPC and ATX/LPA axes**. Biochim Biophys Acta. **1831**(1): p. 42-60.
84. Heilbronn, L. K., Coster, A. C., Campbell, L. V., Greenfield, J. R., Lange, K., Christopher, M. J., Meikle, P. J. and Samocha-Bonet, D. (2013), **The effect of short-term overfeeding on serum lipids in healthy humans**. Obesity. **21**(12): p. E649-659.
85. Buckley, J. T., Halasa, L. N. and MacIntyre, S. (1982), **Purification and partial characterization of a bacterial phospholipid:cholesterol acyltransferase**. The Journal of biological chemistry. **257**(6): p. 3320-3325.
86. Glomset, J. A. (1968), **The plasma lecithins:cholesterol acyltransferase reaction**. Journal of lipid research. **9**(2): p. 155-167.
87. Fuchs, B., Muller, K., Paasch, U. and Schiller, J. (2012), **Lysophospholipids: potential markers of diseases and infertility?** Mini Rev Med Chem. **12**(1): p. 74-86.
88. Arnhold, J., Osipov, A. N., Spalteholz, H., Panasenko, O. M. and Schiller, J. (2001), **Effects of hypochlorous acid on unsaturated phosphatidylcholines**. Free Radic Biol Med. **31**(9): p. 1111-1119.
89. Arnhold, J., Osipov, A. N., Spalteholz, H., Panasenko, O. M. and Schiller, J. (2002), **Formation of lysophospholipids from unsaturated phosphatidyl-cholines under the influence of hypochlorous acid**. Biochim Biophys Acta. **1572**(1): p. 91-100.
90. Sugasini, D. and Subbaiah, P. V. (2017), **Rate of acyl migration in lysophosphatidylcholine (LPC) is dependent upon the nature of the acyl group. Greater stability of *sn*-2 docosahexaenoyl LPC compared to the more saturated LPC species**. PloS one. **12**(11): p. e0187826.

91. Dawson, R. M. (1958), **Studies on the hydrolysis of lecithin by a *Penicillium notatum* phospholipase B preparation**. Biochem J. **70**(4): p. 559-570.
92. Shapiro, B. (1953), **Purification and properties of a lysolecithinase from pancreas**. Biochem J. **53**(4): p. 663-666.
93. Van Den Bosch, H., Aarsman, A. J., De Jong, J. G. and Van Deenem, L. L. (1973), **Studies on lysophospholipases. I. Purification and some properties of a lysophospholipase from beef pancreas**. Biochim Biophys Acta. **296**(1): p. 94-104.
94. Van Tienhoven, M., Atkins, J., Li, Y. and Glynn, P. (2002), **Human neuropathy target esterase catalyzes hydrolysis of membrane lipids**. The Journal of biological chemistry. **277**(23): p. 20942-20948.
95. Quistad, G. B., Barlow, C., Winrow, C. J., Sparks, S. E. and Casida, J. E. (2003), **Evidence that mouse brain neuropathy target esterase is a lysophospholipase**. Proceedings of the National Academy of Sciences of the United States of America. **100**(13): p. 7983-7987.
96. Barbayianni, E., Kaffe, E., Aidinis, V. and Kokotos, G. (2015), **Autotaxin, a secreted lysophospholipase D, as a promising therapeutic target in chronic inflammation and cancer**. Progress in lipid research. **58**: p. 76-96.
97. Hayaishi, O. and Kornberg, A. (1954), **Metabolism of phospholipids by bacterial enzymes**. The Journal of biological chemistry. **206**(2): p. 647-663.
98. Webster, G. R., Marples, E. A. and Thompson, R. H. (1957), **Glyceryl-phosphorylcholine diesterase activity of nervous tissue**. Biochem J. **65**(2): p. 374-377.
99. Van Zoelen, E. J., De Kruijff, B. and Van Deenen, L. L. (1978), **Protein-mediated transbilayer movement of lysophosphatidylcholine in glycophorin-containing vesicles**. Biochim Biophys Acta. **508**(1): p. 97-108.
100. Van Den Besselaar, A. M., Van Den Bosch, H. and Van Deenen, L. L. (1977), **Transbilayer distribution and movement of lysophosphatidylcholine in liposomal membranes**. Biochim Biophys Acta. **465**(3): p. 454-465.
101. Van Den Besselaar, A. M., De Kruijff, B., Van Den Bosch, H. and Van Deenen, L. L. (1979), **Transverse distribution and movement of lysophosphatidyl-choline in sarcoplasmic reticulum membranes as determined by ^{13}C NMR and lysophospholipase**. Biochim Biophys Acta. **555**(2): p. 193-199.
102. De Oliveira Filgueiras, O. M., Van Den Besselaar, A. M. and Van Den Bosch, H. (1977), **Distribution of lysophosphatidylcholine in single bilayer vesicles prepared without sonication**. Biochim Biophys Acta. **471**(3): p. 391-400.
103. Wallace, M., Morris, C., O'Grada, C. M., Ryan, M., Dillon, E. T., Coleman, E., Gibney, E. R., Gibney, M. J., Roche, H. M. and Brennan, L. (2014), **Relationship between the lipidome, inflammatory markers and insulin resistance**. Molecular Biosystems. **10**(6): p. 1586-1595.
104. Barber, M. N., Risis, S., Yang, C., Meikle, P. J., Staples, M., Febbraio, M. A. and Bruce, C. R. (2012), **Plasma lysophosphatidylcholine levels are reduced in obesity and type 2 diabetes**. PloS one. **7**(7): p. e41456.
105. Schmitz, G. and Ruebsaamen, K. (2010), **Metabolism and atherogenic disease association of lysophosphatidylcholine**. Atherosclerosis. **208**(1): p. 10-18.
106. Kim, Y. L., Im, Y. J., Ha, N. C. and Im, D. S. (2007), **Albumin inhibits cytotoxic activity of lysophosphatidylcholine by direct binding**. Prostaglandins Other Lipid Mediat. **83**(1-2): p. 130-138.

107. Ojala, P. J., Hermansson, M., Tolvanen, M., Polvinen, K., Hirvonen, T., Impola, U., Jauhiainen, M., Somerharju, P. and Parkkinen, J. (2006), **Identification of alpha-1 acid glycoprotein as a lysophospholipid-binding protein: a complementary role to albumin in the scavenging of lysophosphatidylcholine**. Biochemistry. **45**(47): p. 14021-14031.
108. Wiesner, P., Leidl, K., Boettcher, A., Schmitz, G. and Liebisch, G. (2009), **Lipid profiling of FPLC-separated lipoprotein fractions by electrospray ionization tandem mass spectrometry**. Journal of lipid research. **50**(3): p. 574-585.
109. Hoofnagle, A. N., Vaisar, T., Mitra, P. and Chait, A. (2010), **HDL lipids and insulin resistance**. Current diabetes reports. **10**(1): p. 78-86.
110. Kabarowski, J. H., Zhu, K., Le, L. Q., Witte, O. N. and Xu, Y. (2001), **Lysophosphatidylcholine as a ligand for the immunoregulatory receptor G2A**. Science. **293**(5530): p. 702-705.
111. Zhu, K., Baudhuin, L. M., Hong, G., Williams, F. S., Cristina, K. L., Kabarowski, J. H., Witte, O. N. and Xu, Y. (2001), **Sphingosylphosphorylcholine and lysophosphatidylcholine are ligands for the G protein-coupled receptor GPR4**. The Journal of biological chemistry. **276**(44): p. 41325-41335.
112. Hirosumi, J., Tuncman, G., Chang, L., Gorgun, C. Z., Uysal, K. T., Maeda, K., Karin, M. and Hotamisligil, G. S. (2002), **A central role for JNK in obesity and insulin resistance**. Nature. **420**(6913): p. 333-336.
113. Solinas, G., Naugler, W., Galimi, F., Lee, M. S. and Karin, M. (2006), **Saturated fatty acids inhibit induction of insulin gene transcription by JNK-mediated phosphorylation of insulin receptor substrates**. Proceedings of the National Academy of Sciences of the United States of America. **103**(44): p. 16454-16459.
114. Yea, K., Kim, J., Yoon, J. H., Kwon, T., Kim, J. H., Lee, B. D., Lee, H. J., Lee, S. J., Kim, J. I., Lee, T. G., Baek, M. C., Park, H. S., Park, K. S., Ohba, M., Suh, P. G. and Ryu, S. H. (2009), **Lysophosphatidylcholine activates adipocyte glucose uptake and lowers blood glucose levels in murine models of diabetes**. The Journal of biological chemistry. **284**(49): p. 33833-33840.
115. Soga, T., Ohishi, T., Matsui, T., Saito, T., Matsumoto, M., Takasaki, J., Matsumoto, S., Kamohara, M., Hiyama, H., Yoshida, S., Momose, K., Ueda, Y., Matsushime, H., Kobori, M. and Furuichi, K. (2005), **Lysophosphatidylcholine enhances glucose-dependent insulin secretion *via* an orphan G protein-coupled receptor**. Biochem Biophys Res Commun. **326**(4): p. 744-751.
116. Xu, Y. (2002), **Sphingosylphosphorylcholine and lysophosphatidylcholine: G protein-coupled receptors and receptor-mediated signal transduction**. Biochim Biophys Acta. **1582**(1-3): p. 81-88.
117. Xu, Y., Fang, X. J., Casey, G. and Mills, G. B. (1995), **Lysophospholipids activate ovarian and breast cancer cells**. Biochem J. **309 (Pt 3)**: p. 933-940.
118. Xing, F., Liu, J., Mo, Y., Liu, Z., Qin, Q., Wang, J., Fan, Z., Long, Y., Liu, N., Zhao, K. and Jiang, Y. (2009), **Lysophosphatidylcholine up-regulates human endothelial nitric oxide synthase gene transactivity by c-Jun *N*-terminal kinase signalling pathway**. Journal of cellular and molecular medicine. **13**(6): p. 1136-1148.
119. Wang, L., Radu, C. G., Yang, L. V., Bentolila, L. A., Riedinger, M. and Witte, O. N. (2005), **Lysophosphatidylcholine-induced surface redistribution regulates signaling of the murine G protein-coupled receptor G2A**. Molecular biology of the cell. **16**(5): p. 2234-2247.

120. Sakai, M., Miyazaki, A., Hakamata, H., Sasaki, T., Yui, S., Yamazaki, M., Shichiri, M. and Horiuchi, S. (1994), **Lysophosphatidylcholine plays an essential role in the mitogenic effect of oxidized low density lipoprotein on murine macrophages**. The Journal of biological chemistry. **269**(50): p. 31430-31435.
121. Yui, S., Sasaki, T., Miyazaki, A., Horiuchi, S. and Yamazaki, M. (1993), **Induction of murine macrophage growth by modified LDLs**. Arterioscler Thromb. **13**(3): p. 331-337.
122. Sakai, M., Miyazaki, A., Hakamata, H., Sato, Y., Matsumura, T., Kobori, S., Shichiri, M. and Horiuchi, S. (1996), **Lysophosphatidylcholine potentiates the mitogenic activity of modified LDL for human monocyte-derived macrophages**. Arterioscler Thromb Vasc Biol. **16**(4): p. 600-605.
123. Quinn, M. T., Parthasarathy, S., Fong, L. G. and Steinberg, D. (1987), **Oxidatively modified low density lipoproteins: a potential role in recruitment and retention of monocyte/macrophages during atherogenesis**. Proceedings of the National Academy of Sciences of the United States of America. **84**(9): p. 2995-2998.
124. Quinn, M. T., Parthasarathy, S. and Steinberg, D. (1988), **Lysophosphatidyl-choline: a chemotactic factor for human monocytes and its potential role in atherogenesis**. Proceedings of the National Academy of Sciences of the United States of America. **85**(8): p. 2805-2809.
125. Kugiyama, K., Kerns, S. A., Morrisett, J. D., Roberts, R. and Henry, P. D. (1990), **Impairment of endothelium-dependent arterial relaxation by lysolecithin in modified low density lipoproteins**. Nature. **344**(6262): p. 160-162.
126. Morel, D. W., Dicorleto, P. E. and Chisolm, G. M. (1984), **Endothelial and smooth muscle cells alter low density lipoprotein *in vitro* by free radical oxidation**. Arteriosclerosis. **4**(4): p. 357-364.
127. Resink, T. J., Tkachuk, V. A., Bernhardt, J. and Buhler, F. R. (1992), **Oxidized low density lipoproteins stimulate phosphoinositide turnover in cultured vascular smooth muscle cells**. Arterioscler Thromb. **12**(3): p. 278-285.
128. Schackelford, R. E., Misra, U. K., Florine-Casteel, K., Thai, S. F., Pizzo, S. V. and Adams, D. O. (1995), **Oxidized low density lipoprotein suppresses activation of NF kappa B in macrophages *via* a pertussis toxin-sensitive signaling mechanism**. The Journal of biological chemistry. **270**(8): p. 3475-3478.
129. De Kruijff, B. and Wirtz, K. W. (1977), **Induction of a relatively fast transbilayer movement of phosphatidylcholine in vesicles. A ^{13}C-NMR study**. Biochim Biophys Acta. **468**(2): p. 318-326.
130. De Kruyff, B., Van Den Besselaar, A. M. and Van Deenen, L. L. (1977), **Outside-inside distribution and translocation of lysophosphatidylcholine in phosphatidylcholine vesicles as determined by ^{13}C-NMR using (*N*-$^{13}CH_3$)-enriched lipids**. Biochim Biophys Acta. **465**(3): p. 443-453.
131. De Kruijff, B., Van Zoelen, E. J. and Van Deenen, L. L. (1978), **Glycophorin facilitates the transbilayer movement of phosphatidylcholine in vesicles**. Biochim Biophys Acta. **509**(3): p. 537-542.
132. Stanton, L. W., White, R. T., Bryant, C. M., Protter, A. A. and Endemann, G. (1992), **A macrophage Fc receptor for IgG is also a receptor for oxidized low density lipoprotein**. The Journal of biological chemistry. **267**(31): p. 22446-22451.

133. Endemann, G., Stanton, L. W., Madden, K. S., Bryant, C. M., White, R. T. and Protter, A. A. (1993), **CD36 is a receptor for oxidized low density lipoprotein**. The Journal of biological chemistry. **268**(16): p. 11811-11816.
134. Acton, S. L., Scherer, P. E., Lodish, H. F. and Krieger, M. (1994), **Expression cloning of SR-BI, a CD36-related class B scavenger receptor**. The Journal of biological chemistry. **269**(33): p. 21003-21009.
135. Ottnad, E., Parthasarathy, S., Sambrano, G. R., Ramprasad, M. P., Quehenberger, O., Kondratenko, N., Green, S. and Steinberg, D. (1995), **A macrophage receptor for oxidized low density lipoprotein distinct from the receptor for acetyl low density lipoprotein: partial purification and role in recognition of oxidatively damaged cells**. Proceedings of the National Academy of Sciences of the United States of America. **92**(5): p. 1391-1395.
136. Sambrano, G. R. and Steinberg, D. (1995), **Recognition of oxidatively damaged and apoptotic cells by an oxidized low density lipoprotein receptor on mouse peritoneal macrophages: role of membrane phosphatidylserine**. Proceedings of the National Academy of Sciences of the United States of America. **92**(5): p. 1396-1400.
137. Arai, H., Kita, T., Yokode, M., Narumiya, S. and Kawai, C. (1989), **Multiple receptors for modified low density lipoproteins in mouse peritoneal macrophages: different uptake mechanisms for acetylated and oxidized low density lipoproteins**. Biochem Biophys Res Commun. **159**(3): p. 1375-1382.
138. Van Berkel, T. J., De Rijke, Y. B. and Kruijt, J. K. (1991), **Different fate *in vivo* of oxidatively modified low density lipoprotein and acetylated low density lipoprotein in rats. Recognition by various scavenger receptors on Kupffer and endothelial liver cells**. The Journal of biological chemistry. **266**(4): p. 2282-2289.
139. De Rijke, Y. B. and Van Berkel, T. J. (1994), **Rat liver Kupffer and endothelial cells express different binding proteins for modified low density lipoproteins. Kupffer cells express a 95-kDa membrane protein as a specific binding site for oxidized low density lipoproteins**. The Journal of biological chemistry. **269**(2): p. 824-827.
140. Melkko, J., Hellevik, T., Risteli, L., Risteli, J. and Smedsrod, B. (1994), **Clearance of NH2-terminal propeptides of types I and III procollagen is a physiological function of the scavenger receptor in liver endothelial cells**. J Exp Med. **179**(2): p. 405-412.
141. Heery, J. M., Kozak, M., Stafforini, D. M., Jones, D. A., Zimmerman, G. A., McIntyre, T. M. and Prescott, S. M. (1995), **Oxidatively modified LDL contains phospholipids with platelet-activating factor-like activity and stimulates the growth of smooth muscle cells**. The Journal of clinical investigation. **96**(5): p. 2322-2330.
142. Shaw, J. M. and Thompson, T. E. (1982), **Effect of phospholipid oxidation products on transbilayer movement of phospholipids in single lamellar vesicles**. Biochemistry. **21**(5): p. 920-927.
143. Kus, V., Flachs, P., Kuda, O., Bardova, K., Janovska, P., Svobodova, M., Jilkova, Z. M., Rossmeisl, M., Wang-Sattler, R., Yu, Z., Illig, T. and Kopecky, J. (2011), **Unmasking differential effects of rosiglitazone and pioglitazone in the combination treatment with n-3 fatty acids in mice fed a high-fat diet**. PloS one. **6**(11): p. e27126.

144. Weir, J. M., Wong, G., Barlow, C. K., Greeve, M. A., Kowalczyk, A., Almasy, L., Comuzzie, A. G., Mahaney, M. C., Jowett, J. B., Shaw, J., Curran, J. E., Blangero, J. and Meikle, P. J. (2013), **Plasma lipid profiling in a large population-based cohort**. Journal of lipid research. **54**(10): p. 2898-2908.
145. Meikle, P. J. and Christopher, M. J. (2011), **Lipidomics is providing new insight into the metabolic syndrome and its *sequelae***. Current opinion in lipidology. **22**(3): p. 210-215.
146. Boden, G. and Shulman, G. I. (2002), **Free fatty acids in obesity and type 2 diabetes: defining their role in the development of insulin resistance and beta-cell dysfunction**. Eur J Clin Invest. **32 Suppl 3**: p. 14-23.
147. Bernstein, R. M., Davis, B. M., Olefsky, J. M. and Reaven, G. M. (1978), **Hepatic insulin responsiveness in patients with endogenous hypertriglyceridaemia**. Diabetologia. **14**(4): p. 249-253.
148. Reaven, G. M., Hollenbeck, C., Jeng, C. Y., Wu, M. S. and Chen, Y. D. (1988), **Measurement of plasma glucose, free fatty acid, lactate, and insulin for 24 h in patients with NIDDM**. Diabetes. **37**(8): p. 1020-1024.
149. Graessler, J., Schwudke, D., Schwarz, P. E., Herzog, R., Shevchenko, A. and Bornstein, S. R. (2009), **Top-down lipidomics reveals ether lipid deficiency in blood plasma of hypertensive patients**. PloS one. **4**(7): p. e6261.
150. Pietiläinen, K. H., Sysi-Aho, M., Rissanen, A., Seppänen-Laakso, T., Yki-Järvinen, H., Kaprio, J. and Oresic, M. (2007), **Acquired obesity is associated with changes in the serum lipidomic profile independent of genetic effects - a monozygotic twin study**. PloS one. **2**(2): p. e218.
151. Kim, H. J., Kim, M. Y., Hwang, J. S., Lee, J. H., Chang, K. C., Kim, J. H., Han, C. W. and Seo, H. G. (2010), **PPARdelta inhibits IL-1beta-stimulated proliferation and migration of vascular smooth muscle cells *via* up-regulation of IL-1Ra**. Cellular and molecular life sciences: CMLS. **67**(12): p. 2119-2130.
152. Tanaka, N., Matsubara, T., Krausz, K. W., Patterson, A. D. and Gonzalez, F. J. (2012), **Disruption of phospholipid and bile acid homeostasis in mice with nonalcoholic steatohepatitis**. Hepatology. **56**(1): p. 118-129.
153. Zhao, X., Fritsche, J., Wang, J., Chen, J., Rittig, K., Schmitt-Kopplin, P., Fritsche, A., Häring, H. U., Schleicher, E. D., Xu, G. and Lehmann, R. (2010), **Metabolomic fingerprints of fasting plasma and spot urine reveal human pre-diabetic metabolic traits**. Metabolomics: Official journal of the Metabolomic Society. **6**(3): p. 362-374.
154. Lehmann, R., Franken, H., Dammeier, S., Rosenbaum, L., Kantartzis, K., Peter, A., Zell, A., Adam, P., Li, J., Xu, G., Königsrainer, A., Machann, J., Schick, F., Hrabe De Angelis, M., Schwab, M., Staiger, H., Schleicher, E., Gastaldelli, A., Fritsche, A., Häring, H. U. and Stefan, N. (2013), **Circulating lysophosphatidylcholines are markers of a metabolically benign nonalcoholic fatty liver**. Diabetes Care. **36**(8): p. 2331-2338.
155. Rhee, E. P., Cheng, S., Larson, M. G., Walford, G. A., Lewis, G. D., McCabe, E., Yang, E., Farrell, L., Fox, C. S., O'Donnell, C. J., Carr, S. A., Vasan, R. S., Florez, J. C., Clish, C. B., Wang, T. J. and Gerszten, R. E. (2011), **Lipid profiling identifies a triacylglycerol signature of insulin resistance and improves diabetes prediction in humans**. The Journal of clinical investigation. **121**(4): p. 1402-1411.

156. Karpe, F., Dickmann, J. R. and Frayn, K. N. (2011), **Fatty acids, obesity, and insulin resistance: time for a reevaluation**. Diabetes. **60**(10): p. 2441-2449.
157. Schwab, U., Seppänen-Laakso, T., Yetukuri, L., Agren, J., Kolehmainen, M., Laaksonen, D. E., Ruskeepää, A. L., Gylling, H., Uusitupa, M. and Oresic, M. (2008), **Triacylglycerol fatty acid composition in diet-induced weight loss in subjects with abnormal glucose metabolism - the GENOBIN study**. PloS one. **3**(7): p. e2630.
158. Rabini, R. A., Galassi, R., Fumelli, P., Dousset, N., Solera, M. L., Valdiguie, P., Curatola, G., Ferretti, G., Taus, M. and Mazzanti, L. (1994), **Reduced Na^+-K^+-ATPase activity and plasma lysophosphatidylcholine concentrations in diabetic patients**. Diabetes. **43**(7): p. 915-919.
159. Motley, E. D., Kabir, S. M., Gardner, C. D., Eguchi, K., Frank, G. D., Kuroki, T., Ohba, M., Yamakawa, T. and Eguchi, S. (2002), **Lysophosphatidylcholine inhibits insulin-induced Akt activation through protein kinase C-alpha in vascular smooth muscle cells**. Hypertension. **39**(2 Pt 2): p. 508-512.
160. Li, J., Hoene, M., Zhao, X., Chen, S., Wei, H., Häring, H. U., Lin, X., Zeng, Z., Weigert, C., Lehmann, R. and Xu, G. (2013), **Stable isotope-assisted lipidomics combined with nontargeted isotopomer filtering, a tool to unravel the complex dynamics of lipid metabolism**. Analytical chemistry. **85**(9): p. 4651-4657.
161. Huang, Y., Fu, J. F., Shi, H. B. and Liu, L. R. (2011), **Metformin prevents non-alcoholic fatty liver disease in rats: role of phospholipase A2/lysophosphatidylcholine lipoapoptosis pathway in hepatocytes**. Zhonghua Er Ke Za Zhi. **49**(2): p. 139-145.
162. Bao, S., Song, H., Wohltmann, M., Ramanadham, S., Jin, W., Bohrer, A. and Turk, J. (2006), **Insulin secretory responses and phospholipid composition of pancreatic islets from mice that do not express group VIA phospholipase A2 and effects of metabolic stress on glucose homeostasis**. The Journal of biological chemistry. **281**(30): p. 20958-20973.
163. Mancuso, D. J., Sims, H. F., Yang, K., Kiebish, M. A., Su, X., Jenkins, C. M., Guan, S., Moon, S. H., Pietka, T., Nassir, F., Schappe, T., Moore, K., Han, X., Abumrad, N. A. and Gross, R. W. (2010), **Genetic ablation of calcium-independent phospholipase A2gamma prevents obesity and insulin resistance during high-fat-feeding by mitochondrial uncoupling and increased adipocyte fatty acid oxidation**. The Journal of biological chemistry. **285**(47): p. 36495-36510.
164. Song, H., Wohltmann, M., Bao, S., Ladenson, J. H., Semenkovich, C. F. and Turk, J. (2010), **Mice deficient in group VIB phospholipase A2 (iPLA2gamma) exhibit relative resistance to obesity and metabolic abnormalities induced by a Western diet**. Am J Physiol Endocrinol Metab. **298**(6): p. E1097-1114.
165. Falcao-Pires, I., Castro-Chaves, P., Miranda-Silva, D., Lourenco, A. P. and Leite-Moreira, A. F. (2012), **Physiological, pathological and potential therapeutic roles of adipokines**. Drug Discov Today. **17**(15-16): p. 880-889.
166. Rasouli, N. and Kern, P. A. (2008), **Adipocytokines and the metabolic complications of obesity**. The Journal of clinical endocrinology and metabolism. **93**(11 Suppl 1): p. S64-73.
167. Ross, R. (1993), **The pathogenesis of atherosclerosis: a perspective for the 1990s**. Nature. **362**(6423): p. 801-809.

168. Palinski, W., Rosenfeld, M. E., Yla-Herttuala, S., Gurtner, G. C., Socher, S. S., Butler, S. W., Parthasarathy, S., Carew, T. E., Steinberg, D. and Witztum, J. L. (1989), **Low density lipoprotein undergoes oxidative modification *in vivo***. Proceedings of the National Academy of Sciences of the United States of America. **86**(4): p. 1372-1376.
169. Yla-Herttuala, S., Palinski, W., Rosenfeld, M. E., Parthasarathy, S., Carew, T. E., Butler, S., Witztum, J. L. and Steinberg, D. (1989), **Evidence for the presence of oxidatively modified low density lipoprotein in atherosclerotic lesions of rabbit and man**. The Journal of clinical investigation. **84**(4): p. 1086-1095.
170. Kume, N., Cybulsky, M. I. and Gimbrone, M. A., Jr. (1992), **Lysophosphatidylcholine, a component of atherogenic lipoproteins, induces mononuclear leukocyte adhesion molecules in cultured human and rabbit arterial endothelial cells**. The Journal of clinical investigation. **90**(3): p. 1138-1144.
171. Kume, N. and Gimbrone, M. A., Jr. (1994), **Lysophosphatidylcholine transcriptionally induces growth factor gene expression in cultured human endothelial cells**. The Journal of clinical investigation. **93**(2): p. 907-911.
172. Kugiyama, K., Sakamoto, T., Misumi, I., Sugiyama, S., Ohgushi, M., Ogawa, H., Horiguchi, M. and Yasue, H. (1993), **Transferable lipids in oxidized low-density lipoprotein stimulate plasminogen activator inhibitor-1 and inhibit tissue-type plasminogen activator release from endothelial cells**. Circ Res. **73**(2): p. 335-343.
173. Zhou, Y. P. and Grill, V. E. (1994), **Long-term exposure of rat pancreatic islets to fatty acids inhibits glucose-induced insulin secretion and biosynthesis through a glucose fatty acid cycle**. The Journal of clinical investigation. **93**(2): p. 870-876.
174. Shimabukuro, M., Wang, M. Y., Zhou, Y. T., Newgard, C. B. and Unger, R. H. (1998), **Protection against lipoapoptosis of beta cells through leptin-dependent maintenance of Bcl-2 expression**. Proceedings of the National Academy of Sciences of the United States of America. **95**(16): p. 9558-9561.
175. Listenberger, L. L., Han, X., Lewis, S. E., Cases, S., Farese, R. V., Jr., Ory, D. S. and Schaffer, J. E. (2003), **Triglyceride accumulation protects against fatty acid-induced lipotoxicity**. Proceedings of the National Academy of Sciences of the United States of America. **100**(6): p. 3077-3082.
176. Weyrich, P., Machicao, F., Reinhardt, J., Machann, J., Schick, F., Tschritter, O., Stefan, N., Fritsche, A. and Häring, H. U. (2008), ***SIRT1* genetic variants associate with the metabolic response of Caucasians to a controlled lifestyle intervention - the TULIP Study**. BMC medical genetics. **9**: p. 100.
177. Stefan, N., Machicao, F., Staiger, H., Machann, J., Schick, F., Tschritter, O., Spieth, C., Weigert, C., Fritsche, A., Stumvoll, M. and Häring, H. U. (2005), **Polymorphisms in the gene encoding adiponectin receptor 1 are associated with insulin resistance and high liver fat**. Diabetologia. **48**(11): p. 2282-2291.
178. Thamer, C., Machann, J., Bachmann, O., Haap, M., Dahl, D., Wietek, B., Tschritter, O., Niess, A., Brechtel, K., Fritsche, A., Claussen, C., Jacob, S., Schick, F., Häring, H. U. and Stumvoll, M. (2003), **Intramyocellular lipids: anthropometric determinants and relationships with maximal aerobic capacity and insulin sensitivity**. The Journal of clinical endocrinology and metabolism. **88**(4): p. 1785-1791.

179. Alberti, K. G. and Zimmet, P. Z. (1998), **Definition, diagnosis and classification of diabetes mellitus and its complications. Part 1: diagnosis and classification of diabetes mellitus provisional report of a WHO consultation**. Diabet Med. **15**(7): p. 539-553.
180. **Report of the Expert Committee on the Diagnosis and Classification of Diabetes Mellitus** (1997). Diabetes Care. **20**(7): p. 1183-1197.
181. Stumvoll, M., Mitrakou, A., Pimenta, W., Jenssen, T., Yki-Järvinen, H., Van Haeften, T., Häring, H. U., Fritsche, A. and Gerich, J. (2000), **Assessment of insulin secretion from the oral glucose tolerance test in white patients with type 2 diabetes**. Diabetes Care. **23**(9): p. 1440-1441.
182. Stumvoll, M., Mitrakou, A., Pimenta, W., Jenssen, T., Yki-Järvinen, H., Van Haeften, T., Renn, W. and Gerich, J. (2000), **Use of the oral glucose tolerance test to assess insulin release and insulin sensitivity**. Diabetes Care. **23**(3): p. 295-301.
183. Matsuda, M. and DeFronzo, R. A. (1999), **Insulin sensitivity indices obtained from oral glucose tolerance testing: comparison with the euglycemic insulin clamp**. Diabetes Care. **22**(9): p. 1462-1470.
184. Hansen, J. E., Sue, D. Y. and Wasserman, K. (1984), **Predicted values for clinical exercise testing**. Am Rev Respir Dis. **129**(2 Pt 2): p. S49-55.
185. Thamer, C., Machann, J., Stefan, N., Schäfer, S. A., Machicao, F., Staiger, H., Laakso, M., Böttcher, M., Claussen, C., Schick, F., Fritsche, A. and Häring, H. U. (2008), **Variations in *PPARD* determine the change in body composition during lifestyle intervention: a whole-body magnetic resonance study**. The Journal of clinical endocrinology and metabolism. **93**(4): p. 1497-1500.
186. Szczepaniak, L. S., Babcock, E. E., Schick, F., Dobbins, R. L., Garg, A., Burns, D. K., McGarry, J. D. and Stein, D. T. (1999), **Measurement of intracellular triglyceride stores by H spectroscopy: validation *in vivo***. Am J Physiol. **276**(5 Pt 1): p. E977-989.
187. Wolf, Magnus, Chen, S., Zhao, X., Scheler, M., Irmler, M., Staiger, H., Beckers, J., De Angelis, M. H., Fritsche, A., Häring, H. U., Schleicher, E. D., Xu, G., Lehmann, R. and Weigert, C. (2013), **Production and release of acylcarnitines by primary myotubes reflect the differences in fasting fat oxidation of the donors**. The Journal of clinical endocrinology and metabolism. **98**(6): p. E1137-1142.
188. Wolf, Magnus (2011), **Bestimmung von Fettsäure-Oxidations-Parametern in humanen Muskelzellen von Probanden mit unterschiedlicher Fettsäure-Oxidations-Kapazität.** *Diplomarbeit der Biochemie*, Mathematisch-Naturwissenschaftliche Fakultät, Interfakultäres Institut für Biochemie, Eberhard Karls Universität Tübingen.
189. Liebisch, G., Drobnik, W., Lieser, B. and Schmitz, G. (2002), **High-throughput quantification of lysophosphatidylcholine by electrospray ionization tandem mass spectrometry**. Clinical chemistry. **48**(12): p. 2217-2224.
190. Bradford, M. M. (1976), **A rapid and sensitive method for the quantitation of microgram quantities of protein utilizing the principle of protein-dye binding**. Analytical biochemistry. **72**: p. 248-254.

191. Linz, P. E., Lovato, L. C., Byington, R. P., O'Connor, P. J., Leiter, L. A., Weiss, D., Force, R. W., Crouse, J. R., Ismail-Beigi, F., Simmons, D. L., Papademetriou, V., Ginsberg, H. N. and Elam, M. B. (2014), **Paradoxical reduction in HDL-C with fenofibrate and thiazolidinedione therapy in type 2 diabetes: the ACCORD Lipid Trial**. Diabetes Care. **37**(3): p. 686-693.
192. Buse, J. B., Bigger, J. T., Byington, R. P., Cooper, L. S., Cushman, W. C., Friedewald, W. T., Genuth, S., Gerstein, H. C., Ginsberg, H. N., Goff, D. C., Jr., Grimm, R. H., Jr., Margolis, K. L., Probstfield, J. L., Simons-Morton, D. G. and Sullivan, M. D. (2007), **Action to Control Cardiovascular Risk in Diabetes (ACCORD) trial: design and methods**. The American journal of cardiology. **99**(12A): p. 21i-33i.
193. Goff, D. C., Jr., Gerstein, H. C., Ginsberg, H. N., Cushman, W. C., Margolis, K. L., Byington, R. P., Buse, J. B., Genuth, S., Probstfield, J. L. and Simons-Morton, D. G. (2007), **Prevention of cardiovascular disease in persons with type 2 diabetes mellitus: current knowledge and rationale for the Action to Control Cardiovascular Risk in Diabetes (ACCORD) trial**. The American journal of cardiology. **99**(12A): p. 4i-20i.
194. Ginsberg, H. N., Bonds, D. E., Lovato, L. C., Crouse, J. R., Elam, M. B., Linz, P. E., O'Connor, P. J., Leiter, L. A., Weiss, D., Lipkin, E. and Fleg, J. L. (2007), **Evolution of the lipid trial protocol of the Action to Control Cardiovascular Risk in Diabetes (ACCORD) trial**. The American journal of cardiology. **99**(12A): p. 56i-67i.
195. Chalmers, J. (2003), **ADVANCE study: objectives, design and current status**. Drugs. **63 Spec No 1**: p. 39-44.
196. Floege, J., Raggi, P., Block, G. A., Torres, P. U., Csiky, B., Naso, A., Nossuli, K., Moustafa, M., Goodman, W. G., Lopez, N., Downey, G., Dehmel, B. and Chertow, G. M. (2010), **Study design and subject baseline characteristics in the ADVANCE Study: effects of cinacalcet on vascular calcification in haemodialysis patients**. Nephrology, dialysis, transplantation: official publication of the European Dialysis and Transplant Association - European Renal Association. **25**(6): p. 1916-1923.
197. Malmberg, K., Ryden, L., Wedel, H., Birkeland, K., Bootsma, A., Dickstein, K., Efendic, S., Fisher, M., Hamsten, A., Herlitz, J., Hildebrandt, P., MacLeod, K., Laakso, M., Torp-Pedersen, C. and Waldenstrom, A. (2005), **Intense metabolic control by means of insulin in patients with diabetes mellitus and acute myocardial infarction (DIGAMI 2): effects on mortality and morbidity**. Eur Heart J. **26**(7): p. 650-661.
198. Malmberg, K., Ryden, L., Efendic, S., Herlitz, J., Nicol, P., Waldenstrom, A., Wedel, H. and Welin, L. (1995), **Randomized trial of insulin-glucose infusion followed by subcutaneous insulin treatment in diabetic patients with acute myocardial infarction (DIGAMI study): effects on mortality at 1 year**. J Am Coll Cardiol. **26**(1): p. 57-65.
199. United Kingdom Prospective Diabetes Study Group (1998), **United Kingdom Prospective Diabetes Study 24: a 6-year, randomized, controlled trial comparing sulfonylurea, insulin, and metformin therapy in patients with newly diagnosed type 2 diabetes that could not be controlled with diet therapy.** Ann Intern Med. **128**(3): p. 165-175.

200. United Kingdom Prospective Diabetes Study Group (1998), **Effect of intensive blood-glucose control with metformin on complications in overweight patients with type 2 diabetes (UKPDS 34)**. The Lancet. **352**(9131): p. 854-865.
201. United Kingdom Prospective Diabetes Study Group (1998), **Intensive blood-glucose control with sulphonylureas or insulin compared with conventional treatment and risk of complications in patients with type 2 diabetes (UKPDS 33)**. The Lancet. **352**(9131): p. 837-853.
202. Friedrich, B., Weyrich, P., Stancakova, A., Wang, J., Kuusisto, J., Laakso, M., Sesti, G., Succurro, E., Smith, U., Hansen, T., Pedersen, O., Machicao, F., Schäfer, S., Lang, F., Risler, T., Ullrich, S., Stefan, N., Fritsche, A. and Häring, H. U. (2008), **Variance of the *SGK1* gene is associated with insulin secretion in different European populations: results from the TUEF, EUGENE2, and METSIM studies**. PloS one. **3**(11): p. e3506.
203. Stumvoll, M., Fritsche, A., Stefan, N., Hardt, E. and Häring, H. U. (2001), **Evidence against a rate-limiting role of proinsulin processing for maximal insulin secretion in subjects with impaired glucose tolerance and beta-cell dysfunction**. The Journal of clinical endocrinology and metabolism. **86**(3): p. 1235-1239.
204. Eaton, R. P., Allen, R. C., Schade, D. S., Erickson, K. M. and Standefer, J. (1980), **Prehepatic insulin production in man: kinetic analysis using peripheral connecting peptide behavior**. J Clin Endocrinol Metab. **51**(3): p. 520-528.
205. Jacob, S., Machann, J., Rett, K., Brechtel, K., Volk, A., Renn, W., Maerker, E., Matthaei, S., Schick, F., Claussen, C. D. and Häring, H. U. (1999), **Association of increased intramyocellular lipid content with insulin resistance in lean non-diabetic offspring of type 2 diabetic subjects**. Diabetes. **48**(5): p. 1113-1119.
206. Brechtel, K., Jacob, S., Machann, J., Hauer, B., Nielsen, M., Meissner, H. P., Matthaei, S., Häring, H. U., Claussen, C. D. and Schick, F. (2000), **Acquired generalized lipoatrophy (AGL): highly selective MR lipid imaging and localized ^{1}H-MRS**. J Magn Reson Imaging. **12**(2): p. 306-310.
207. Fritsche, A., Madaus, A., Stefan, N., Tschritter, O., Maerker, E., Teigeler, A., Häring, H. U. and Stumvoll, M. (2002), **Relationships among age, proinsulin conversion, and beta-cell function in nondiabetic humans**. Diabetes. 51 Suppl 1: p. S234-239.
208. Fritsche, A., Wahl, H. G., Metzinger, E., Renn, W., Kellerer, M., Häring, H. U. and Stumvoll, M. (1998), **Evidence for inhibition of leptin secretion by catecholamines in man**. Exp Clin Endocrinol Diabetes. **106**(5): p. 415-418.
209. Tschritter, O., Fritsche, A., Thamer, C., Haap, M., Shirkavand, F., Rahe, S., Staiger, H., Maerker, E., Häring, H. U. and Stumvoll, M. (2003), **Plasma adiponectin concentrations predict insulin sensitivity of both glucose and lipid metabolism**. Diabetes. **52**(2): p. 239-243.
210. Ravussin, E., Lillioja, S., Anderson, T. E., Christin, L. and Bogardus, C. (1986), **Determinants of 24-hour energy expenditure in man. Methods and results using a respiratory chamber**. The Journal of clinical investigation. **78**(6): p. 1568-1578.
211. Luke, A., Durazo-Arvizu, R., Cao, G., Adeyemo, A., Tayo, B. and Cooper, R. (2006), **Positive association between resting energy expenditure and weight gain in a lean adult population**. The American journal of clinical nutrition. **83**(5): p. 1076-1081.

212. Weyer, C., Snitker, S., Rising, R., Bogardus, C. and Ravussin, E. (1999), **Determinants of energy expenditure and fuel utilization in man: effects of body composition, age, sex, ethnicity and glucose tolerance in 916 subjects**. Int J Obes Relat Metab Disord. **23**(7): p. 715-722.
213. Xie, Y., Gibbs, T. C. and Meier, K. E. (2002), **Lysophosphatidic acid as an autocrine and paracrine mediator**. Biochim Biophys Acta. **1582**(1-3): p. 270-281.
214. Metzler, D. E. (2003), **Regulation of biosynthesis**, in *Biochemistry – The Chemical Reactions of Living Cells*, Elsevier Science Academic Press. p. 996-1005.
215. Metzler, D. E. (2003), **Eukaryotic cells**, in *Biochemistry – The Chemical Reactions of Living Cells*, Elsevier Science Academic Press. p. 11-15.
216. Metzler, D. E. (2003), **The organization of metabolism**, in *Biochemistry – The Chemical Reactions of Living Cells*, Elsevier Science Academic Press. p. 939-947.
217. Metzler, D. E. (2003), **The biosynthesis of fatty acids and their esters**, in *Biochemistry – The Chemical Reactions of Living Cells*, Elsevier Science Academic Press. p. 1185-1196.
218. Metzler, D. E. (2003), **The citric acid cycle**, in *Biochemistry – The Chemical Reactions of Living Cells*, Elsevier Science Academic Press. p. 950-958.
219. Metzler, D. E. (2003), **Pacemakers and the control of metabolic flux**, in *Biochemistry – The Chemical Reactions of Living Cells*, Elsevier Science Academic Press. p. 535-537.
220. Rothman, K. J. (1990), **No adjustments are needed for multiple comparisons**. Epidemiology. **1**(1): p. 43-46.
221. Klingler, C., Zhao, X., Adhikary, T., Li, J., Xu, G., Häring, H. U., Schleicher, E., Lehmann, R. and Weigert, C. (2016), **Lysophosphatidylcholines activate PPARdelta and protect human skeletal muscle cells from lipotoxicity**. Biochim Biophys Acta. **1861**(12 Pt A): p. 1980-1992.
222. Lee, Y. J., Lee, A., Yoo, H. J., Kim, M., Jee, S. H., Shin, D. Y. and Lee, J. H. (2018), **Effect of weight loss on circulating fatty acid profiles in overweight subjects with high visceral fat area: a 12-week randomized controlled trial**. Nutr J. **17**(1): p. 28.
223. Narkar, V. A., Downes, M., Yu, R. T., Embler, E., Wang, Y. X., Banayo, E., Mihaylova, M. M., Nelson, M. C., Zou, Y., Juguilon, H., Kang, H., Shaw, R. J. and Evans, R. M. (2008), **AMPK and PPARdelta agonists are exercise mimetics**. Cell. **134**(3): p. 405-415.
224. Takahashi, H., Goto, T., Yamazaki, Y., Kamakari, K., Hirata, M., Suzuki, H., Shibata, D., Nakata, R., Inoue, H., Takahashi, N. and Kawada, T. (2015), **Metabolomics reveal 1-palmitoyl lysophosphatidylcholine production by peroxisome proliferator-activated receptor alpha**. Journal of lipid research. **56**(2): p. 254-265.
225. Kim, J. Y., Park, J. Y., Kim, O. Y., Ham, B. M., Kim, H. J., Kwon, D. Y., Jang, Y. and Lee, J. H. (2010), **Metabolic profiling of plasma in overweight/obese and lean men using ultra performance liquid chromatography and Q-TOF mass spectrometry (UPLC-Q-TOF MS)**. J Proteome Res. **9**(9): p. 4368-4375.

226. Galili, O., Versari, D., Sattler, K. J., Olson, M. L., Mannheim, D., McConnell, J. P., Chade, A. R., Lerman, L. O. and Lerman, A. (2007), **Early experimental obesity is associated with coronary endothelial dysfunction and oxidative stress**. Am J Physiol Heart Circ Physiol. **292**(2): p. H904-911.
227. Loftus, N., Miseki, K., Iida, J., Gika, H. G., Theodoridis, G. and Wilson, I. D. (2008), **Profiling and biomarker identification in plasma from different Zucker rat strains *via* high mass accuracy multistage mass spectrometric analysis using liquid chromatography/mass spectrometry with a quadrupole ion trap-time of flight mass spectrometer**. Rapid Commun Mass Spectrom. **22**(16): p. 2547-2554.
228. Pan, D. A., Lillioja, S., Kriketos, A. D., Milner, M. R., Baur, L. A., Bogardus, C., Jenkins, A. B. and Storlien, L. H. (1997), **Skeletal muscle triglyceride levels are inversely related to insulin action**. Diabetes. **46**(6): p. 983-988.
229. Krssak, M., Falk Petersen, K., Dresner, A., DiPietro, L., Vogel, S. M., Rothman, D. L., Roden, M. and Shulman, G. I. (1999), **Intramyocellular lipid concentrations are correlated with insulin sensitivity in humans: a ^{1}H NMR spectroscopy study**. Diabetologia. **42**(1): p. 113-116.
230. Danforth, E., Jr. (2000), **Failure of adipocyte differentiation causes type II diabetes mellitus?** Nature genetics. **26**(1): p. 13.
231. Wang, H., Zhang, H., Jia, Y., Zhang, Z., Craig, R., Wang, X. and Elbein, S. C. (2004), **Adiponectin receptor 1 gene (*ADIPOR1*) as a candidate for type 2 diabetes and insulin resistance**. Diabetes. **53**(8): p. 2132-2136.
232. Weiss, R., Dufour, S., Taksali, S. E., Tamborlane, W. V., Petersen, K. F., Bonadonna, R. C., Boselli, L., Barbetta, G., Allen, K., Rife, F., Savoye, M., Dziura, J., Sherwin, R., Shulman, G. I. and Caprio, S. (2003), **Prediabetes in obese youth: a syndrome of impaired glucose tolerance, severe insulin resistance, and altered myocellular and abdominal fat partitioning**. Lancet. **362**(9388): p. 951-957.
233. Tiikkainen, M., Tamminen, M., Häkkinen, A. M., Bergholm, R., Vehkavaara, S., Halavaara, J., Teramo, K., Rissanen, A. and Yki-Järvinen, H. (2002), **Liver-fat accumulation and insulin resistance in obese women with previous gestational diabetes**. Obes Res. **10**(9): p. 859-867.
234. Kelley, D. E., McKolanis, T. M., Hegazi, R. A., Kuller, L. H. and Kalhan, S. C. (2003), **Fatty liver in type 2 diabetes mellitus: relation to regional adiposity, fatty acids, and insulin resistance**. Am J Physiol Endocrinol Metab. **285**(4): p. E906-916.
235. Brons, C., Jacobsen, S., Nilsson, E., Ronn, T., Jensen, C. B., Storgaard, H., Poulsen, P., Groop, L., Ling, C., Astrup, A. and Vaag, A. (2010), **Deoxyribonucleic acid methylation and gene expression of *PPARGC1A* in human muscle is influenced by high-fat overfeeding in a birth-weight-dependent manner**. The Journal of clinical endocrinology and metabolism. **95**(6): p. 3048-3056.

8 Erklärung zum Eigenanteil der Dissertationsschrift

Die vorliegende Arbeit wurde in der Arbeitsgruppe für Pathobiochemie der Abteilung Innere Medizin IV für Endokrinologie und Diabetologie, Angiologie, Nephrologie und Klinische Chemie des Universitätsklinikums Tübingen unter der Betreuung von Frau Prof. Dr. rer. nat. Cora Weigert durchgeführt, die auch an der Konzeption der Studie beteiligt war.

Die anthropometrischen und physiologischen Parameter der Donoren wurden im Rahmen der TUEF-Studie erhoben. Hierbei wurden auch durch autorisiertes ärztliches Personal die primären humanen Myotuben der Probanden durch Skelettmuskelbiopsien akquiriert.

Sämtliche Zellkulturversuche sowie alle Versuche zur Protein-, DNA- und RNA-Quantifizierung wurden von mir eigenständig im Rahmen meiner Diplomarbeit für das Studienfach Biochemie durchgeführt. Die Bestimmung der Fettsäureoxidationskapazität der primären humanen Myotuben erfolgte in Zusammenarbeit mit der medizinisch-technischen Angestellten Heike Runge im nuklearmedizinischen Labor der Universität Tübingen. Die Ergebnisse dieser Versuche sind in meiner Diplomarbeit aufgeführt [188] und zudem in einem Fachjournal publiziert worden [187] und daher nicht in dieser Dissertationsschrift präsentiert. Sie wurden lediglich für die Korrelationen mit den neu bestimmten Lysophosphatidylcholin-Konzentrationen herangezogen.

Die massenspektrometrischen Analysen wurden durch unsere Kooperationspartner Xinjie Zhao und Shili Chen vom *Key Laboratory of Separation Science for Analytical Chemistry of the Dalian Institute of Chemical Physics of the Chinese Academy of Sciences* in Dalian (China) durchgeführt.

Die statistische Auswertung erfolgte nach Beratung durch das Institut für Biometrie eigenständig durch mich.

Ich versichere, das Manuskript selbstständig verfasst zu haben und keine weiteren als die von mir angegebenen Quellen und Hilfsmittel verwendet zu haben.

Tübingen, den 02.12.2020

9 Supplemental Data

9.1 Calculations

First phase insulin secretion was calculated by using glucose and insulin concentrations from OGTT according to **Supplemental Equation 1**. ISI was reckoned both by using glucose and insulin concentrations from OGTT according to **Supplemental Equation 2** (ISI_{OGTT}) and by using results from the euglycemic-hyperinsulinemic clamp according to **Supplemental Equation 3** (ISI_{clamp}).

$$\text{First phase insulin secretion} = 1283 + 1.829\ [\text{insulin}]_{30} - 138.7\ [\text{glucose}]_{30} + 3.772\ [\text{insulin}]_{0}$$

Supplemental Equation 1: Calculation of first phase insulin secretion (1^{st}pIS) from insulin and glucose concentrations measured during an oral glucose tolerance test (OGTT) [177, 181, 182]. Basal insulin concentration at the beginning of OGTT ($[\text{insulin}]_0$), insulin concentration after the first 30 minutes of OGTT ($[\text{insulin}]_{30}$) and glucose concentration after the first 30 minutes of OGTT ($[\text{glucose}]_{30}$) are required for determination of 1^{st}pIS.

$$ISI_{OGTT} = \frac{10{,}000}{\sqrt{([\text{glucose}]_0 \cdot [\text{insulin}]_0 \cdot \text{mean}\ [\text{glucose}]_{OGTT} \cdot \text{mean}\ [\text{insulin}]_{OGTT})}}$$

Supplemental Equation 2: Calculation of insulin sensitivity index (ISI) according to Matsuda and DeFronzo [183]. The ISI computation incorporates fasting plasma glucose concentration ($[\text{glucose}]_0$), fasting plasma insulin concentration ($[\text{insulin}]_0$), the mean of all glucose concentration measurements during OGTT (mean $[\text{glucose}]_{OGTT}$) and the mean of all insulin concentration measurements during OGTT (mean $[\text{insulin}]_{OGTT}$).

$$ISI_{clamp} = \frac{\text{mean}\ GIR_{2^{nd}hour}}{[\text{insulin}]_{\text{steady state}}}$$

Supplemental Equation 3: Calculation of insulin sensitivity index (ISI) by division of the mean glucose infusion rate (GIR) during the second hour of the euglycemic-hyperinsulinemic clamp (mean $GIR_{2^{nd}\ hour}$) by the concentration of plasma insulin during the steady-state phase of the euglycemic-hyperinsulinemic clamp ($[\text{insulin}]_{\text{steady state}}$). As the glucose infusion rate is given in $\mu mol \cdot kg^{-1} \cdot min^{-1}$ and insulin concentration is given in pM, the unit of ISI_{clamp} results in $\mu mol \cdot kg^{-1} \cdot min^{-1} \cdot pM^{-1}$ [177, 178].

9.2 Labeled [^{13}C]lysophosphatidylcholines in Trial Medium

As [^{13}C]-labeled LPCs were detected in pure Trial Medium in very few instances and if anything then in vanishingly low amounts, comparisons between amounts in the cell culture supernatants and those in pure Trial Medium are not considered meaningful: Out of the five investigated Trial Medium samples, one sample showed very small quantities of [$^{13}C_{14}$]LPC C14:0 ($n = 1.3 \cdot 10^{-4}$ nmol) and [$^{13}C_{16}$]LPC C16:0 ($n = 1.5 \cdot 10^{-2}$ nmol) as another sample did for [$^{13}C_{16}$]LPC C16:0 ($n = 1.1 \cdot 10^{-2}$ nmol) and a third one for [$^{13}C_{16}$]LPC C16:1 ($n = 2.8 \cdot 10^{-5}$ nmol). In the remaining two pure Trial Medium

samples no single [^{13}C]LPC species was detected. It follows from the foregoing that [$^{13}C_{16}$]LPC C18:0, [$^{13}C_{18}$]LPC C18:0, [$^{13}C_{16}$]LPC C18:1 and [$^{13}C_{18}$]LPC C18:1 were not found at all in the five pure Trial Medium samples. The proportions of the mean amounts of the detected [^{13}C]-labeled species in pure Trial Medium in comparison to the mean amounts in the cell culture supernatants after 24-hour stimulation were 0.25 % for [$^{13}C_{14}$]LPC C14:0, 0.37 % for [$^{13}C_{16}$]LPC C16:0 and 0.01 % for [$^{13}C_{16}$]LPC C16:1 whereas the respective proportions for the nonlabeled derivatives were 82 % (LPC C14:0), 147 % (LPC C16:0) and 129 % (LPC C16:1).

These vanishingly low concentrations of [^{13}C]LPCs in pure Trial Medium might be the consequence of carryover contaminations during sample preparation or during mass spectrometric measurements or of inaccurate peak selection in mass spectrogram evaluation.

9.3 Kinetics of [^{13}C]lysophosphatidylcholines: percental increases and emergence

All [^{13}C]LPC species distinctly and permanently increased in the course of time without exception both intra- and extracellularly. Accordingly, total intracellular [^{13}C]-metabolites elevated by a factor of 6.7 after 4 hours of stimulation (*vs.* 30 min: + 571 %) with an additional triplication after 24 hours (*vs.* 4 h: + 198 %) resulting in a 20-fold increase in total (*vs.* 30 min: + 1900 %). Total extracellular [^{13}C]-species showed a more than 27-fold increase after 4 hours (*vs.* 30 min: + 2647 %) further increasing by a factor of 18 after 24 hours (*vs.* 4 h: + 1707 %) and thus nearly reaching altogether a 500-fold increase (*vs.* 30 min: + 49521 %).

The individual [^{13}C]-species endorsed very similar kinetics permanently increasing. Whereas all 7 [^{13}C]-isotopes were already detected after 30 minutes in the cell lysates of all donors, release into the supernatants was delayed: After 30 minutes, exclusively [$^{13}C_{16}$]LPC C16:0 was measured in supernatants of 8 out of the 10 donors as well as [$^{13}C_{16}$]LPC C16:1 in the supernatants of 4 donors. After 4 hours, all donors featured [$^{13}C_{16}$]LPC C16:0 and [$^{13}C_{16}$]LPC C16:1 in their human myotubes' supernatants, 5 donors [$^{13}C_{16}$]LPC C18:0, 3 donors [$^{13}C_{14}$]LPC C14:0 and one single donor [$^{13}C_{18}$]LPC C18:0. All 7 [^{13}C]-isotopes were contained in the supernatants of all donors after 24 hours of stimulation with [$^{13}C_{16}$]LPC C18:1 and [$^{13}C_{18}$]LPC C18:1 not being monitored before.

9.4 Congruousness of intra- and extracellular kinetics

Interestingly, the congruence of intra- and extracellular changes notably differed between the different stimulation periods. Comparing the 24-hour *stimuli* with the 30-minute *stimuli*, kinetics of only 4 out of the 18 (22 %) both intra- and extracellularly detected LPC species were congruent in cell lysates and supernatants: LPC C16:0, LPC C20:1, LPC C20:2 and LPC C22:3 significantly decreased in both cell lysates and supernatants with LPC C20:0 showing a similar trend (in cell lysate). *Au contraire*, LPC C18:2, LPC C18:3, LPC C20:3, LPC C20:5 and LPC C22:6 significantly reducing in supernatants were significantly elevated (LPC C20:3) in cell lysates or tended to be elevated (LPC C18:2, LPC C18:3, LPC C20:5 and LPC C22:6) and - *vice versa* - LPC C22:1 intracellularly decreased but tended to increase extracellularly. And 6 (33 %) of the LPC species (LPC C16:1, LPC C18:0, LPC C18:1, LPC C20:4, LPC C22:4 and LPC C22:5) were intracellularly unaltered and extracellularly diminished whereas LPC C14:0 was intracellularly diminished and extracellularly unaltered. LPC C14:1 was exclusively found in cell lysates as it was the case with LPC C22:0 in supernatants. Altogether, comparing the 24-hour *stimuli* with the 30-minute *stimuli*, the species-specific comparison of the kinetics between intra- and extracellular compartments revealed 40 % (8/20) isolated decreases, 20 % (4/20) congruent decreases plus 5 % (1/20) analog trends and 5 % (1/20) incongruent alternations plus 25 % (5/20) analog trends. After 4 hours (*versus* 30 minutes) 20 % (4/20) isolated increases (intracellular LPC C18:2 and LPC C18:3 plus extracellular LPC C14:0 and LPC C22:0) plus 15 % (3/20) analog trends (intracellular LPC C16:1, LPC C18:1 and LPC C20:2) and 35 % (7/20) incongruent changes (LPC C20:3, LPC C20:4, LPC C20:5, LPC C22:4, LPC C22:5 and LPC C22:6 intracellularly increasing and extracellularly decreasing and LPC C22:1 showing the opposite) were found, without any congruent changes being found. Quite the contrary, results from 24-hour *stimuli* compared with 4-hour *stimuli* revealed 45 % (9/20) congruent decreases (LPC C14:0, LPC C16:0, LPC C18:0, LPC C18:1, LPC C20:1, LPC C20:2, LPC C22:3, LPC C22:4 and LPC C22:5) plus 15 % (3/20) analog trends (LPC C16:1, LPC C20:0 and LPC C20:4) and 35 % (7/20) isolated decreases (intracellular LPC C14:1 and LPC C22:1, extracellular LPC C18:2, LPC C18:3, LPC C20:3, LPC C20:5 and LPC C22:6) without any incongruent kinetic being found.

The decreased LPC levels found in overfeeding [84, 104], obesity [103, 104, 144, 149-151], insulin resistance [153, 154] and type 2 diabetes mellitus [104] raise the question whether these declines result from reduced production of LPCs or rather from increased consumption in consequence of either degradation or uptake from blood by metabolically active tissues. Revealingly, the reduction of LPC levels in consequence of a high-fat diet in mice is much more marked in plasma than in tissues such as liver, adipose tissue or skeletal muscle [104]. Furthermore, nearly all significant alterations of LPC species found in tissues by Barber *et al.* were consistent with the respective alterations in plasma after 12 weeks of high-fat-feeding: LPC C18:0 was increased in both adipose tissue and plasma, whereas all LPC species decreased in liver (LPC C20:0 and LPC C20:1) and/or in skeletal muscle (LPC C16:1 and LPC C20:1) were also diminished in plasma [104]. These observations could be brought into accordance with the hypothesis of an (intra-) cellular uptake of extracellular LPC species possibly with subsequent intracellular metabolization. However, many other hypotheses are conceivable such as metabolization and/or degradation of LPCs both intra- and extracellularly to take a single example.

LPCs are produced from PCs by secretory phospholipases [84], LCAT [84] or ROS [87-89]. However, diminished production by ROS appears unlikely because an overfeeding study with human subjects was accompanied by a marked systemic oxidative stress response indicated by the systemic oxidative stress marker urinary F2-isoprostanes, while 7 out of 22 LPC species decreased [84]. Alternatively, decreased LPC levels could be the result of a reduced LCAT activity possibly caused by increased levels of cholesteryl esters (CE) in the sense of a product repression.

9.5 Impact of the degree of unsaturation of acyl groups on LPC level alteration

Time course analysis of the LPC total concentrations in cell lysates and supernatants (referring the LPC amounts of substance to the protein mass of the corresponding cell lysate) revealed distinct decreases of total [^{12}C]LPCs after 24 hours in both supernatants (*vs*. 4-hour stimulation: - 51 %, $p = 0.0002$*; *vs*. 30-min stimulation: - 51 %, $p < 0.0001$*) and cell lysates (*vs*. 4-hour stimulation: - 24 %, $p = 0.0031$*) with a trend to increase after 4 hours being only found intracellularly (*vs*. 30-min stimulation: + 18 %, $p = 0.0666$) but not extracellularly (*vs*. 30-min stimulation: + 2 %, $p = 0.8425$).

Species-specific LPC profiling mirrored these observations of decreased concentrations after 24 hours of stimulation by 7 out of 19 (37 %) intracellular as well as by 16 out of 19 (84 %) extracellular [^{12}C]LPC species when compared with the 30-minute stimulation period. Relating the 24-hour *stimuli* to the 4-hour *stimuli* affirmed significant decreases after 24 hours for 11 intracellular (58 %) and 17 extracellular (89 %) species. This superior coverage results from elevations after 4 hours (*versus* 30 minutes) which were observed to be significant for 8 intracellular (42 %) and 3 extracellular (16 %) [^{12}C]-species.

There is evidence to suggest that the alterations after both 4 hours and 24 hours occur as a function of the degree of unsaturation of the respectively equivalent acyl group chain length: A higher degree of unsaturation seems to promote intracellular increases as well as extracellular decreases as visualized in **Figure 20** (always focusing on LPC species of the respectively equivalent acyl group chain length).

Accordingly, not only LPC C18:1 (+ 20 %), LPC C18:2 (+ 35 %) and LPC C18:3 (+ 48 %) as well as LPC C20:2 (+ 19 %), LPC C20:3 (+ 44 %), LPC C20:4 (+ 42 %) and LPC C20:5 (+ 60 %) plus LPC C22:1 (- 20 %), LPC C22:4 (+ 27 %), LPC C22:5 (+ 37 %) and LPC C22:6 (+ 45 %) successively increased after 4 hours in cell lysates (*versus* 30 minutes), but LPC C22:1 (+ 35 %), LPC C22:4 (- 17 %), LPC C22:5 (- 22 %) and LPC C22:6 (- 29 %) successively decreased in supernatants.

Similarly, comparison of 24-hour *stimuli* with 30-min *stimuli* revealed waxing decreases in supernatants for LPC C18:0 (- 42 %), LPC C18:1 (- 44 %), LPC C18:2 (- 74 %) and LPC C18:3 (- 78 %) as well as for LPC C20:0 (- 21 %), LPC C20:1 (- 32 %), LPC C20:2 (- 51 %), LPC C20:3 (- 74 %), LPC C20:4 (- 83 %) and LPC C20:5 (- 83 %) plus for LPC C22:1 (+ 26 %), LPC C22:3 (- 37 %), LPC C22:4 (- 71 %), LPC C22:5 (- 79 %) and LPC C22:6 (- 83 %). Intracellularly, first, LPC C14:0 (- 52 %) and LPC C14:1 (- 38 %), second, LPC C20:1 (- 39 %) and LPC C20:2 (- 30 %), and third, LPC C22:1 (- 52 %) and LPC C22:3 (- 44 %) featured shrinking decreases, whereas, fourth, polyunsaturated LPC C18:2 (+ 45 %) and LPC C18:3 (+ 80 %), fifth, LPC C20:3 (+ 47 %) and LPC C20:5 (+ 60 %), and sixth, LPC C22:5 (+ 16 %) and LPC C22:6 (+ 42 %) progressively increased.

Analogously, after 24 hours *versus* 4 hours, incremental extracellular decreases were found for LPC C18:0 (- 45 %), LPC C18:1 (- 48 %), LPC C18:2 (- 71 %) and

LPC C18:3 (- 75 %) as well as for LPC C20:0 (- 27 %), LPC C20:1 (- 38 %), LPC C20:2 (- 51 %), LPC C20:3 (- 69 %), LPC C20:4 (- 78 %) and LPC C20:5 (- 78 %) plus for LPC C22:3 (- 45 %), LPC C22:4 (- 65 %), LPC C22:5 (- 73 %) and LPC C22:6 (- 76 %).

Notably, unvarying extracellular decreases were also found for LPC C20:3 (- 16 %), LPC C20:4 (- 22 %) and LPC C20:5 (- 20 %) after 4 hours *versus* 30 minutes, for LPC C16:0 (- 35 %) and LPC C16:1 (- 34 %) after 24 hours *versus* 30 minutes and for LPC C16:0 (- 43 %) and LPC C16:1 (- 43 %) after 24 hours *versus* 4 hours and analogously constant intracellular decreases of LPC C18:0 (- 19 %) and LPC C18:1 (- 23 %).

This dependence of LPC dynamics on the degree of unsaturation of respectively equivalent acyl group chain lengths may be the consequence of differing binding affinities with a major degree of unsaturation implicating a higher binding affinity with, for example, transmembrane transport proteins and/or with metabolizing enzymes entailing a greater decline for more unsaturated species in supernatants. The fact, that a major degree of unsaturation was not only associated with greater extracellular declines but also with greater intracellular increases, rather lends credence to the hypothesis that species with major degree of unsaturation may bind with a higher affinity to transmembrane transport proteins.

Another explanation may be found in a facilitated (noncatalyzed) transmembrane migration for more unsaturated LPC species. Revealingly, as elaborated in detail in chapter **1.1.5**, equilibration between the two membrane leaflets of sarcoplasmic reticulum membranes after administration of [*N*-$^{13}CH_3$]-labeled LPC C16:0 was completed *in vitro* within 30 minutes at 20 °C [101]. Interestingly, the majority of [*N*-$^{13}CH_3$]LPCs was incorporated into the outer leaflet [130], with approximately 42 % of [*N*-$^{13}CH_3$]LPCs being incorporated into the inner leaflet [101], pointing again to the beforehand discussed possibility of an incorporation of LPCs into the membrane instead of a (complete) transmembrane migration.

9.6 Investigation of gender-dependent LPC kinetics

As depicted in **Supplemental Table 1**, investigating a potential gender effect on LPC concentrations, no single LPC species significantly differs between male and female donors.

Supplemental Table 1: Species-specific differences between male (n = 6) and female (n = 4) subjects determined by unpaired Student's *t*-tests in JMP® and expressed as p-values. LPCs were isolated from both cell lysates and supernatants of cultured primary human myotubes from 10 different donors after stimulation with 100 µM L-carnitine plus 125 µM [$^{13}C_{16}$]palmitate for 30 minutes (0.5 h), 4 hours (4 h) or 24 hours (24 h). The amounts of LPCs were referred to the protein mass of the corresponding cell lysate.

LPC species	CELL LYSATE			SUPERNATANT		
	0.5 h	4 h	24 h	0.5 h	4 h	24 h
[$^{13}C_{14}$]LPC C14:0	0.9259	0.4381	0.1758			0.4593
[$^{13}C_{16}$]LPC C16:0	0.8517	0.3383	0.2531	0.4659	0.8178	0.3604
[$^{13}C_{16}$]LPC C16:1	0.7702	0.5068	0.4757		0.9828	0.9811
[$^{13}C_{16}$]LPC C18:0	0.2521	0.8390	0.3048			0.7188
[$^{13}C_{18}$]LPC C18:0	0.9546	0.9080	0.3602			0.9493
[$^{13}C_{16}$]LPC C18:1	0.3557	0.6553	0.1722			0.6175
[$^{13}C_{18}$]LPC C18:1	0.6038	0.5361	0.2285			0.4421
LPC C14:0	0.6992	0.5190	0.3628	0.7037	0.8820	0.5678
LPC C14:1	0.5100	0.4035	0.6287			
LPC C16:0	0.7262	0.4260	0.0608	0.8438	0.8433	0.6429
LPC C16:1	0.2788	0.3499	0.5370	0.7018	0.9490	0.5241
LPC C18:0	0.6144	0.7651	0.4225	0.9506	0.7322	0.7449
LPC C18:1	0.5879	0.4076	0.1654	0.8645	0.8173	0.7255
LPC C18:2	0.6802	0.4686	0.6877	0.6553	0.9105	0.6184
LPC C18:3	0.4447	0.3015	0.9357	0.6535	0.9437	0.5790
LPC C20:0	0.3942	0.4491	0.5239	0.9662	0.6537	0.8085
LPC C20:1	0.3483	0.4798	0.5717	0.9661	0.5759	0.9550
LPC C20:2	0.3809	0.8146	0.9293	0.7903	0.6775	0.8820
LPC C20:3	0.6236	0.9911	0.7802	0.8942	0.7977	0.8929
LPC C20:4	0.6872	0.5673	0.5692	0.7381	0.9800	0.6345
LPC C20:5	0.2008	0.1778	0.4492	0.5622	0.9612	0.4537
LPC C22:0				0.9748	0.2563	0.8094
LPC C22:1	0.7518	0.5482	0.5235	0.8919	0.5314	0.8747
LPC C22:3	0.0563	0.2267	0.5601	0.6277	0.8600	0.9920
LPC C22:4	0.2248	0.4025	0.6742	0.8733	0.7915	0.8600
LPC C22:5	0.7658	0.9737	0.8233	0.8205	0.8494	0.9140
LPC C22:6	0.7743	0.9760	0.9526	0.7315	0.9389	0.8664

9.7 Supplemental correlation analyses

The results of all LPC species-specific correlation analyses with *in vivo* and further *in vitro* parameters of the donors are represented by color coding in the heat maps of **Supplemental Table 2**, **Supplemental Table 3** and **Supplemental Table 4**.

Supplemental Table 2: Heat map for the correlations ($p \leq 0.05$, $n \geq 6$) of [^{12}C]- or [^{13}C]-sums and of the individual [^{13}C]-species with the *in vivo* and *in vitro* parameters of the donors.
Please refer to the List of Abbreviations for specification of abbreviations.

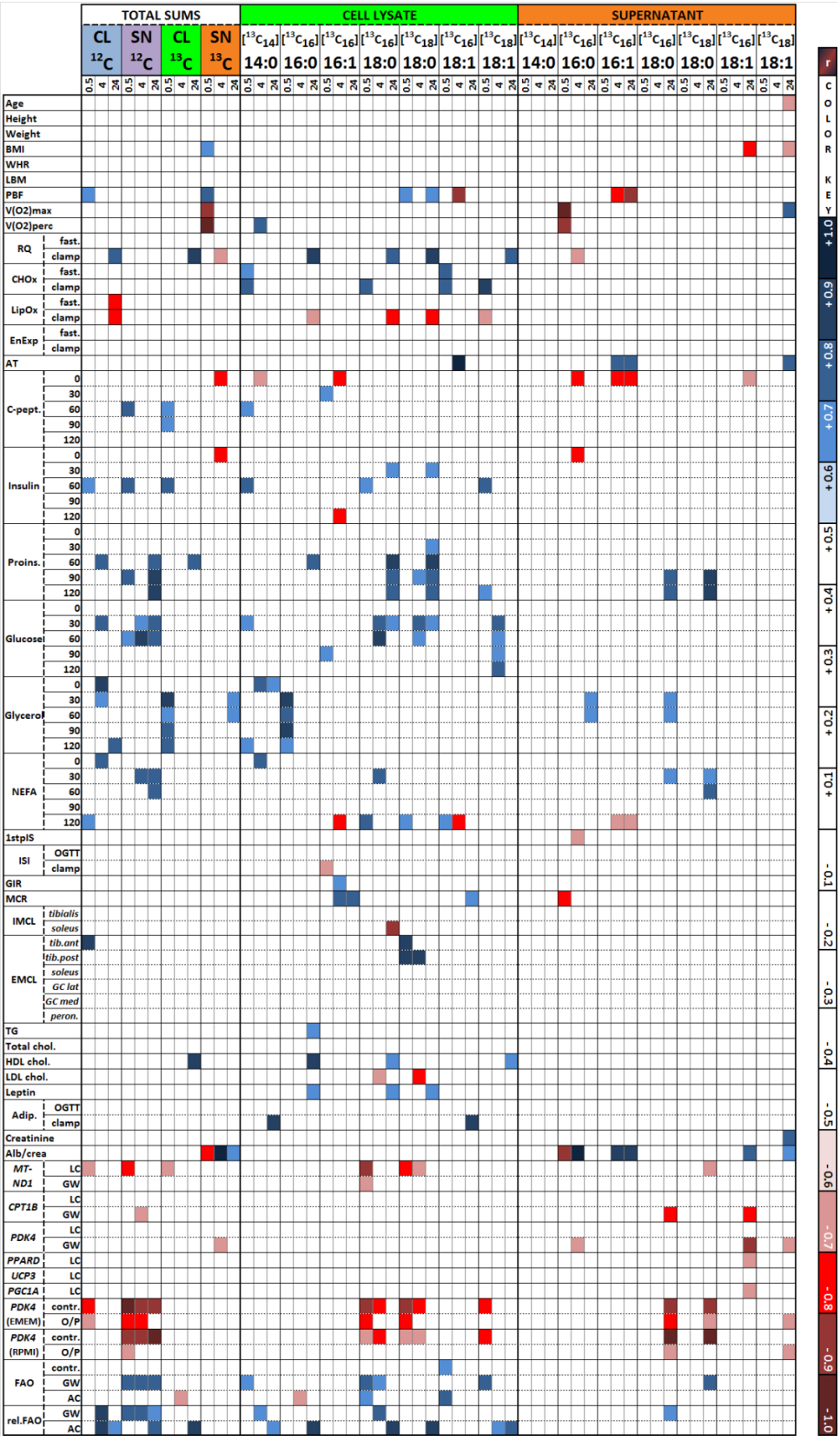

Supplemental Table 3: Heat map of the species-specific associations ($p \leq 0.05$, $n \geq 6$) of the intracellular [^{12}C]-species with the *in vivo* and *in vitro* parameters of the donors.
Please refer to the List of Abbreviations for specification of abbreviations.

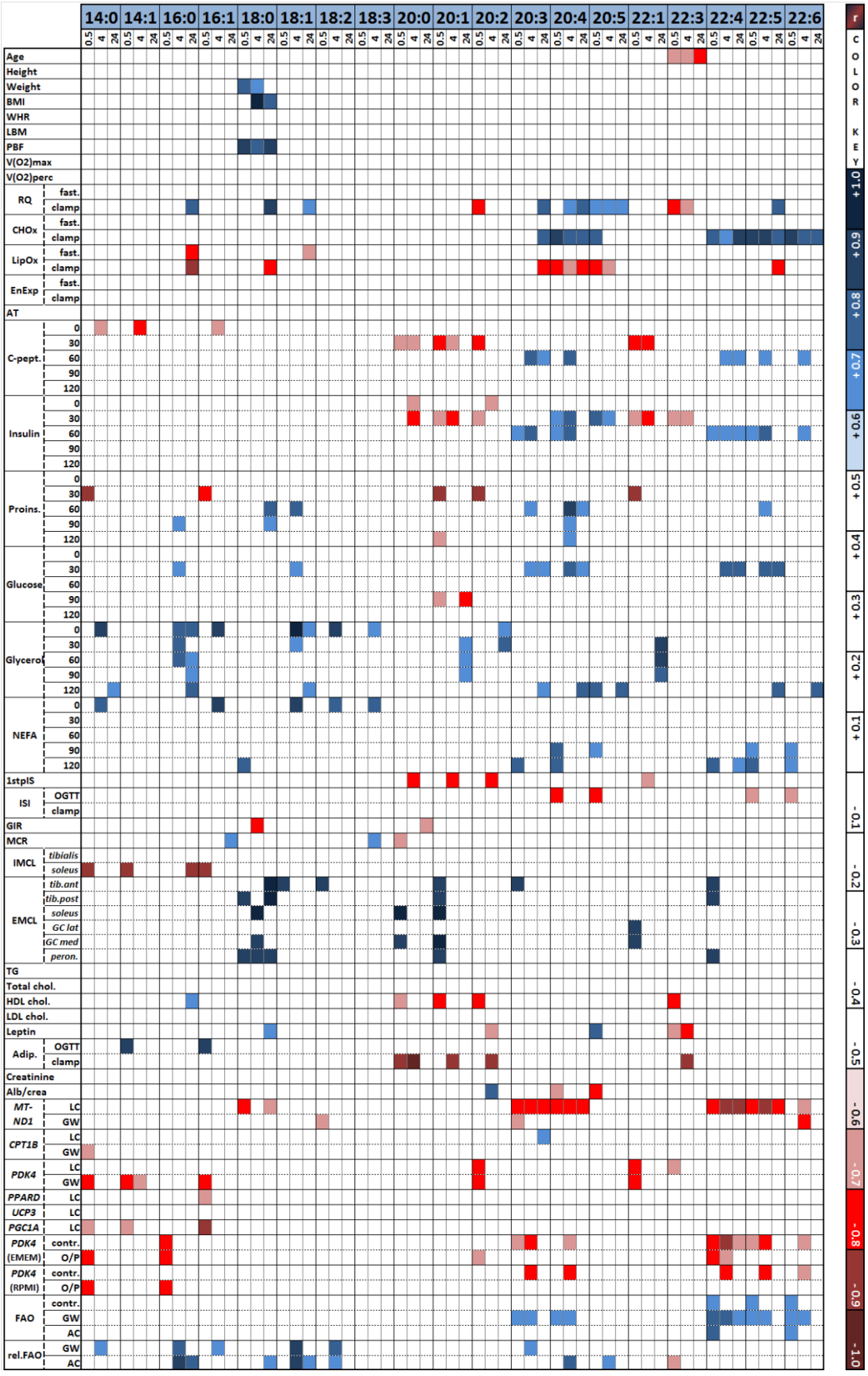

Supplemental Table 4: Heat map of the species-specific associations ($p \leq 0.05$, $n \geq 6$) of the extracellular [^{12}C]-species with the *in vivo* and *in vitro* parameters of the donors.
Please refer to the List of Abbreviations for specification of abbreviations.

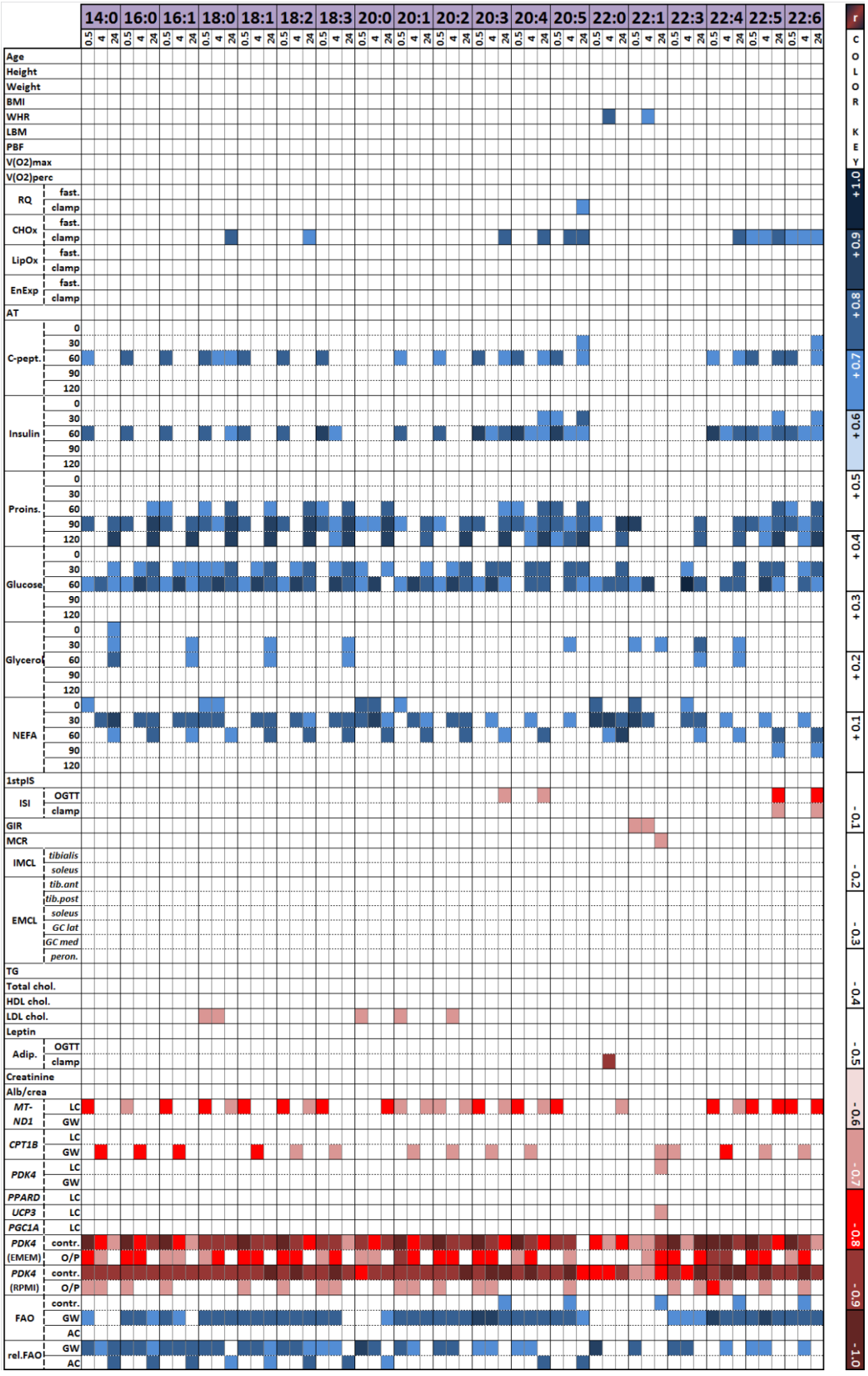

9.7.1 Coherency of correlation analyses with [^{12}C]LPCs and [^{13}C]LPCs

Although the kinetics strikingly differed between [^{12}C]LPC species, predominantly markedly decreasing, and [^{13}C]LPC species, exclusively markedly increasing, there were obvious coherencies between the correlation results of [^{12}C]- and [^{13}C]-species. So 4 out of 15 significant associations (≈ 27 %) of intracellular [$^{13}C_{14}$]LPC C14:0 were affirmed by LPC C14:0, 4 out of 12 significant associations (≈ 33 %) of intracellular [$^{13}C_{16}$]LPC C16:0 by LPC C16:0, 2 out of 9 significant associations (≈ 22 %) of intracellular [$^{13}C_{16}$]LPC C16:1 by LPC C16:1, 8 out of 29 significant associations (≈ 28 %) of intracellular [$^{13}C_{16}$]LPC C18:0 by LPC C18:0, 11 out of 27 significant associations (≈ 41 %) of intracellular [$^{13}C_{18}$]LPC C18:0 by LPC C18:0, 4 out of 15 significant associations (≈ 27 %) of intracellular [$^{13}C_{18}$]LPC C18:1 by LPC C18:1, 4 out of 10 significant associations (40 %) of extracellular [$^{13}C_{16}$]LPC C18:0 by LPC C18:0 and 7 out of 9 significant associations (≈ 78 %) of extracellular [$^{13}C_{18}$]LPC C18:0 by LPC C18:0. However, no coherent correlations were found between intracellular [$^{13}C_{16}$]LPC C18:1 and LPC C18:1, extracellular [$^{13}C_{16}$]LPC C16:0 and LPC C16:0, extracellular [$^{13}C_{16}$]LPC C16:1 and LPC C16:1, extracellular [$^{13}C_{16}$]LPC C18:1 and LPC C18:1 or extracellular [$^{13}C_{18}$]LPC C18:1 and LPC C18:1. Extracellular [$^{13}C_{14}$]LPC C14:0 showed no significant association at all.

Importantly, all (100 %) of these 44 coherent associations as well as additional 20 significant associations of [^{13}C]-species tendentially affirmed by their respective [^{12}C]-homologue were consistent with the direction of the association, respectively. This clearly indicates that those myotubes presenting higher levels of [^{13}C]LPCs also show higher levels of [^{12}C]LPCs. But as [^{13}C]-species distinctly increase in the course of time whereas most [^{12}C]-species decrease this means also that those myotubes with a superior production of [^{13}C]LPCs show a minor reduction of [^{12}C]LPCs. For example, intracellular [$^{13}C_{16}$]LPC C16:0 was highly significantly increased after 24 hours of stimulation (*vs.* 0.5 h: $p = 0.0048$*) whereas intracellular LPC C16:0 was highly significantly decreased after 24 hours (*vs.* 0.5 h: $p = 0.0029$*) but at this stimulation period of 24 hours both showed positive associations with RQ_{clamp}, negative associations with $LipOx_{clamp}$, positive associations with HDL cholesterol and positive associations with relFAO (AC) (**Supplemental Table 2** and **Supplemental Table 3**).

The observation that a superior *de novo* synthesis of [^{13}C]LPCs may be accompanied by an attenuated decrease of the respective [^{12}C]-homologues suggest that the reductions of the [^{12}C]LPC concentrations may be (at least partly) the consequence of their reduced production as the *de novo* synthesis of [^{12}C]LPCs presumably also continues to occur at an individually correspondent activity.

9.7.2 Correlation analyses with anthropometric parameters

Significant correlations of extracellular [^{13}C]LPCs after 30 minutes of [$^{13}C_{16}$]palmitate stimulation are found with BMI (r = + 0.68, p = 0.0441*), PBF (r = + 0.73, p = 0.0270*) and aerobic capacity ($V(O_2)_{max}$: r = - 0.89, p = 0.0065* and $V(O_2)_{perc}$: r = - 0.99, p < 0.0001*) as shown in **Table 13** in the Results section. PBF also correlates with intracellular [^{12}C]LPCs at the same time point (r = + 0.66, p = 0.0386*). Further significant correlations are absent for BMI, PBF, $V(O_2)_{max}$ (**Table 13**) and $V(O_2)_{perc}$ (**Supplemental Table 5**).

Species-specific correlation analyses are represented by color coding in the heat maps of **Supplemental Table 2**, **Supplemental Table 3** and **Supplemental Table 4**.

Age exclusively correlates with extracellular [$^{13}C_{18}$]LPC C18:1 (24 h: r = - 0.65, p = 0.0406*) and intracellular LPC C22:3 but this latter association is confirmed for all three points in time (0.5 h: r = - 0.65, p = 0.0413*; 4 h: r = - 0.67, p = 0.0336*; 24 h: r = - 0.77, p = 0.0091*).

WHR (applied as a method of estimation for body fat distribution [177]) correlates at the time of 4 hours with extracellular LPC C22:0 (r = + 0.74, p = 0.0142*) and extracellular LPC C22:1 (r = + 0.66, p = 0.0397*).

Weight solely correlates significantly with intracellular LPC C18:0 at the time of 30 minutes (r = + 0.77, p = 0.0092*) and at the time of 4 hours (r = + 0.69, p = 0.0258*).

Height and **LBM** do not correlate with any species.

BMI shows significant correlations with intracellular LPC C18:0 at the time of 4 hours (r = + 0.91, p = 0.0003*) and 24 hours (r = + 0.76, p = 0.0113*) as well as a clear trend at the time of 30 minutes (r = + 0.63, p = 0.0519).

None of the extracellular [^{13}C]LPC species at the time of 30 minutes correlates with BMI ($p \geq 0.1872$) although their sum does ($r = + 0.68$, $p = 0.0441$*), whereas at the time of 24 hours extracellular [$^{13}C_{16}$]LPC C18:1 ($r = - 0.71$, $p = 0.0220$*) and extracellular [$^{13}C_{18}$]LPC C18:1 ($r = - 0.65$, $p = 0.0428$*) correlate with BMI although the sum of extracellular [^{13}C]LPC species at the time of 24 hours doesn't ($r = - 0.19$, $p = 0.5960$).

The positive correlation of **PBF** with total intracellular [^{12}C]LPCs after 30 minutes of stimulation is retained in species-specific analysis for LPC C18:0 ($r = + 0.82$, $p = 0.0038$*) and tendentially for LPC C16:0 ($r = + 0.57$, $p = 0.0870$), LPC C18:1 ($r = + 0.59$, $p = 0.0711$), LPC C18:2 ($r = + 0.63$, $p = 0.0529$) and LPC C20:3 ($r = + 0.60$, $p = 0.0665$). Notably, LPC C18:0 also correlates with PBF at the time of 4 hours ($r = + 0.78$, $p = 0.0073$*) and 24 hours ($r = + 0.84$, $p = 0.0023$*).

Extracellularly, 8 out of the 19 [^{12}C]-species (42 %) tend to be positively associated with PBF after 30 minutes: LPC C14:0 ($r = + 0.55$, $p = 0.0985$), LPC C16:1 ($r = + 0.56$, $p = 0.0957$), LPC C18:2 ($r = + 0.58$, $p = 0.0798$), LPC C18:3 ($r = + 0.56$, $p = 0.0926$), LPC C20:4 ($r = + 0.57$, $p = 0.0824$), LPC C22:3 ($r = + 0.57$, $p = 0.0879$), LPC C22:5 ($r = + 0.57$, $p = 0.0834$) and LPC C22:6 ($r = + 0.56$, $p = 0.0923$).

The positive correlation of PBF with total extracellular [^{13}C]LPCs after 30 minutes ($r = + 0.73$, $p = 0.0270$*) is only tendentially confirmed by [$^{13}C_{16}$]LPC C16:0 ($r = + 0.67$, $p = 0.0687$) but PBF correlates negatively with extracellular [$^{13}C_{16}$]LPC C16:1 after 4 hours ($r = - 0.73$, $p = 0.0169$*) and after 24 hours ($r = - 0.81$, $p = 0.0043$*) as well as with intracellular [$^{13}C_{16}$]LPC C18:1 after 4 hours ($r = - 0.86$, $p = 0.0012$*). In contrast, PBF correlates positively with intracellular [$^{13}C_{18}$]LPC C18:0 after 30 minutes ($r = + 0.69$, $p = 0.0279$*), 4 hours ($r = + 0.61$, $p = 0.0626$) and 24 hours ($r = + 0.67$, $p = 0.0339$*).

The negative associations of **$V(O_2)_{max}$** and **$V(O_2)_{perc}$** with total extracellular [^{13}C]LPCs at the time of 30 minutes ($V(O_2)_{max}$: $r = - 0.89$, $p = 0.0065$*, $n = 7$; $V(O_2)_{perc}$: $r = - 0.99$, $p < 0.0001$*, $n = 7$) is confirmed in species-specific analysis for [$^{13}C_{16}$]LPC C16:0 ($V(O_2)_{max}$: $r = - 0.91$, $p = 0.0042$*, $n = 7$; $V(O_2)_{perc}$: $r = - 0.86$, $p = 0.0133$*, $n = 7$) and tendentially for [$^{13}C_{16}$]LPC C16:1 ($V(O_2)_{max}$: $r = - 0.99$, $p = 0.0852$, $n = 3$; $V(O_2)_{perc}$: $r = - 0.98$, $p = 0.1118$, $n = 3$). By contrast, intracellular [$^{13}C_{14}$]LPC C14:0 at the time of 4 hours shows a positive relationship with $V(O_2)_{perc}$ ($r = + 0.73$, $p = 0.0391$*, $n = 8$) and intracellular [$^{13}C_{16}$]LPC C16:1 also tends to correlate positively with $V(O_2)_{perc}$ at the

time of 4 hours (r = + 0.68, p = 0.0638, n = 8) as well as extracellular [$^{13}C_{16}$]LPC C16:1 at the time of 24 hours with $V(O_2)_{max}$ (r = + 0.70, p = 0.0509, n = 8) and $V(O_2)_{perc}$ (r = + 0.70, p = 0.0547, n = 8). Extracellular [$^{13}C_{18}$]LPC C18:1 after 24 hours correlates with $V(O_2)_{max}$ (r = + 0.75, p = 0.0324*, n = 8) and tends to with $V(O_2)_{perc}$ (r = + 0.68, p = 0.0624, n = 8).

9.7.3 Correlation analyses with *in vivo* physiologic and metabolic parameters

Correlation results with sums of [^{12}C]- or [^{13}C]-labeled LPCs are shown in **Supplemental Table 5** for additional physiologic parameters which were excluded from the Results section: $V(O_2)_{perc}$, $EnExp_{fasting}$, $EnExp_{clamp}$ and anaerobic threshold (AT).

Species-specific correlation analyses with all *in vivo* and *in vitro* parameters are represented by color coding in the heat maps of **Supplemental Table 2**, **Supplemental Table 3** and **Supplemental Table 4**.

$RQ_{fasting}$ doesn't show any correlation with the sums of intra- or extracellular LPCs, neither with [^{12}C]- nor with [^{13}C]-labeled derivatives. However, species-specific analysis reveals a positive correlation with extracellular [$^{13}C_{16}$]LPC C16:1 after 30 minutes of [$^{13}C_{16}$]palmitate stimulation (r = + 0.98, p = 0.0155*, n = 4).

The positive relationship of **RQ_{clamp}** with 24-hour intracellular [^{12}C]LPCs (r = + 0.79, p = 0.0067*) and 24-hour intracellular [^{13}C]LPCs (r = + 0.82, p = 0.0034*) is reflected by the species LPC C16:0 (r = + 0.78, p = 0.0075*), [$^{13}C_{16}$]LPC C16:0 (r = + 0.84, p = 0.0026*), LPC C18:0 (r = + 0.83, p = 0.0030*), [$^{13}C_{16}$]LPC C18:0 (r = + 0.80, p = 0.0056*), [$^{13}C_{18}$]LPC C18:0 (r = + 0.83, p = 0.0028*), LPC C18:1 (r = + 0.70, p = 0.0244*), [$^{13}C_{18}$]LPC C18:1 (r = + 0.75, p = 0.0124*), LPC C20:3 (r = + 0.74, p = 0.0142*), LPC C20:4 (r = + 0.77, p = 0.0096*), LPC C20:5 (r = + 0.66, p = 0.0378*) and LPC C22:5 (r = + 0.73, p = 0.0156*) plus analog trends for LPC C18:2 (r = + 0.60, p = 0.0681), LPC C22:4 (r = + 0.63, p = 0.0525) and LPC C22:6 (r = + 0.62, p = 0.0534). Intracellular [$^{13}C_{18}$]LPC C18:1 (0.5 h: r = + 0.56, p = 0.0889; 4 h: r = + 0.60, p = 0.0656), LPC C20:4 (0.5 h: r = + 0.61, p = 0.0636; 4 h: r = + 0.67, p = 0.0331*), LPC C20:5 (0.5 h: r = + 0.67, p = 0.0353*; 4 h: r = + 0.66, p = 0.0383*) and LPC C22:5 (4 h: r = + 0.61, p = 0.0603) additionally show (a trend for) positive correlations after 30 minutes and/or 4 hours of stimulation.

In contrast, intracellular LPC C20:2 after 30 minutes (r = - 0.73, p = 0.0159*) as well as intracellular LPC C22:3 after 30 minutes (r = - 0.79, p = 0.0071*) and after 4 hours (r = - 0.66, p = 0.0393*) correlate negatively with RQ_{clamp}. Moreover, the negative correlation of total extracellular [^{13}C]LPCs after 4 hours (r = - 0.65, p = 0.0405*) with RQ_{clamp} is also observed for (extracellular) [$^{13}C_{16}$]LPC C16:0 after 4 hours (r = - 0.64, p = 0.0456*) as well as tendentially for [$^{13}C_{16}$]LPC C16:1 after 4 hours (r = - 0.57, p = 0.0876) plus after 24 hours (r = - 0.56, p = 0.0894) and for [$^{13}C_{18}$]LPC C18:1 after 24 hours (r = - 0.60, p = 0.0654). The only extracellular species correlating positively with RQ_{clamp} is LPC C20:5 after 24 hours (r = + 0.65, p = 0.0406*).

Both **$CHOx_{fasting}$** and **$CHOx_{clamp}$** do not show any association with total concentrations of intra- nor extracellular [^{12}C]- nor [^{13}C]LPCs (**Table 14**). Nonetheless, individual intracellular [^{13}C]-isotopes positively correlate after 30 minutes of stimulation with CHOx such as intracellular [$^{13}C_{14}$]LPC C14:0 ($CHOx_{fasting}$: r = + 0.67, p = 0.0488*, n = 9; $CHOx_{clamp}$: r = + 0.80, p = 0.0098*, n = 9), intracellular [$^{13}C_{16}$]LPC C18:0 ($CHOx_{clamp}$: r = + 0.72, p = 0.0292*, n = 9), intracellular [$^{13}C_{16}$]LPC C18:1 ($CHOx_{fasting}$: r = + 0.72, p = 0.0276*, n = 9; $CHOx_{clamp}$: r = + 0.77, p = 0.0158*, n = 9) and intracellular [$^{13}C_{18}$]LPC C18:1 ($CHOx_{clamp}$: r = + 0.87, p = 0.0023*, n = 9). Extracellular [^{13}C]-metabolites lack significant associations.

Concerning [^{12}C]-species, in agreement with the results for RQ reported above, the discrepancy between fasting condition and steady-state phase of the clamp is elucidated as not a single [^{12}C]-species (0 %) associates with $CHOx_{fasting}$ (n = 9) but 6 out of 19 intracellular (32 %) and 8 out of 19 extracellular (42 %) species positively associate with $CHOx_{clamp}$ (n = 9) – predominantly those with polyunsaturated long-chain acyl groups: extracellular LPC C18:0 (24 h: r = + 0.71, p = 0.0338*), extracellular LPC C18:2 (0.5 h: r = + 0.59, p = 0.0933; 4 h: r = + 0.59, p = 0.0976; 24 h: r = + 0.68, p = 0.0454*), intracellular LPC C20:3 (0.5 h: r = + 0.60, p = 0.0876; 4 h: r = + 0.64, p = 0.0634; 24 h: r = + 0.76, p = 0.0165*), extracellular LPC C20:3 (0.5 h: r = + 0.66, p = 0.0530; 4 h: r = + 0.64, p = 0.0660; 24 h: r = + 0.73, p = 0.0253*), intracellular LPC C20:4 (0.5 h: r = + 0.82, p = 0.0073*; 4 h: r = + 0.73, p = 0.0256*; 24 h: r = + 0.78, p = 0.0140*), extracellular LPC C20:4 (0.5 h: r = + 0.64, p = 0.0608; 4 h: r = + 0.66, p = 0.0554; 24 h: r = + 0.72, p = 0.0283*), intracellular LPC C20:5 (0.5 h: r = + 0.71, p = 0.0330*; 24 h: r = + 0.62, p = 0.0779), extracellular LPC C20:5 (0.5 h:

r = + 0.66, p = 0.0546; 4 h: r = + 0.70, p = 0.0355*; 24 h: r = + 0.73, p = 0.0263*), intracellular LPC C22:4 (0.5 h: r = + 0.70, p = 0.0347*; 4 h: r = + 0.70, p = 0.0361*; 24 h: r = + 0.81, p = 0.0085*), extracellular LPC C22:4 (0.5 h: r = + 0.64, p = 0.0631; 4 h: r = + 0.60, p = 0.0850; 24 h: r = + 0.70, p = 0.0344*), intracellular LPC C22:5 (0.5 h: r = + 0.82, p = 0.0064*; 4 h: r = + 0.80, p = 0.0090*; 24 h: r = + 0.80, p = 0.0099*), extracellular LPC C22:5 (0.5 h: r = + 0.68, p = 0.0420*; 4 h: r = + 0.67, p = 0.0461*; 24 h: r = + 0.70, p = 0.0357*), intracellular LPC C22:6 (0.5 h: r = + 0.82, p = 0.0072*; 4 h: r = + 0.76, p = 0.0184*; 24 h: r = + 0.78, p = 0.0125*) and extracellular LPC C22:6 (0.5 h: r = + 0.69, p = 0.0407*; 4 h: r = + 0.69, p = 0.0415*; 24 h: r = + 0.69, p = 0.0400*).

Correlating total intra- or extracellular [^{12}C]- or [^{13}C]LPCs with *in vivo* LipOx yields significant negative relationships for [^{12}C]LPCs after 24 hours in cell lysates with both **LipOx$_{fasting}$** (r = - 0.73, p = 0.0266*, n = 9) and **LipOx$_{clamp}$** (r = - 0.79, p = 0.0112*, n = 9). Specifically, associations with LipOx$_{fasting}$ are found for intracellular LPC C16:0 (24 h: r = - 0.76, p = 0.0178*) and LPC C18:1 (24 h: r = - 0.68, p = 0.0438*). LipOx$_{clamp}$ (n = 9) negatively associates with the intracellular species LPC C16:0 (24 h: r = - 0.85, p = 0.0035*), LPC C18:0 (24 h: r = - 0.77, p = 0.0155*), LPC C20:3 (24 h: r = - 0.71, p = 0.0316*), LPC C20:4 (0.5 h: r = - 0.75, p = 0.0206*; 4 h: r = - 0.67, p = 0.0477*; 24 h: r = - 0.75, p = 0.0201*), LPC C20:5 (0.5 h: r = - 0.78, p = 0.0124*; 4 h: r = - 0.67, p = 0.0497*; 24 h: r = - 0.65, p = 0.0595) and LPC C22:5 (0.5 h: r = - 0.65, p = 0.0570; 4 h: r = - 0.65, p = 0.0603; 24 h: r = - 0.72, p = 0.0274*).
Whereas LipOx$_{fasting}$ does not correlate with any [^{13}C]-labeled metabolite, LipOx$_{clamp}$ correlates negatively with 4 out of 7 intracellular species (57 %) which are [$^{13}C_{16}$]LPC C16:0 after 24 hours (r = - 0.69, p = 0.0393*), [$^{13}C_{16}$]LPC C18:0 after 24 hours (r = - 0.73, p = 0.0251*), [$^{13}C_{18}$]LPC C18:0 after 24 hours (r = - 0.76, p = 0.0185*) and [$^{13}C_{18}$]LPC C18:1 after 30 minutes (r = - 0.67, p = 0.0482*).

Both **EnExp$_{fasting}$** and **EnExp$_{clamp}$** show not a single relationship with LPCs, neither with the sums (**Supplemental Table 5**) nor with individual species (**Supplemental Table 2**, **Supplemental Table 3** and **Supplemental Table 4**), neither with intracellular nor with extracellular concentrations, neither with [^{12}C]- nor with [^{13}C]-isotopes.

AT (n = 8) doesn't show any correlation with [^{12}C]LPCs, neither with their intra- nor extracellular sums (**Supplemental Table 5**) nor with the individual species (**Supplemental Table 3** and **Supplemental Table 4**).
While total [^{13}C]LPCs also lack significant associations, extracellular [$^{13}C_{16}$]LPC C16:1 after 4 hours (r = + 0.77, p = 0.0259*) and after 24 hours (r = + 0.78, p = 0.0216*), intracellular [$^{13}C_{16}$]LPC C18:1 after 4 hours (r = + 0.91, p = 0.0015*) and extracellular [$^{13}C_{18}$]LPC C18:1 after 24 hours (r = + 0.78, p = 0.0211*) positively correlate with AT (**Supplemental Table 2**).

In conclusion, the comparison of the two physiologically different conditions (fasting *vs*. clamp) reveals fundamental discrepancies in correlation analyses: None out of the 52 monitored LPC species (0 %) correlate with $RQ_{fasting}$, 2 species (≈ 4 %) with $CHOx_{fasting}$ and 2 species (≈ 4 %) with $LipOx_{fasting}$, whereas 15 species (≈ 29 %) correlate with RQ_{clamp}, 18 species (≈ 35 %) with $CHOx_{clamp}$ and 10 species (≈ 19 %) with $LipOx_{clamp}$. These considerable differences suggest that the *in vitro* LPC levels measured after stimulation with a fatty acid load are associated with *in vivo* energy metabolism after stimulation with intravenous insulin and glucose (clamp) but not with basal energy metabolism during fasting condition.

Detailed analysis of the associated LPC species highlights the relevance of the chemical structure of the species, as species with acyl groups containing up to 18 carbon atoms as well as with polyunsaturated C_{20} or C_{22} acyl groups show correlations in favor of an enhanced carbohydrate oxidation, while intracellular LPC C20:2 (after 0.5 h) plus LPC C22:3 (after 0.5 h and 4 h) exhibit a negative relationship with RQ_{clamp} (in favor of an enhanced lipid oxidation).
As opposed to this, intracellular [$^{13}C_{16}$]LPC C16:0 (after 24 h), [$^{13}C_{16}$]LPC C18:0 (after 24 h), [$^{13}C_{18}$]LPC C18:0 (after 24 h), [$^{13}C_{18}$]LPC C18:1 (after 24 h), LPC C16:0 (after 24 h), LPC C18:0 (after 24 h), LPC C18:1 (after 24 h), LPC C20:3 (after 24 h), LPC C20:4 (after 4 h and 24 h), LPC C20:5 (after 0.5 h, 4 h and 24 h) and LPC C22:5 (after 24 h) plus extracellular LPC C20:5 (after 24 h) exhibit a positive relationship with RQ_{clamp}.
In accordance with these associations, positive correlations are also found between $CHOx_{clamp}$ and intracellular [$^{13}C_{14}$]LPC C14:0 (after 0.5 h), [$^{13}C_{16}$]LPC C18:0

(after 0.5 h), [$^{13}C_{16}$]LPC C18:1 (after 0.5 h), [$^{13}C_{18}$]LPC C18:1 (after 0.5 h), LPC C20:3 (after 24 h), LPC C20:4 (after 0.5 h, 4 h and 24 h), LPC C20:5 (after 0.5 h), LPC C22:4 (after 0.5 h, 4 h and 24 h), LPC C22:5 (after 0.5 h, 4 h and 24 h) and LPC C22:6 (after 0.5 h, 4 h and 24 h) plus extracellular LPC C18:0 (after 24 h), LPC C18:2 (after 24 h), LPC C20:3 (after 24 h), LPC C20:4 (after 24 h), LPC C20:5 (after 4 h and 24 h), LPC C22:4 (after 24 h), LPC C22:5 (after 0.5 h, 4 h and 24 h) and LPC C22:6 (after 0.5 h, 4 h and 24 h) underlining the relevance of the entities with polyunsaturated C_{20} or C_{22} acyl groups as these species associate both intracellularly and extracellularly.
Analogously, $LipOx_{clamp}$ negatively correlates with intracellular [$^{13}C_{16}$]LPC C16:0 (after 24 h), [$^{13}C_{16}$]LPC C18:0 (after 24 h), [$^{13}C_{18}$]LPC C18:0 (after 24 h), [$^{13}C_{18}$]LPC C18:1 (after 0.5 h), LPC C16:0 (after 24 h), LPC C18:0 (after 24 h), LPC C20:3 (after 24 h), LPC C20:4 (after 0.5 h, 4 h and 24 h), LPC C20:5 (after 0.5 h and 4 h) and LPC C22:5 (after 24 h).
Thus, the only species correlating with RQ_{clamp} ($r > 0$), $CHOx_{clamp}$ ($r > 0$) and $LipOx_{clamp}$ ($r < 0$) are intracellular LPC C20:3 (after 24 h), LPC C20:4 (after 4 h and 24 h), LPC C20:5 (after 0.5 h) and LPC C22:5 (after 24 h).

Furthermore, the importance of species-specific lipidomics profiling is once more elucidated by the associations of LPC species with ISI determined *in vivo* during OGTT (**ISI_{OGTT}**) because (inverse) correlations are exclusively observed with polyunsaturated long-chain species, both intracellularly and extracellularly, but not with other species: ISI_{OGTT} negatively correlates with intracellular LPC C20:4, LPC C20:5, LPC C22:5 and LPC C22:6 (after 0.5 h) as well as with extracellular LPC C20:3, LPC C20:4, LPC C22:5 and LPC C22:6 (after 24 h).
Notably, none of these associations is reflected by the LPC sums but ISI determined *in vivo* during a euglycemic-hyperinsulinemic clamp (**ISI_{clamp}**) affirms the negative relationships with extracellular LPC C22:5 (after 24 h) and LPC C22:6 (after 24 h) and shows appropriate trends with intracellular LPC C20:4 (after 0.5 h: $r = -0.62$; $p = 0.0568$) and LPC C20:5 (after 0.5 h: $r = -0.56$; $p = 0.0949$) as well as with extracellular LPC C20:3 (after 24 h: $r = -0.56$; $p = 0.0901$) and LPC C20:4 (after 24 h: $r = -0.56$; $p = 0.0906$).
However, these overlaps may also be explained mathematically as ISI_{OGTT} and ISI_{clamp} are highly associated ($r = +0.91$; $p = 0.0003$*).

Supplemental Table 5: Correlation analyses between total concentrations of [^{12}C]- or [^{13}C]-labeled lysophosphatidylcholines (LPC) in cell lysates or supernatants of primary human myotubes after different stimulation periods and the physiologic *in vivo* parameters percentage of the maximal aerobic capacity $V(O_2)_{max}$ of the individually predicted peak $V(O_2)$ ($V(O_2)_p$), energy expenditure (EnExp), anaerobic threshold (AT), first phase insulin secretion (1stpIS), glucose infusion rate (GIR) and metabolic clearance rate (MCR). EnExp was measured both in fasting condition ($EnExp_{fasting}$) and during steady-state phase of a euglycemic-hyperinsulinemic clamp ($EnExp_{clamp}$). GIR and MCR are parameters of the euglycemic-hyperinsulinemic clamp, whereas 1stpIS was determined by oral glucose tolerance tests (OGTT). Human myotubes from 10 different individuals (n = 10) were stimulated for 30 minutes (0.5), 4 hours (4) or 24 hours (24) with 100 µM L-carnitine and 125 µM [$^{13}C_{16}$]palmitate. LPC amounts were mass spectrometrically quantified and referred to the protein mass of the corresponding cell lysate. As Shapiro-Wilk W tests in JMP® revealed log-normal distributions for LPC concentrations, $EnExp_{fasting}$, $EnExp_{clamp}$, 1stpIS, GIR and MCR, these variables were log_e-transformed (ln) for utilization in correlation analyses.

		TP		$V(O_2)_p$	EnExp fasting [ln]	EnExp clamp [ln]	AT	1stpIS OGTT [ln]	GIR clamp [ln]	MCR clamp [ln]
CELL LYSATE	[^{12}C]LPC	0.5	r	- 0.40	- 0.18	- 0.13	- 0.59	+ 0.19	- 0.33	- 0.41
			p	0.3328	0.6371	0.7419	0.1246	0.5968	0.3567	0.2456
			n	8	9	9	8	10	10	10
		4	r	+ 0.03	- 0.24	- 0.21	- 0.26	- 0.18	- 0.17	- 0.01
			p	0.9428	0.5397	0.5872	0.5305	0.6102	0.6371	0.9885
			n	8	9	9	8	10	10	10
		24	r	- 0.07	- 0.31	- 0.31	- 0.36	+ 0.11	+ 0.19	+ 0.31
			p	0.8662	0.4139	0.4241	0.3766	0.7659	0.5917	0.3812
			n	8	9	9	8	10	10	10
	[^{13}C]LPC	0.5	r	- 0.14	+ 0.09	+ 0.16	+ 0.04	+ 0.06	- 0.53	- 0.51
			p	0.7499	0.8252	0.6844	0.9254	0.8737	0.1124	0.1277
			n	8	9	9	8	10	10	10
		4	r	+ 0.15	- 0.14	- 0.23	+ 0.07	- 0.30	+ 0.01	+ 0.23
			p	0.7207	0.7197	0.5450	0.8681	0.4014	0.9883	0.5257
			n	8	9	9	8	10	10	10
		24	r	- 0.06	- 0.21	- 0.27	- 0.36	+ 0.26	+ 0.19	+ 0.31
			p	0.8854	0.5834	0.4818	0.3815	0.4627	0.6014	0.3763
			n	8	9	9	8	10	10	10
SUPERNATANT	[^{12}C]LPC	0.5	r	- 0.06	+ 0.03	+ 0.14	- 0.20	+ 0.06	- 0.30	- 0.30
			p	0.8922	0.9335	0.7192	0.6342	0.8743	0.3982	0.4034
			n	8	9	9	8	10	10	10
		4	r	+ 0.15	+ 0.39	+ 0.45	+ 0.27	- 0.30	- 0.36	- 0.35
			p	0.7171	0.3004	0.2290	0.5237	0.4066	0.3058	0.3171
			n	8	9	9	8	10	10	10
		24	r	+ 0.17	+ 0.20	+ 0.27	+ 0.04	+ 0.09	- 0.22	- 0.23
			p	0.6857	0.6032	0.4855	0.9268	0.8115	0.5388	0.5205
			n	8	9	9	8	10	10	10
	[^{13}C]LPC	0.5	r	- 0.99	- 0.03	- 0.18	- 0.74	+ 0.07	- 0.55	- 0.50
			p	<0.0001	0.9407	0.6696	0.0581	0.8582	0.1241	0.1667
			n	7	8	8	7	9	9	9
		4	r	+ 0.41	+ 0.10	+ 0.16	+ 0.58	- 0.63	- 0.11	- 0.06
			p	0.3149	0.8018	0.6723	0.1311	0.0510	0.7607	0.8767
			n	8	9	9	8	10	10	10
		24	r	+ 0.55	+ 0.02	+ 0.03	+ 0.41	- 0.28	- 0.04	+ 0.03
			p	0.1601	0.9573	0.9490	0.3149	0.4377	0.9087	0.9283
			n	8	9	9	8	10	10	10

Remarkably, the intracellular long-chain LPC species with no or few double bonds LPC C20:0, LPC C20:1, LPC C20:2 and LPC C22:1 as well as extracellular [$^{13}C_{16}$]LPC C16:0 (always after 4 hours of *in vitro* stimulation) negatively correlate with 1stpIS calculated by use of insulin and glucose concentrations from OGTT [177, 181, 182]. As **Supplemental Equation 1** and **Supplemental Equation 2** indicate that the numeric value of ISI_{OGTT} decreases but that of 1stpIS increases with ascending OGTT insulin levels, these results represent opposing relationships in comparison to the negative associations with ISI. This finding is highly consistent with the discrepancies observed for *in vivo* levels of C-peptide, insulin and proinsulin during OGTT also identifying extracellular [$^{13}C_{16}$]LPC C16:0 plus intracellular LPC C20:0, LPC C20:1, LPC C20:2 and LPC C22:1 as deviantly associating species (see **Supplemental Table 2** and **Supplemental Table 3**).

Additionally, GIR and MCR confirm intracellular LPC C20:0 and extracellular [$^{13}C_{16}$]LPC C16:0 as deviantly associating species but expand this group of species by intracellular LPC C18:0 and extracellular LPC C22:1: GIR correlates positively with intracellular [$^{13}C_{16}$]LPC C16:1 (after 4 h) but negatively with intracellular LPC C18:0 (after 4 h) and LPC C20:0 (after 24 h) plus extracellular LPC C22:1 (after 0.5 h and 4 h). Similarly, MCR correlates positively with intracellular [$^{13}C_{16}$]LPC C16:1 (after 4 h and 24 h), [$^{13}C_{16}$]LPC C18:1 (after 24 h), LPC C16:1 (after 24 h) and LPC C18:3 (after 4 h) but negatively with intracellular LPC C20:0 (after 0.5 h) plus extracellular [$^{13}C_{16}$]LPC C16:0 (after 0.5 h) and LPC C22:1 (after 24 h).

9.7.4 Correlation analyses with *in vivo* muscular lipid content

No significant correlations are observed between *in vivo* **IMCL** and *in vitro* total LPCs. IMCL of *M. tibialis* neither associates with an individual species and IMCL of *M. soleus* (n = 7) only associates inversely with intracellular LPC C14:0 (0.5 h: r = - 0.87, p = 0.0117*), LPC C14:1 (0.5 h: r = - 0.81, p = 0.0259*; 4 h: r = - 0.73, p = 0.0649), LPC C16:0 (24 h: r = - 0.80, p = 0.0301*), LPC C16:1 (0.5 h: r = - 0.84, p = 0.0177*) and [$^{13}C_{16}$]LPC C18:0 (24 h: r = - 0.82, p = 0.0225*).

EMCL of different muscles shows various significant relationships with LPC levels: EMCL of *M. tibialis anterior* (*M tib. ant.*; n = 6) positively correlates with total intracellular [^{12}C]LPCs after 30-minute stimulation (r = + 0.85, p = 0.0309*) reflected

by individual correlations with intracellular LPC C18:1 (r = + 0.88, p = 0.0218*), LPC C18:2 (r = + 0.83, p = 0.0425*), LPC C20:1 (r = + 0.84, p = 0.0377*), LPC C20:3 (r = + 0.83, p = 0.0426*) and LPC C22:4 (r = + 0.89, p = 0.0172*).

EMCLs (n = 6) of other muscles lack significant relationships with [^{12}C]LPC sums but correlate with specific intracellular [^{12}C]-species: LPC C18:0 correlates with EMCL of *M. tib. ant.* (24 h: r = + 0.93, p = 0.0082*), *M. tib. post.* (0.5 h: r = + 0.82, p = 0.0471*; 4 h: r = + 0.76, p = 0.0778; 24 h: r = + 0.91, p = 0.0107*), *M. soleus* (4 h: r = + 0.97, p = 0.0015*) and *M. peroneus* (0.5 h: r = + 0.83, p = 0.0428*; 4 h: r = + 0.86, p = 0.0282*; 24 h: r = + 0.89, p = 0.0185*), LPC C20:0 with EMCL of *M. soleus* (0.5 h: r = + 0.92, p = 0.0097*) and *M. gastrocnemius medialis* (*M. GC med.*; 0.5 h: r = + 0.85, p = 0.0314*), LPC C20:1 with EMCL of *M. tib. ant.* (see above), *M. tib. post.* (0.5 h: r = + 0.82, p = 0.0447*), *M. soleus* (0.5 h: r = + 0.96, p = 0.0021*), *M. GC med.* (0.5 h: r = + 0.91, p = 0.0130*) and *M. peroneus* (0.5 h: r = + 0.89, p = 0.0171*), LPC C22:1 with EMCL of *M. GC lat.* (0.5 h: r = + 0.82, p = 0.0465*) *et med.* (0.5 h: r = + 0.82, p = 0.0479*) and LPC C22:4 with EMCL of *M. tib. ant.* (see above), *M. tib. post.* (0.5 h: r = + 0.88, p = 0.0223*; 4 h: r = + 0.80, p = 0.0554) and *M. peroneus* (0.5 h: r = + 0.82, p = 0.0438*). Moreover, intracellular [$^{13}C_{18}$]LPC C18:0 associates with EMCL of *M. tib. ant.* (0.5 h: r = + 0.87, p = 0.0253*; 24 h: r = + 0.81, p = 0.0524; n = 6) and *M. tib. post.* (0.5 h: r = + 0.84, p = 0.0378*; 4 h: r = + 0.84, p = 0.0386*; 24 h: r = + 0.78, p = 0.0656; n = 6) and extracellular [$^{13}C_{16}$]LPC C16:0 with EMCL of *M. GC lat.* (0.5 h: r = + 0.95, p = 0.0150*; n = 5) reflecting the correlations between total extracellular [^{13}C]LPCs and EMCL of *M. GC lat.* (0.5 h: r = + 0.89, p = 0.0458*) *et med.* (0.5 h: r = + 0.95, p = 0.0145*; n = 5).

In summary, both IMCL and EMCL significantly correlate with various intracellular but with not a single extracellular LPC species. Moreover, IMCL shows exclusively negative and EMCL exclusively positive relationships with the associated species differing.

Revealingly, ectopic fat deposits such as increased liver fat content have been described as relevant risk factors for development of insulin resistance and type 2 diabetes mellitus [230, 231]. Interestingly, liver density assessed by CT, which is inversely proportional to liver fat content, correlated positively in a human cohort (BMI: 25.6 kg/m² ± 0.6 kg/m², n = 40) with serum LPC C18:0, LPC C18:2, LPC C20:0,

LPC C20:2, LPC C22:0, LPC C22:1 and LPC C24:0 and after a 28-day overfeeding period the changes in liver density positively correlated with the changes of LPC C15:0, LPC C17:0, LPC C20:1 and LPC C22:1 with no other of the remaining 329 lipid species significantly ($p \leq 0.01$) associating with the change of liver density [84].

Concerning EMCL determined in 6 different shank muscles of the donors in this present study, the LPC species associating with several of these muscles' EMCL were extensively similar as 4 out of 5 of them (80 %) were also reported to be associated with liver fat content [84]: These were LPC C18:0 (associating with EMCL of 5 out of 6 (≈ 83 %) shank muscles), LPC C20:0 (2 out of 6 (≈ 33 %) muscles), LPC C20:1 (5 out of 6 (≈ 83 %) muscles) and LPC C22:1 (2 out of 6 (≈ 33 %) muscles) but not LPC C22:4 (3 out of 6 (50 %) muscles). But in contrast to the reported negative associations with liver fat content [84] all of these associations with EMCL showed a positive direction and only intracellular but not any extracellular species significantly associated.

These opposed directions of the correlations may hint at opposed metabolic functions of liver fat content and EMCL or they may be a consequence of the anthropometric and metabolic differences of the investigated cohorts as the metabolically healthy lean human donors of this present project ($n = 10$ in correlation analyses) and the metabolically healthy borderline normal weight human subjects of the study by Heilbronn *et al.* ($n = 40$) were commensurable in regard to fasting blood glucose (4.7 mM ± 0.4 mM *vs.* 4.5 mM ± 0.6 mM), fasting NEFAs (390 µM ± 216 µM *vs.* 300 µM ± 130 µM), total cholesterol (179 mg/dl ± 43 mg/dl *vs.* 178 mg/dl ± 49 mg/dl), HDL cholesterol (58 mg/dl ± 14 mg/dl *vs.* 50 mg/dl ± 25 mg/dl), LDL cholesterol (110 mg/dl ± 35 mg/dl *vs.* 108 mg/dl ± 25 mg/dl) and GIR (36.7 µmol/kg/min ± 7.7 µmol/kg/min *vs.* 36.6 µmol/kg/min ± 11.8 µmol/kg/min) but different in regard to BMI (21.8 kg/m² ± 1.9 kg/m² *vs.* 25.6 kg/m² ± 3.8 kg/m²), PBF (20 % ± 8 % *vs.* 33 % ± 8 %) and fasting insulin (36 pM ± 12 pM *vs.* 69 pM ± 25 pM) as shown in **Supplemental Table 6**.

Congruously, obesity and aerobic fitness have been described as important influencing factors for IMCL [178] as Thamer *et al.* found significant correlations between IMCL of *M. tibialis* and PBF ($r = + 0.28$, $p = 0.01$) as well as between IMCL of *M. soleus* and WHR ($r = + 0.41$, $p < 0.0001$) [178] but without performing adjustments IMCL was not

significantly correlated with age nor with $V(O_2)_{max}$ [178]. Insulin sensitivity correlated neither with IMCL of *M. tibialis* (p = 0.20) nor with IMCL of *M. soleus* (p = 0.72) [178] but intramyocellular lipids have been described to relevantly influence insulin resistance in humans [232-234]. However, the specific lipid species mediating these pathobiochemical effects are not known yet.

9.7.5 Correlation analyses with *in vitro* mitochondrial DNA content, gene expression and [^{3}H]palmitate oxidation activity of cultured human myotubes

Although LPC levels are predominantly positively associated with both *in vivo* $CHOx_{clamp}$ (see chapter **3.3.2**) and *in vitro* FAO activity (see chapter **3.3.6**), exclusively negative relationships are found with **mitochondrial DNA content**: After supplementation with 100 µM L-carnitine during fusion phase (*MT-ND1* L**C**) 2 intracellular [^{13}C]-, 6 intracellular [^{12}C]-, 1 extracellular [^{13}C]- and 17 extracellular [^{12}C]-species negatively correlate with the amount of mitochondrial *MT-ND1* in relation to chromosomal *LPL*. These species are intracellular [$^{13}C_{16}$]LPC C18:0 (after 0.5 h), [$^{13}C_{18}$]LPC C18:0 (after 0.5 h and 4 h), LPC C18:0 (after 0.5 h and 24 h), LPC C20:3 (after 0.5 h, 4 h and 24 h), LPC C20:4 (after 0.5 h, 4 h and 24 h), LPC C22:4 (after 0.5 h, 4 h and 24 h), LPC C22:5 (after 0.5 h, 4 h and 24 h) and LPC C22:6 (after 4 h) plus extracellular [$^{13}C_{18}$]LPC C18:0 (after 24 h), LPC C14:0 (after 0.5 h), LPC C16:0 (after 0.5 h), LPC C16:1 (after 0.5 h), LPC C18:0 (after 0.5 h and 24 h), LPC C18:1 (after 0.5 h), LPC C18:2 (after 0.5 h and 24 h), LPC C18:3 (after 0.5 h), LPC C20:0 (after 24 h), LPC C20:1 (after 0.5 h and 24 h), LPC C20:2 (after 0.5 h and 24 h), LPC C20:3 (after 0.5 h and 24 h), LPC C20:4 (after 0.5 h and 24 h), LPC C20:5 (after 0.5 h), LPC C22:0 (after 24 h), LPC C22:4 (after 0.5 h and 24 h), LPC C22:5 (after 0.5 h and 24 h) and LPC C22:6 (after 0.5 h and 24 h).

These negative relationships with mitochondrial DNA content appear contradictory to the hypothesis that LPCs may act as an indicator for increased aerobic capacity and increased metabolic flexibility of cultivated human myotubes from young, lean donors (see above) but possibly increased mitochondrial DNA content may provide a counter mechanism to cope with the enhanced metabolic strain if the aerobic functionality of the myotubes is impaired.

Notably, only three of these numerous associations reported above are also found after supplementation with 100 µM L-carnitine plus 1 µM GW501516 during fusion phase

(*MT-ND1* GW) despite lacking differences between these two incubation modes in mitochondrial DNA content [188]. The three confirmed relationships are those with intracellular [$^{13}C_{16}$]LPC C18:0 (after 0.5 h), LPC C20:3 (after 0.5 h) and LPC C22:6 (after 4 h). Moreover, an additional inverse relationship is observed with intracellular LPC C18:2 (after 0.5 h).
One explanation for this obviously attenuated interdependency may be a compensatory effect by *PPARD*-inducing GW501516 on the aerobic functionality of the human myotubes during fusion phase.

The expression of *PDK4* (referred to *ACTB* expression) in primary human myotubes is highly significantly increased by a 24-hour stimulation with 125 µM oleate plus 125 µM palmitate ($p < 0.0001$*) both in glucose-containing EMEM Medium and glucose-free RPMI Medium [188]. In contrast, stimulations with 100 µM L-carnitine (LC) or 100 µM of an equimolar mixture of the mcACs C8-, C10- and C12-AC (mcAC) do not alter the *PDK4* expression, neither uncombined nor in combination with oleate plus palmitate (data not shown) [188]. Consequently, the results of the correlation analyses for the stimulations with LC or mcAC resemble those for the stimulations without them and therefore are excluded from **Supplemental Table 2**, **Supplemental Table 3** and **Supplemental Table 4**.

Notably, the remarkable relationships observed between LPC concentrations and *PDK4* expression after cultivation in both glucose-containing EMEM Medium and glucose-free RPMI Medium are not reaffirmed by the **gene expression results from the 10 cm dishes** incubated for 6 days during fusion phase with Fusion Medium supplemented with 100 µM L-carnitine, 100 µM mcAC or 100 µM L-carnitine plus 1 µM GW501516. These media were renewed every 2 days. Thus, the incubations without GW501516 differed from the stimulations reported above in the used medium (Fusion Medium *vs.* Trial Medium), the time period since the last change of the medium (48 hours *vs.* 24 hours), the cell culture vessels (10 cm dishes *vs.* 6-well plates), the confluency of the myotubes at differentiation initiation (70 % to 90 % *vs.* 95 % to 100 %) and the time point for supplementation (during *vs.* after fusion phase).

By contrast to the stimulations in Trial Medium, *PDK4* expression after incubation in Fusion Medium merely correlates with intracellular LPC C14:0 (after 0.5 h),

LPC C16:0 (after 0.5 h), LPC C16:1 (after 0.5 h), LPC C20:2 (after 0.5 h), LPC C22:1 (after 0.5 h) and LPC C22:3 (after 0.5 h) plus extracellular LPC C22:1 (after 24 h) and [$^{13}C_{16}$]LPC C18:1 (after 24 h). Apart from intracellular LPC C22:1 all these correlations are only significant for one of the two incubation modes without GW501516.

Similarly, induced by GW501516, *PDK4* expression negatively associates with intracellular LPC C14:0 (after 0.5 h), LPC C14:1 (after 0.5 h and 4 h), LPC C16:1 (after 0.5 h), LPC C20:2 (after 0.5 h) and LPC C22:1 (after 0.5 h) plus extracellular [$^{13}C_{16}$]LPC C16:0 (after 4 h), [$^{13}C_{16}$]LPC C18:1 and [$^{13}C_{18}$]LPC C18:1 (both after 24 h).

Expression data of the three genes ***PPARD***, ***UCP3*** and ***PPARGC1A*** show very similar association patterns negatively correlating in each case with the four LPC species intracellular LPC C14:0 (after 0.5 h), LPC C14:1 (after 0.5 h) and LPC C16:1 (after 0.5 h) plus extracellular [$^{13}C_{16}$]LPC C18:1 (after 24 h).

As the three incubation modes (LC, mcAC or GW501516) didn't differ for these genes [188], the incubation modes can be interpreted as triple repeat determinations. In this way, the reliability of the results is enhanced affirming the negative associations of intracellular LPC C14:0, LPC C14:1, LPC C16:1 and extracellular [$^{13}C_{16}$]LPC C18:1 with the expression of *PPARD* by 2, 2, 3 and 3 incubation modes, those with the expression of *UCP3* by 2, 2, 2 and 1 incubation modes and those with the expression of *PPARGC1A* by 1, 2, 2 and 1 incubation modes, respectively.

Additionally, *PPARD* expression negatively correlates with intracellular LPC C20:2 (after 0.5 h; 1 incubation mode) and *UCP3* expression with extracellular LPC C22:1 (after 24 h; 1 incubation mode). Interestingly, gene expression of *PPARGC1A* in human muscle was found to be altered by high-fat-overfeeding [235].

Notably, whereas *CPT1B* expression lacks any negative relationship after incubation modes without GW501516, induced *CPT1B* expression negatively associates with 2 out of 7 extracellular [^{13}C]-species (≈ 29 %) and 15 out of 19 extracellular [^{12}C]-species (≈ 79 %): [$^{13}C_{16}$]LPC C18:0 (after 24 h), [$^{13}C_{16}$]LPC C18:1 (after 24 h), LPC C14:0 (after 4 h), LPC C16:0 (after 4 h), LPC C16:1 (after 4 h), LPC C18:1 (after 4 h), LPC C18:2 (after 4 h), LPC C18:3 (after 4 h), LPC C20:1 (after 4 h), LPC C20:2 (after 4 h), LPC C20:3 (after 4 h), LPC C20:4 (after 4 h) , LPC C22:1 (after 24 h), LPC C22:3 (after 0.5 h), LPC C22:4 (after 4 h), LPC C22:5 (after 4 h) and LPC C22:6 (after 4 h) plus intracellular LPC C14:0 (after 0.5 h).

The ***in vitro*** **activity of [^{3}H]palmitate oxidation** was used for correlation analyses in two ways: On the one hand as absolute measures of the activities of the individual stimulation modes (**FAO**) and on the other hand as relative increases compared to the activity without supplementation (**relFAO**).

The activity of [^{3}H]palmitate oxidation without supplementation (**FAO contr.**) positively correlates with intracellular [$^{13}C_{16}$]LPC C18:1, LPC C22:4, LPC C22:5 and LPC C22:6 (after 0.5 h) plus extracellular LPC C20:3 (after 24 h), LPC C20:5 (after 4 h), LPC C22:1 (after 24 h), LPC C22:4 (after 24 h) and LPC C22:6 (after 4 h).

FAO activity enhanced by mcAC (**FAO AC**) shows positive relationships with intracellular [$^{13}C_{16}$]LPC C18:0, [$^{13}C_{16}$]LPC C18:1, LPC C22:4 and LPC C22:6 (after 0.5 h) as well as a negative relationship with intracellular [$^{13}C_{16}$]LPC C16:0 (after 4 h).

Considerably more positive relationships are observed when the relative increases of the FAO activity by mcAC in relation to FAO without supplementation (**relFAO AC**) are used for correlation analyses: Positive correlations emerge for intracellular [$^{13}C_{14}$]LPC C14:0 (after 24 h), [$^{13}C_{16}$]LPC C16:0 (after 24 h), [$^{13}C_{16}$]LPC C18:0 (after 24 h), [$^{13}C_{18}$]LPC C18:0 (after 24 h), [$^{13}C_{18}$]LPC C18:1 (after 4 h and 24 h), LPC C16:0 (after 4 h and 24 h), LPC C18:0 (after 24 h), LPC C18:1 (after 4 h and 24 h), LPC C18:2 (after 4 h), LPC C20:4 (after 4 h) and LPC C20:5 (after 4 h) as well as for extracellular LPC C14:0, LPC C16:0, LPC C16:1, LPC C18:0, LPC C18:1, LPC C18:2, LPC C18:3, LPC C20:0, LPC C20:4 and LPC C20:5 (after 24 h). Moreover, a negative correlation emerges with intracellular LPC C22:3 (after 0.5 h).

FAO activity boosted by GW501516 (**FAO GW**) positively associates with 8 intracellular and 18 extracellular species which are intracellular [$^{13}C_{14}$]LPC C14:0 (after 0.5 h), [$^{13}C_{16}$]LPC C18:0 (after 0.5 h and 4 h), [$^{13}C_{18}$]LPC C18:1 (after 0.5 h), LPC C20:3 (after 0.5 h and 4 h), LPC C20:4 (after 0.5 h and 4 h), LPC C22:4 (after 0.5 h, 4 h and 24 h), LPC C22:5 (after 0.5 h and 4 h) and LPC C22:6 (after 0.5 h and 4 h) plus extracellular [$^{13}C_{18}$]LPC C18:0 (after 24 h), LPC C14:0 (after 0.5 h), LPC C16:0 (after 0.5 h, 4 h and 24 h), LPC C16:1 (after 0.5 h and 4 h), LPC C18:0 (after 0.5 h, 4 h and 24 h), LPC C18:1 (after 0.5 h, 4 h and 24 h), LPC C18:2 (after 0.5 h, 4 h and 24 h), LPC C18:3 (after 0.5 h and 4 h), LPC C20:0 (after 24 h), LPC C20:1 (after 0.5 h, 4 h and 24 h), LPC C20:2 (after 0.5 h, 4 h and 24 h), LPC C20:3 (after 0.5 h, 4 h and 24 h), LPC C20:4 (after 0.5 h, 4 h and 24 h),

LPC C20:5 (after 0.5 h, 4 h and 24 h), LPC C22:3 (after 0.5 h, 4 h and 24 h), LPC C22:4 (after 0.5 h, 4 h and 24 h), LPC C22:5 (after 0.5 h, 4 h and 24 h) and LPC C22:6 (after 0.5 h, 4 h and 24 h).

Similarly, the relative increase of the FAO activity by GW501516 in relation to FAO activity without supplementation (**relFAO GW**) positively associates with 8 intracellular and 19 extracellular species even though partly differing in the chemical structure of the LPC species: intracellular [$^{13}C_{14}$]LPC C14:0 (after 4 h), [$^{13}C_{16}$]LPC C18:0 (after 4 h), LPC C14:0 (after 4 h), LPC C16:0 (after 4 h), LPC C16:1 (after 4 h), LPC C18:1 (after 4 h), LPC C18:2 (after 4 h) and LPC C20:3 (after 4 h) plus extracellular [$^{13}C_{16}$]LPC C18:0 (after 24 h), LPC C14:0 (after 0.5 h, 4 h and 24 h), LPC C16:0 (after 0.5 h, 4 h and 24 h), LPC C16:1 (after 0.5 h, 4 h and 24 h), LPC C18:0 (after 0.5 h and 4 h), LPC C18:1 (after 0.5 h, 4 h and 24 h), LPC C18:2 (after 0.5 h, 4 h and 24 h), LPC C18:3 (after 0.5 h and 4 h), LPC C20:0 (after 0.5 h and 4 h), LPC C20:1 (after 0.5 h and 4 h), LPC C20:2 (after 0.5 h and 4 h), LPC C20:3 (after 0.5 h and 4 h), LPC C20:4 (after 0.5 h and 4 h), LPC C22:0 (after 0.5 h), LPC C22:1 (after 0.5 h), LPC C22:3 (after 0.5 h and 4 h), LPC C22:4 (after 4 h), LPC C22:5 (after 0.5 h and 4 h) and LPC C22:6 (after 4 h).

In conclusion, the vast majority of the observed significant correlations of FAO activity with LPC species have a positive direction (144 out of 146; ≈ 99 %) with only two correlations being inverse. Therefore, high *in vitro* LPC concentrations seem to be indicative of a high *in vitro* FAO activity under metabolic strain by [^{3}H]palmitate.

9.8 Comparison of study designs

The intracellular LPC content was also studied by Li *et al.* in primary human myotubes (n = 4) after 12 hours and after 24 hours of stimulation with 250 µM [$^{13}C_{16}$]palmitate [160] as well as by Han *et al.* in L6 myotubes after 12-hour stimulation with 600 µM to 1000 µM palmitate [67]. The intracellular LPC content was found to be increased approximately twofold after 12 hours of stimulation and approximately threefold after 24 hours of stimulation with 250 µM [$^{13}C_{16}$]palmitate in comparison to the control cells cultured without addition of palmitate [160]. Similarly, 12-hour stimulation of L6 myotubes with 600 µM to 1000 µM palmitate led to an approximately twofold to fourfold increase of the total intracellular LPC content [67].

These reports substantially differ from our findings of predominantly decreasing intracellular [^{12}C]LPC species in response to stimulation with 100 µM L-carnitine and 125 µM [$^{13}C_{16}$]palmitate with 7 species (≈ 37 %) significantly decreased but only 1 species (≈ 5 %) significantly increased after 24 hours (*vs*. 30 minutes). These inconsistencies may be caused by the higher palmitate concentrations but discrepancies between the donors' anthropometric and (patho-) physiologic properties may also be an explanation. However, Han *et al.* omitted phenotyping of the donor of the L6 myotubes. Possibly, the donor suffered from insulin resistance or type 2 diabetes as increased concentrations of LPCs have also been reported in the skeletal muscle and liver of obese diabetic *db/db* mice in comparison with C57BL/6 mice [67]. Furthermore, Han *et al.* newly plated the myoblasts after proliferation for differentiation into myotubes and proliferation phase was conducted with αMEM Medium containing 10 % FBS [67] instead of 20 % FBS. Similarly, Han *et al.* started stimulation after 6 to 8 days of differentiation [67] as we did after 6 to 7 days but LPC content was determined enzymatically [67] and not mass spectrometrically.

Most importantly, stimulation was performed with unlabeled [^{12}C]palmitate which is why LPC content was not distinguished into [^{12}C]- and [^{13}C]LPCs and species-specific profiling was omitted [67]. So these results should be compared with our sums of [^{12}C]- plus [^{13}C]LPCs which consistently showed significant increases of total intracellular concentrations after 4 hours of stimulation.

As outlined in the chapters **3.3.3** and **4.5.5,** correlation analyses of this work in hand revealed inverse associations of *in vivo* ISI_{OGTT} with various polyunsaturated long-chain LPC species both from cell lysates and from supernatants. These found negative associations with insulin sensitivity are markedly confronted by repeatedly reported negative associations with insulin resistance in studies investigating *in vivo* plasma or serum LPC levels in human individuals [84, 103] or mice [104].

One explanation for these oppositional observations may be differences in regard to the metabolic strain as both Wallace *et al.* and Heilbronn *et al.* performed *in vivo* lipidomics analyses after a 12-hour overnight fasting period in their human cohorts [84, 103] and mice were also fasted for 5 hours prior to plasma sampling [104] whereas *in vitro* LPC profiling of primary human myotubes in this project was directly conducted after

the metabolic strain by a fatty acid load employing 125 µM [$^{13}C_{16}$]palmitate for 30 minutes, 4 hours or 24 hours.

Moreover, anthropometric and physiologic differences between the investigated cohorts may cause the contrary relationships as HOMA-IR score was assessed by Wallace *et al.* in human individuals with higher BMI and PBF plus higher levels of fasting plasma glucose (with individuals with elevated fasting glucose levels ≥ 7 mM being excluded), fasting plasma insulin, fasting NEFAs and fasting TGs but comparable levels of total cholesterol, HDL cholesterol and LDL cholesterol [103] compared to the donors who were chosen and whose ISI was determined in this present project.

The human cohort of sedentary, nondiabetic subjects studied by Heilbronn *et al.* [84] exhibited similar fasting glucose concentrations like the cohort in this present project but concerning age, BMI, PBF, fasting insulin and fasting TG concentrations the cohort's properties resembled more those of the cohort studied by Wallace *et al.* [103] as depicted in **Supplemental Table 6**.

Similarly, mice exhibited an increased body mass (+ 26 %), fat mass (+ 210 %) and HOMA-IR score (+ 650 %) plus elevated levels of 5-hour fasting blood glucose (+ 11 %) and plasma insulin (+ 546 %) after 12 weeks of high-fat diet [104].

Supplemental Table 6: Comparison of anthropometric and biochemical parameters of various human cohorts used for LPC profiling. Data are presented as mean ± standard deviation.
Abbreviations: n, number of subjects; BMI, body mass index; PBF, percentage of body fat; NEFAs, non-esterified fatty acids; TGs, triglycerides; HDL, high density lipoprotein; LDL, low density lipoprotein; GIR, glucose infusion rate; HOMA-IR, homeostatic model assessment of insulin resistance.

Parameter	**Cohort of the myotubes' donors (n = 10)**	**Heilbronn *et al.* (n = 40) [84]**	**Wallace *et al.* (n = 39) [103]**
Age [years]	24 ± 3	37 ± 13	34 ± 13
BMI [kg/m²]	22 ± 2	26 ± 4	26 ± 6
PBF [%]	20 ± 8	33 ± 8	28 ± 14
Fasting glucose [mM]	4.69 ± 0.44	4.5 ± 0.6	5.27 ± 0.55
Fasting insulin [pM]	36.0 ± 11.6	69 ± 25	64.7 ± 55.6
Fasting NEFAs [µM]	390 ± 216	300 ± 130	600 ± 350
Fasting TGs [mg/dl]	78.9 ± 23.7	96.3 ± 55.7	95.4 ± 43.8
Total cholesterol [mg/dl]	178.9 ± 42.7	178.0 ± 48.7	184.2 ± 41.4
HDL cholesterol [mg/dl]	58.1 ± 14.2	50.3 ± 24.7	55.7 ± 17.8
LDL cholesterol [mg/dl]	109.6 ± 35.4	108.4 ± 24.7	104.5 ± 37.5
GIR [µmol/kg/min]	36.7 ± 7.7	36.6 ± 11.8	
HOMA-IR [-]		1.9 ± 0.6	2.28 ± 2.17